AD-A104 992 NAVAL COASTAL SYSTEMS CENTER PANAMA CITY FL F/G 6/19
HEAT AND WATER VAPOR TRANSFER IN THE HUMAN RESPIRATORY SYSTEM A--ETC(U)
SEP 81 M L NUCKOLS
UNCLASSIFIED NCSC-TR-364-81 SBIE-AD-F200 009 NL

1 OF 4
AD
A104992

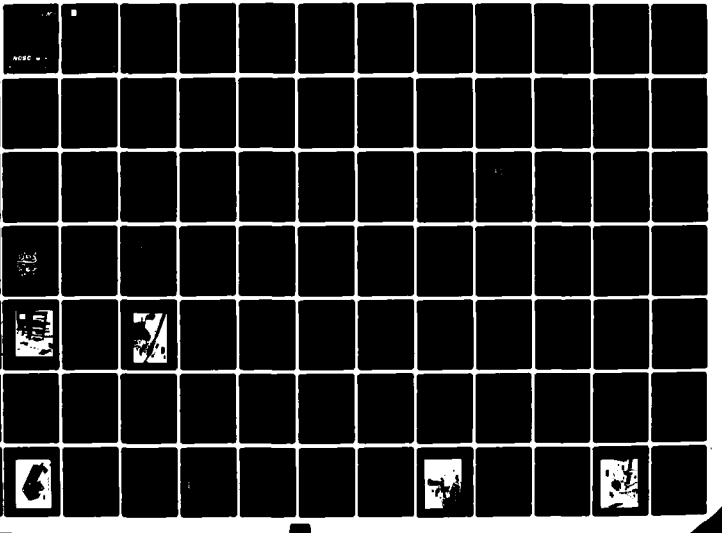

10

TECHNICAL
REPORT
NCSC TR364-81

SEPTEMBER 1981

LEVEL II

HEAT AND WATER VAPOR TRANSFER IN THE HUMAN RESPIRATORY SYSTEM AT HYPERBARIC CONDITIONS

MARSHALL L. NUCKOLS

PREPARED FOR DOCTORAL DISSERTATION, DUKE UNIVERSITY, DURHAM, N.C.

NAVAL COASTAL SYSTEMS CENTER
NCSC
PANAMA CITY, FLORIDA 32407

NAVAL COASTAL SYSTEMS CENTER

PANAMA CITY, FLORIDA 32407

CAPT RAYMOND D. BENNETT, USN
Commanding Officer

GUY C. DILWORTH
Technical Director

ADMINISTRATIVE INFORMATION

(U) The research described in this report was performed during fiscal years 1980-1981 as a principal part of a doctoral thesis and was supported by the NCSC Independent Research Program through funding by the Office of the Assistant Deputy Chief of Naval Material for Laboratory Management (Program Element 61152N, Project Number R00001, Task R041-01). This research is intended to characterize the heat and water vapor transfer mechanisms in the human airways.

(U) In the interest of costs and timeliness and the best interests of NCSC and the Navy, certain deviations from format and style were allowed in publishing this Technical Report from a doctoral thesis.

(U) The author wishes to acknowledge the help and suggestions of Dr. C. E. Johnson, Duke University; Dr. David L. Swift, Johns Hopkins School of Hygiene and Public Health; Dr. Eugene Wissler, University of Texas; Dr. J. L. Zumrick, Naval Experimental Diving Unit; Mr. P. G. Sexton, Code 753, NCSC; and the staff of the Hyperbaric Test Facility at NCSC.

Released by:
William H. Williams, Head
Engineering Department
September 1981

Under authority of:
Guy C. Dilworth
Technical Director

UNCLASSIFIED

SECURITY CLASSIFICATION OF THIS PAGE (When Data Entered)

REPORT DOCUMENTATION PAGE		READ INSTRUCTIONS BEFORE COMPLETING FORM
1. REPORT NUMBER TR 364-81	2. GOVT ACCESSION NO. AD-A104992	3. RECIPIENT'S CATALOG NUMBER
4. TITLE (and Subtitle) Heat and Water Vapor Transfer in the Human Respiratory System at Hyperbaric Conditions		5. TYPE OF REPORT & PERIOD COVERED 6. PERFORMING ORG. REPORT NUMBER
7. AUTHOR(s) Marshall L. Nuckols		8. CONTRACT OR GRANT NUMBER(s)
9. PERFORMING ORGANIZATION NAME AND ADDRESS Naval Coastal Systems Center Panama City, FL 32407		10. PROGRAM ELEMENT, PROJECT, TASK AREA & WORK UNIT NUMBERS Program Element 61152N; Project R00001, TA R041-01; Work Unit 0401-69
11. CONTROLLING OFFICE NAME AND ADDRESS		12. REPORT DATE September 1981 13. NUMBER OF PAGES 302
14. MONITORING AGENCY NAME & ADDRESS(if different from Controlling Office)		15. SECURITY CLASS. (of this report) UNCLASSIFIED 15a. DECLASSIFICATION/DOWNGRADING SCHEDULE N/A

16. DISTRIBUTION STATEMENT (of this Report)

Approved for public release: distribution unlimited.

17. DISTRIBUTION STATEMENT (of the abstract entered in Block 20, if different from Report)

18. SUPPLEMENTARY NOTES

19. KEY WORDS (Continue on reverse side if necessary and identify by block number)

Respiratory System; Heat Transfer; Mass Transfer; Swimmer Divers; Heat Loss; Diving; Nose (Anatomy); Gas Flow; Anatomical Models; Instrumentation; Hyperbraic Conditions; Human Body

20. ABSTRACT (Continue on reverse side if necessary and identify by block number)

Heat and mass transfer mechanisms are characterized in physical models of the human upper respiratory tract (nares to trachea) and lower respiratory tract (main bronchus to alveoli) to simulated depths of 305 metres with various gas mixtures. Such characterizations offer a detailed understanding of the effects of environmental pressures, gas composition, and respiratory rates on the body cooling capacity of the respiratory airways. Empirically derived heat transfer relationships found in this investigation follow:

(continued)

20. ABSTRACT (continued):

Upper Airways

Nasal Breathing/Inhalation: $\overline{Nu} = 0.028\ (RePr)^{0.854}$

Nasal Breathing/Exhalation: $\overline{Nu} = 0.0045\ (RePr)^{1.080}$ for $Re \leq 7800$

$\overline{Nu} = 0.310\ (RePr)^{0.585}$ for $Re > 7800$

Oral Breathing/Inhalation: $\overline{Nu} = 0.035\ (RePr)^{0.804}$

Oral Breathing/Exhalation: $\overline{Nu} = 0.0006\ (RePr)^{1.269}$ for $Re \leq 12{,}000$

$\overline{Nu} = 0.094\ (RePr)^{0.704}$ for $Re > 12{,}000$

Lower Airways

Inspiration: $\overline{Nu} = 0.0777\ (RePr)^{0.726}$

Expiration: $\overline{Nu} = 0.0589\ (RePr)^{0.752}$

Combined: $\overline{Nu} = 0.0733\ (RePr)^{0.731}$

$\overline{Nu}$, Re, and Pr are the dimensionless Nusselt, Reynolds, and Prandtl numbers, respectively. The above relationships are based on the physical dimensions and gas flow properties in the trachea and are applicable to Reynolds number values up to 70,000.

The Chilton-Colburn j-factor analogy is used to derive corresponding mass transfer data from the experimental recordings.

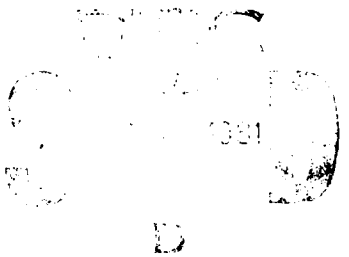

TABLE OF CONTENTS

TABLE OF CONTENTS (Continued)

LIST OF FIGURES

LIST OF TABLES

NOMENCLATURE

A	Area, cm^2
C	Molar Density, gm-moles/cm^3
C_p	Specific Heat, joules/gm °C
D	Diameter, cm
D_v	Mass Diffusivity Coefficient, cm^2/sec
f	Friction Factor
h	Heat transfer coefficient, Watts/cm^2 °C
h_D	Mass transfer coefficient, cm/sec
h_{fg}	Latent heat of vaporization, joule/g
j	Chilton - Colburn j-Factor
K	Thermal Conductivity, Watts/cm °C
k_x	Mass transfer coefficient, gm-moles/cm^2 - sec
L	Passageway length, cm
M	Molecular weight, gm/gm-moles
$\dot{m}$	Mass transfer rate, g/sec
Nu	Nusselt number, hD/K
P	Pressure, kPa
Pr	Prandtl number, Cp μ/K
q	Heat flow, joules/sec
$\dot{Q}$	Heat flow, joules/sec
Ru	Universal gas constant, joule/Kg-mole °C
R	Tube radius, cm
R	Gas constant, joule/Kg °C
Re	Reynolds number, ρVD/μ
RMV	Respiratory minute volume, L/min

Sc	Schmidt number, $\mu/\rho D_v$
Sh	Sherwood number, $h_D D/D_v$
t_s	Endurance limit, min
T	temperature, °C
V	Flow velocity, cm/sec
$\dot{V}$	Volumetric flow rate, cm^3/sec
W	Humidity ratio, gm of water/gm dry air
x	Mole fraction
α	Thermal diffusivity, cm^2/sec
ΔT	Differential temperature, °C
μ	Viscosity, g/cm-sec
ρ	Mass density, g/cm^3
ϕ	Relative humidity

Subscripts

A, B	Gas Constituent Designation
B	Blood Conditions
D	Mass Diffusion
e	Exit Conditions
g	Dry Gas Conditions
H	Heat Transfer
H_2O	Water Vapor
i	Entrance Conditions
i+1	Exit Conditions
L	Latent Heat
M	Interface Condition

0	Exit Conditions
S	Sensible Heat
T	Trachea
V	Saturated Vapor
W	Wall or water conditions
∞	Free Stream Conditions
1, 2, ··	Branch Number

Superscripts

—	Mean Value
·	Rate

HEAT AND WATER VAPOR TRANSFER IN THE HUMAN RESPIRATORY SYSTEM AT HYPERBARIC CONDITIONS

CHAPTER I

INTRODUCTION

Background

The diver's environment presents numerous adverse conditions which must be understood or compensated for to sustain life. In the recent past these conditions offered severe limitations to the diver's practical operating depths and mission durations. As late as 1950, the maximum practical operating depth for divers did not exceed 60 metres. Reduced visibility, impaired mobility, and assorted groups of dangerous marine life all contribute to rendering a diver's task far more difficult than a similar job on the surface. Additionally, other factors act as more immediate and direct threats to the diver's life.

For example, the very same gas that we breathe daily to support life on the surface becomes poisonous to the diver at increased pressures. This phenomenon, referred to as oxygen toxicity, has been shown to occur in humans whenever the partial pressure of oxygen exceeds approximately 3 atmospheres (absolute pressure). Although individual tolerances have been shown to vary widely, as a rule a diver is limited to a depth of 90 metres when breathing air before oxygen toxicity sets in. Nausea, blurred vision, convulsions, and death might ultimately occur from oxygen poisoning.

A second phenomenon due to the other major constituent of the air we breathe is termed nitrogen narcosis, or so called "rapture of the deep". As a diver descends, the partial pressure of nitrogen in the air he breathes increases. At depths beyond 30 metres (again individual tolerances vary widely) the nitrogen produces an intoxicating effect similar to that of alcohol. This narcosis is characterized by a slowing of mental activity and a general feeling of euphoria, perhaps leading to a false sense of security.

These conditions, as well as the more popularly known occurrences of decompression sickness ("bends" or caisson disease) and high pressure nervous syndrome (HPNS), have all been found manageable in recent years through the use of proper gas mixtures and dive procedures. Replacing nitrogen with helium has been shown to eliminate the symptoms of nitrogen narcosis. To allow divers to reach greater depths, the proportion of oxygen in this helium/ oxygen mix can be reduced sufficiently to sustain life while avoiding oxygen toxicity. While extensive research continues in all of these gas related dive ailments, one hazard of the diver is perhaps less understood and far more difficult to manage, i.e., body heat loss to his surroundings.

The sea offers a severe thermal environment for the surface swimmer or diver. The thermal properties of seawater, i.e., conductivity and specific heat, were for many years unsuspected for the deaths of many accidental overboard victims in what was considered mild water temperatures. Coupled with the gradual decrease in sea temperatures as a diver descends, approaching 0°C at 305 metres even in tropical waters, these properties of seawater provide the potential for an extreme heat loss from the diver's body through

convective cooling. Keatinge [1] gives as an example the accident of the Lakonia which caught fire near Madeira in December 1963 in relatively warm water (17° to 18°C). Even though rescue ships arrived within 3 hours, 113 of the approximately 200 people who entered the water were dead. Even though all victims were found floating in their lifejackets in fairly calm sea, death was attributed to drowning for lack of a better explanation.

It is now known that cold is responsible for most deaths after major shipwrecks and many of the immersion deaths of inland and coastal waters, but until recently even experts regarded drowning as the only important hazard to life in the water, Keatinge [1]. Several investigators have recently attempted to predict body heat losses and their effects on the endurance limits of man submerged in cold water. Hayward, Eckerson, and Collis [2] gives an experimentally derived expression for this endurance limit for lightly clothed subjects in water less than 23°C, as

$$t_s = 15 + 7.2/(0.0785 - 0.0034T_w)$$

T_w = water temperature, °C

t_s = endurance limit, min (death assumed at 30°C rectal temperature).

Although of minor concern in surface environments, heat lost through the diver's cyclic breathing pattern is a second major potential source of body heat drain. A number of investigations, primarily funded by the Office of Naval Research, were conducted in the late 1960s to characterize the significance of this avenue of body heat loss for the diver or habitat dweller in high pressure environments. Webb and Annis [3] recorded heat losses from the respiratory tract ranging from less than 10 percent of total body heat loss at the surface to over 25 percent of total body heat loss at

70 metres of seawater. In investigations by Goodman et al [4] to simulated depths of 305 metres of seawater, recordings of heat loss from the respiratory tract of human subjects were seen to exceed total body metabolic outputs at depths beyond approximately 180 metres when inspiring 1.5 °C gas temperatures. Beyond this depth the divers were in a state of net body heat drain even though their thermally protective garments were most effective in eliminating body surface convective cooling due to cold water immersion.

Unlike the heat losses from surface convective cooling, the potential losses from the respiratory tract remove heat, via the pulmonary - vascular system, directly from the body's "core" containing the vital body organs. As such, excessive respiratory heat losses represent a much greater immediate life-threatening situation than does body surface cooling. In fact the body has built up a complex thermal regulatory system to minimize central body core cooling even at the expense of sacrificing less critical peripheral tissue to cold injury, Guyton [5]. The potentially serious role of this avenue of heat drain in hyperbaric environments makes it mandatory for us to understand the heat transfer mechanism in the human respiratory tract.

The two major concerns in the investigation of the effects of breathing cold, dense gases fall into two categories. One, the previously mentioned concern with excessive heat loss directly from the body core, and second, the potential damage that may result to the pulmonary mucosa from the cold, dry breathing gas. In the previously mentioned studies of Goodman et al [4], an inspiration temperature was observed at various simulated ocean depths below which copious secretions from the pulmonary airway were observed. Hoke, Jackson, Alexander, and Flynn [6] likewise observed such secretions

and acute respiratory difficulty in similar tests to 244 metres of seawater when 0°C gas temperatures were used and at 305 metres of seawater when 7°C gas temperatures were used. They concluded that a rate of respiratory heat loss exceeding 350 watts was detrimental to pulmonary function and overall thermal balance in spite of exercise.

Injury to the respiratory tract may not be limited only to the effects of cold, dense gases. The lack of moisture content in the inspired gas may likewise contribute to damaging effects on the pulmonary airways. Marfatia, Donahoe, and Hendren [7] observed severe pathologic changes to rabbits' respiratory epithelium following 6 hours respiration of dry (18 percent RH) gases at 23°C at surface pressure. Characteristic changes included destruction of cilia and mucous glands in the upper respiratory passages, and up to 2 percent loss in total body weight. Similar experiments with humidified (90 percent RH) gases at 22°C showed no pathologic changes or weight loss. Burton [8] indicates that similar results have been observed in man during mouth-breathing of dry gases during postoperative periods.

The inability of the respiratory tract to keep up with the fluid and heat demands required to condition the inspiratory gases appears to be the major contributor to these pathologic changes. This conditioning capability, especially of the upper respiratory tract, has been identified for many years as a major protective weapon in defense of the lungs. Whether called a "passive heat exchanger" (Webb [9]) a "countercurrent heat exchanger" (Jackson, Schmidt-Nielsen [10]), or a "heat and moisture exchanger apparatus" (Cole [11]), the proximal 10 to 15 cm length of upper respiratory tract has an efficient design to condition incoming gases to near body temperature and

humidity saturation prior to entering the lungs at 1 ATA during nasal breathing. Webb [9] demonstrated this phenomena by recording gas temperatures of 25° to 33°C only 9 cm back from the anterior nares while subjects breathed gases at temperatures ranging from -20° to 31°C at the surface. This data is supported by Armstrong [12] who reported no direct laryngeal injury during 2 to 6 hours breathing air at -80°F at high altitudes, and by Spealman [13] during exposures to temperatures ranging from -83°F to 133°F at surface conditions. This conditioning ability of the respiratory tract will of course be jeopardized as pressure increases, as in a diving operation, due to the increased heat and moisture demand of these dry, high density respiratory gases. Under these severe conditions, the inspired gases will continue to drain heat and moisture from the lower respiratory tract until saturated with water vapor at body temperature. This condition may not be reached until the gases have penetrated through several bifurcations of the lower respiratory tract [17].

The experiments of Moritz, Hendriques, and McLean [14] offer further support of the excellent conditioning capabilities of the upper airways in extreme environments, and also demonstrate the importance of the moisture content of the inspired gases. In these experiments, the effects of forced inhalation of hot gases, steam-air mixtures, and flame inhalation on the respiratory tract and lungs of dogs was investigated. The inhalation for short durations of hot, relatively dry furnace gases (350°C) and flames (up to 550°C recorded in larynx) were observed to rapidly cool to as low as 50°C by the time the lower trachea was reached. Autopsies revealed mild-to-no damage in the lungs. On the other hand, during inspiration of a steam-air mix (approximately 100°C), temperatures up to 94°C were recorded at the lower trachea. Moderate to severe pathologic changes were observed in the

airways at autopsy. These additional experiments may indicate that the primary means for the upper respiratory tract to condition the inhalation of hot, dry gases is to convert the high temperature energy into latent heat. Although these extremely high temperatures would never be expected to be seen by a diver, this data does serve as supporting evidence of the significant protective capability of the upper respiratory tract. In a diving situation this protective mechanism must necessarily work somewhat differently. During the inhalation of cold, dry gases the upper respiratory tract must supply sufficient heat to warm the gas to body temperature, and the moisture and latent heat to saturate the gas at body temperature. As previously noted, this moisture and heat requirement can put a serious strain on the body's fight to maintain thermal neutrality.

Fortunately, all of the heat and water vapor given up by the respiratory tract during cold gas inhalation is not lost. Bouhuys reports that a man breathing dry air at 0°C and 1 ATA would use nearly all his basal metabolic heat production merely to warm and humidify the air he inspired without any protective mechanism [15]. Clearly, protective mechanisms within the respiratory tract prevent this occurrence. Webb [9] demonstrated the heat and water vapor conservation features of the upper respiratory tract in man during expiration. In a series of tests 18 subjects inspired an air environment at the surface at ambient temperatures of 75°C, 55°C, 25°C, 5°C, and -25°C. Nasal airway temperatures were continually monitored with shielded thermocouples at 1 cm, 5 cm, and 9 cm back from the nasal opening. In all tests, Webb found that expired temperatures were less than body temperature unless the inspired air temperature exceeded 75°C (dry) or 55°C (vapor pressure above 45 mm Hg). Webb explains that during expiration, the vapor

saturated gas gives up heat and moisture through condensation to the airway walls that were previously cooled during inspiration. (Webb noted that this cooling and condensation of the expired gas probably causes the watery nasal drip when breathing cold air.) In so doing the conserved heat and water vapor can be available for the next inspiration. The overall result of this process is the net loss from the respiratory tract per day of about 350 Kcal of heat (about 17% of the basal metabolic rate) and 250-400 ml of water [72, 73] under resting conditions.

Although not as pronounced in humans, this conserving feature plays a major role in the ability of small mammals to exist in arid climates with little or no external water supply [16]. Expiration temperatures 10°C below ambient temperatures have been recorded in the Kangaroo rat; evidence of the superior conservation features in these desert rodents.

It is clear then, from previous research that the heat and water vapor transport mechanisms in the respiratory system are extremely important in the body's defense against climatic extremes. Additionally, many respiratory dysfunctions diagnosed clinically are now being attributed to a breakdown of these defense mechanisms. For example, these processes apparently play an essential role in the dysfunction of the ventilatory system in some diseases such as cystic fibrosis [79]. Also, recent studies at Peter Bent Brigham Hospital have found evidence that heat loss from the mucosa due to heating and humidifying inspired air is a major stimulus for exercise-induced asthma [80, 81, 82]. In fact, recent reports have stated a probable connection between the mucosa temperature, water content, and heat fluxes in the respiratory tract with many other diseases, which collectively, are the leading causes of bed disability and work loss in the US [83, 84].

A full understanding of these exchange mechanisms in the upper and lower respiratory tracts are thus desirable. Past investigators (Goodman et al [4], Webb [3], Hoke [6]) have given much information to characterize these processes under experimentally defined conditions (i.e., metabolic rate, respiratory minute volume, gas composition, etc). They have derived empirical expressions of expired temperature as a function of inspired temperature which can be used for predicting respiratory heat loss over a range of conditions. Braithwaite [24] used the results of these past studies to derive limits of minimal safe inspired gas temperatures for divers at depths of 180 to 305 metres of seawater, Figure 1. Although recognized as significant in their value as a good first estimate these guidelines were derived using an overall "black box" approach as given in Appendix G without an assessment of the local heat and mass exchange mechanisms that occur in the respiratory tract. As such, Braithwaite recognized that the proposed limits did not adequately address the effects of respiratory minute volume, gas density, gas composition, metabolic heat production and water vapor content on these exchange mechanisms.

Unfortunately, these heat and water vapor transport mechanisms have not been characterized quantitatively in the human airways. This is primarily due to the complex geometry and flow patterns in the airways which complicate modeling efforts. This research is directed toward fulfilling these characterizations.

DEPTH FSW	TEMPERATURE °C	°F
600	-1.0	30.1
650	1.7	35.0
700	4.0	39.2
750	6.0	42.9
800	7.8	46.1
850	9.4	48.9
900	10.8	51.5
950	12.1	53.8
1000	13.3	55.9

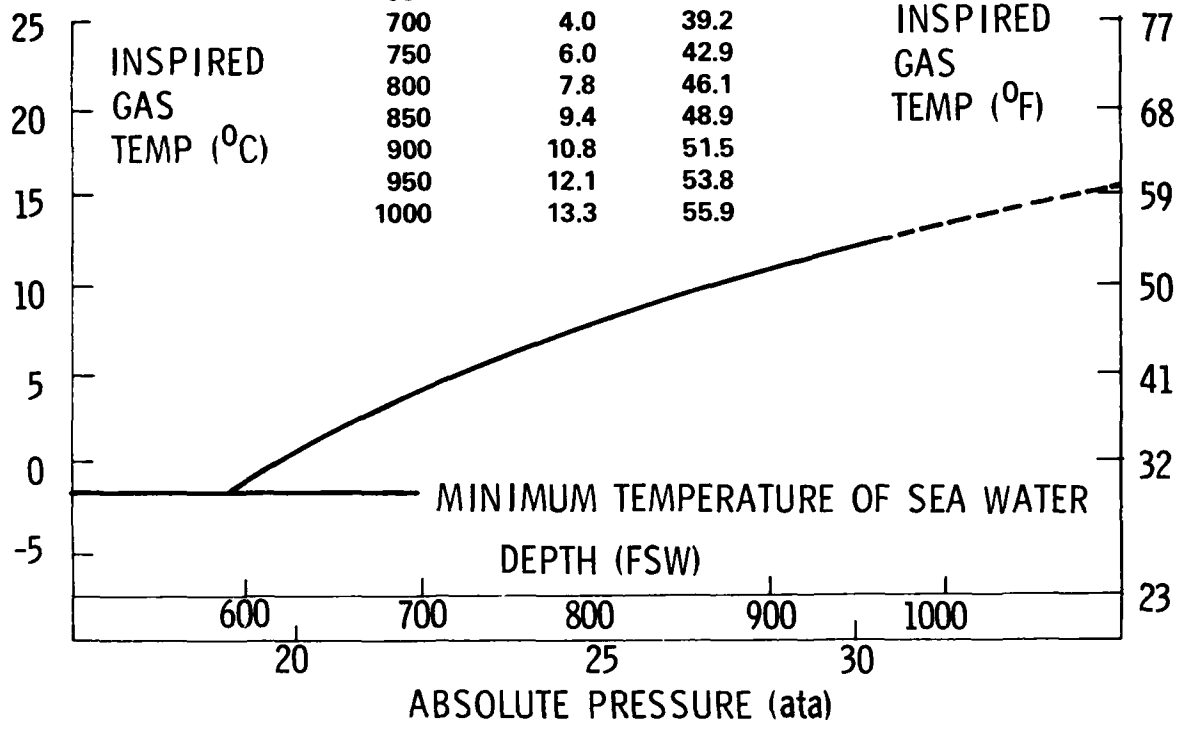

FIGURE 1: MINIMUM SAFE INSPIRED GAS TEMPERATURE LIMITS (FROM BRAITHWAITE [24])

Approach

When considering the local heat and mass exchange from any segment within the respiratory airway, as shown in Figure 2, individual expressions can be written for these two transport processes. At the interface between the gas stream and passageway wall (the mucous membrane) evaporation takes place and a saturation state exists at the interface temperature, T_w. The mass transfer from this interface to the gas stream occurs because of a difference in concentration of the water vapor according to the expression [60]

$$\dot{m}/A = h_D (\rho_w - \rho_i)$$

where

$\dot{m}$ = mass transfer rate, g/sec

A = heat transfer surface area, cm^2

h_D = mass transfer coefficient, cm/sec

ρ_w = partial mass density of water vapor at interface, g/cm^3

ρ_i = partial mass density of water vapor of incoming gas stream, g/cm^3

Likewise, sensible heat transfer between the gas stream and interface can be expressed as the product of a heat transfer coefficient, h, and the difference between the interface and gas stream temperatures.

$$q_s/A = h(T_w - T_i)$$

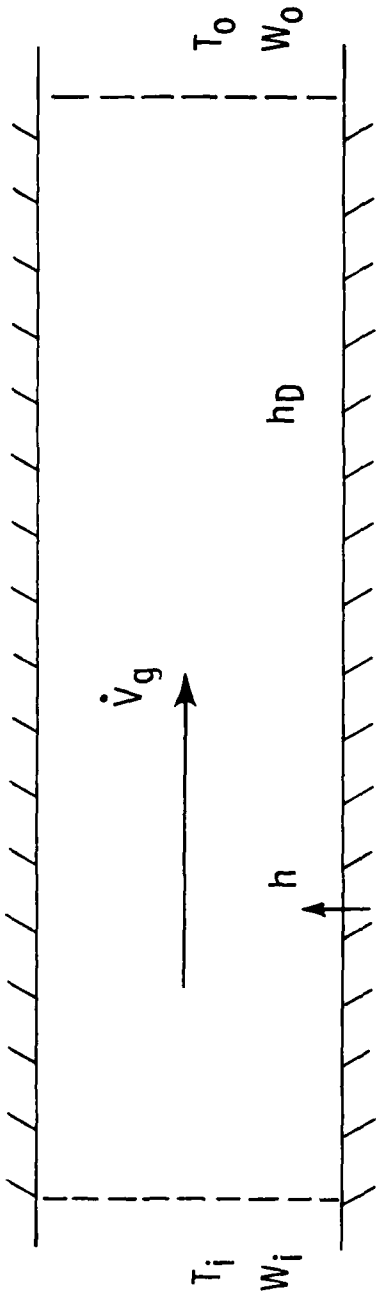

FIGURE 2: SEGMENT OF AIRWAY

where

q_s = sensible heat transfer rate between the gas stream and mucosa, Watts

h = heat transfer coefficient, Watts/cm^2 °C

T_i = temperature of incoming gas stream, °C

Since the water vapor transferred to the gas stream must be supplied with its latent heat of vaporization, h_{fg}, the total heat flux between any segment of the mucous membrane and the respiratory gas is

$$q/A = h(T_w - T_i) + h_D (\rho_w - \rho_i) h_{fg}$$

where

h_{fg} = latent heat of vaporization, joules/g.

The key to properly understanding heat and water vapor transport in the human airways is to fully characterize the heat and mass transfer coefficients, h and h_D, over the full range of conditions encountered in respiration at the surface and deep sea conditions. These characterizations would be practically insurmountable if the many pertinent flow and gas parameters (i.e., flow rate, gas properties, etc) were allowed to vary independently. This complexity is minimized through the use of dimensionless groups in determining the behavior of these transfer coefficients. A thorough discussion of these dimensionless groups will be delayed until Chapter V. However, briefly stated the primary objective of this research effort will be to characterize in the human airways the dimensionless heat transfer parameter, Nu, defined as

$$Nu = \frac{h\ D}{K}$$

where

Nu = dimensionless Nusselt number

D = characteristic dimension, cm

K = gas thermal conductivity, Watts/cm °C

and the dimensionless mass transfer parameter, Sh, defined as

$$Sh = \frac{h_D D}{D_v}$$

where

Sh = dimensionless Sherwood number

D_v = mass diffusivity coefficient of water vapor to respiratory gases, cm^2/sec

over the full range of conditions encountered during breathing in hyperbaric gas environments. The assessments of their behaviors will be made over a range of Reynolds numbers, Re, to adequately address respiratory heat loss to 610 metres of seawater (2000 FSW)

where

$$Re = \frac{4\rho \dot{V}g}{\pi D \mu}$$

ρ = gas density, g/cm^3

μ = gas viscosity, g/cm-sec

$\dot{V}g$ = volumetric flow rate, cm^3/sec.

It was shown previously that Reynolds number values between 0 and approximately 62,000 (based on the diameter and flow velocity in the trachea) would be adequate for this desired range of applications [25].

In the research about to be described, the local heat transfer characteristics from castings of the human upper airways (trachea and upward) and a model of the lower airways are measured in both surface (1ATA) and hyperbaric environments. Heat transfer relationships are derived for mouth and nasal breathing during quasi-steady inspiratory and expiratory flows while simulating constant mucosa temperatures. Mass transfer relationships have been derived by analogy from these heat transfer measurements. A comparative conditioning efficiency evaluation is also made between the oral and nasal passageways from these relationships. The use of these transport relationships, in conjunction with a mathematical model of flow in the human airways, gives a detailed insight into the effects of environmental conditions and respiratory requirements on the temperatures and heat fluxes of the airway mucosa.

In going about these characterizations the results of past investigations at Duke University were utilized. Linderoth and Kuonen [17] and Nuckols [25] determined experimentally the inspirational heat transfer characteristics of physical models of the lower respiratory tract in unidirectional, steady flow conditions. Heat transfer relationships, $\overline{Nu} = f(Re, Pr)$ as seen in Figure 3, were derived based on these models, and they were found to be applicable over a wide range of hyperbaric conditions and respiratory rates. Johnson [26] verified these relationships during <u>in vivo</u> measurements of the gas stream and lumen wall temperatures of anesthetized dogs at hyperbaric conditions.

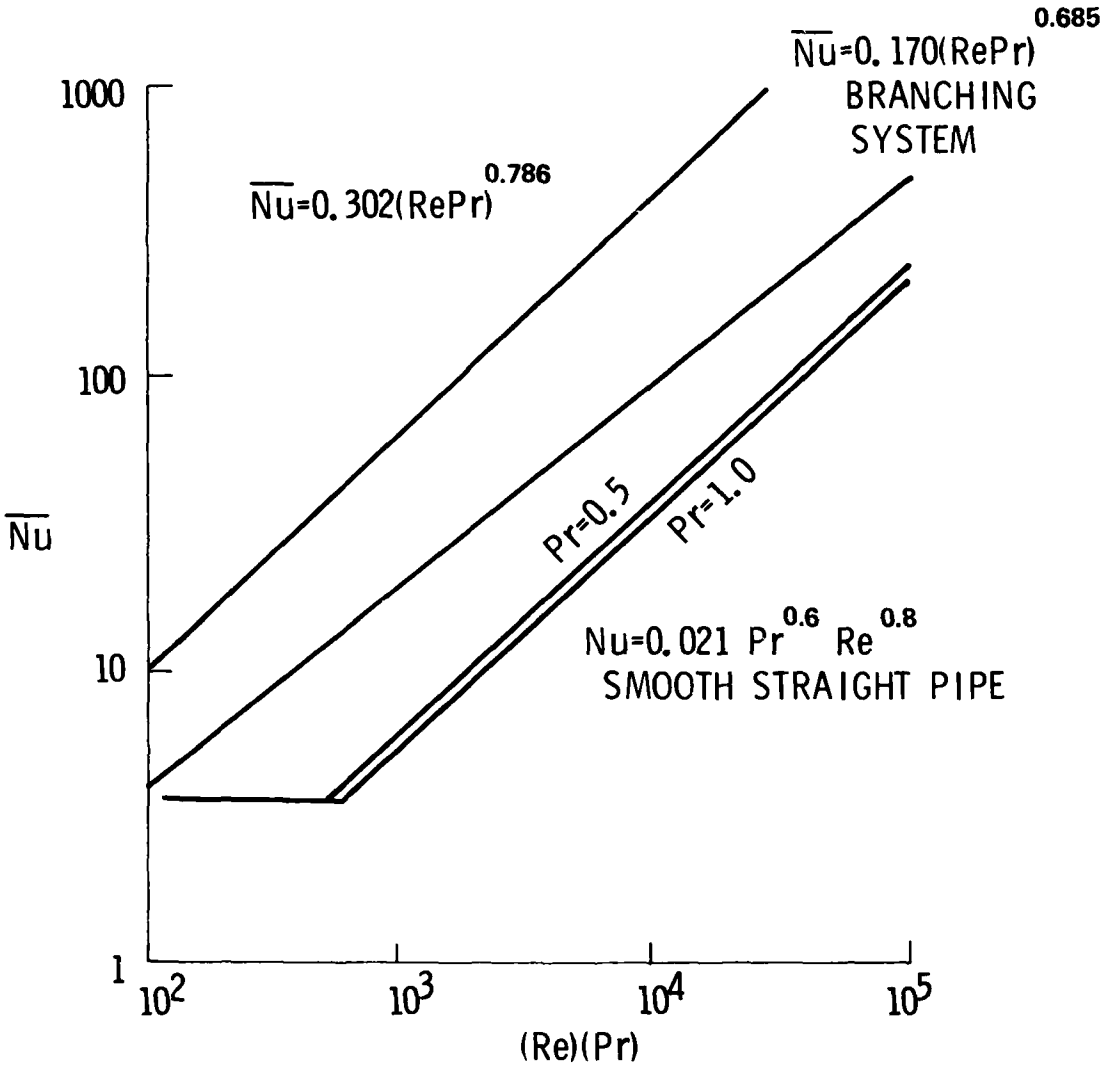

FIGURE 3: HEAT TRANSFER CHARACTERIZATIONS FROM PAST STUDIES OF LOWER RESPIRATORY TRACT (FROM JOHNSON [26])

It was necessary in this study, to verify or modify the above desired relationships in an expiratory flow direction using the same model. Mass transfer coefficients are then derived from the above relationships using the Chilton-Colburn j-factor analogy. It was additionally necessary to derive heat and mass transfer coefficients for the upper respiratory tract. These were determined experimentally from a cast of the upper respiratory airways of a human cadaver. Heat and mass transfer coefficients are derived in both the oral and nasal breathing modes. These two relationships are compared to quantify the relative effectiveness of these two respiratory passageways.

Throughout the experimental recordings, two fundamental assumptions have necessarily been made in the modeling efforts.

a) heat transfer characterizations in the human respiratory system using quasi-steady flow are representative of the actual unsteady flow state of cyclic breathing and

b) heat transfer characterizations from physical models of the human airways having constant wall temperatures are applicable to the conditioning processes in the living system.

The use of these assumptions has widespread precedence and justifying evidence in past flow characterization studies [17, 25, 38, 53, 56]. These assumptions and rationales for their use are discussed in Appendix A.

Following the experimental phase of this study a mathematical model of the human respiratory system is introduced. When used in conjuction with the derived relationships for heat and mass transfer in the upper and lower

respiratory tracts, regional airway temperatures and water vapor contents and expiratory temperatures under varying ambient conditions can be determined.

An additional utilization of this model would also provide a new analytical tool for the investigation of the controversy surrounding the use of the respiratory tract in active surface rewarming and/or as a region of supplemental heating. Harrison, Hysing, and Bo [28] reported that the effectiveness of the respiratory tract is limited as a means of inducing body cooling for surgical purposes at 1 ata. (Body cooling rates of 1.1°C/hr obtained by cooling with cold $He-O_2-CO_2$ inspiratory mixes was considered not rapid enough for surgical needs). However, it was suggested that it may have application for adding supplemental heat in high pressure environments. Lloyd, Conliffe, Orgel, and Walker [29] have proposed an apparatus which features inhalation rewarming that has been used as an ancillary first aid treatment of hypothermia victims in hill climbing in Scotland. Hayward and Steinman [30] have used a similar apparatus in comparative investigations of inhalation and immersion rewarming. They claim that although no significant difference in core temperature rise is seen in these experiments, rapid esophageal temperature increases are seen with inhalation rewarming. They argue that this temperature rise is closely related to the heart and great vessel temperature which would indicate a reduced chance of ventricular fibrillation when using this method. Although an investigation of the merits of these arguments are beyond the scope of this study, the model will allow a good estimation of the quantity of heat which can feasibly be transferred to the body during inhalation warming and/or supplemental heating under various environmental conditions.

In the next chapter, the anatomy and functions of the human respiratory tract will be discussed briefly to explore the necessary considerations in modeling this living system. Model fabrications and testing will be discussed in detail in Chapters III and IV, followed by an analysis of the test results in Chapter V. Simple analytical models will be utilized in Chapter VI to show several methods in which the results of this investigation can give meaningful information concerning the heat and mass transfer in the human airways at hyperbaric conditions. A liberal use of Appendices will be made to describe supporting sub-investigations to most effectively streamline the main study.

CHAPTER II

THE RESPIRATORY SYSTEM: DESCRIPTION AND FUNCTIONS

The human respiratory tract serves many functions other than its primary role as a passageway to conduct inspired and expired gases to and from the gas-exchanging surfaces in the lungs. In addition, it is instrumental in other important functions--gas filtration, producing voice sounds, chemically monitoring inspired gases, and warming and humidifying respiratory gases [15].

As a filter, the air passages rid inspired gases of aerosol particles prior to reaching the delicate alveoli. This is accomplished through the design of the airway shape. Continual turns and branches in the airway passage cause particulate matter to be propelled to the walls where they are trapped by mucus coating the air passage epithelium. Paddling motion of microscopic, hairlike structures, called cilia, push the dirt-laden mucus of the upper passages down into the throat and upward from the lungs into the throat thereby maintaining a clean air passageway.

Additionally, particulate matter in the nasal passages and the lungs are cleared, respectively, through sneeze and cough reflexes. These reflexes are additional protective mechanisms, triggered by tiny nerve endings in the respiratory tract, to rid the air passageways of irritants in the air. Similar nerve endings just inside the nasal cavity also serve as the first line of defense against our breathing contaminated air. Very sensitive to odors,

these nerve endings alert us early to noxious gases which may be damaging to the lungs.

Perhaps of even greater importance to the defense of the alveoli is the temperature and humidity conditioning of inspired gases by the respiratory tract. This conditioning capability has been demonstrated by numerous investigators in both extreme hot and extreme cold climates [74]. One early documented investigation in 1775 was conducted by Dr. Charles Blagden of the Royal Society of London. He and three colleagues exposed themselves to a 150°F dry environment for 20 minutes without apparent ill effects to their respiratory systems. More recently, a student of the University of California at Los Angeles volunteered to remain in a laboratory enclosure with the internal air at 115°C. Even though the delicate alveoli would have been severely damaged during only a few minutes at this temperature, this student was capable of remaining a full 26 minutes before he voluntarily terminated his exposure [74].

These and many other investigations previously discussed clearly demonstrate evidence of temperature and humidity conditioning capabilities of the respiratory tract. A look at the physical makeup of the air passageways helps us to understand this conditioning capability.

Physical Description

During normal breathing through the nasal passages, the inspiratory gas first passes through a bony entrance region of the upper respiratory tract, Figure 4. This region composed of the turbinates, nasopharynx, septum, and

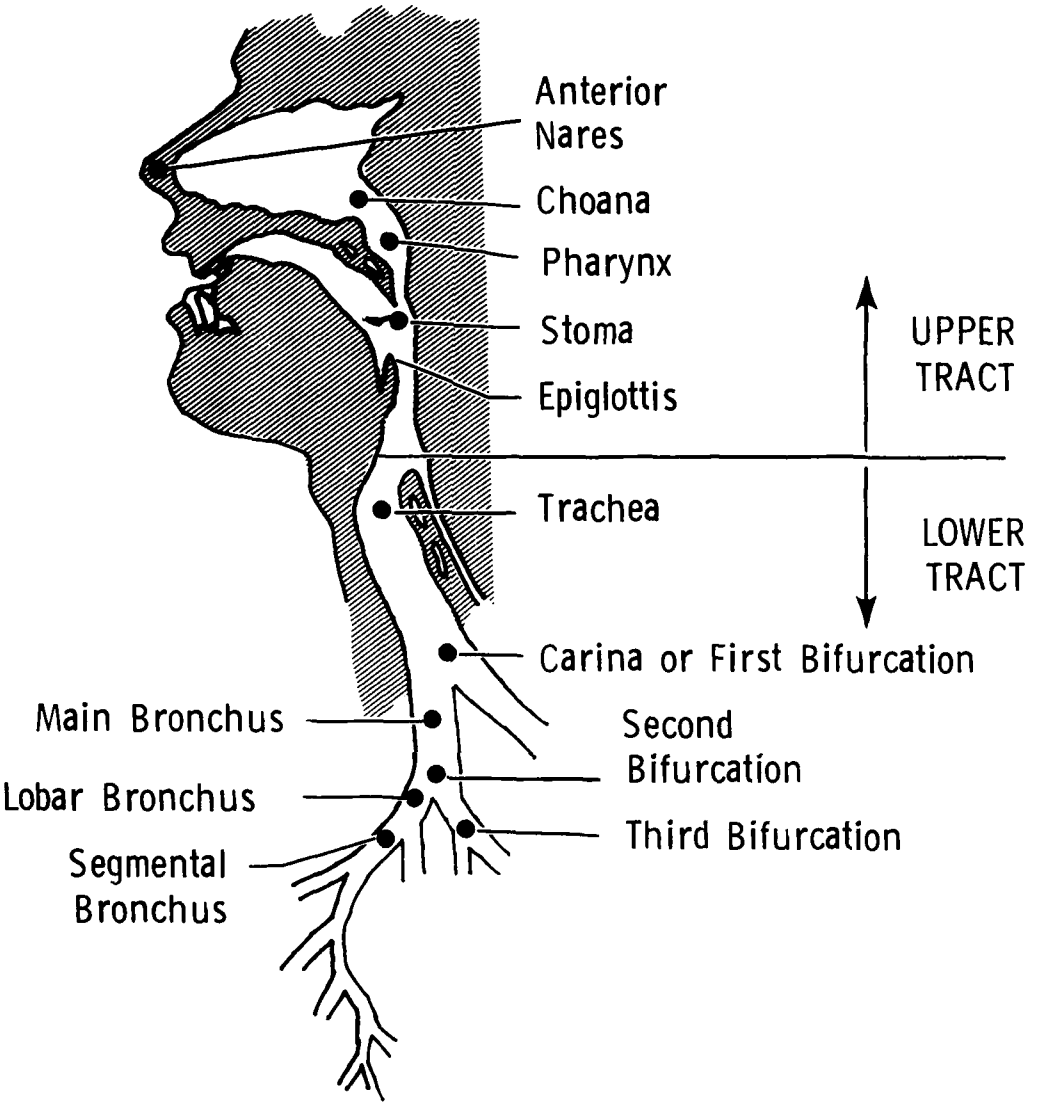

FIGURE 4: HUMAN RESPIRATORY TRACT

choana, serves as an excellent gas conditioning space for warming and humidifying the inspired gas. Up to 160 cm^2 of mucous membrane surface [15] in this upper portion provides a good surface area for these conditioning processes during inspiration, and the heat and moisture recovery during expiration. Continuing its travels past the stoma, the inspiratory gas conditioning continues. Under normal atmospheric conditions, the inspired gas will reach within 2 to 3 percent of body temperature and come to within 2 to 3 percent of full saturation with moisture prior to reaching the trachea [5].

When the gas is inspired through the mouth, the conditioning process will be less efficient due to the reduced surface contact area in the oral passage. However, under normal atmospheric conditions, it is doubtful that significant conditioning occurs beyond the third or fourth generation of branching in the lower respiratory tract [17].

The lower respiratory tract, composed of a system of multibranched tubes as represented by Weibel's morphological model (Table 1), is capable of continuing the gas warming and humidification during more extreme ambient conditions. This ever-branching system ensures the completion of the inspiratory gas heating and humidification prior to reaching the alveoli. In so doing, this natural air conditioning system protects the lungs from extremes in environmental temperature and humidity.

The upper and lower tract epithelium, composed of ciliated columnar cells contain mucous secreting glands. The wavelike motion of the hairlike cilia provide a continual fluid layer along the airway walls [15]. This fluid, called mucus, is a viscoelastic semi-solid substance of gelatinous consistency.

TABLE 1

WEIBEL'S MORPHOLOGICAL DIMENSIONS OF THE HUMAN LUNG*

Generation Z	Number Per Generation n(z)	Diameter D(z) cm	Length L(z) cm	Total Cross Section cm^2	Total Volume cm^3	Accumulative Volume cm^3
0	1	1.8	12.0	2.54	30.50	30.5
1	2	1.22	4.76	2.33	11.25	41.8
2	4	0.83	1.90	2.13	3.97	45.8
3	8	0.56	0.76	2.00	1.52	47.2
4	16	0.45	1.27	2.48	3.46	50.7
5	32	0.35	1.07	3.11	3.30	54.0
6	64	0.28	0.90	3.96	3.53	57.5
8	256	0.186	0.64	6.95	4.45	65.8
9	512	0.154	0.54	9.56	5.17	71.0
10	1,024	0.130	0.46	13.4	6.21	77.2
11	2,048	0.109	0.39	19.6	7.56	84.8
12	4,096	0.095	0.33	28.8	9.82	94.6
13	8,192	0.082	0.27	44.5	12.45	106.0
14	16,384	0.074	0.23	69.4	16.40	123.4
15	32,768	0.066	0.20	113.0	21.70	145.1
16	65,536	0.060	0.165	180.0	29.70	174.8
17	131,072	0.054	0.141	300.0	41.80	216.6
18	262,144	0.050	0.117	534.0	61.10	277.7
19	524,288	0.047	0.099	944.0	93.20	370.0
20	1,048,576	0.045	0.083	1,600.0	139.50	510.4
21	2,097,152	0.043	0.070	3,220.0	224.30	734.7
22	4,194,304	0.041	0.059	5,880.0	350.00	1,084.7
23	8,388,608	0.041	0.050	11,800.0	591.00	1,675.0

*From Weibel [27]

Mucoid sputum is reported to be 95% water and contains saliva with many bacterial enzymes [38]. The nasal mucosae continually regenerates itself with new mucus secreting and ciliated cells while shedding dead cells. This process occurs following trauma or during normal cell turnover, with a normal cell life in the human mucosae of 7.5-9 days [38].

Gas Flow in the Lower Tract

Gas flow in a branching system representative of the lower respiratory tract has been characterized extensively by researchers at Imperial College in England [53, 54, 55, 56] using pipe models and actual castings of the lower airways. Complex secondary flows were shown to be generated downstream of each succeeding bifurcation as a result of the inertial forces of the fluid stream. A complete summary of these flow studies is given by Johnson [26].

All of the experimental flow studies conducted in the past have utilized quasi-steady flow through models or castings of the airways. This procedent will be followed in the experimentals phase of this research with justifications outlined in Appendix A.

Gasflow in the Upper Tract

With the exception of periods of heavy exercise or chronic nasal obstructions, most humans are preferentially nasal breathers. This appears paradoxical since nasal breathing requires about 50 percent more effort than mouth breathing under normal conditions [38]. Fortunately for us, this instinctive behavior is followed due to the excellent advantage we apparently receive from the point of view of respiratory gas conditioning and particle filtration. For infants, Polgar [18] indicated that nasal breathing, except during crying, is compulsory and can lead to death if nasal obstructions are not detected early. This obligate nose breathing of infants may in fact be facilitated by lower nasal flow resistance than oral flow resistance [19].

A look at the anatomy of the nasal passages, Figures 5 and 6, will clearly demonstrate how its structure best fits the function of conditioning and filtering our breathing gases. A relatively large cross-sectional area in the main nasal passage is broken into narrow widths by the nasal septum, dividing the nasal airway into two, and further by the folds of the turbinates. This assures maximum contact between the respiratory gas and the mucosal surfaces.

During mouth breathing, as must be employed when using many diving apparatus, the resulting airway can be maintained nearly as efficiently in filtration as the nose by positioning the tongue close to the palate [38]. However, during heavy exercise, inspiration will usually occur through a wide open oropharynx, with most of the conditioning and filtration of the breathing gas lost.

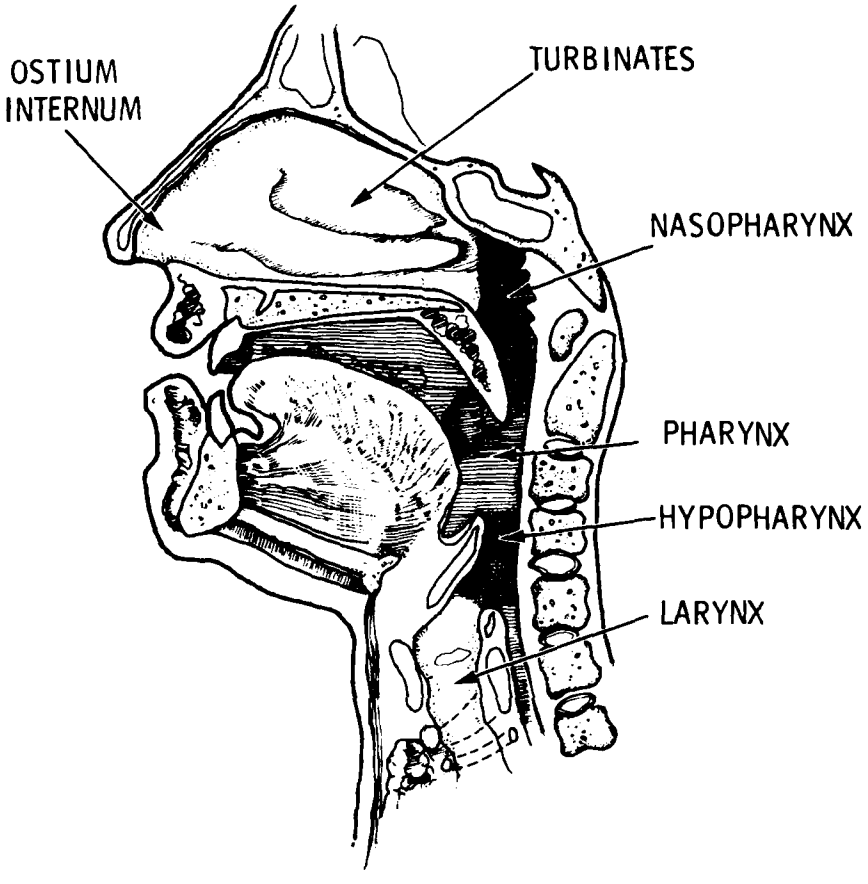

FIGURE 5: UPPER RESPIRATORY TRACT: ORAL AND NASAL PASSAGEWAYS

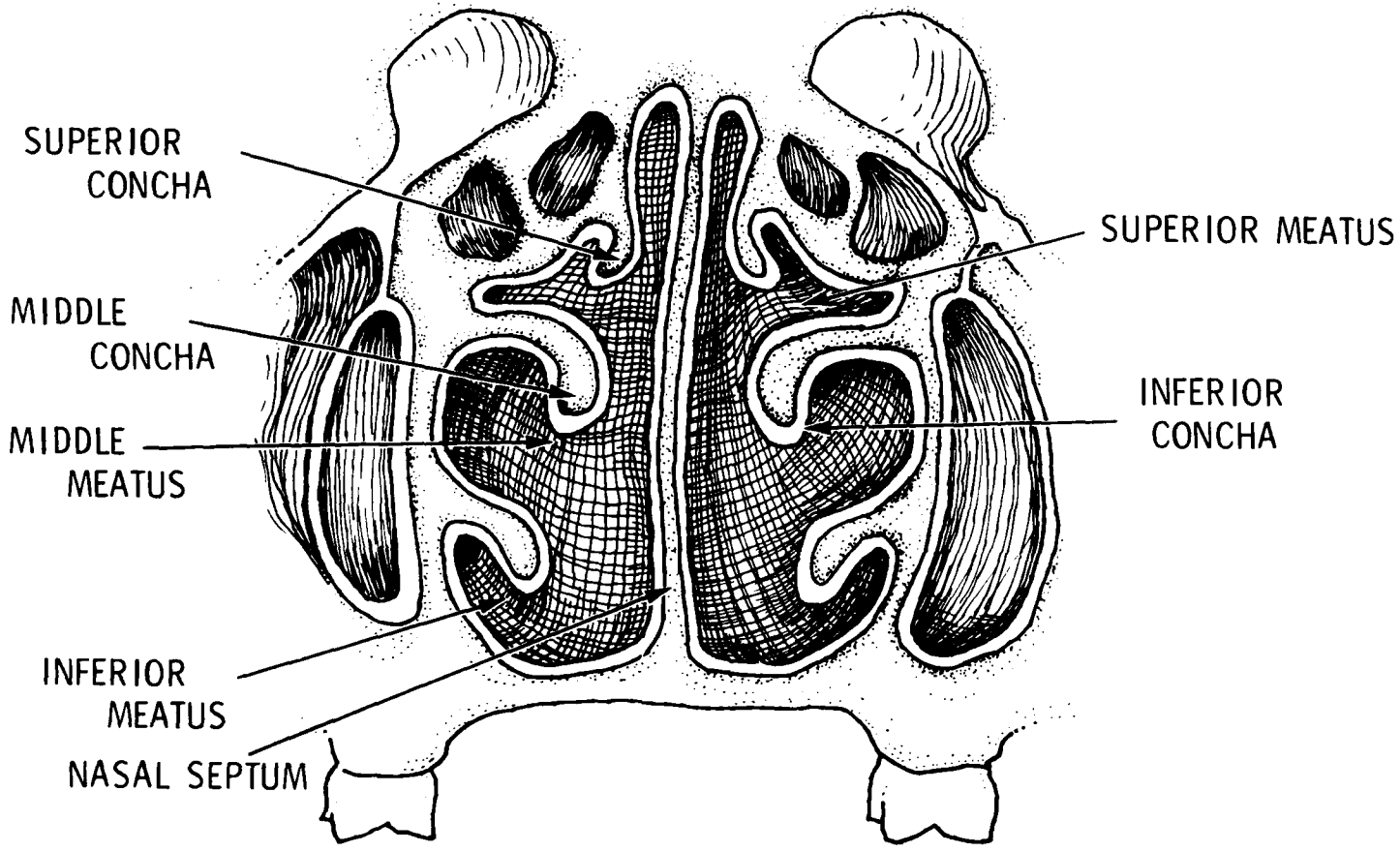

FIGURE 6: FRONTAL SECTION THROUGH NASAL CAVITIES

During mouth breathing, very little air passes through the nose due to the relatively high nasal resistance [15].

Very little is known about the airflow through the oral cavity during heavy exercise. However, thanks to the efforts of Proctor and Swift [38] the nature of airflow in the nasal passages has been clearly demonstrated through the use of clear polyester casts. In some of their studies, waterflow (flow-rates chosen to maintain appropriate Reynolds number) was used to provide streamline markings with dye injections at various locations in the nasal cavity. This method allowed a visualization of the direction of flow, and also indicated regions of laminar and turbulent flow. Figure 7 summarizes these flow visualization studies during inspiration. Note that most of the flow in the main nasal cavity appears to pass between the middle meatus during inspiration. A small portion of the incoming flow travels upward to the olfactory area to join a standing eddy current. This eddy current is possibly optimum to sample the gas for toxic smells without damaging the olfactory mucosa. By contrast to this inspiratory flow behavior, they saw roughly equal flow along the main nasal passage during expiration with complete flushing of the olfactory area.

Table 2 summarizes the airflow behavior during inspiration for their model studies at a half-passage flow rate of 12.5 liters/min. Note here that even for flow rates approximating that of a resting subject, turbulence persists in the flow stream beyond the ostium internum. This mixing behavior aids in the conditioning capability of the upper respiratory tract.

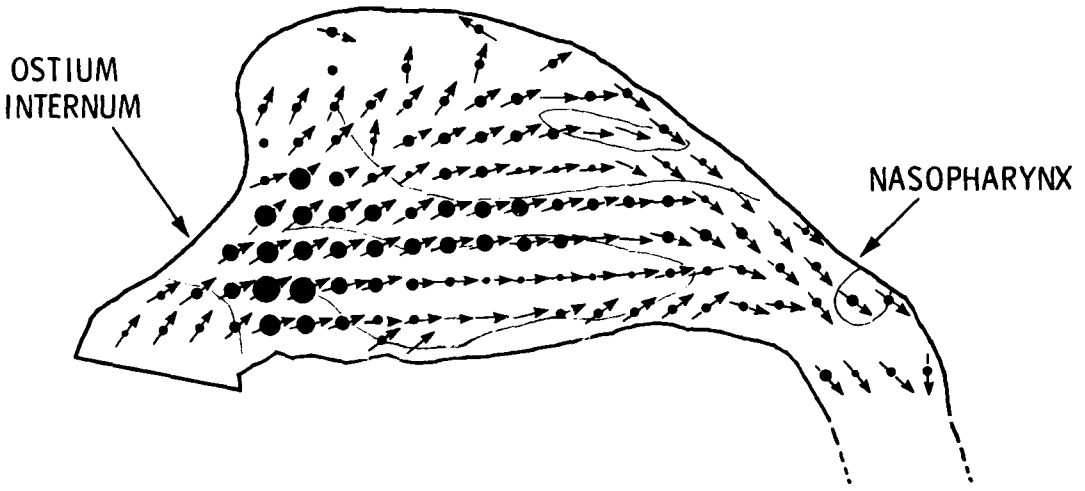

FIGURE 7: LINEAR VELOCITY OF THE INSPIRATORY NASAL AIRFLOW AS DERIVED FROM MODEL STUDIES. THE NOSTRIL IS TO THE LEFT. THE SIZE OF EACH DOT INDICATES VELOCITY AND THE ARROW DIRECTION. (REPRINTED FROM RESPIRATORY DEFENSE MECHANISMS [38] PART 1, PG 80, BY COURTESY OF MARCEL DEKKER, INC.)

TABLE 2

FLOW BEHAVIOR IN THE UPPER AIRWAY DURING INSPIRATION AT A RESTING HALF FLOW RATE OF 12.5L/MIN*

Location	Total Area (cm^2)	Flow Velocity (m/sec)	Flow Type
Nostril	1.8	2.3	Laminar
Ostium Internum	0.64	6.5	Laminar
Main Nasal Cavity	5.5	2-3	Turbulence
Nasopharynx	3-5	4	Turbulence

*From Proctor and Swift [38]

They also found that during quiet breathing of normal subjects, the resistance of the nasal passage represents approximately one-half of the entire respiratory tract resistance. However, essentially no pressure change was recorded beyond the first 1.5 cm of the main nasal chamber; i.e., just beyond the ostium internum. Thus, the entire transnasal pressure drop is found in the first 1.5 cm of the airway, with the remainder of the passage acting essentially as a plenum. In fact, the ostium internum region has been found to act as a built-in flow-limiting device. When inspiratory airflow reaches 1 to 1.25 litre/sec, this portion of the airway tends to collapse and any additional inspiratory force produces no further airflow. Beyond this flow requirement, mouth breathing becomes a necessity.

One further note must be made when considering the flow characteristics in a single nasal passageway. There appears to be a wide range in nasal airflow resistance between normal individuals and in any one individual from time to time. Many factors have been identified which influence this varying nasal resistance. Among them:

a. Cold air increases nasal resistance and decreases peak airflows [20].

b. Exercise reduces nasal resistance [21, 22].

c. Various noxious gases in the environment increase nasal resistance.

In addition, normal individuals are known to have a systematic variation in the nasal resistance first in one side of the nose and then the other [23]. This phenomena, known in the rhinological literature as the "nasal cycle" is thought by some to serve as a built-in safety mechanism to assure that neither side of the nose is continuously burdened with conditioning and filtering the breathing gas. Whatever the function and mechanism may be for this cyclic variation in nasal resistance, it certainly complicates any attempt to characterize the gas flow and conditioning capability of the nasal passageway through the use of a single cast model. However, by characterizing the heat and mass transfer mechanisms in models based on mean nasal resistance values of numerous in vivo measurements, nominal transfer characteristics can be identified. Such as approach was followed in this research. It remains to be explored the effects of variations in nasal resistance values on the heat and mass transfer mechanisms in the human airways.

CHAPTER III

LOWER RESPIRATORY TRACT

EXPERIMENTAL APPARATUS, INSTRUMENTATION, TESTING

As reported earlier, the heat transfer characteristics of the lower respiratory tract were recorded in previous investigations during simulated inspiration flow studies [17, 25]. Rigid pipe models were used in these past studies to simulate a typical three branch "unit" in the branching tree system of the lower respiratory tract. These tests confirmed that a single relationship could be found which described the heat transfer characteristics of the lower respiratory tract over a wide range of breathing gas mixtures and ambient pressures. A significant finding from these past studies was that further characterizations of this system could be made at the surface (1 ATA) which properly described its performance at hyperbaric conditions.

The experimental effort during this investigation of the lower tract was conducted to further characterize this branching system in the exhalation flow mode. Based on the findings of the previous studies, all tests in this investigation were conducted at 1 ATA to facilitate the test procedure and data acquisition. Data from this and the previous studies are used to complete the characterization of the heat transfer in the lower respiratory tract during the entire breathing cycle.

Model Description

The rigid pipe model utilized in one of these previous investigations [25] served as the test apparatus in this continued study. This model of the trachea and the first two branchings of the lower respiratory tract was made using schedule 40 and 80 black iron pipe. Scaling for the model was made according to the morphometric data collected by Weibel [31] for the adult human lung as seen in Table 1 of the previous chapter. An overall scale, based on Weibel, of approximately 2:1 was chosen to allow easy entrance into a man-rated chamber for hyperbaric studies during the previous studies. An angle of 60 degrees was used for both branchings based on the measurements made by Horsfield and Cummings [32]. A schematic of this model is shown in Figure 8 with the branch and data locations identified. Sixteen data taps were positioned as seen in Figure 8 so that horizontal and vertical temperature profiles could be obtained near the entrances and exits of each branch.

The pipe model was mounted inside a watertight plywood box in which the model entrance and second branches penetrate. This box provided a constant temperature water bath which surrounded the model to provide a uniform and constant wall temperature. The water bath was maintained at a preset temperature with variations of less than 1°C by means of a submersible heater featuring automatic feedback control (FTS Systems, Inc.). A laboratory stirrer (Cole-Parmer Model 4554) was used to maintain continual water movement around the heat coils, thereby minimizing temperature variations.

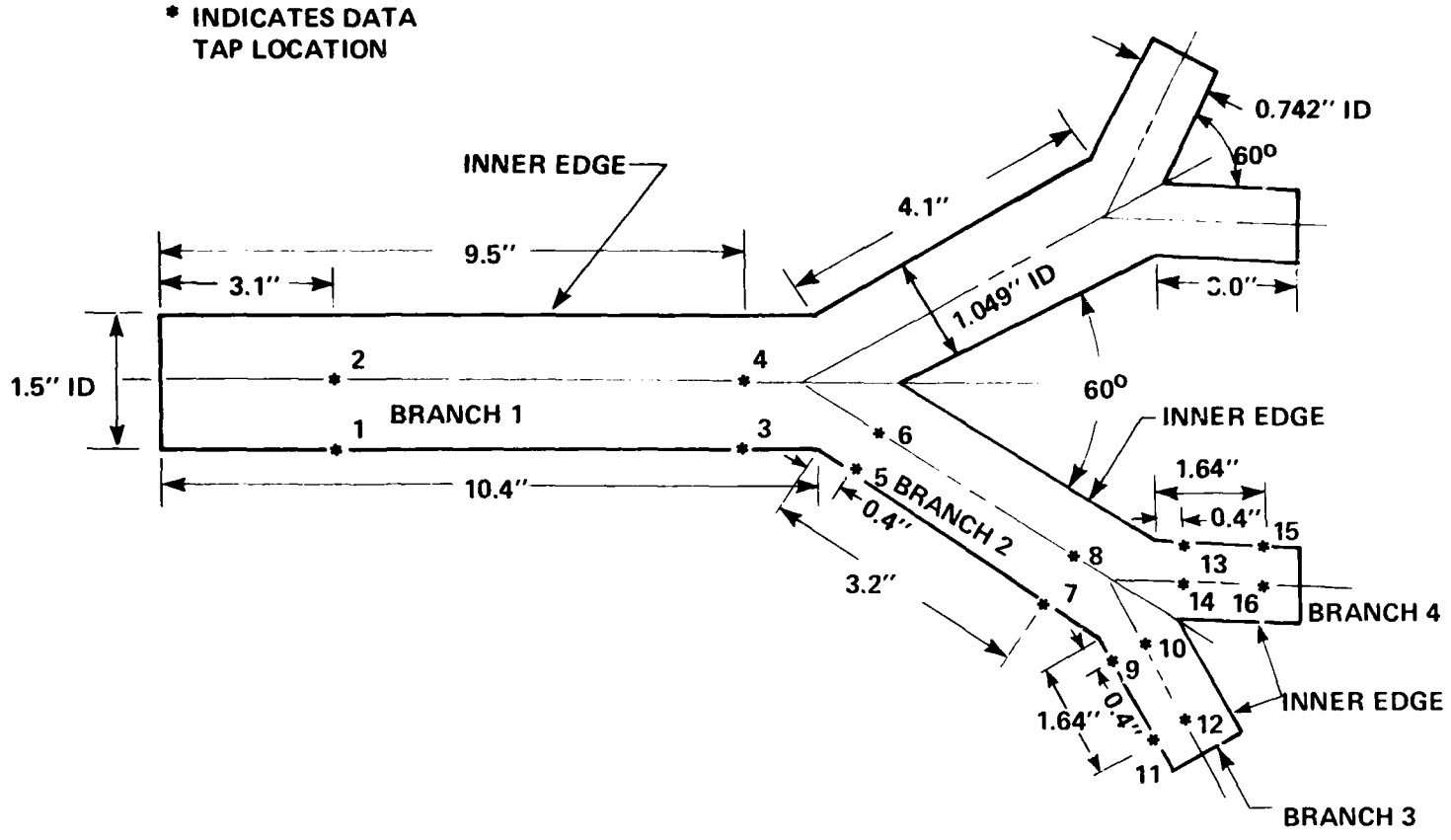

FIGURE 8: MODEL DESCRIPTION AND DATA TAP LOCATION:
LOWER RESPIRATORY TRACT

During each series of investigations, the gas under study was drawn through an entry pipe into branch 1, and exited through the four smallest branches into a plenum (for expiratory studies the flow path was reversed). This plenum ensured equal static pressures at the ends of the four small branches, simulating the intrapleural pressure in the lung. A commercial centrifugal blower (McMaster-Carr No. 1954N11) provided the gas movement through the model by connection of the model exhaust to the blower intake.

Instrumentation and Data Acquistion

Flow and temperature measurements required to characterize the heat transfer characteristics of the lower respiratory tract were obtained and stored by means of an automated data acquisition system. This system provided a minimum time duration for temperature profile measurements within the model, thereby minimizing possible variations in the desired ambient conditions during these measurements.

a. Temperature Measurement. Thermocouple probes shown in Figure 9 were used to measure the temperature profiles (radial) at each data tap location. Each thermocouple junction was made using 30 gauge copper and constantan wire with nylon insulation. A rosin core solder was used to make the junction surfaces as reflective as possible to minimize radiation effects from the surrounding model walls. The exposed wire leading to each thermocouple junction was coated with an insulating varnish to reduce chances of electrical short circuits with the probe casing. The thermocouple wire was then threaded through a 3-inch length of stainless steel capillary tubing (0.12 cm ID/0.17 cm OD) until the junction extended approximately 2 cm out

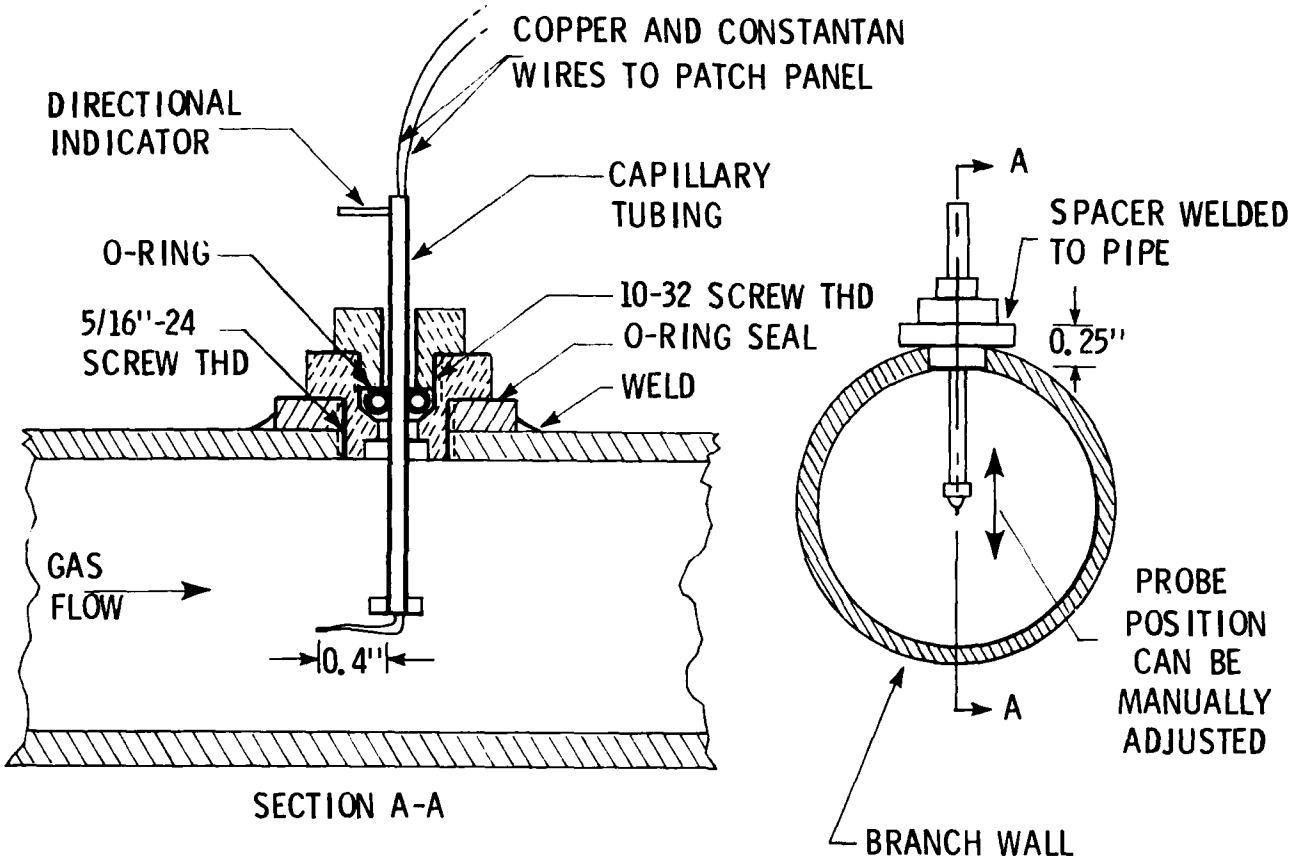

FIGURE 9: THERMOCOUPLE PROBE DESIGN

of the tubing. The exposed wires were bent allowing the junction to extend 1 cm upstream from the capillary tubing axis. Electrical potting resin provided a waterproof seal between the thermocouple wire and the inside of the capillary tubing. This probe design was found to be highly dependable for these temperature profile measurements, and showed readings quite comparable to those obtained with a hot film anemometer. Its reliability, durability, and low cost made its use desirable over anemometer or thermistor probes.

Each probe was inserted into an O-ring sealed mounting assembly which provided a dynamic seal, allowing the probe to move freely across the branch diameter. The output voltages from each probe were relayed through an electronic ice point (Omega Model MCJ) prior to their connection to the data acquisition system.

The ambient and water bath temperatures were each recorded using a Yellow Springs YSI701 thermistor. Their outputs were each processed by a Sire 700 signal conditioner prior to entering the data acquisition system.

b. Flow Measurement. A laminar flow element (Meriam Model 50 MC2-4) was placed in series wih the pipe model to record gas volumetric flow rates. The pressure differential generated by the LFE was monitored continually by a Statham differential pressure transducer (Model PM96TC). This signal was then processed by an HP 8805B carrier amplifier prior to being recorded by the data acquisition system.

c. Data Acquisition System. The data acquisition system is represented schematically in Figure 10. The heart of this system consists of a HP 9830A

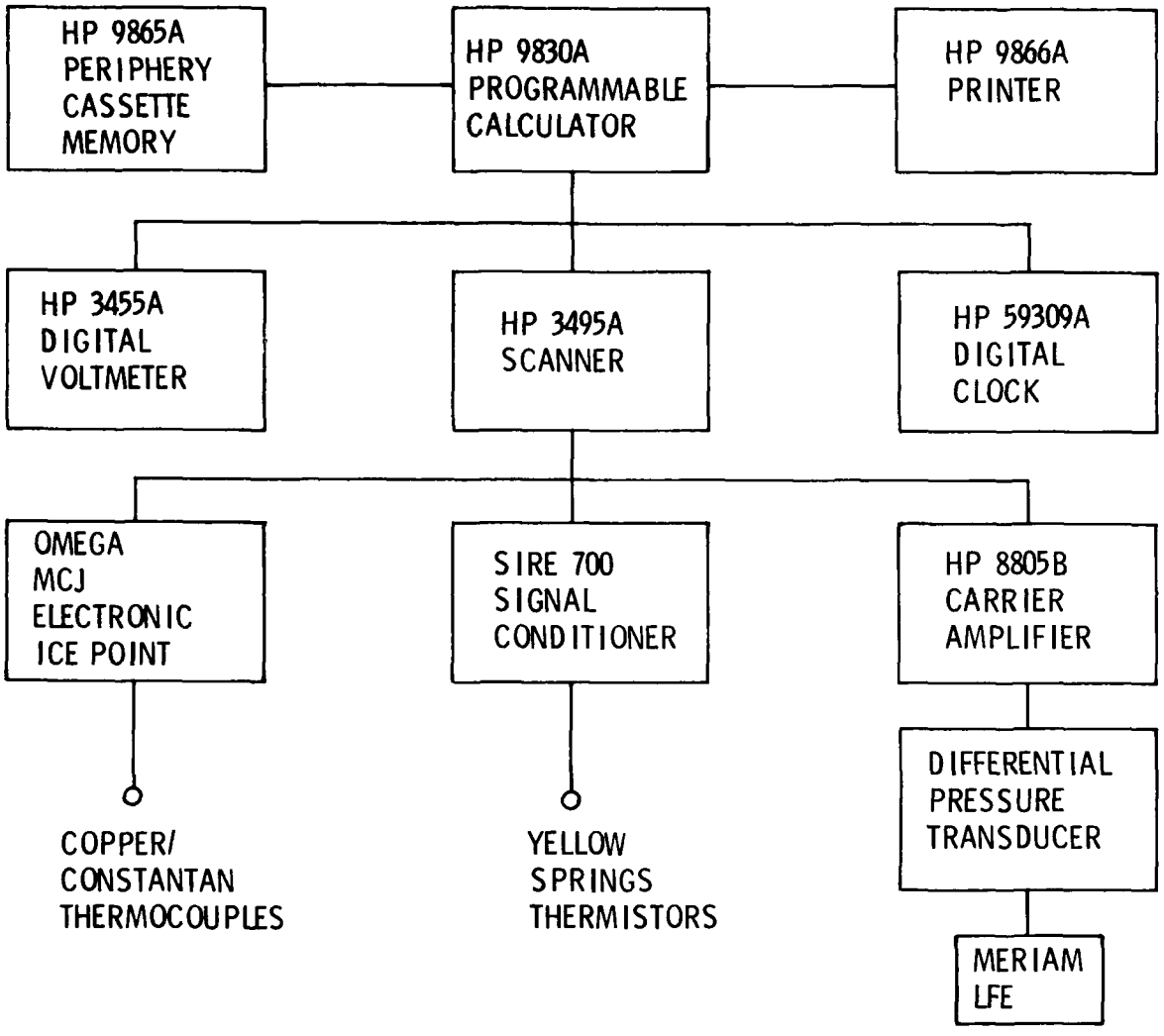

FIGURE 10: RESPIRATORY HEAT LOSS DATA ACQUISITION SYSTEM

programmable calculator with an interface bus system (HP-1B) which allows two-way communication between measurement and recording instruments and the calculator. Data collection was initiated by the calculator's command to the scanner (HP 3495A) to scan all data channels successively. While this scanning operation took place, a digital voltmeter (HP 3455A) was internally instructed to read the signal from each data channel and enter it into the calculator's memory bank. This procedure could be repeated as often as desired, and was programmed to trigger at a predetermined time interval as measured by a HP 59309A digital clock.

Once the data had entered the calculator's memory, it was processed for the determination of heat transfer characteristics. It was then printed (HP 9866A Printer) and stored for later retrieval on a periphery memory cassette (HP 9865A).

A photograph of the test setup and associated instrumentation is shown in Figures 11a and 11b.

Instrument Calibrations

Prior to the initiation of these tests, the digital voltmeter (HP 3455A) was calibrated in the Naval Coastal Systems Center calibration laboratory, a Type II facility, traceable to the National Bureau of Standards. All other instruments critical to the data acquisition during these tests were calibrated prior to each day's testing, and checked periodically throughout the day.

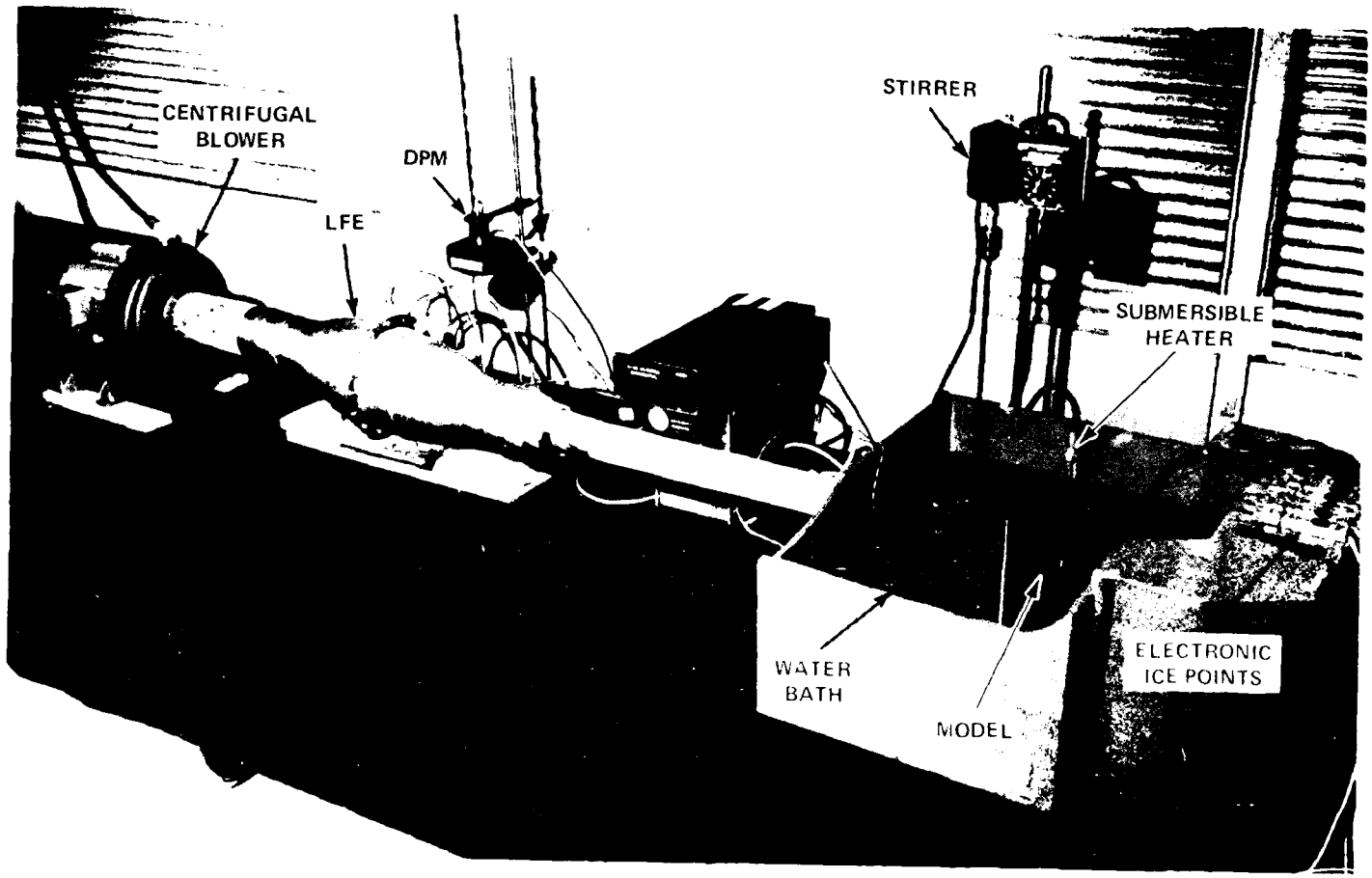

FIGURE 11a. TEST SETUP AND ASSOCIATED INSTRUMENTATION: MODEL FLOW SYSTEM

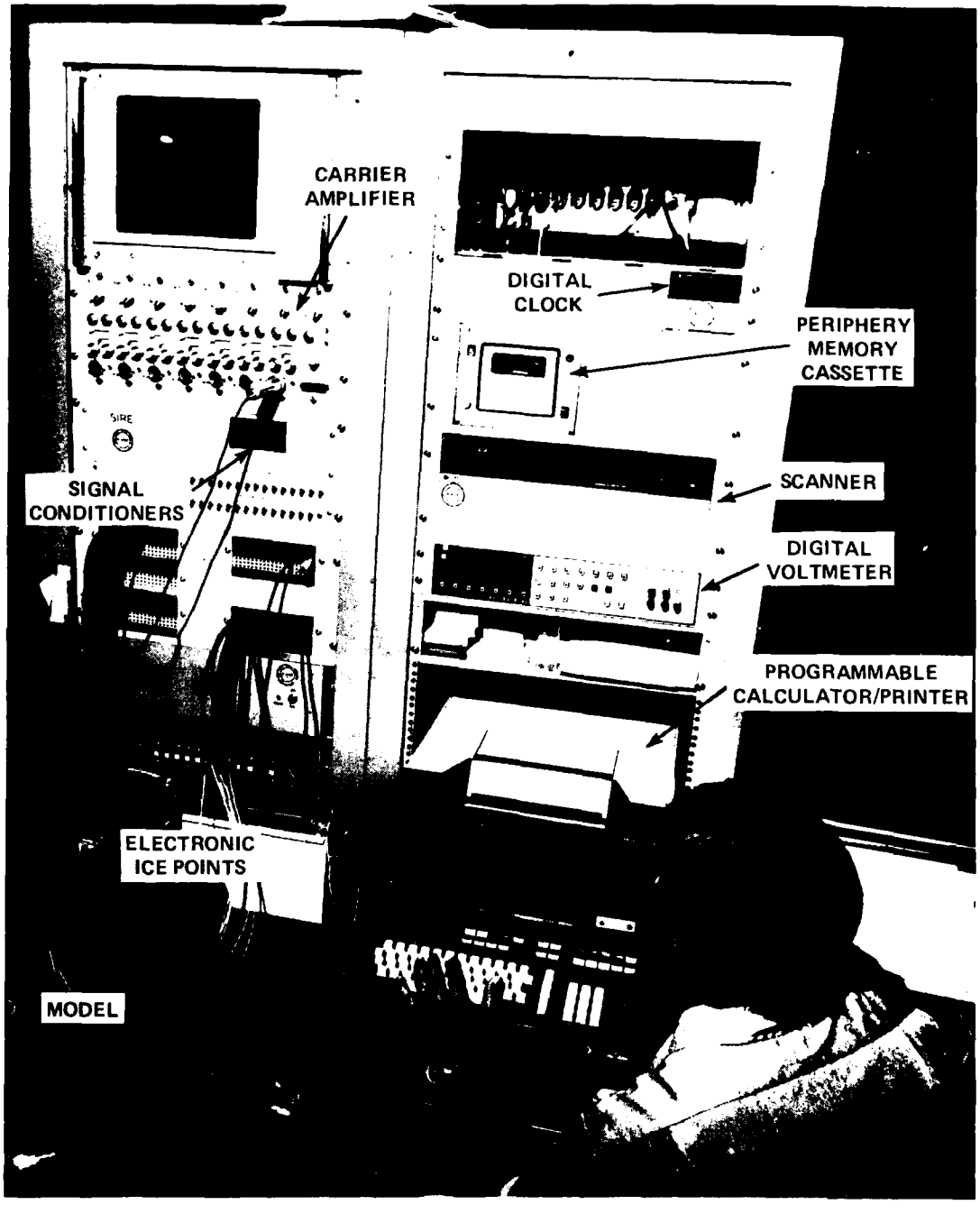

FIGURE 11b: TEST SETUP AND ASSOCIATED INSTRUMENTATION:
DATA ACQUISITION SYSTEM

a. Flow Measurement

The Meriam laminar flow element (LFE) depends for its accuracy and metering indication on the principles of laminar flow. A slight differential pressure is created by the insertion of a resistance element in the flowing stream. Due to the forced laminar behavior of the flow through this resistance element, the differential pressure follows a near linear relationship with flow*. The LFE is factory calibrated using air flow versus differential pressure at 70°F and 29.92-inch Mercury absolute. When the flow temperature and pressure are at other than calibrated conditions, corrected flow is obtained by application of the ideal gas relationship

$$\dot{V}_1 = \dot{V}_2 \cdot \frac{P_2}{P_1} \cdot \frac{T_1}{T_2}$$

or

$$\text{Corrected flow (LPM)} = \text{Measured flow (LPM)} \times \frac{29.92}{P_f} \times \frac{460+T_f}{(530)}$$

where:

P_f = actual inlet pressure, in of H_g

T_f = observed flow temperature , °F

The differential pressure transducer (DPM), used in this flow measurement, was calibrated against an inclined manometer and an electronic digigauge (Ashcroft 0-50 in H_2O) prior to each day's run, see Figure 12. A custom-made syringe having a hand crank screw mechanism was connected by tubing in parallel to the DPM and either the inclined manometer or the

---

*Complete linearity is not achieved due to the dynamic losses seen on entry to and exit from the resistance element.

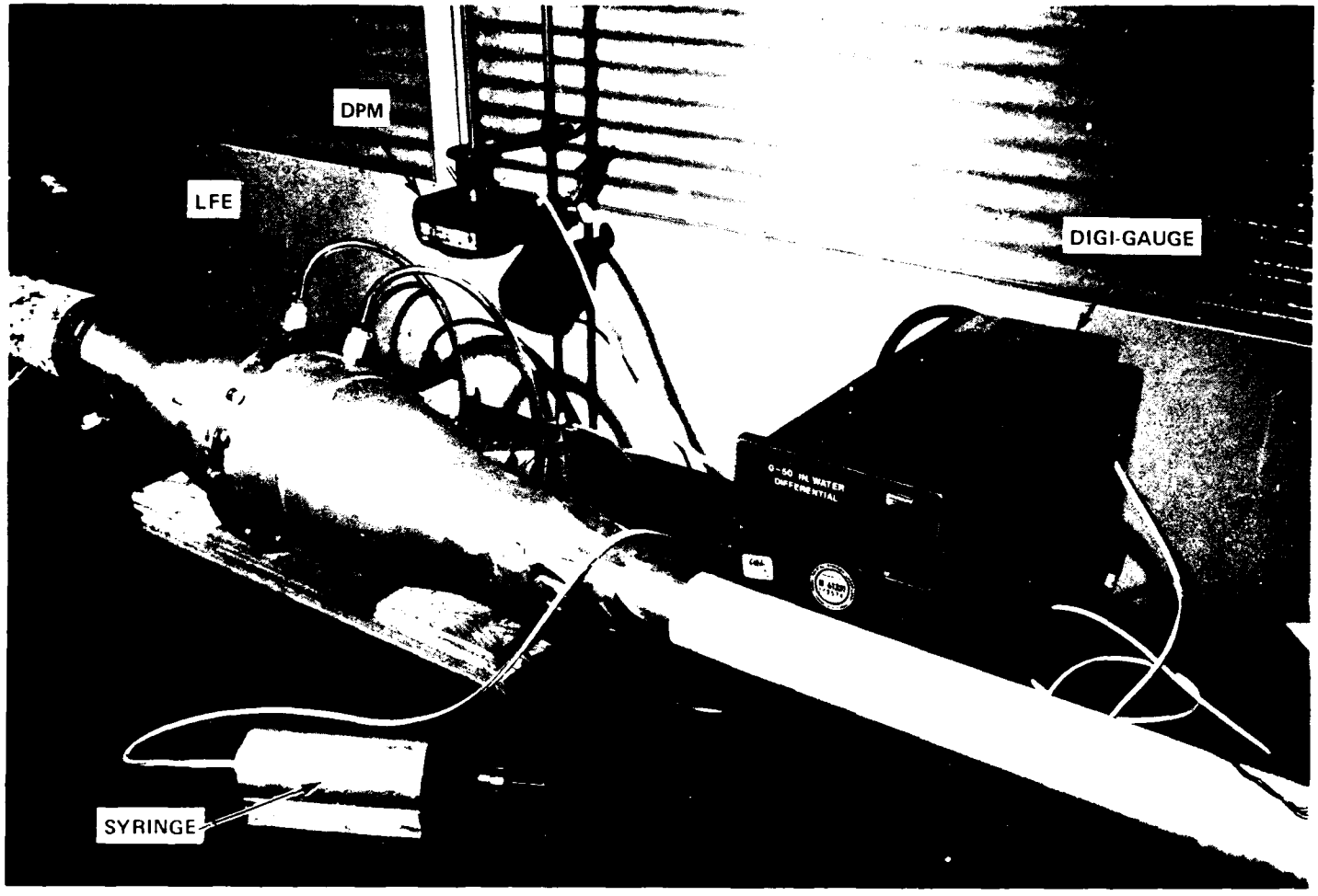

FIGURE 12: DIFFERENTIAL PRESSURE TRANSDUCER CALIBRATION AND FLOW MEASUREMENT

digi-gauge. By advancing the syringe plunger with the hand crank, a known pressure, as read on the manometer or digi-gauge, was applied to one side of the DPM. By allowing the other side of the DPM to remain open to ambient pressure, this differential pressure could be used in the DPM calibration. The gain and zero point were then set on the carrier amplifier to give a convenient voltage output at this pressure level.

Prior to each day's run, this zero point and gain setting was checked as described above to ensure their continued accuracy.

b. Temperature Measurement

The electronic ice point contains a self-compensating electronic circuit built into a standard female quick-disconnect. This system, Figure 13, incorporates a temperature sensitive element which is thermally integrated with cold junctions T2 and T3 inside the ice point reference. In this system, the emf generated by the ice point compensator is equivalent to that produced at the measuring junction at 0°C.

As the ambient temperature surrounding the cold junction T2 and T3 varies, a change in thermal emf is generated. This thermal emf induced into the circuit would create an error in the output unless otherwise compensated for. To accomplish this, an equal and opposite voltage is injected into the circuit automatically by a "compensating voltage generator" which in turn cancels out this error emf. This "compensating voltage generator" is temperature sensitive and produces a compensating emf that tracks the error signal over a wide ambient temperature range. The manufacturer specifies a compensation accuracy, for a reference temperature setting of 0°C, of ±½°C over a

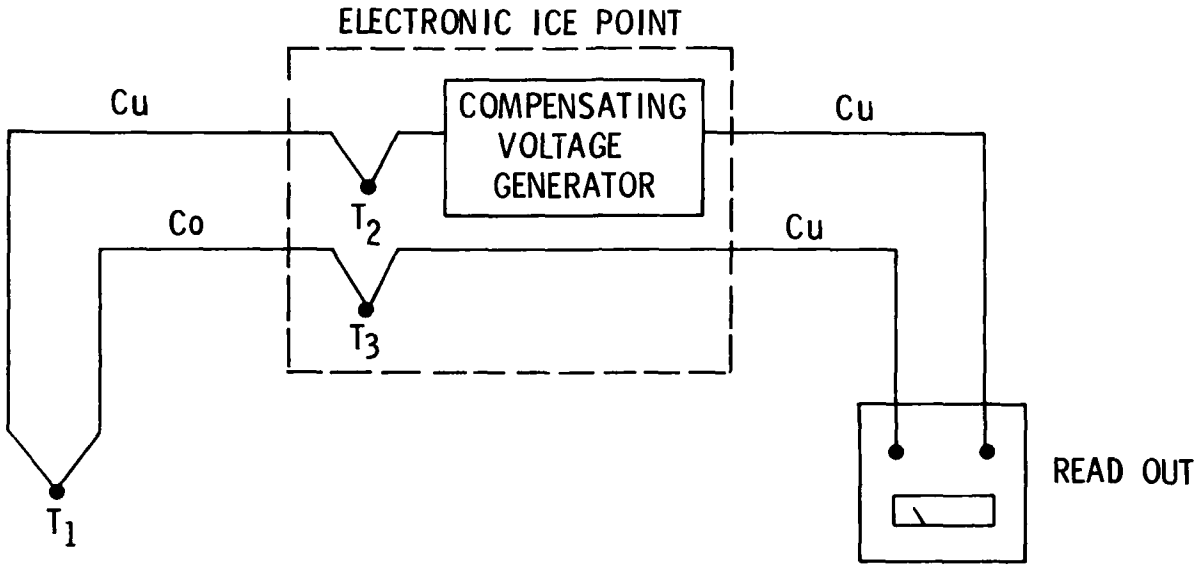

FIGURE 13: ELECTRONIC ICE POINT

temperature range of 15°C to 30°C [33]. To verify this accuracy, each thermocouple probe in series with the electronic ice point was immersed in a well-stirred ice bath while recording their emf's. All emf generated by these probes were within this specified accuracy.

Experimental Procedure and Results

Using the instrumentation scheme described earlier, temperature profiles were recorded at the entrance to branch 3 and 4 and the exit of branch 1 during expiratory flow studies, see Figure 8*. Eleven temperature points were recorded across the model diameter at each location, both vertically and horizontally. Typical temperature profiles are shown in Figures 14 through 18. These profiles are consistent with those recorded in previous investigations of inspiratory flow in pipe models of the lower respiratory tract having constant wall temperatures [17, 25]. As in the inspiratory flow studies, the temperature profiles throughout the model were seen to be the most asymmetric at the lower Reynolds number flows. This is due to the reduced flow stream mixing and secondary flows that exist at the lower Reynolds numbers. At the higher flow rates, near symmetrical temperature profiles were observed.

Likewise, higher model exit temperatures were observed at the lower Reynolds number values during these expiratory flow studies, as shown in Figure 19. This is due partly to the increased dwell time these gas flows

*Several preliminary tests were conducted in the inspiratory flow mode to first confirm the results of this test setup with those previously reported in Reference [25].

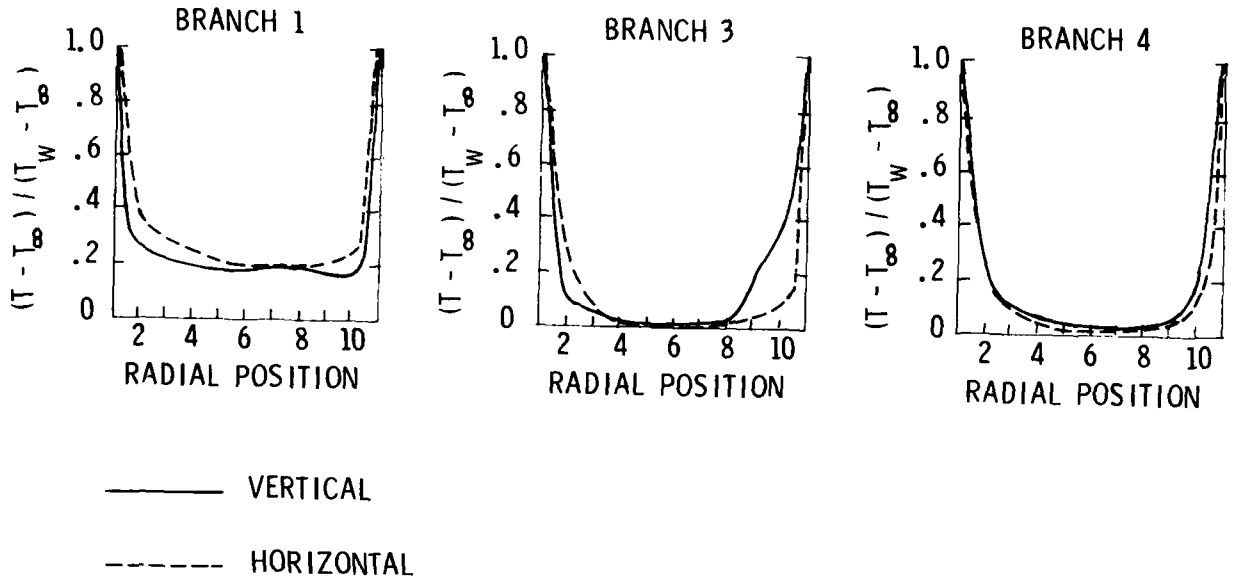

FIGURE 14: TEMPERATURE PROFILES AT VARIOUS LOCATIONS IN THE LOWER TRACT MODEL (RE=34,438)

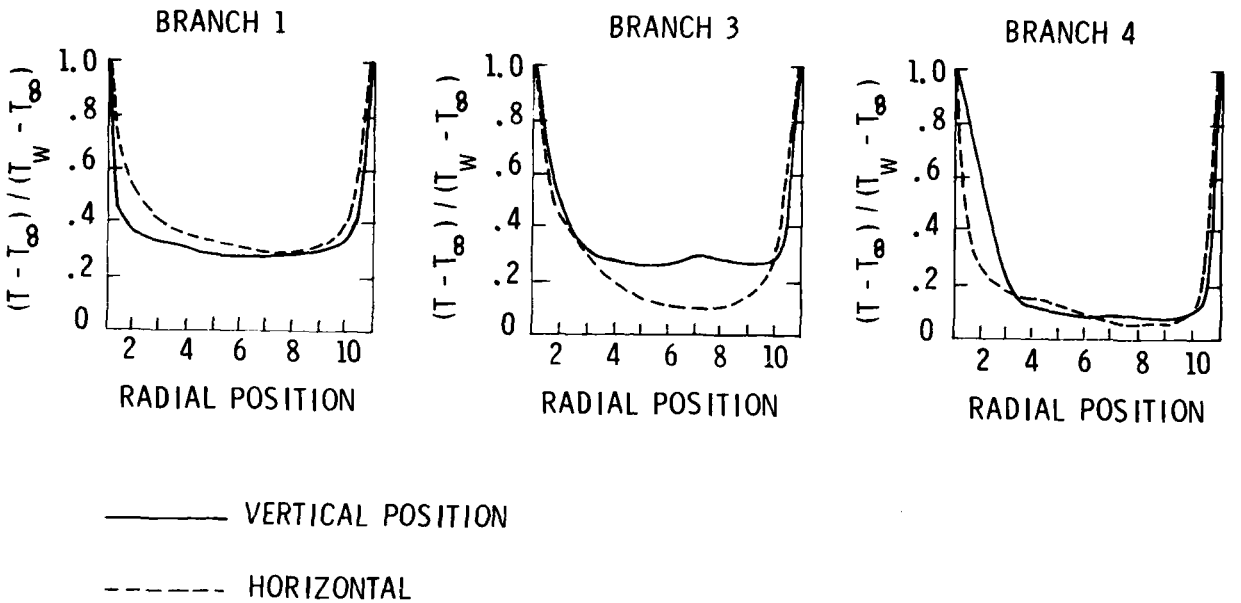

FIGURE 15: TEMPERATURE PROFILES AT VARIOUS LOCATIONS IN THE LOWER TRACT MODEL (RE=21,210)

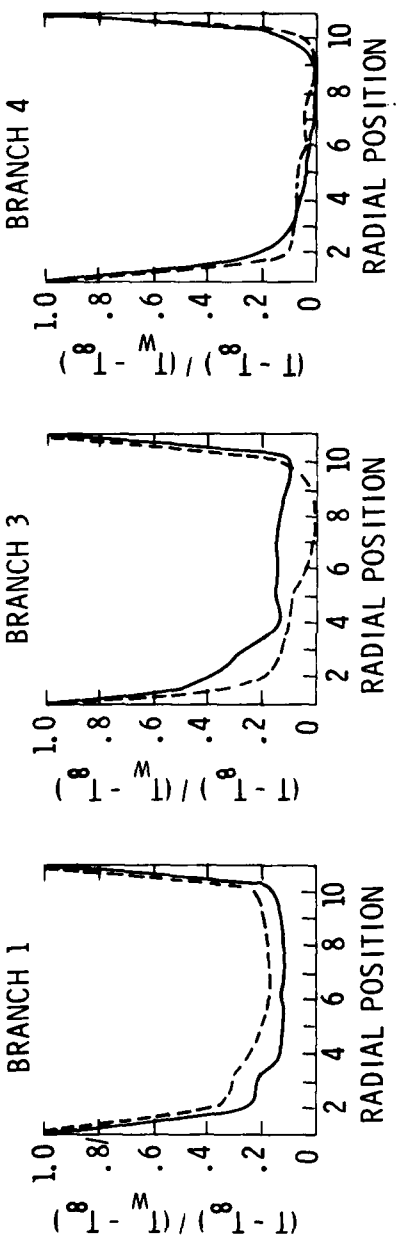

FIGURE 16: TEMPERATURE PROFILES AT VARIOUS LOCATIONS IN THE LOWER TRACT MODEL (RE=56,873)

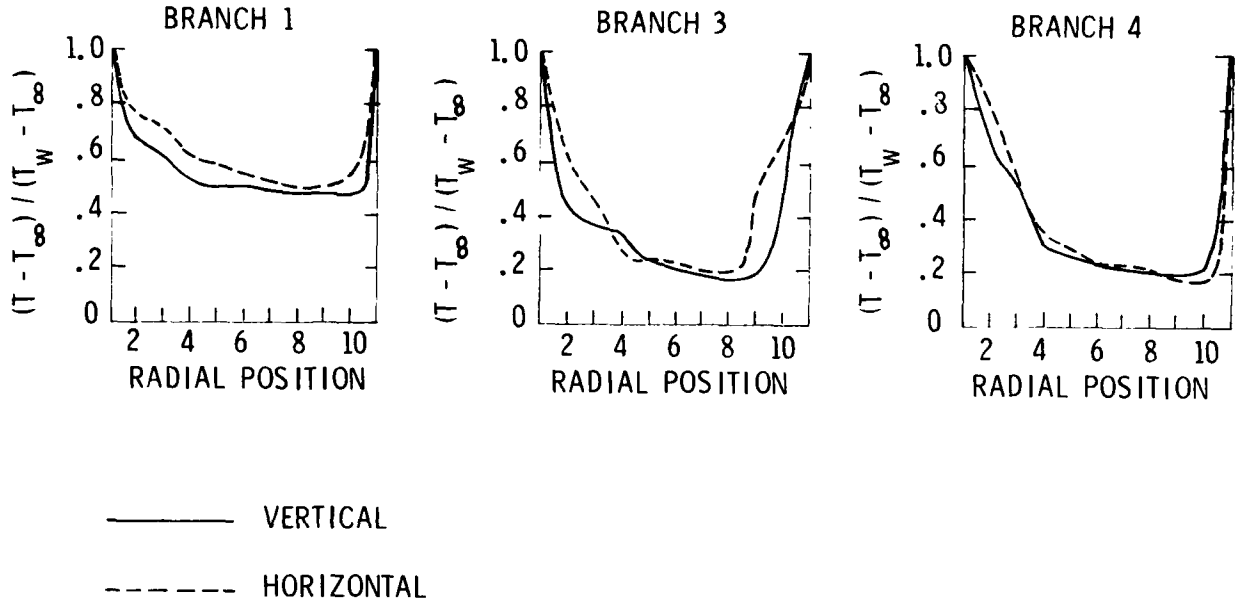

FIGURE 17: TEMPERATURE PROFILES AT VARIOUS LOCATIONS IN THE LOWER TRACT MODEL (RE=5,733)

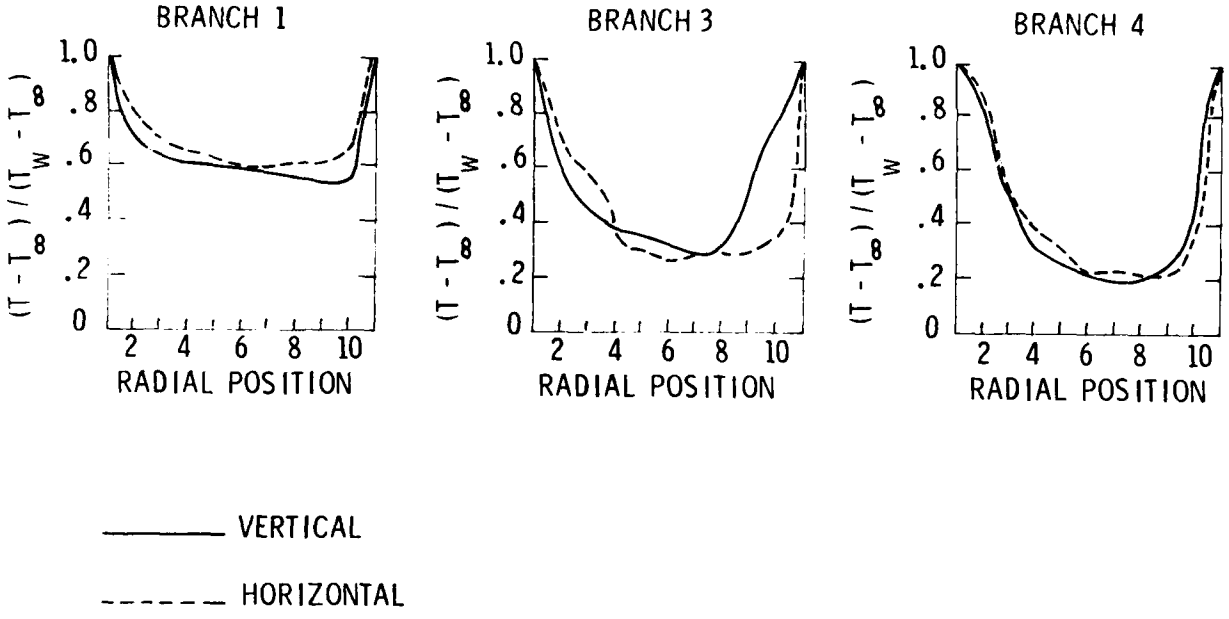

FIGURE 18: TEMPERATURE PROFILES AT VARIOUS LOCATIONS IN THE LOWER TRACT MODEL (RE=2,917)

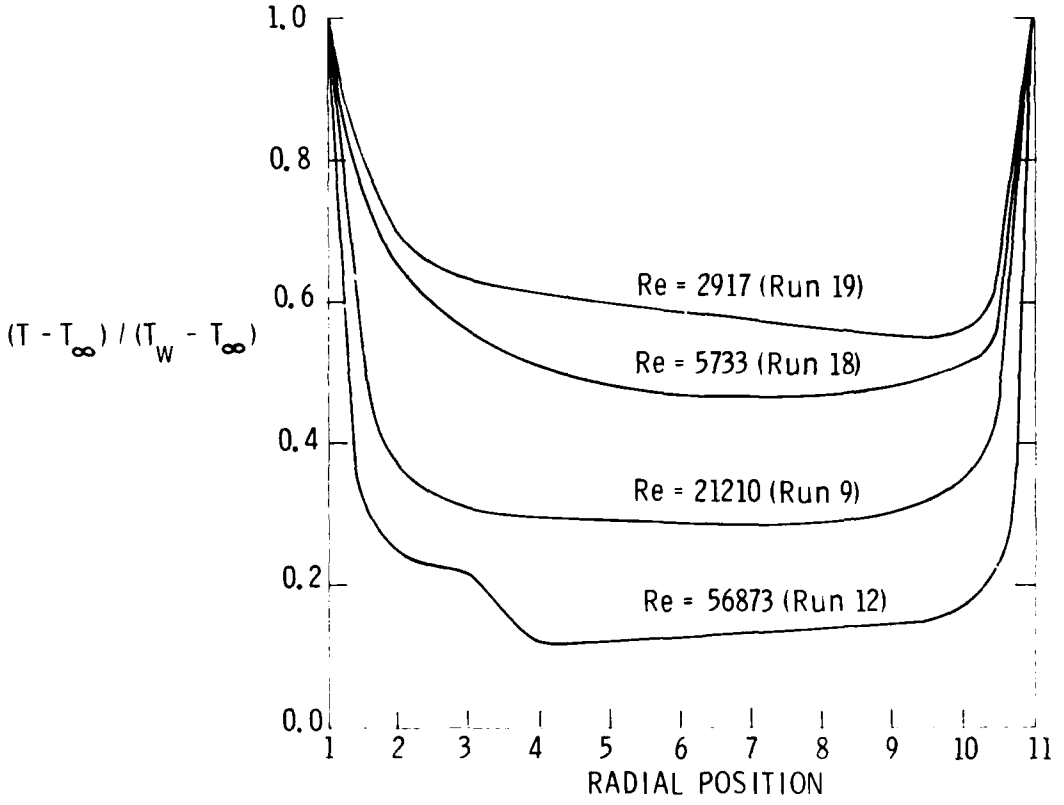

FIGURE 19: EFFECT OF REYNOLDS NUMBER ON VERTICAL TEMPERATURE PROFILES OF BRANCH 1

see while traversing the model at the reduced flow rates. Additionally, the more dense gases will tend to have a high thermal capacity (ρC_p), resulting in lower exit temperatures at comparable flow velocities than the less dense gases. From the above recordings a bulk gas temperature was calculated at each position as the arithmetic average of the horizontal and vertical recordings.

The volumetric flow rate recorded with the Meriam laminar flow element was used to calculate average velocities in each branch of the model according to the findings of previous flow studies in similar branching models [17, 25, 36]:

$$\bar{V}_1 = \dot{V}/A_1 \tag{1}$$

$$\bar{V}_2 = \frac{1}{2}\,\bar{V}_1\,\frac{A_1}{A_2} \tag{2}$$

$$\bar{V}_3 = \frac{\bar{V}_2}{2.26}\,\frac{A_2}{A_3} \tag{3}$$

$$\bar{V}_4 = 1.26\,\bar{V}_3 \tag{4}$$

where

$\bar{V}_1, \bar{V}_2, \bar{V}_3, \bar{V}_4$ = average velocities in branches 1, 2, 3, and 4, respectively (cm/sec).

A_1, A_2, A_3, A_4 = cross-sectional area of branches 1, 2, 3, and 4, respectively (cm^2).

$\dot{V}$ = volumetric flow rate in branch 1 (cc/sec).

These expressions for local flows in the model branches were used due to the consistent finding that flow in branch 4 exceeded branch 3 by 26% during inspiration flow studies. Note that this finding is relatively insignificant during expiration flow studies since the weighted average inlet temperature in branches 3 and 4 is equal to the ambient temperature during expiration studies.

Heat Transfer Coefficient Calculations

Using the recorded bulk temperatures, average flow velocities, and the model bath temperature (used as the approximate model wall temperature), overall heat transfer coefficients were calculated over a wide range of model flow rates in the expiratory flow mode. Constant gas properties were assumed during each test run based on the average bulk temperature of the gas within the model (average of inlet and exit temperatures).

As indicated in Figure 20, the heat balance for the branching model during expiratory flow can be written as follows (based on flow symmetry out of branch 1):

Heat Entering + Heat Added = Heat Exiting

or

$$\dot{m}\, C_p\, T_i + \dot{Q} = \dot{m}\, C_p\, \dot{T}_{i+1}$$

By defining an average heat transfer coefficient, $\bar{h}$, for this branching system based on the geometry of branch 1 as was done in the previous investi-

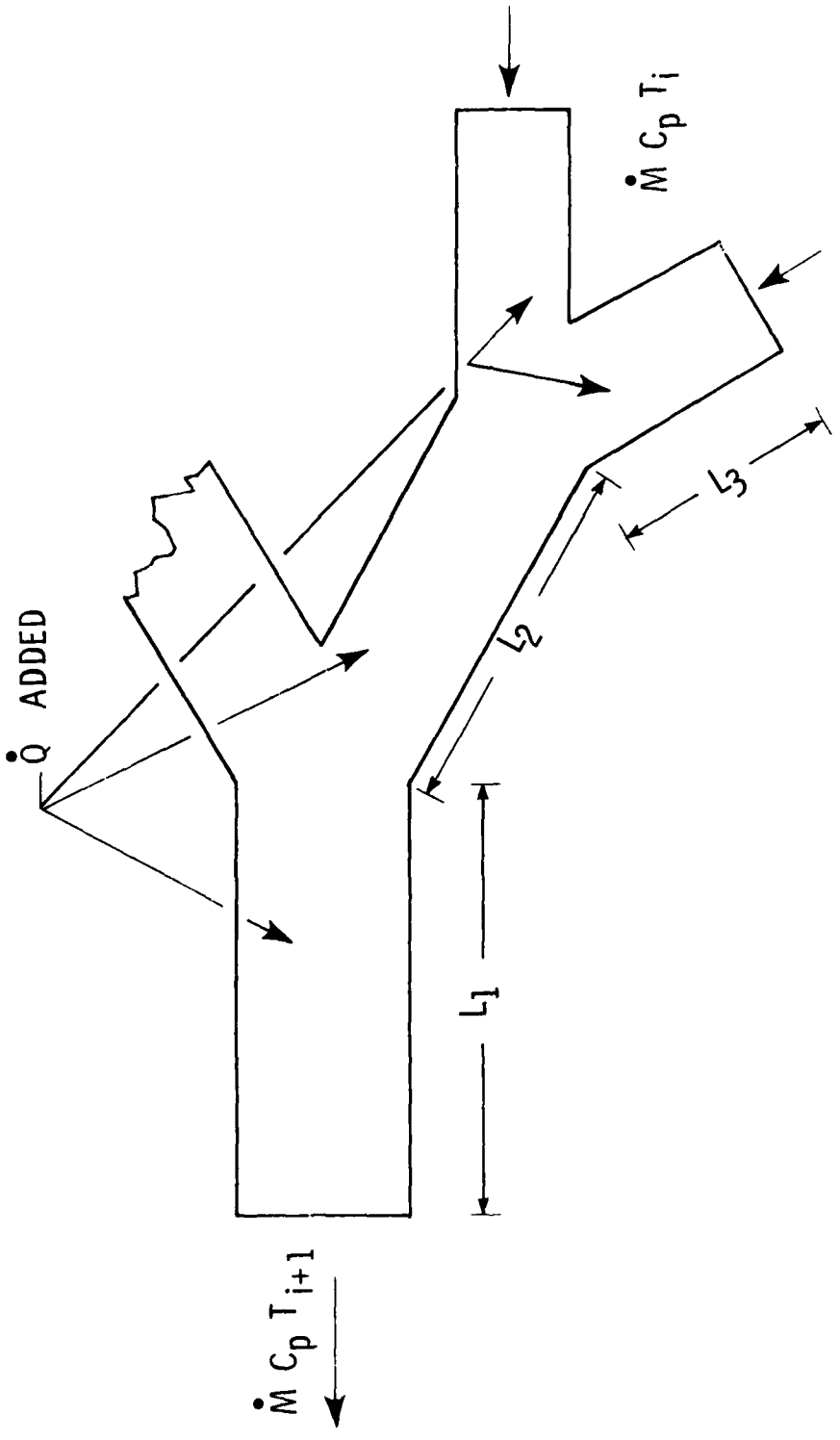

FIGURE 20: HEAT TRANSFER IN BRANCHING SYSTEM DURING EXHALATION

gations [17, 25, 26], we obtain

$$\dot{m}\, C_p\, T_i + \pi D L \bar{h}\, \Delta T_w = \dot{m}\, C_p\, T_{i+1}$$

where

T_{i+1} = bulk temperature upstream (°C)

T_i = weighted average entrance temperature (°C)

$$= \frac{V_3 T_3 + V_4 T_4}{V_3 + V_4}$$

T_3, T_4 = bulk temperatures recorded at entrances to branches 3 and 4, respectively (°C)

$\Delta T_w = T_w - T_i$

T_w = wall temperature (°C)

$\dot{m}$ = mass flow rate (gm/sec)

C_p = gas specific heat (joules/gm -°C)

$\dot{Q}$ = heat added through walls (joules/sec)

$\bar{h}$ = average model heat transfer coefficient based on branch 1 (watts/cm^2-°C)

D = branch 1 diameter (cm)

L = model length (cm)

$= L_1 + L_2 + L_3$

ρ = gas mass density (gm/cm^3).

However, since

$$\dot{m} = \rho \bar{V}_1\, \pi D^2/4$$

and by defining

$$\Delta T = T_{i+1} - T_i$$

the average model heat transfer coefficient can be written

$$\bar{h} = \rho C_p \, (\Delta T/\Delta T_w) \cdot (\bar{V}_1 \, D/4L). \tag{5}$$

Additionally, nondimensionalized heat transfer coefficients and flow based on branch 1 can be defined as

$$\overline{Nu} = \frac{\bar{h} \, D}{K} = \text{overall model Nusselt number} \tag{6}$$

and

$$Re = \frac{\rho \bar{V}_1 \, D}{\mu} = \text{branch 1 Reynolds number} \tag{7}$$

where

K = gas thermal conductivity (watts/cm-°C)

μ = gas absolute viscosity (gm/cm-sec).

For flow in the opposite direction; i.e., simulating inspiration, it is only necessary to switch definitions of T_i and T_{i+1} to get comparable Nusselt values for flow in this mode.

A total of 21 test runs were made with flow in the expiratory flow mode. Data from the 18 additional test runs from the past inspiratory flow studies [25] were likewise reduced as described above.

The above expressions were incorporated into the computer program "Data Acquisition - Lower Tract" given in Appendix I to obtain the results tabulated in Tables 3 and 4. (A complete listing of data recorded during these tests is included in Appendix J.) These calculated results of Nusselt number are plotted against the product of Reynolds number and Prandtl number in Figures 21

and 22 for flow in each direction. Figure 23 superimposes these previous two charts to show that a single functional relationship appears to hold for flow in both directions over the range of flow investigated.

A curve-fitting subroutine was utilized to obtain least square fits of the data given in Figures 21-23. This routine as described in Reference [37] gave the following relationships for heat transfer in the branching system:

Inspiration:

$$\overline{Nu} = 0.0777\ (RePr)^{0.726} \tag{8}$$

Expiration:

$$\overline{Nu} = 0.0589\ (RePr)^{0.752} \tag{9}$$

Combined:

$$\overline{Nu} = 0.0733\ (RePr)^{0.731} \tag{10}$$

The above combined relationship was derived from a data range of $195 < Re < 62{,}000$ with Prantl numbers of approximately 0.7.

TABLE 3a. EXPERIMENTAL RESULTS DURING EXPIRATION FLOW STUDIES: LOWER RESPIRATORY TRACT

				Branch Velocities (cm/sec)				
File	Gas Mix	Depth (M)	Flow (L/sec)	Branch 1	Branch 2	Branch 3	Branch 4	Branch 1 Re
0	air	0	0.83	72.2	73.8	65.2	82.3	1830
1	air	0	15.48	1356.4	1386.8	1228.3	1545.3	34438
2	air	0	12.75	1118.6	1143.6	1011.4	1274.3	28383
3	air	0	8.20	718.9	735.0	650.0	819.0	18243
4	air	0	27.74	2433.3	2487.7	2200.1	2772.1	61743
5	air	0	27.84	2441.7	2496.3	2207.6	2781.6	61960
6	air	0	6.03	528.5	540.3	477.8	602.1	13410
7	air	0	20.73	1817.9	1858.6	1643.7	2071.0	46133
8	air	0	5.51	482.9	493.7	436.6	550.1	12254
9	air	0	9.53	836.0	854.7	755.8	952.3	21210
10	air	0	17.09	1498.6	1532.2	1355.0	1707.3	38032
11	air	0	23.24	2038.2	2083.8	1842.8	2321.9	51713
12	air	0	25.55	2241.0	2291.1	2026.2	2553.0	56873
13	air	0	19.53	1712.8	1751.1	1548.6	1951.3	43471
14	air	0	24.45	2144.2	2192.2	1938.7	2442.8	54417
15	air	0	22.44	1968.1	2012.1	1779.5	2242.1	49937
16	air	0	12.40	1087.8	1112.2	983.6	1239.3	27604
17	air	0	14.69	1288.2	1317.0	1164.7	1467.5	32689
18	air	0	2.58	225.9	231.0	204.3	257.4	5733
19	air	0	1.31	114.9	117.5	103.9	130.9	2917
20	air	0	0.40	34.7	35.5	31.4	39.5	880

TABLE 3b. EXPERIMENTAL RESULTS DURING EXPIRATION FLOW STUDIES:
LOWER RESPIRATORY TRACT

				Bulk Temperature (C)			
File	Gas Mix	Depth (M)	Bath Temp (C)	Enter Branch 4	Enter Branch 3	Exit Branch 1	Nu
0	air	0	46.4	36.1	35.9	39.1	10.8
1	air	0	45.1	30.4	30.6	32.9	115.3
2	air	0	45.5	30.8	31.1	33.7	107.8
3	air	0	45.5	32.6	33.0	35.5	77.6
4	air	0	45.3	30.5	29.6	32.2	169.6
5	air	0	45.0	30.4	30.0	32.4	185.2
6	air	0	45.1	32.6	32.8	35.2	54.7
7	air	0	45.0	31.1	31.5	33.0	120.0
8	air	0	44.4	33.0	34.7	35.5	40.0
9	air	0	44.4	31.5	33.0	34.5	80.1
10	air	0	44.3	30.6	32.2	33.6	136.4
11	air	0	44.2	30.3	31.6	33.0	164.9
12	air	0	44.1	30.1	31.2	32.2	137.2
13	air	0	51.9	33.2	35.2	36.9	140.4
14	air	0	46.6	32.1	33.0	34.2	132.8
15	air	0	44.0	30.5	30.8	33.1	182.5
16	air	0	44.6	31.2	31.9	34.3	117.9
17	air	0	44.9	31.1	30.9	33.9	133.7
18	air	0	45.1	34.5	34.7	38.2	38.8
19	air	0	45.2	35.5	36.1	39.6	23.7
20	air	0	46.5	36.4	36.9	40.2	6.4

≠ TABLE 4a. EXPERIMENTAL RESULTS DURING INSPIRATION FLOW STUDIES: LOWER RESPIRATORY TRACT

File	Gas Mix	Depth (M)	Flow (L/sec)	Branch Velocities (cm/sec)				
				Branch 1	Branch 2	Branch 3	Branch 4	Branch 1 Re
21	air	0	14.4	1261.9	1289.3	1140.0	1438.7	30987
22	$He/0_2$*	0	18.5	1627.6	1664.2	1472.2	1853.2	9952
23	$He/0_2$	30.48	15.8	1380.7	1411.2	1246.6	1572.8	33937
24	$He/0_2$	30.48	10.7	935.7	957.1	847.3	1066.8	22999
25	$He/0_2$	30.48	7.3	640.1	655.3	579.1	728.5	15732
26	$He/0_2$	12.19	15.6	1365.5	1396.0	1234.4	1554.5	18437
27	$He/0_2$	12.19	10.2	893.1	914.4	807.7	1018.0	12058
29	$He/0_2$	12.19	7.5	652.3	667.5	591.3	743.7	8807
30	$He/0_2$	12.19	5.2	460.2	469.4	417.6	524.3	6214
31	$He/0_2$	12.19	8.1	710.2	725.4	643.1	807.7	9589
32	$He/0_2$	12.19	4.0	347.5	356.6	313.9	396.2	4692
33	air	12.19	2.7	237.7	243.8	216.4	271.3	12904
34	air	12.19	4.8	420.6	429.8	381.0	478.5	22831
35	air	0	1.3	109.7	112.8	100.6	125.0	2695
36	air	0	0.47	42.7	42.7	39.6	48.8	1040
37	air	0	0.76	67.1	67.1	61.0	76.2	1617
38	air	0	0.28	24.4	24.4	21.3	27.4	614
39	air	0	0.09	9.1	9.1	6.1	9.1	195

*All $He/0_2$ mixes were 83.2% He/16.8% 0_2.

≠From Reference [25]

TABLE 4b. EXPERIMENTAL RESULTS DURING INSPIRATION FLOW STUDIES: LOWER RESPIRATORY TRACT

			Bulk Temperatures (C)				
File	Gas Mix	Depth (M)	Bath Temp (C)	Enter Branch 1	Exit Branch 3	Exit Branch 4	Nu
21	air	0	50.0	28.2	34.9	30.3	117.2
22	He/O_{2}*	0	46.1	28.7	36.9	31.1	42.1
23	He/O_2	30.48	44.4	26.8	32.1	27.8	83.3
24	He/O_2	30.48	42.8	26.4	31.3	27.3	55.4
25	He/O_2	30.48	42.2	26.1	31.7	27.7	48.9
26	He/O_2	12.19	41.7	25.9	31.0	27.4	53.8
27	He/O_2	12.19	41.7	26.7	32.1	27.8	35.7
29	He/O_2	12.19	42.2	29.4	35.4	31.4	38.8
30	He/O_2	12.19	43.3	29.1	36.3	31.7	30.4
31	He/O_2	12.19	43.3	27.2	34.7	30.3	44.5
32	He/O_2	12.19	43.3	29.7	36.7	31.3	20.3
33	air	12.19	46.7	29.4	36.4	31.3	62.0
34	air	12.19	46.7	28.0	34.3	30.1	95.5
35	air	0	43.9	31.5	38.7	34.1	20.0
36	air	0	43.9	33.5	41.1	36.1	9.6
37	air	0	43.9	32.6	40.7	35.4	14.7
38	air	0	48.3	36.2	45.5	41.7	7.2
39	air	0	48.9	37.6	44.4	43.4	2.2

*All He/O_2 mixes were 83.2% He/16.8% O_2.

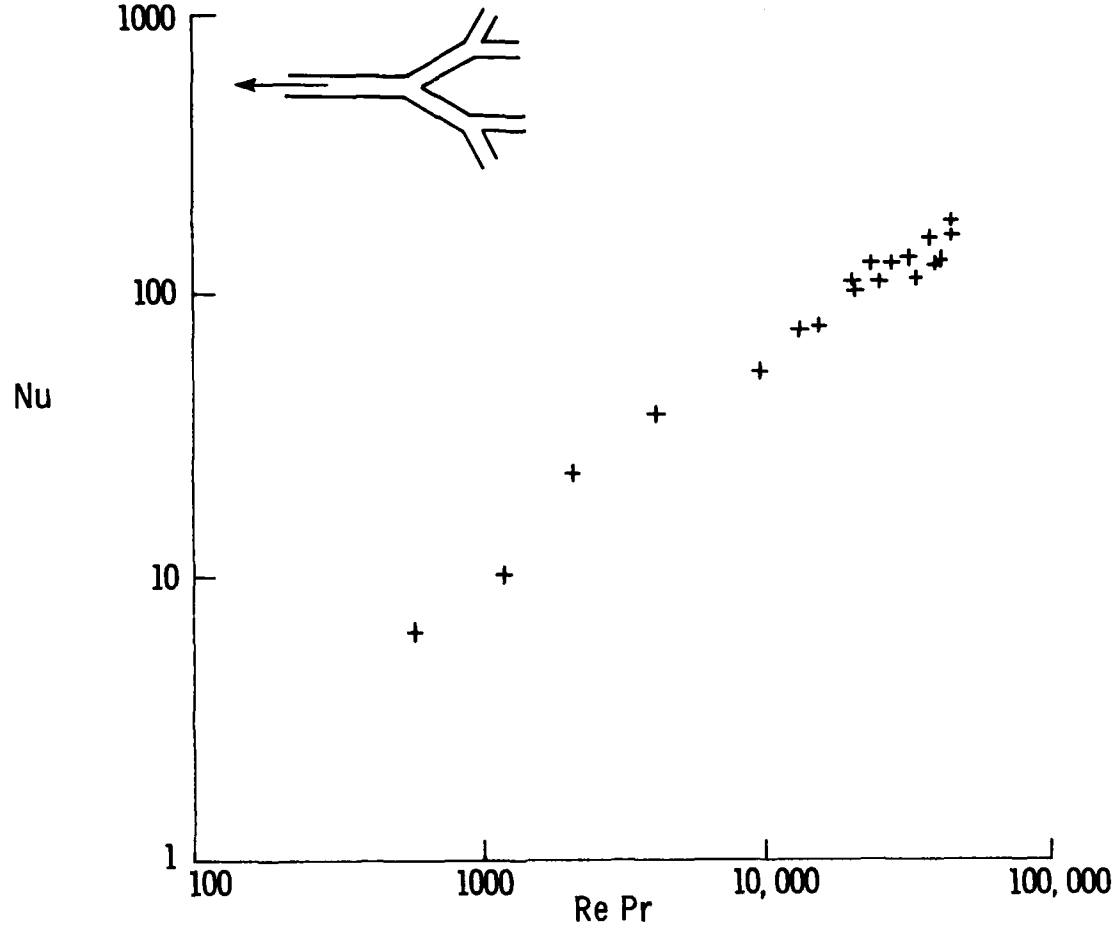

FIGURE 21: HEAT TRANSFER CHARACTERISTICS OF BRANCHING SYSTEM DURING EXPIRATION

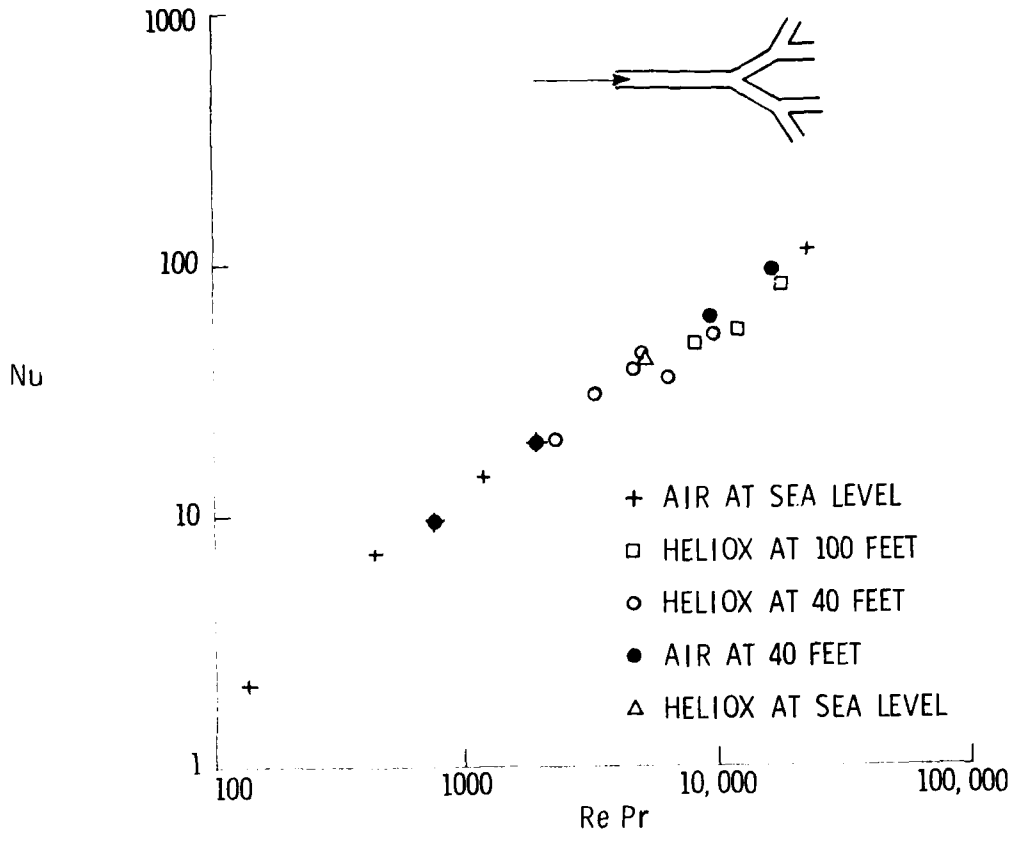

FIGURE 22: HEAT TRANSFER CHARACTERISTICS OF BRANCHING SYSTEM DURING INSPIRATION

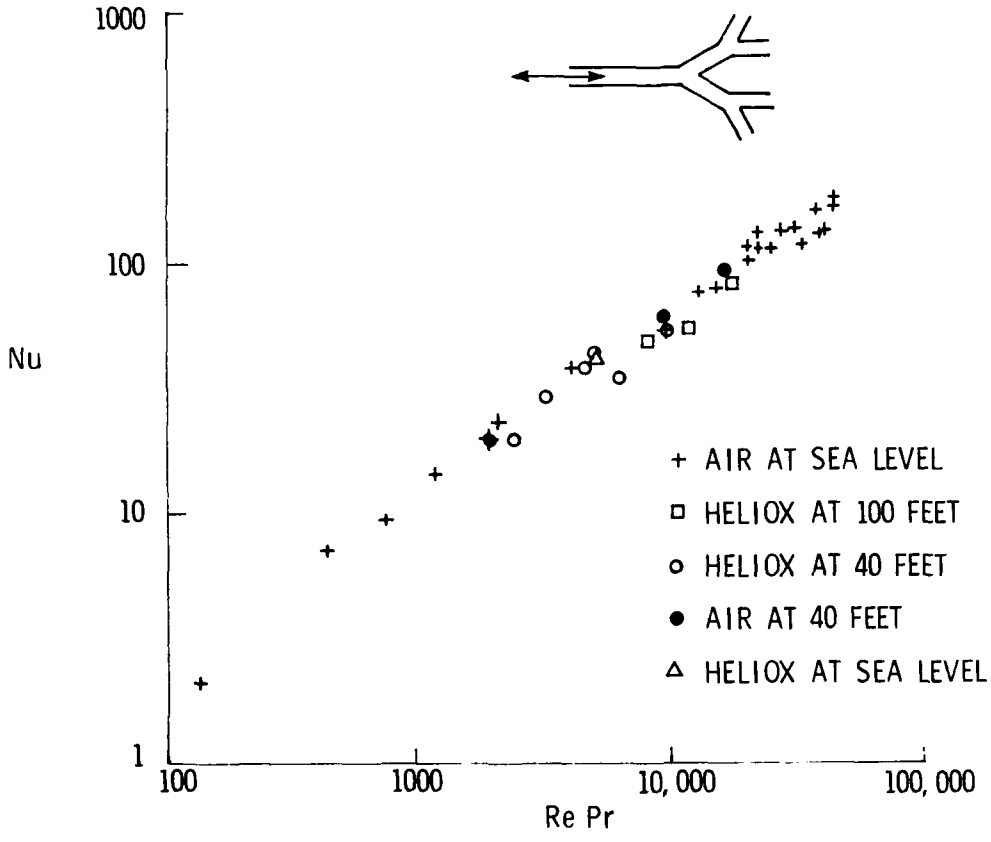

FIGURE 23: OVERALL HEAT TRANSFER CHARACTERISTICS OF BRANCHING SYSTEM DURING INSPIRATION AND EXPIRATION

CHAPTER IV

UPPER RESPIRATORY TRACT
EXPERIMENTAL APPARATUS, INSTRUMENTATION, TESTING

Model Description

In order to accurately assess the heat and mass transfer in the upper respiratory tract, a geometrically accurate physical model was required. Unlike the lower respiratory tract, the complexity of the flow channels in the upper tract do not lend themselves to morphometry. It was thus necessary to obtain a true likeness of these airways through a casting process from a human cadaver. Such a model was obtained from researchers at Johns Hopkins University, who had used similar models in the past to study flow patterns in the upper airways [38].

The model was fabricated through a two-step process from the cadaver of a male adult who had no signs of respiratory abnormalities [39]. First, half negatives were made of the upper airways (both oral and nasal cavities) on each side of the midsagittal plane using a pourable silicone rubber compound capable of reproducing intricate detail (Dow Corning Silastic E RTV). Its excellent duplicating qualities and high tear resistance/high strength properties made it a good choice for this application. Following curing, these half negatives were then embedded in molds filled, by layering, with a clear casting plastic (Ward's Bio-Plastic), leaving the midsagittal

planes uncovered. Following cure of the casting resin, the silicone rubber negatives were removed leaving the intricate detail of the upper airways intact as shown in Figure 24. Following grinding and polishing of the casting exterior surfaces, the two clear plastic halves were assembled with machine screws as seen in Figure 25. Prior to final assembly, a thin brass plate (0.010 cm thick) was inserted between the two plastic halves in the region of the turbinates to serve as the nasal septum. (The thin brass plate was chosen to facilitate heat transfer into the septum in the attempt to maintain constant surface temperature.)

Nasal and oral openings were then machined into the assembled model as specified below:

Nasal openings:* 0.64 cm

Mouth opening: 2.54 cm x 0.64 cm (OVAL)

Measured airway dimensions of the model (see Figure 26) to be used in data reduction were

Trachea diameter: 1.27 cm
Nasal passageway length: 24.1 cm
Oral passageway length: 19.7 cm

*These dimensions were later modified, as discussed later, to match in vivo pressure drop recordings in the nasal airways and those recorded in a similar model at Johns Hopkins University.

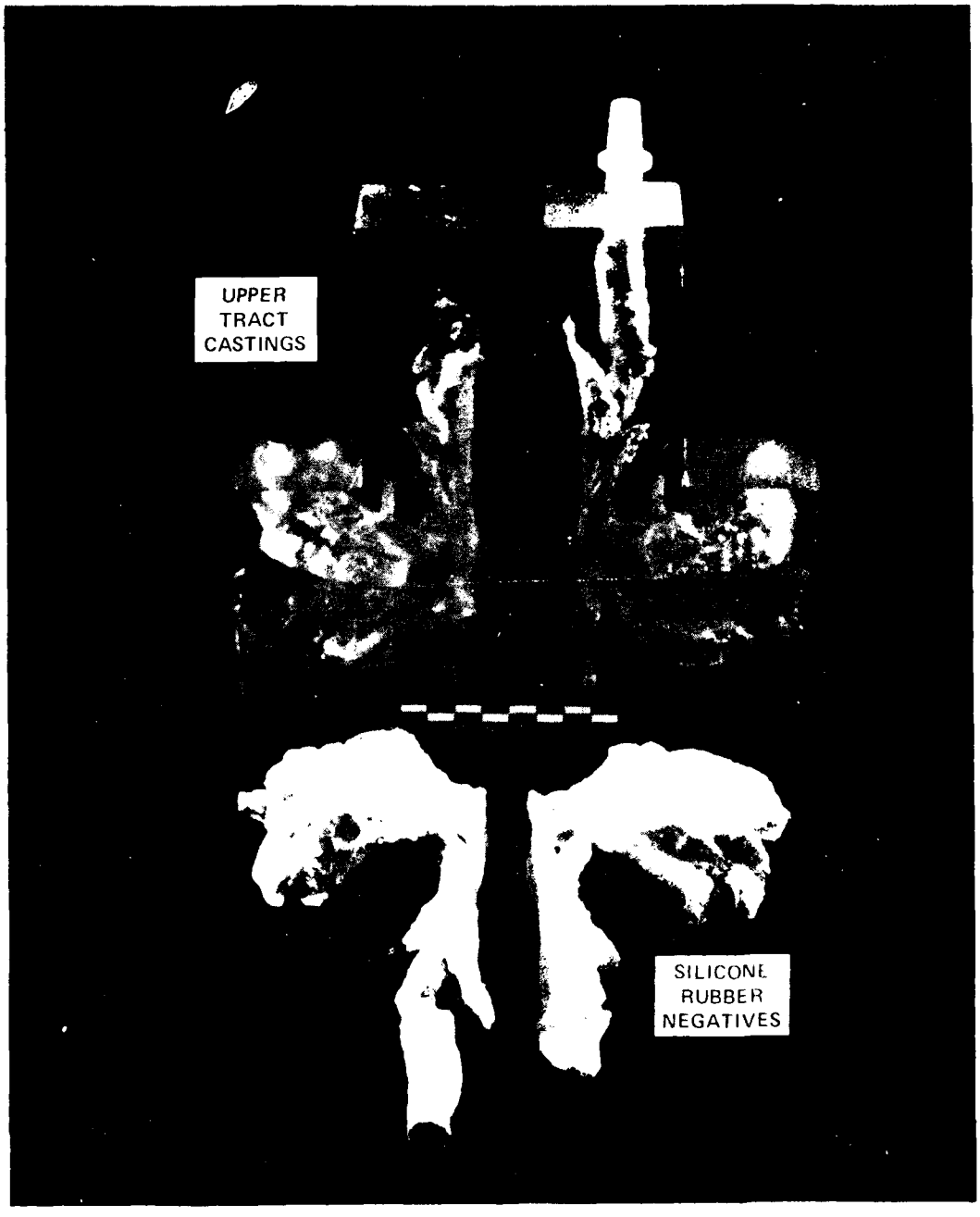

FIGURE 24: POSITIVE AND NEGATIVE CASTINGS OF THE HUMAN UPPER RESPIRATORY TRACT USED FOR HEAT TRANSFER ANALYSIS

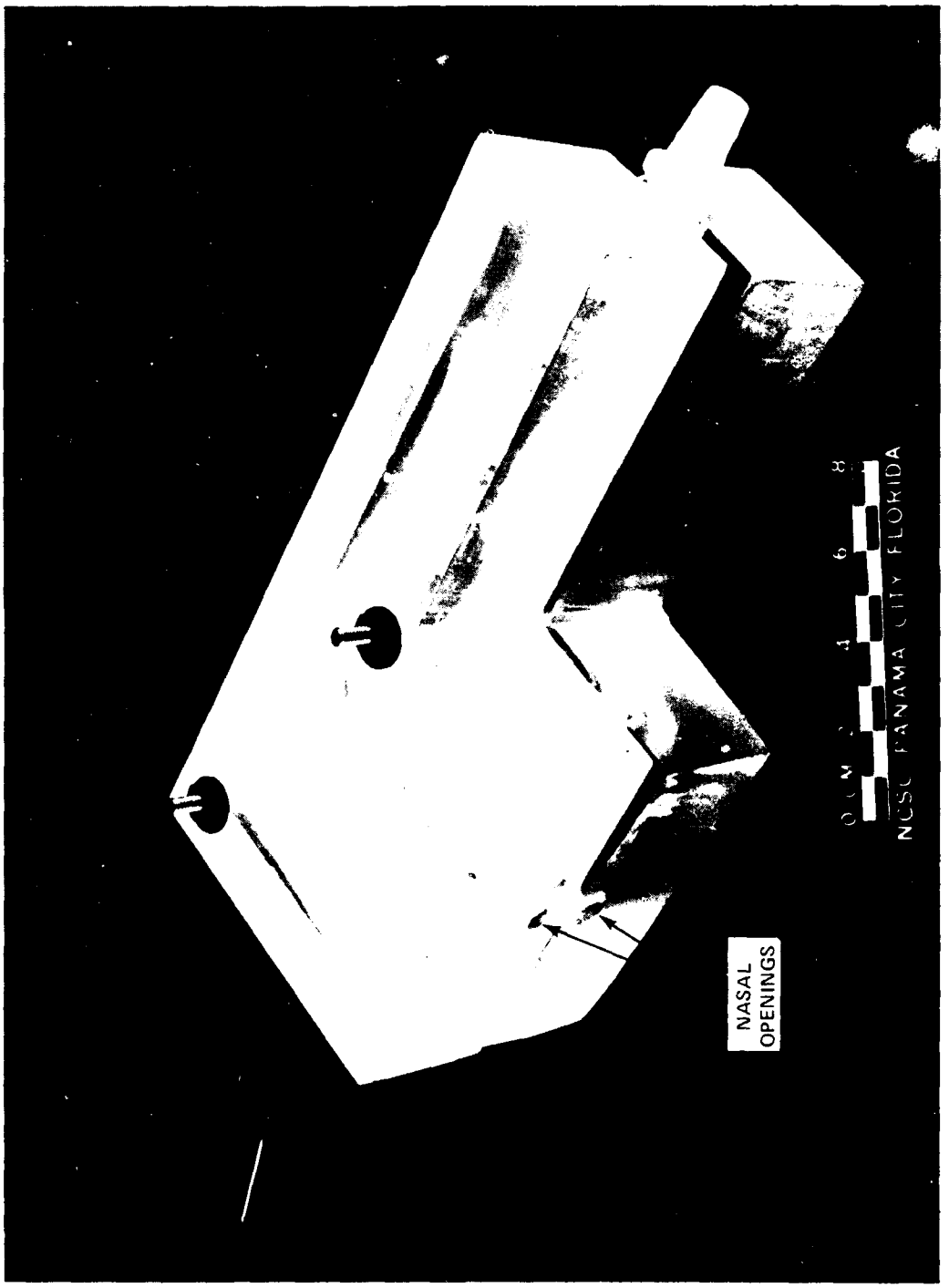

FIGURE 25: MODEL ASSEMBLED PRIOR TO INSTRUMENTING

Following model assembly, all joints were sealed with a clear silicone sealing compound. After the model was instrumented for temperature and flow measurements (to be described later), the entire assembly was submerged in a well-stirred, hot water bath (approximately 375-litre capacity). A short section of PVC pipe (3.2 cm od) surrounding the oral or nasal openings allowed the model to be fully submerged in the bath while preventing water to enter the model airways.

Instrumentation

A similar automated data acquisition system, as used in the previous investigation of the lower respiratory tract, was used in this investigation. However, the size limitations inherent with this model required a different temperature and flow measurement system from that used previously. Additionally, special considerations were made in this test setup to allow testing at simulated depths to confirm the independent behavior of these heat transfer characterizations with depth (as was previously done for the lower tract model).

a. Temperature Measurements

As with the model of the lower respiratory tract, attempts were made to maintain a constant wall temperature during this thermal evaluation. The fundamental assumption made during this and the previous test series was that heat transfer relationships derived from a constant wall temperature model would reasonably represent the *in vivo* situation. This assumption appears to be justified by human and dog airway temperature measurements by

Cole [86] and Johnson [26]. Oscillatory changes in the mucosal surface temperatures were not observed in these studies even though oscillatory changes in air temperature were.

Unlike the pipe model, however, the thermal properties of the clear plastic model (approximate properties shown in Table 5) are not as capable of maintaining constant temperature, particularly when dense cold gases are passed through the model. To monitor the status of the model wall temperature during testing, five copper/constantan thermocouples (30 gauge) were positioned as shown in Figure 26. The junction of each thermocouple was inserted into a small hole (0.12 cm diameter) drilled through the model wall and positioned adjacent to the airway. A quick curing epoxy was used to secure the thermocouples in place. As previously described in the lower tract investigation, all thermocouple junctions were referenced to 0°C using electronic ice point reference junctions. Prior to subjecting this temperature monitoring system to hyperbaric environments, it was necessary to insure that the electronic ice points were not adversely effected by elevated pressures. This investigation, reported in Appendix B, showed no adverse effects at hyperbaric environments up to 350 metres of seawater.

TABLE 5: APPROXIMATE THERMAL PROPERTIES OF POLYESTER CASTING MATERIAL [40]

Thermal Conductivity	$1.67 \times 10^{-3} \frac{\text{watts}}{\text{cm} - {}^{\circ}\text{C}}$
Specific Heat	1.046 joule/gm °C
Density	1.10 - 1.46 gm/cm^3

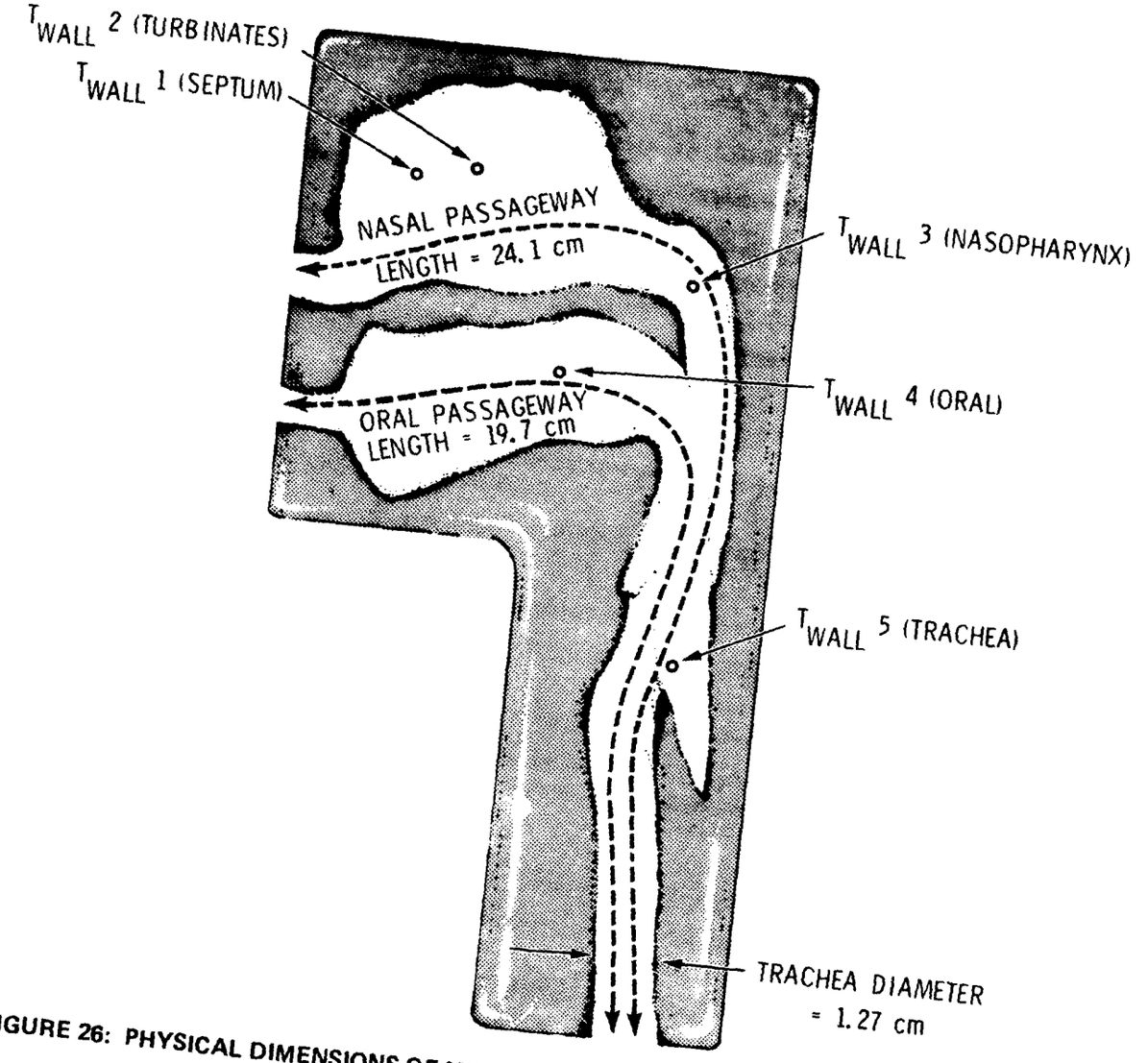

FIGURE 26: PHYSICAL DIMENSIONS OF MODEL AND TEMPERATURE SITE LOCATIONS

One Fastip thermistor probe (Thermometrics, Inc.) was positioned in the trachea midstream, and two similar probes in the center of the oral or nasal openings (depending on the mode of breathing being investigated) to record incoming and outgoing gas temperatures. These thermistor probes were chosen since their small physical size (1/8-inch nominal probe diameter) would tend to least affect the gas flow within the model airways while remaining rugged enough to withstand relatively high flow velocities.

A linearizing network is built within these thermistor probes to function within the temperature range of 0-50°C with an accuracy of 0.25°C. A calibration check on these thermistors was made prior to this investigation to ensure this accuracy. Each thermistor was fully submerged in a temperature controlled water bath (Neslab Instruments) along with a quartz thermometer sensing probe (HP2804A) which had been previously calibrated for the triple point of water. The bath was successively raised from 0°C to 50°C in 1°C steps while recording the Fastip probes and quartz thermometer at each step. Figure 27 shows the temperature differentials recorded for the thermistors as compared with the quartz thermometer. Instead of the desired linear response, the thermistors each exhibited a similar sinusoidal pattern with maximum deviations from the quartz reading of 0.4°C over this temperature range. To obtain the maximum accuracy during this investigation, a temperature correction equation was thus utilized when reading these thermistor probes [41]. This equation was

$$t_{corrected} = t_{reading} + 0.3 \sin [9.73 (t_{reading}-5)]$$

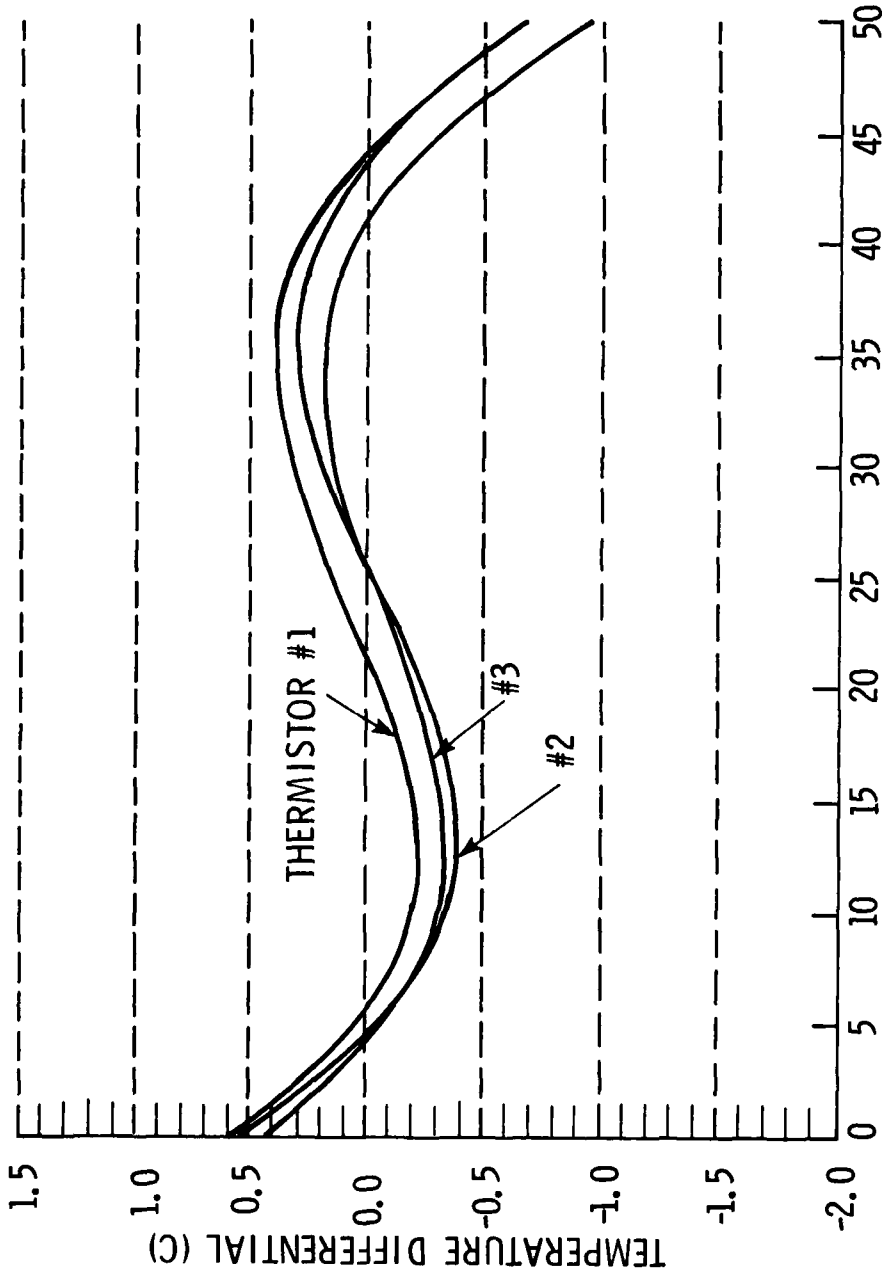

FIGURE 27: FASTIP THERMISTOR/QUARTZ THERMOMETER TEMPERATURE DIFFERENTIAL

where: t is in °C and the argument of sin is in degrees.

The surrounding hot water bath temperature was maintained by a 1.5 kw submersible heater, and monitored with a Yellow Springs YSI 701 thermistor. The instrumented model prior to submergence is shown in Figure 28.

b. Flow Measurement

A laminar flow element, LFE (Meriam Model 50MW20-1-1/2) was placed in series with the model either downstream or upstream of the trachea, depending on whether exhalation or inhalation flow studies were in process. A Validyne differential pressure transducer (Model DP15, Ser 1083, 0.5 psid range) was used to monitor the pressure drop across the LFE. The laminar flow element is factory calibrated for recording the flow of air at 21°C. Since in this investigation the LFE was utilized to record the flow of various gases other than air at temperatures and pressures other than 21°C and 1 atmosphere, it was necessary to perform viscosity corrections throughout this investigation when reading the laminar flow element. This viscosity correction procedure is outlined in Appendix C. The procedure as described previously in the lower tract investigation was used to calibrate the differential pressure transducer.

c. Airway Pressure Drop

The respiratory flow resistance in man during nasal breathing has been recorded in vivo [42, 43]. Attempts were made in this investigation to match the resistance characteristics of this model with those recorded in vivo, as provided by researchers at Johns Hopkins University [44]. This

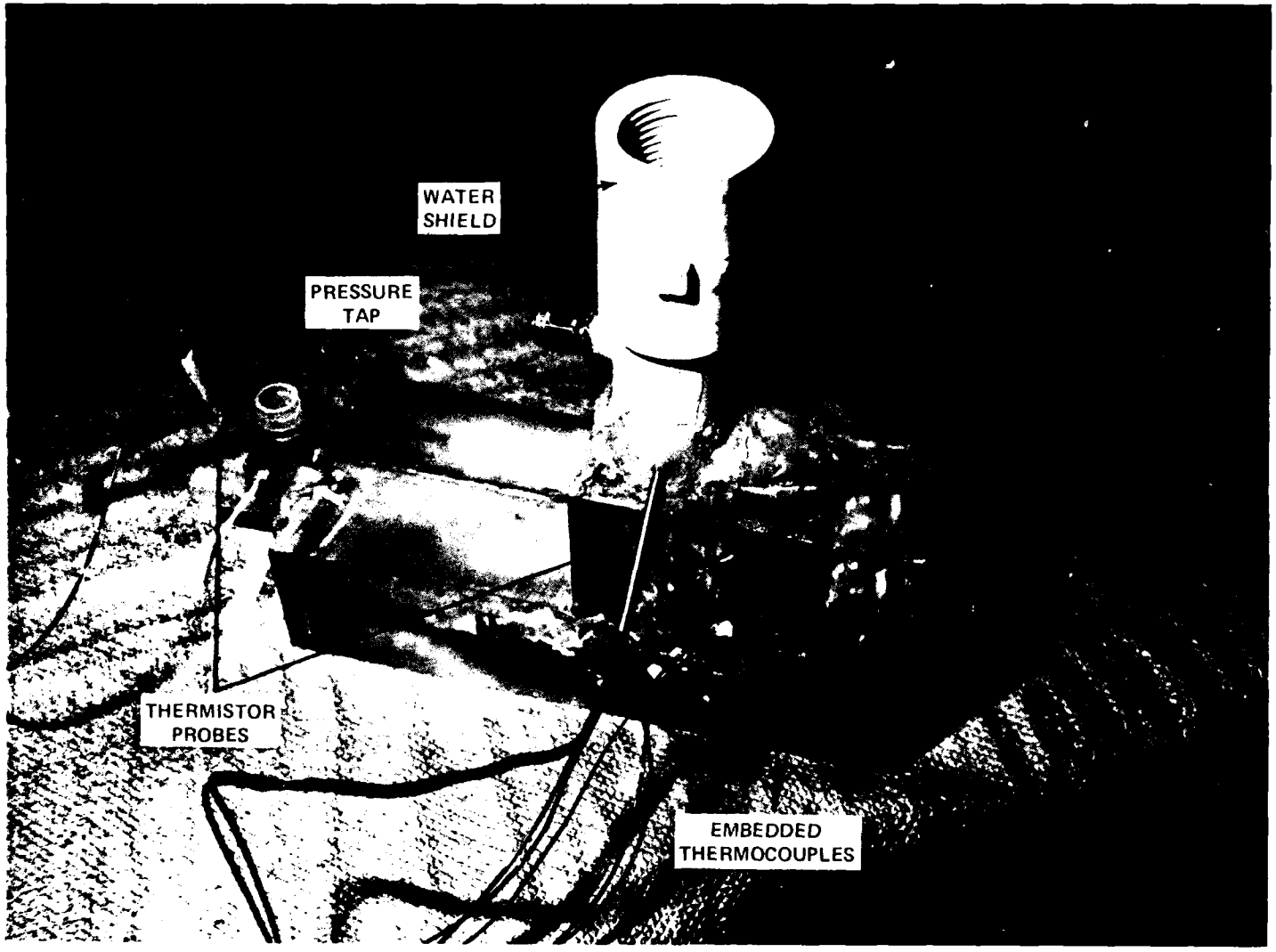

FIGURE 28: TEMPERATURE INSTRUMENTED MODEL PRIOR TO WATER BATH SUBMERGENCE

match was felt necessary due to the strong similarity relationships that are inherent between heat, mass, and momentum transfer. A Validyne differential pressure transducer (Model DP15, Serial 1083, 0.5 psid range) was used to establish and monitor the pressure drop across the model nasal airway, i.e., between the trachea and the anterior nares. A modeling clay was utilized to restrict the nasal passageways near the ostium internum (the nasal location found to be flow limiting) until the resistance characteristics were met. Figure 29 shows a comparison of the flow resistance characteristics of the model used in this investigation with those obtained from Johns Hopkins. Agreement within 8 to 15 percent was observed for flows up to 60 litres/minute. This level of agreement was felt adequate due to the high variability reported in in vivo recordings.

A view of the fully instrumented model ready for inhalation flow measurements through the oral pathway is shown in Figure 30. This assembly was positioned in a 1.2 metre diameter by 3 metre long horizontal hyperbaric chamber rated to 6890 kPa (1000 psig). Gas supply for flow through the model was provided by 689 kPa (100 psi) air lines for testing at the surface, on air, and by 5.7 cubic metre storage cylinders (nominally 17,000 kPa rated) during testing at simulated depths to 305 metres of seawater.

Experimental Procedure and Results

The upper tract test assembly described previously was sealed inside the hyperbaric chamber to be pressurized to the desired simulated depth.

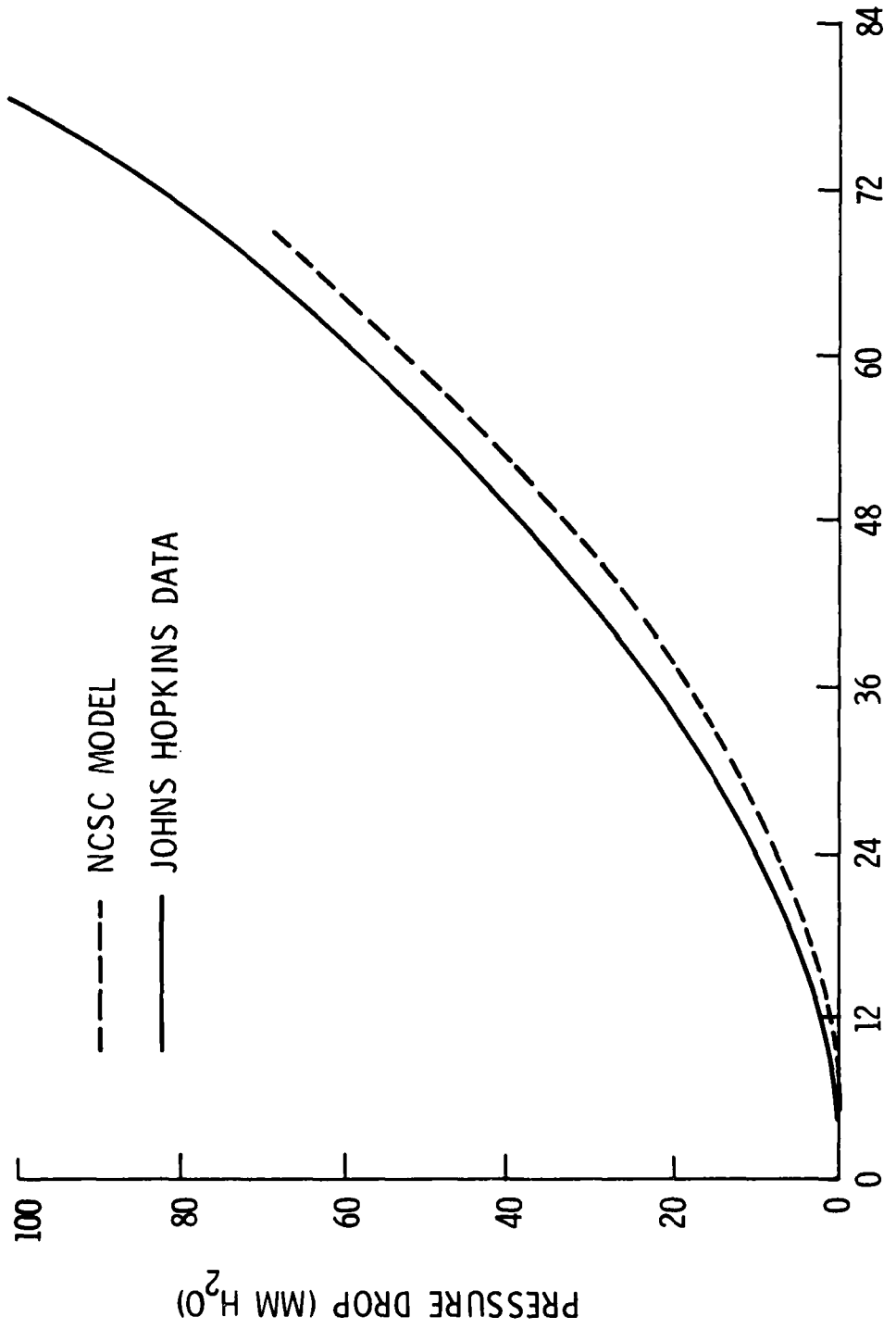

FIGURE 29: PRESSURE DROP THROUGH CASTING OF HUMAN NASAL PASSAGEWAY

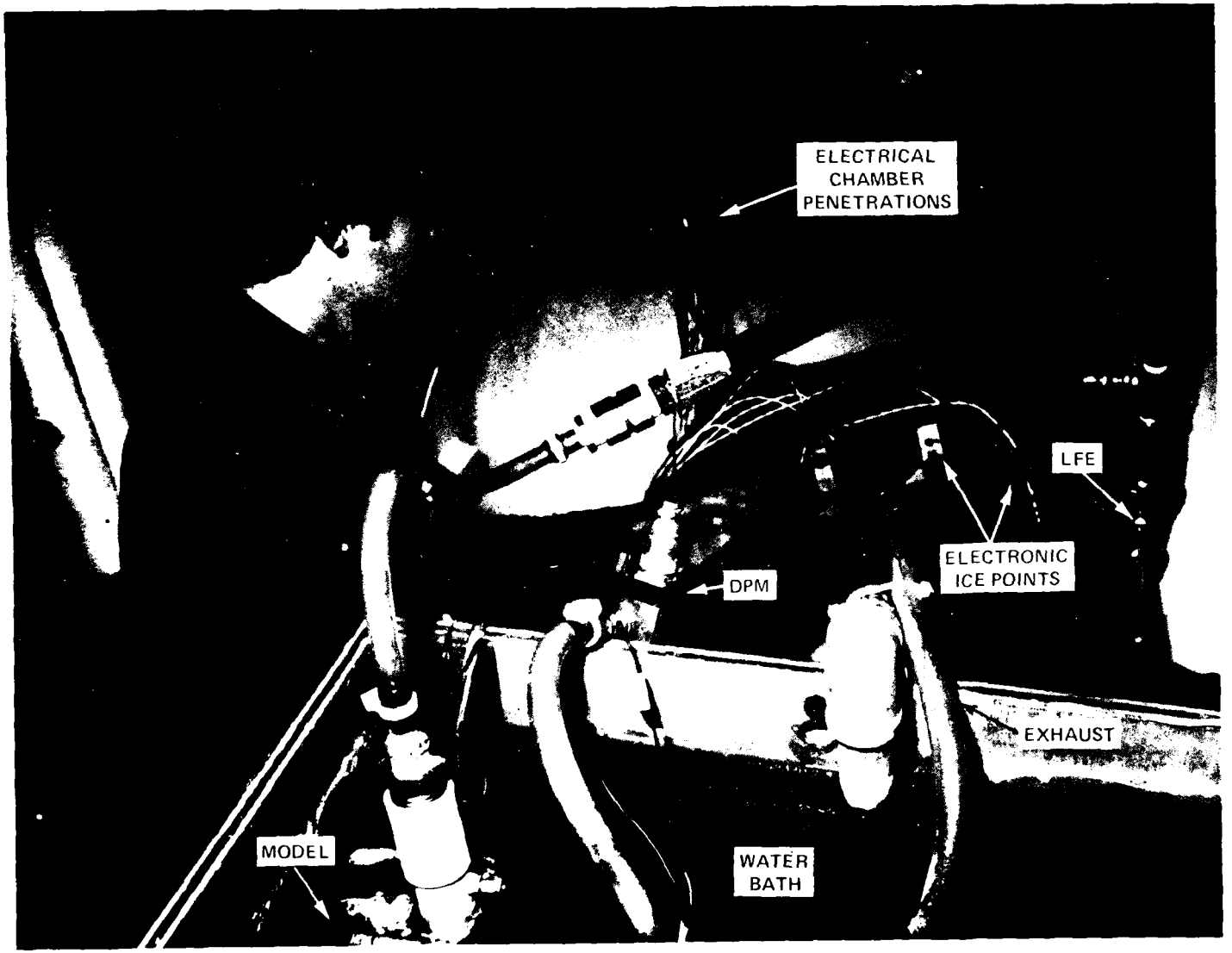

FIGURE 30: MODEL PREPARED FOR INHALATION STUDIES THROUGH ORAL CAVITY

The chamber bath temperature had been previously raised by the submersible heating elements to 50 to 55°C, thus providing a 30-degree minimum differential between the incoming gas and model wall temperatures (large temperature differentials were desired to minimize any instrumentation errors). A Heise pressure comparator (Dresser Industries Model 710 A) was used to control a solenoid actuated valve (Futurecraft, Inc.) to maintain this simulated depth during testing. Following chamber pressurization all temperatures on the model were monitored until stability was observed. At this point gas flow was initiated through the test model by opening a ¼-turn valve while observing the laminar flow element monitor. More or less flow could be introduced through a combination of adjustments with the valve and a two-stage regulator. Once flow had been established model wall temperatures, gas stream temperatures in and out of the model, gas flow rate, and bath temperature were recorded using the automated data acquisition system. This data acquisition was initiated in as soon a time following gas flow as practical to ensure steady flow while minimizing wall cooling.

The above procedure was repeated over a range of flow rates, at simulated depths of 0, 61, and 305 metres of seawater, using three different gas mixtures. The test depths, gas mixtures, and flow rates were arbitrarily selected to provide sufficient data to map the heat transfer characteristics of the model over the desired Reynolds number range of 0-70,000. Additionally, four test modes were evaluated including exhalation flow through the nasal airway, exhalation flow through the oral airway, inhalation flow through the nasal airway, and inhalation flow through the oral airway. A complete listing of data recorded during these tests is included in the NCSC Hydrospace Lab Note 1-81 [45] and Appendix J.

AD-A104 992 NAVAL COASTAL SYSTEMS CENTER PANAMA CITY FL F/G 6/19
HEAT AND WATER VAPOR TRANSFER IN THE HUMAN RESPIRATORY SYSTEM A--ETC(U)
SEP 81 M L NUCKOLS

UNCLASSIFIED NCSC-TR-364-81 SBIE-AD-F200 009 NL

2 of 4
AD
A104992

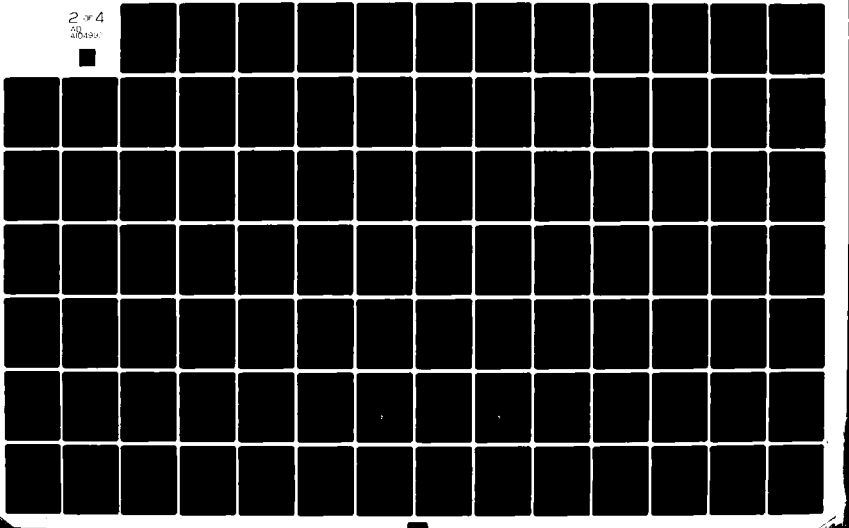

Heat Transfer Coefficient Calculations

As in the investigation of the lower respiratory tract a characteristic dimension must be selected for the reduction of the test data. As before, the trachea diameter was used as a basis for the calculations of model Reynolds number and Nusselt number. This dimension provides a common basis for comparing heat transfer characteristics of the oral and nasal passageways. Constant gas properties were again assumed during each test run based on the average bulk temperature of the gas within the model. Gas mixtures and their properties are shown in Table 6.

From the model gas flow measurement a mean flow velocity was calculated in the trachea as

$$\bar{V} = \frac{\dot{V}}{A} * 1000 \frac{\text{cu cm}}{\text{litre}} \quad .$$

where:

$\bar{V}$ = mean trachea flow velocity $(\frac{cm}{sec})$

$\dot{V}$ = Model flow rate $(\frac{litres}{sec})$

A = cross-sectional area in trachea (cm^2)

$= \frac{\pi}{4} D_T^2$

D_T = trachea diameter (cm)

The model Reynolds number, Re, was then obtained as

$$Re = \frac{\rho \bar{V} D_T}{\mu} \quad .$$

TABLE 6

† PROPERTIES OF GASES USED IN THERMAL EVALUATION OF UPPER RESPIRATORY TRACT

Gas/ Depth (m)	Density gm/cm^3	Specific Heat joules/gm-°C	Viscosity gm/cm-sec	Thermal Conductivity watts/cm-°C	Pr
Air/0	1.178×10^{-3}	1.0059	1.83×10^{-4}	2.637×10^{-4}	0.7
He/0	1.63×10^{-4}	5.1988	1.997×10^{-4}	1.503×10^{-3}	0.69
He/61	1.143×10^{-3}	5.1988	1.997×10^{-4}	1.507×10^{-3}	0.69
He/305	5.01×10^{-3}	5.2030	1.997×10^{-4}	1.532×10^{-3}	0.69
N_2/61	8.037×10^{-3}	1.0427	1.803×10^{-4}	2.637×10^{-4}	0.71
N_2/305	3.571×10^{-2}	1.0640	1.82×10^{-4}	2.763×10^{-4}	0.71

†From US Navy Diving Gas Manual [46]

CONVERSIONS

$$\frac{\text{lbs}}{\text{cu ft}} * 0.01602 = \frac{\text{gm}}{\text{cm}^3}$$

$$\frac{\text{BTU}}{\text{lb - °F}} * 10^{-3} = \frac{\text{Kcal}}{\text{gm - °C}}$$

$$\frac{\text{lb}}{\text{ft - sec}} * 14.9 = \frac{\text{gm}}{\text{cm - sec}}$$

$$\frac{\text{BTU}}{\text{sec - ft - °F}} * 0.01488 = \frac{\text{Kcal}}{\text{cm - sec - °C}}$$

1 joule = 9.478×10^{-4} BTU = 2.388×10^{-4} KCAL

where:

ρ = gas density $(\frac{gm}{cm^3})$

μ = gas viscosity $(\frac{gm}{cm - sec})$

Next, an average model wall temperature was calculated as the average of the five wall temperatures; three temperatures for oral flow (see Figure 26).

$$\bar{T}_w = \frac{T_1 + T_2 + T_3 + T_4 + T_5}{5} \qquad \text{(NASAL)}$$

$$\bar{T}_w = \frac{T_3 + T_4 + T_5}{3} \qquad \text{(ORAL)}$$

A weighted average temperature based on the surface area that was represented by each thermocouple was not attempted due to the difficulty in arriving at the areas of the turbinate folds. However, with the exception of test runs at 305 metres of seawater, the variation between individual thermocouples was small (within 1 °C) which minimized the error from a straight arithmetic averaging. The abnormality seen at 305 metres of seawater will be discussed later.

A mean heat transfer coefficient, $\bar{h}$, was then calculated as described previously in the discussion of the lower respiratory tract as

$$\bar{h} = \rho C_p \left(\frac{\Delta T}{\Delta T_w}\right) \cdot \left(\frac{\bar{V} D_T}{4L}\right)$$

where:

C_p = gas specific heat $(\frac{joule}{gm - {}^oC})$

L = gas passageway length (cm) (see Figure 26)

$$\Delta T = T_{i+1} - T_i \quad (°C)$$

T_i = entering gas temperature (°C)

T_{i+1} = exiting gas temperature (°C)

$\Delta T_w = \bar{T}_w - T_i$ (°C)

An overall model Nusselt number was then calculated based on the trachea diameter as

$$\bar{Nu} = \frac{\bar{h}\, D_T}{K} = \text{overall model Nusselt number}$$

where:

K = gas thermal conductivity ($\frac{\text{watts}}{\text{cm } -°C}$)

The above data collections and calculations were made using the computer program "Data Acquisition-Upper Tract" described in Appendix I in a total of 137 tests as summarized in Tables 7 through 10. This allowed the mapping of the upper respiratory tract heat transfer characteristics during inhalation and exhalation, while breathing solely through the mouth and solely through the nose. This data is plotted in Figures 31 through 34 as the dimensionless Nusselt number versus the product of Reynolds and Prandtl numbers. A review of Figures 31 through 34 reveals a consistent trend of increasing Nusselt number as the product of Reynolds and Prandtl number increase. These relationships appear to hold true for all gases and all simulated depths tested except for helium when tested at 305 metres of seawater. With helium at 305 metres of seawater, especially at the higher values of Re·Pr, the overall Nusselt numbers appear to fall below the trend established by the other gases.

TABLE 7. EXPERIMENTAL RESULTS DURING NASAL/EXHALATION FLOW TESTS

TEST NO	GAS MIX	DEPTH (FSW)	FLOW (LPM)	TIN (C)	TOUT (C)	TWALL (C)	H KC/CM↑2-S-C	RE NO	NU NO	PR NO
0	AIR	0.0	19.1	38.8	42.1	43.1	7.13E-07	2049.2	14.4	.7
1	AIR	0.0	41.1	34.1	40.8	43.1	1.49E-06	4409.5	30.1	.7
2	AIR	0.0	51.5	33.0	39.7	42.9	1.71E-06	5525.2	34.4	.7
3	AIR	0.0	61.4	32.0	39.2	43.0	1.96E-06	6587.4	39.4	.7
4	AIR	0.0	86.1	31.1	38.5	43.1	2.60E-06	9237.3	52.5	.7
5	AIR	0.0	114.1	31.1	37.6	43.4	2.95E-06	12241.3	59.5	.7
6	AIR	0.0	49.3	34.9	41.3	44.5	1.60E-06	5289.2	32.2	.7
7	AIR	0.0	30.1	38.3	42.5	44.9	9.40E-07	3229.3	19.0	.7
8	AIR	0.0	74.0	32.4	40.4	44.5	2.38E-06	7939.2	48.0	.7
9	AIR	0.0	18.2	42.7	44.0	45.6	3.89E-07	1952.6	7.8	.7
10	AIR	0.0	116.8	31.6	39.1	45.1	3.15E-06	12531.0	63.6	.7
27	HE	0.0	58.7	45.8	49.3	51.4	1.28E-06	798.5	4.5	.69
28	HE	0.0	85.1	43.1	48.4	51.1	1.96E-06	1157.7	6.9	.69
29	HE	0.0	119.3	41.4	47.6	50.9	2.71E-06	1622.9	9.6	.69
30	HE	0.0	25.4	48.9	49.2	51.1	1.01E-07	345.5	0.4	.69
31	HE	0.0	47.9	46.0	49.0	51.2	9.71E-07	651.6	3.4	.69
32	HE	0.0	33.7	48.0	49.6	51.4	5.44E-07	458.4	1.9	.69
33	HE	0.0	43.2	46.4	49.4	51.2	9.22E-07	587.7	3.3	.69
34	N2	200.0	12.0	37.0	44.5	49.1	2.55E-06	8915.1	51.4	.71
35	N2	200.0	21.5	34.2	41.3	48.4	3.72E-06	15973.0	74.9	.71
36	N2	200.0	32.4	32.9	39.2	48.0	4.69E-06	24070.9	94.4	.71
37	N2	200.0	37.5	33.7	39.8	48.3	5.39E-06	27859.8	108.7	.71
38	N2	200.0	40.1	32.2	38.1	47.9	5.17E-06	29791.4	104.3	.71
39	N2	200.0	42.4	33.5	38.9	48.2	5.41E-06	31500.2	109.0	.71
54	HE	1000.0	5.0	39.6	46.6	54.1	2.61E-06	2090.6	9.0	.69
55	HE	1000.0	12.7	37.8	43.0	51.4	5.16E-06	5310.2	17.9	.69
56	HE	1000.0	32.5	32.6	37.8	49.2	1.10E-05	13589.1	38.1	.69
57	HE	1000.0	73.8	30.0	32.5	47.5	1.11E-05	30857.8	38.6	.69
58	N2	1000.0	5.0	42.1	45.9	50.1	3.66E-06	16352.1	70.4	.71
59	N2	1000.0	18.6	36.6	42.3	49.1	1.32E-05	60829.8	253.1	.71
60	N2	1000.0	7.4	37.8	42.7	49.5	4.83E-06	24201.1	93.0	.71
61	N2	1000.0	15.9	35.2	39.2	48.5	7.39E-06	51999.7	142.2	.71
62	N2	1000.0	12.2	36.4	40.4	48.6	6.29E-06	39899.1	121.0	.71

TABLE 8. EXPERIMENTAL RESULTS DURING NASAL/INHALATION FLOW TESTS

TEST NO	GAS MIX	DEPTH (FSW)	FLOW (LPM)	TIN (C)	TOUT (C)	TWALL (C)	H KC/CM↑2-S-C	RE NO	NU NO
11	AIR	0.0	25.4	39.8	47.5	49.2	1.01E-06	2725.1	20.4
12	AIR	0.0	31.9	38.2	46.6	49.1	1.20E-06	3422.4	24.3
13	AIR	0.0	47.4	37.4	45.8	48.8	1.72E-06	5085.4	34.6
14	AIR	0.0	59.1	36.6	45.1	48.6	2.05E-06	6340.6	41.4
15	AIR	0.0	79.5	35.2	44.0	48.4	2.59E-06	8529.2	52.2
16	AIR	0.0	96.8	35.0	43.5	48.5	3.00E-06	10385.3	60.4
17	AIR	0.0	113.7	34.8	43.2	48.5	3.41E-06	12198.4	68.8
18	AIR	0.0	88.0	35.9	44.2	48.8	2.77E-06	9441.2	55.8
19	AIR	0.0	66.7	37.6	45.5	49.0	2.26E-06	7156.0	45.5
20	HE	0.0	40.1	36.5	49.1	49.8	1.33E-06	545.5	4.7
21	HE	0.0	81.8	33.8	47.1	49.6	2.41E-06	1112.8	8.5
22	HE	0.0	150.4	31.3	44.5	49.4	3.85E-06	2046.0	13.6
23	HE	0.0	76.0	34.1	47.1	49.2	2.28E-06	1033.9	8.1
24	HE	0.0	52.7	36.1	48.3	49.4	1.70E-06	716.9	6.0
25	HE	0.0	15.2	42.0	50.2	50.3	5.27E-07	206.8	1.9
26	HE	0.0	27.2	39.4	49.7	49.9	9.34E-07	370.0	3.3
40	N2	200.0	12.5	40.2	46.1	49.7	2.70E-06	9286.6	54.3
41	N2	200.0	22.4	36.0	42.7	48.9	4.04E-06	16641.6	81.3
42	N2	200.0	28.8	33.8	40.5	48.4	4.56E-06	21396.3	92.0
43	N2	200.0	45.6	32.2	38.6	48.1	6.37E-06	33877.5	128.5
44	HE	200.0	23.1	37.4	45.4	50.6	3.45E-06	2203.6	12.2
45	HE	200.0	28.2	36.0	45.3	50.4	4.46E-06	2690.1	15.7
46	HE	200.0	49.1	34.5	43.0	50.1	6.58E-06	4683.8	23.2
47	HE	200.0	44.8	34.9	43.3	49.8	6.20E-06	4273.6	21.9
48	HE	1000.0	4.3	40.1	46.4	51.4	2.59E-06	1797.9	9.0
49	HE	1000.0	60.6	33.2	36.9	49.4	1.51E-05	25338.5	52.3
50	HE	1000.0	23.9	35.1	40.8	49.6	1.02E-05	9993.2	35.3
51	N2	1000.0	5.1	38.0	47.0	50.5	5.75E-06	16679.1	110.7
52	N2	1000.0	9.6	37.6	43.8	49.9	7.65E-06	31396.0	147.2
53	N2	1000.0	9.2	37.3	43.0	49.6	5.70E-06	30087.9	129.0

TABLE 9. EXPERIMENTAL RESULTS DURING ORAL/EXHALATION FLOW TESTS

TEST NO	GAS MIX	DEPTH (FSW)	FLOW (LPM)	TIN (C)	TOUT (C)	TWALL (C)	H KC/CM↑2-S-C	RE NO	NU NO
63	AIR	0.0	13.3	45.1	46.5	50.6	2.03E-07	1426.9	4.1
64	AIR	0.0	20.4	45.3	46.2	50.3	2.08E-07	2188.6	4.2
65	AIR	0.0	31.1	42.8	45.2	50.1	5.99E-07	3336.6	12.1
66	AIR	0.0	37.7	41.9	44.2	50.1	6.12E-07	3980.3	12.3
67	AIR	0.0	44.8	39.9	44.2	49.8	1.15E-06	4806.4	23.1
68	AIR	0.0	72.8	37.3	42.7	49.7	1.89E-06	7810.4	38.0
69	AIR	0.0	61.4	38.6	43.7	49.7	1.68E-06	6587.4	33.9
70	AIR	0.0	95.0	36.8	42.8	49.9	2.66E-06	10192.2	53.6
71	AIR	0.0	108.7	36.4	42.5	49.7	2.99E-06	11662.0	60.3
72	HE	0.0	88.6	41.4	41.9	48.8	2.81E-07	1205.3	1.0
73	HE	0.0	27.8	45.0	45.8	48.9	2.44E-07	378.2	0.9
74	HE	0.0	124.3	39.0	40.6	48.8	8.42E-07	1690.9	3.0
75	HE	0.0	211.7	36.6	38.2	48.4	1.23E-06	2879.9	4.3
76	HE	0.0	106.9	41.0	41.2	48.2	1.58E-07	1454.2	0.6
77	HE	0.0	41.0	44.6	44.7	48.4	4.58E-08	557.8	0.2
104	N2	200.0	5.8	45.9	48.4	54.0	7.46E-07	4309.0	15.0
105	N2	200.0	26.9	42.5	46.2	53.7	3.75E-06	19984.8	75.6
106	N2	200.0	6.8	45.8	48.7	54.0	1.02E-06	5051.9	20.6
107	N2	200.0	10.0	40.7	46.7	54.0	1.91E-06	7429.3	38.5
108	N2	200.0	16.2	38.6	44.8	53.9	2.79E-06	12035.4	56.2
109	N2	200.0	35.5	35.7	41.8	53.7	5.09E-06	26374.0	102.7
110	HE	200.0	11.6	45.8	46.9	53.9	4.50E-07	1106.6	1.6
111	HE	200.0	35.6	38.5	44.3	54.1	3.93E-06	3396.0	13.9
112	HE	200.0	15.2	45.3	47.9	53.9	1.35E-06	1450.0	4.8
113	HE	200.0	24.5	43.1	46.1	53.8	2.06E-06	2337.1	7.3
114	HE	200.0	9.1	47.6	49.0	53.9	5.85E-07	868.1	2.1
115	HE	200.0	22.5	43.7	46.5	53.9	1.82E-06	2146.3	6.4
116	HE	200.0	50.7	37.1	42.7	53.6	5.18E-06	4836.4	18.3
117	HE	1000.0	4.5	41.9	46.9	54.4	2.35E-06	1881.6	8.2
118	HE	1000.0	11.2	39.3	44.3	53.9	5.01E-06	4683.0	17.4
119	HE	1000.0	44.4	34.6	38.6	52.6	1.28E-05	18564.8	44.4

TABLE 9. EXPERIMENTAL RESULTS DURING ORAL/EXHALATION FLOW TESTS (Con't)

TEST NO	GAS MIX	DEPTH (FSW)	FLOW (LPM)	TIN (C)	TOUT (C)	TWALL (C)	H KC/CM↑2-S-C	RE NO	NU NO
120	N2	1000.0	2.0	44.7	47.8	53.4	1.35E-06	6540.8	26.0
121	N2	1000.0	20.9	37.1	41.1	52.8	1.01E-05	68351.8	193.9
122	N2	1000.0	13.1	38.5	42.3	52.8	6.58E-06	42842.5	126.6
123	N2	1000.0	7.3	40.7	44.6	52.9	4.47E-06	23874.1	86.0
124	HE	0.0	185.1	40.9	44.3	52.5	2.28E-06	2518..	8.1
125	HE	0.0	60.0	45.6	48.2	52.5	9.49E-07	816.2	3.4
126	HE	0.0	42.1	46.5	48.8	52.4	6.84E-07	572.7	2.4
127	HE	0.0	87.2	43.5	46.7	52.5	1.33E-06	1186.2	4.7
128	HE	0.0	157.6	40.5	43.8	52.4	1.87E-06	2143.9	6.6

TABLE 10. EXPERIMENTAL RESULTS DURING ORAL/INHALATION FLOW TESTS

TEST NO	GAS MIX	DEPTH (FSW)	FLOW (LPM)	TIN (C)	TOUT (C)	TWALL (C)	H KC/CM↑2-S-C	RE NO	NU NO
78	HE	0.0	40.8	32.0	43.4	48.6	1.20E-06	555.0	4.3
79	HE	0.0	98.0	28.9	40.8	48.3	2.58E-06	1333.2	9.1
80	HE	0.0	159.6	26.3	37.1	47.7	3.46E-06	2171.2	12.2
81	HE	0.0	210.7	25.8	36.5	47.9	4.37E-06	2864.9	15.5
82	HE	0.0	97.3	29.1	40.3	48.0	2.48E-06	1323.6	8.8
83	HE	0.0	81.7	31.2	42.6	48.5	2.31E-06	1111.4	8.2
84	AIR	0.0	14.7	39.7	44.8	48.8	4.95E-07	1577.1	10.0
85	AIR	0.0	20.5	39.2	44.1	48.9	6.23E-07	2199.4	12.6
86	AIR	0.0	30.9	38.0	43.1	49.1	8.52E-07	3315.1	17.2
87	AIR	0.0	43.5	36.8	43.0	49.0	1.33E-06	4666.9	26.7
88	AIR	0.0	51.7	36.3	42.4	49.2	1.46E-06	5546.7	29.5
89	AIR	0.0	60.6	35.6	41.9	49.1	1.69E-06	6501.5	34.0
90	AIR	0.0	80.7	33.9	40.1	49.1	1.98E-06	8658.0	39.8
91	AIR	0.0	119.4	32.0	38.2	48.9	2.63E-06	12809.9	53.0
92	AIR	0.0	97.0	33.4	39.8	49.2	2.36E-06	10438.9	47.7
93	AIR	0.0	132.6	32.5	38.6	49.0	2.94E-06	14226.1	59.3
94	N2	200.0	7.7	40.2	48.2	57.4	1.52E-06	5720.5	30.7
95	N2	200.0	20.7	35.0	43.7	56.8	3.52E-06	15378.6	70.9
96	N2	200.0	32.2	32.6	40.5	56.1	4.60E-06	23922.3	92.8
97	N2	200.0	41.1	32.2	39.3	55.6	5.30E-06	30534.4	106.8
98	N2	200.0	48.4	31.6	37.9	55.0	5.54E-06	35957.7	111.7
99	HE	200.0	3.3	41.2	49.4	55.4	5.72E-07	314.8	2.0
100	HE	200.0	41.2	32.5	42.5	54.7	5.60E-06	3930.2	19.7
101	HE	200.0	19.6	34.6	46.1	54.8	3.36E-06	1869.7	11.8
102	HE	200.0	14.3	36.1	47.7	54.9	2.65E-06	1364.1	9.4
103	HE	200.0	7.8	37.7	49.4	54.7	1.62E-06	744.1	5.7
129	N2	1000.0	3.3	37.4	46.0	54.2	3.26E-06	10792.4	62.7
130	N2	1000.0	10.4	31.7	42.1	53.5	9.54E-06	34012.4	183.5
131	N2	1000.0	10.7	31.4	37.2	52.5	5.67E-06	34993.5	109.2
132	N2	1000.0	12.1	32.0	37.4	52.1	6.23E-06	39572.1	119.9
133	N2	1000.0	6.8	33.5	39.8	51.9	4.49E-06	22238.9	86.3
134	N2	1000.0	25.2	31.5	34.9	51.5	8.23E-06	82414.6	158.3

TABLE 10. EXPERIMENTAL RESULTS DURING ORAL/INHALATION FLOW TESTS (Con't)

TEST NO	GAS MIX	DEPTH (FSW)	FLOW (LPM)	TIN (C)	TOUT (C)	TWALL (C)	H KC/CM↑2-S-C	RE NO	NU NO
135	HE	1000.0	3.6	37.2	44.1	51.7	2.26E-06	1505.3	7.8
136	HE	1000.0	15.8	32.7	38.8	51.0	6.92E-06	6606.4	24.0
137	HE	1000.0	6.1	34.1	43.1	51.3	4.20E-06	2550.6	14.6

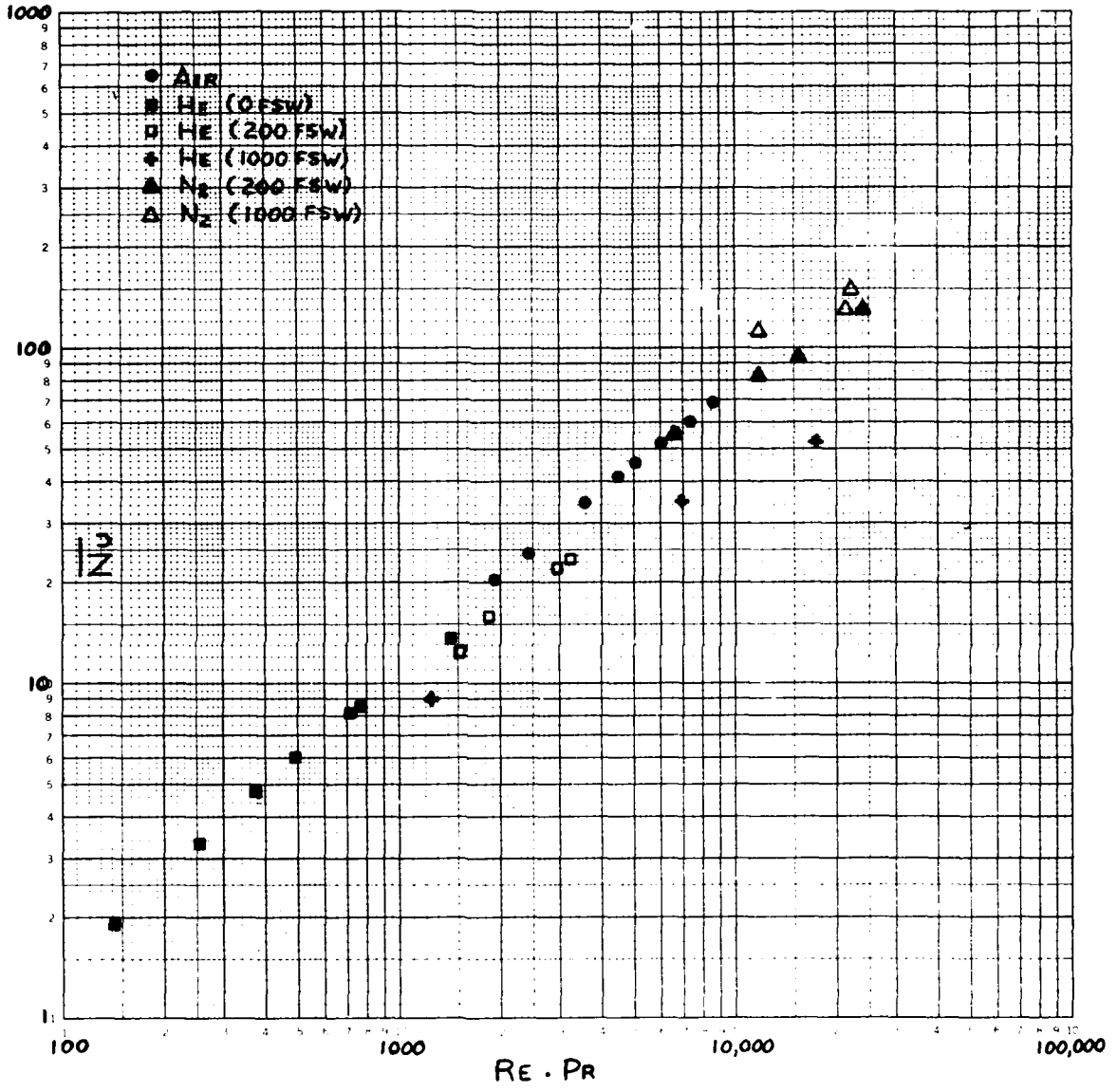

FIGURE 31: HEAT TRANSFER CHARACTERISTICS OF NASAL TRACT DURING INHALATION (PRELIMINARY)

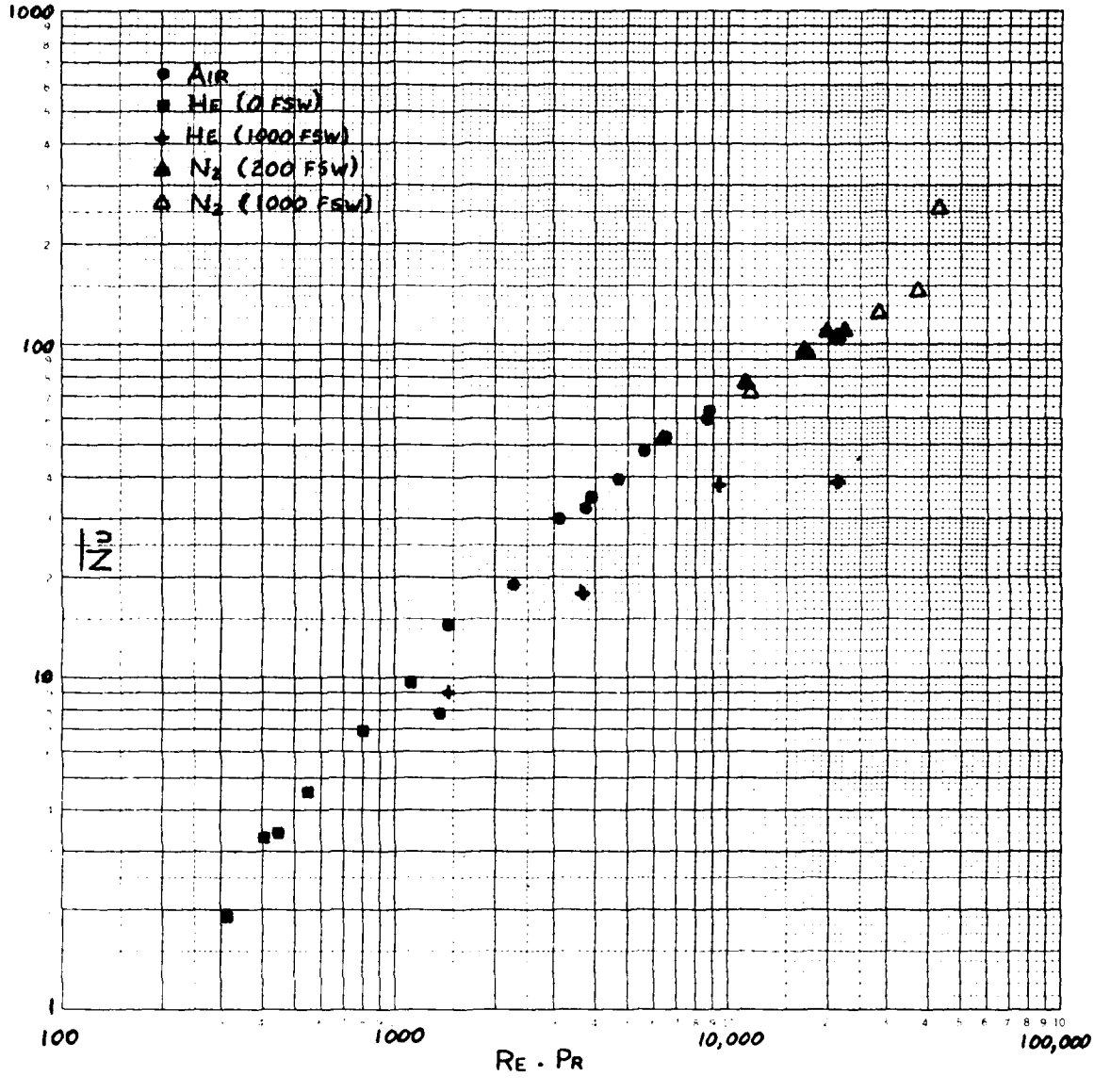

FIGURE 32: HEAT TRANSFER CHARACTERISTICS OF NASAL TRACT DURING EXHALATION (PRELIMINARY)

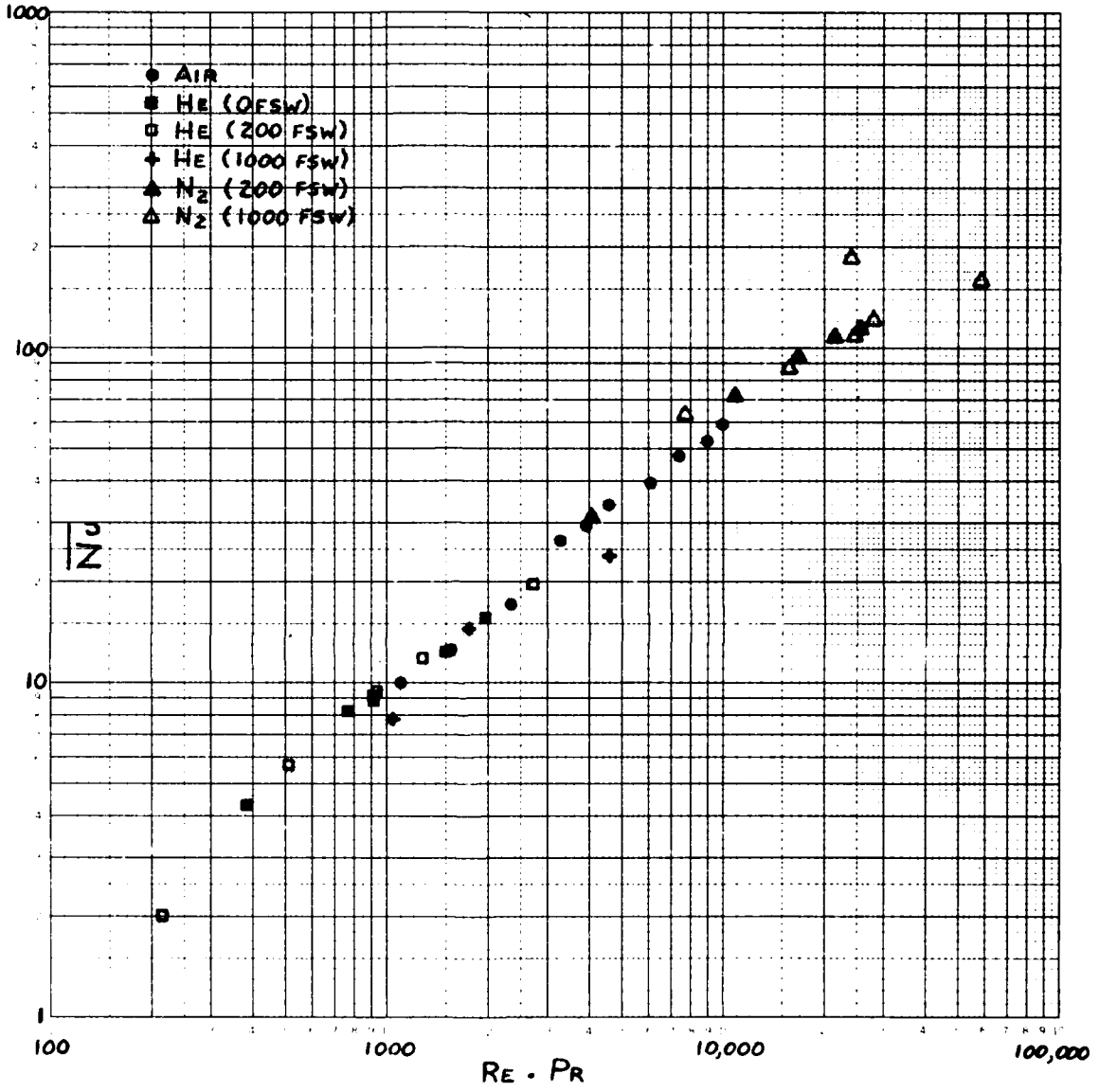

FIGURE 33: HEAT TRANSFER CHARACTERISTICS OF ORAL TRACT DURING INHALATION (PRELIMINARY)

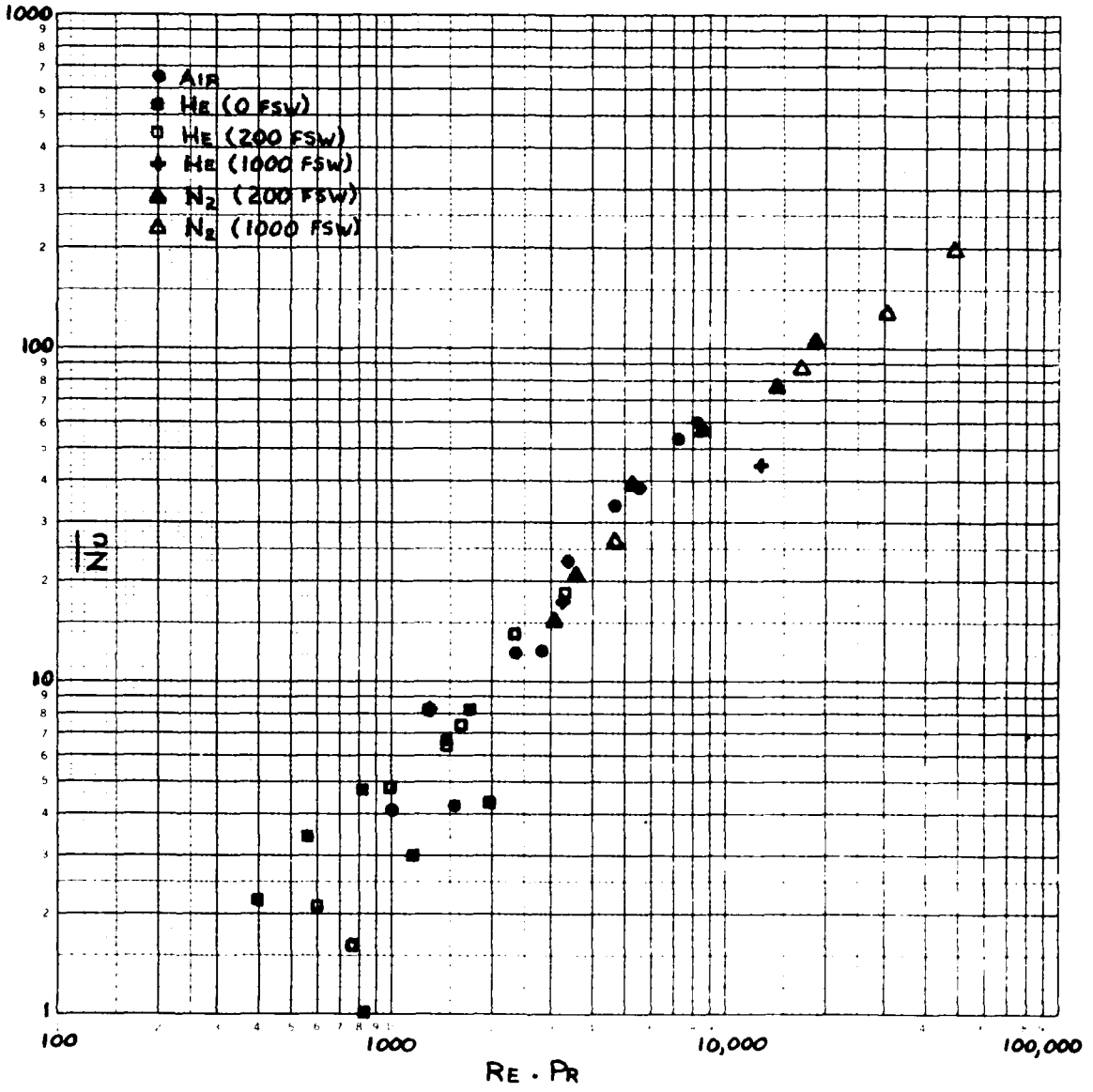

FIGURE 34: HEAT TRANSFER CHARACTERISTICS OF ORAL TRACT DURING EXHALATION (PRELIMINARY)

This apparent discrepancy is felt to be attributable to the initial assumption of a constant wall temperature model. Variations from this assumption, if not detected adequately by the thermocouples embedded in the walls adjacent to the gas stream, would cause erroneously high values for ΔT_w and thus low calculated values of the heat transfer coefficient, $\bar{h}$, and $\overline{Nu}$. To test out this hypothesis finite difference solutions for the model wall temperature distributions were determined under various conditions of simulated depths and test gases in Appendix D. For this idealized representation of the model wall with air at sea level as the test medium (Biot number, $\bar{h}$ L/K, approximately equal to 2.0), it is observed in Figure D-3 that the model wall adjacent to the gas stream has cooled to

$$\frac{T - T_s}{T_\infty - T_s} \simeq 0.93$$

after 3 seconds gas stream flow (This is the approximate time at which data was recorded).

where: T_s is the gas stream temperature, °C, and T_∞ is the water bath temperature, °C. At approximately 1/8 cm (.049 inch) from the model surface this dimensionless temperature would be approximately 0.99 following the 3 second interval. A small thermocouple with a bead diameter of 1/8 cm (having a calculated response time of 0.1 seconds in oil) which is embedded in the model wall would actually record an average temperature based on the above two values of 0.96, or give approximately a 3% error in the model surface temperature. For the same model with a Biot number of 40.0 (typical of helium at 305 MSW) the model surface would have a dimensionless temperature of approximately 0.27 following an interval of 3 seconds and 0.91 at 1/8 cm from the surface after the same 3 seconds. Under these conditions the

thermocouple would now record an average dimensionless temperature of 0.59 for a error of approximately 119% in this parameter. The result of this error would be to record higher wall temperatures, T_w, than actually present. As previously stated, these high values of T_w give high calculated values of ΔT_w, and subsequently low values of $\overline{Nu}$ for helium at 305 MSW. This error diminishes rapidly as the Biot number decreases. This would indicate that the data recorded with models having low Biot numbers (low values of $\bar{h}$ or high values of K for the model walls) would provide the most accurate information for establishing heat transfer relationships for the model of the upper respiratory tract. It should be noted that the data recorded from the lower respiratory tract should offer maximum accuracy since its Biot number was less than 0.05.

Based on the above analysis, the data recorded for helium at 305 MSW was not utilized in establishing the heat transfer characteristics of the upper tract model. The remainder data is shown in Figures 35-38 for establishing the heat transfer mechanisms for each breathing mode. A curve-fitting routine as outlined in Reference 37 was utilized to obtain least square fits of the above data. Results of this curve-fitting are outlined below:

$$\underline{\text{Nasal Breathing}}_{\text{Inhalation}}: \quad \overline{Nu} = 0.028\ (RePr)^{0.854} \tag{11}$$

$$\underline{\text{Nasal Breathing}}_{\text{Exhalation}}: \quad \overline{Nu} = 0.0045\ (RePr)^{1.080} \text{ for } Re \leq 7800 \tag{12a}$$

$$\overline{Nu} = 0.310\ (RePr)^{0.585} \text{ for } Re > 7800 \tag{12b}$$

$$\underline{\text{Oral Breathing}}_{\text{Inhalation}}: \quad \overline{Nu} = 0.035\ (RePr)^{0.804} \tag{13}$$

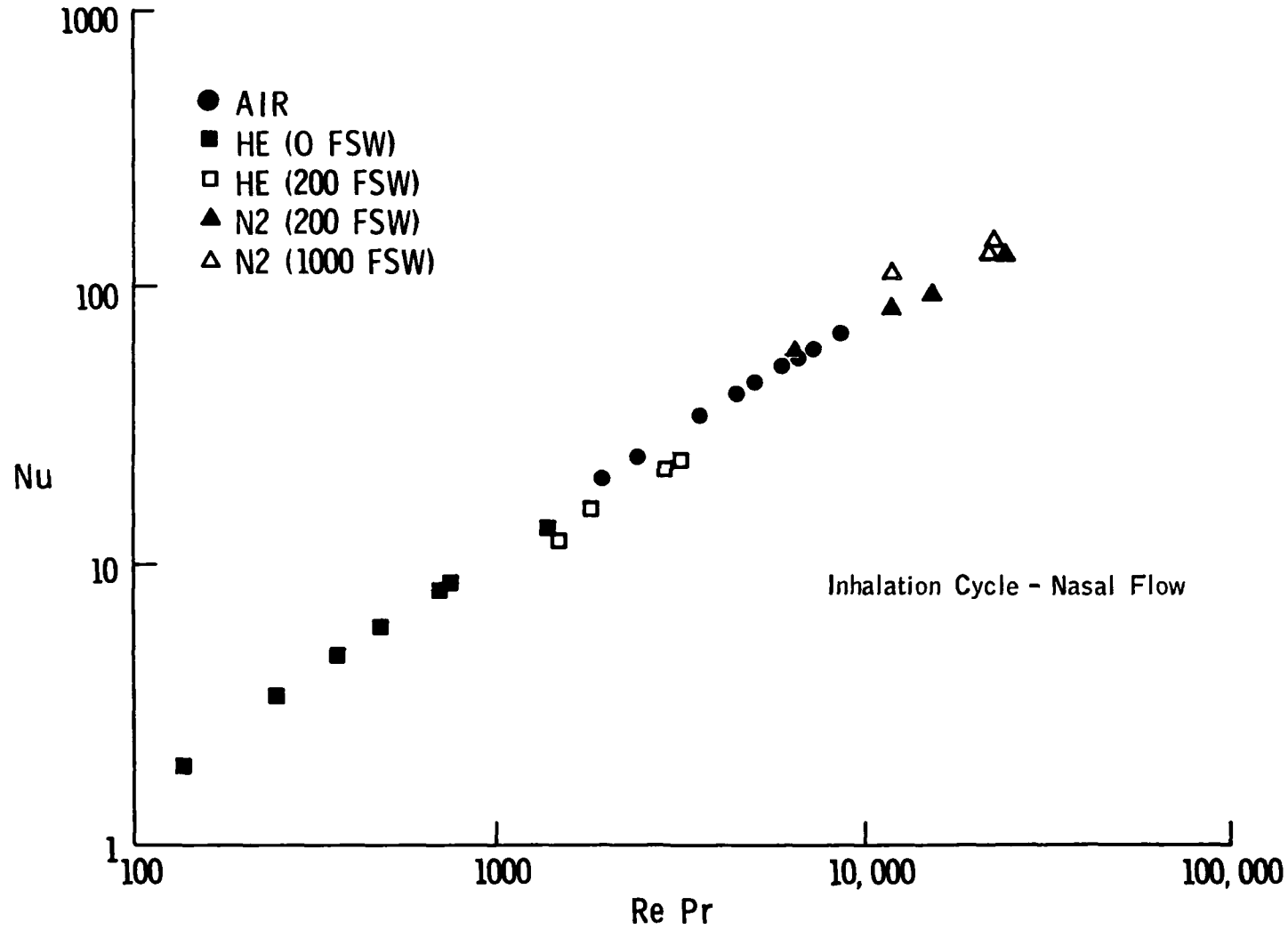

FIGURE 35: HEAT TRANSFER CHARACTERISTICS-UPPER RESPIRATORY TRACT

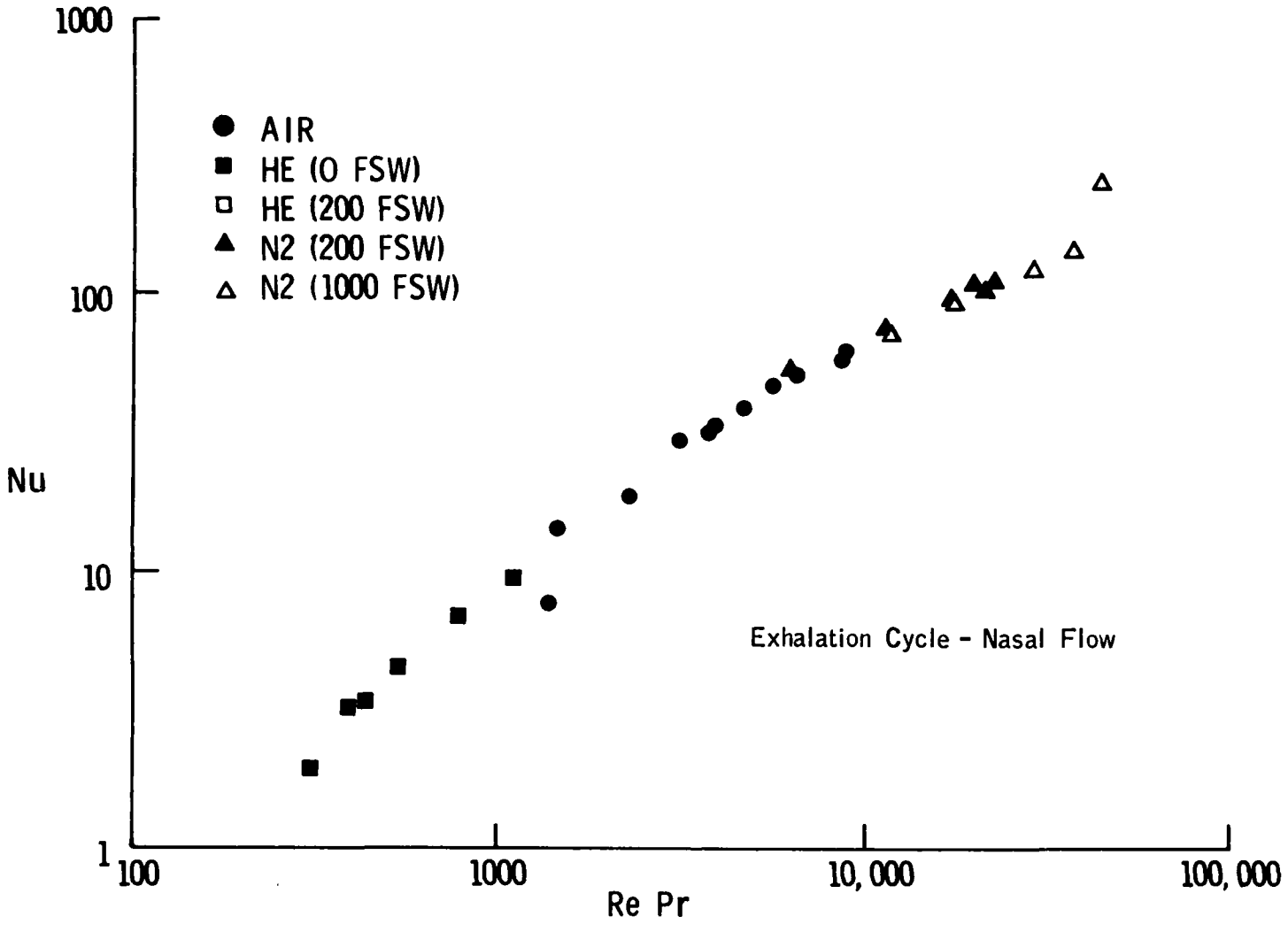

FIGURE 36: HEAT TRANSFER CHARACTERISTICS - UPPER RESPIRATORY TRACT

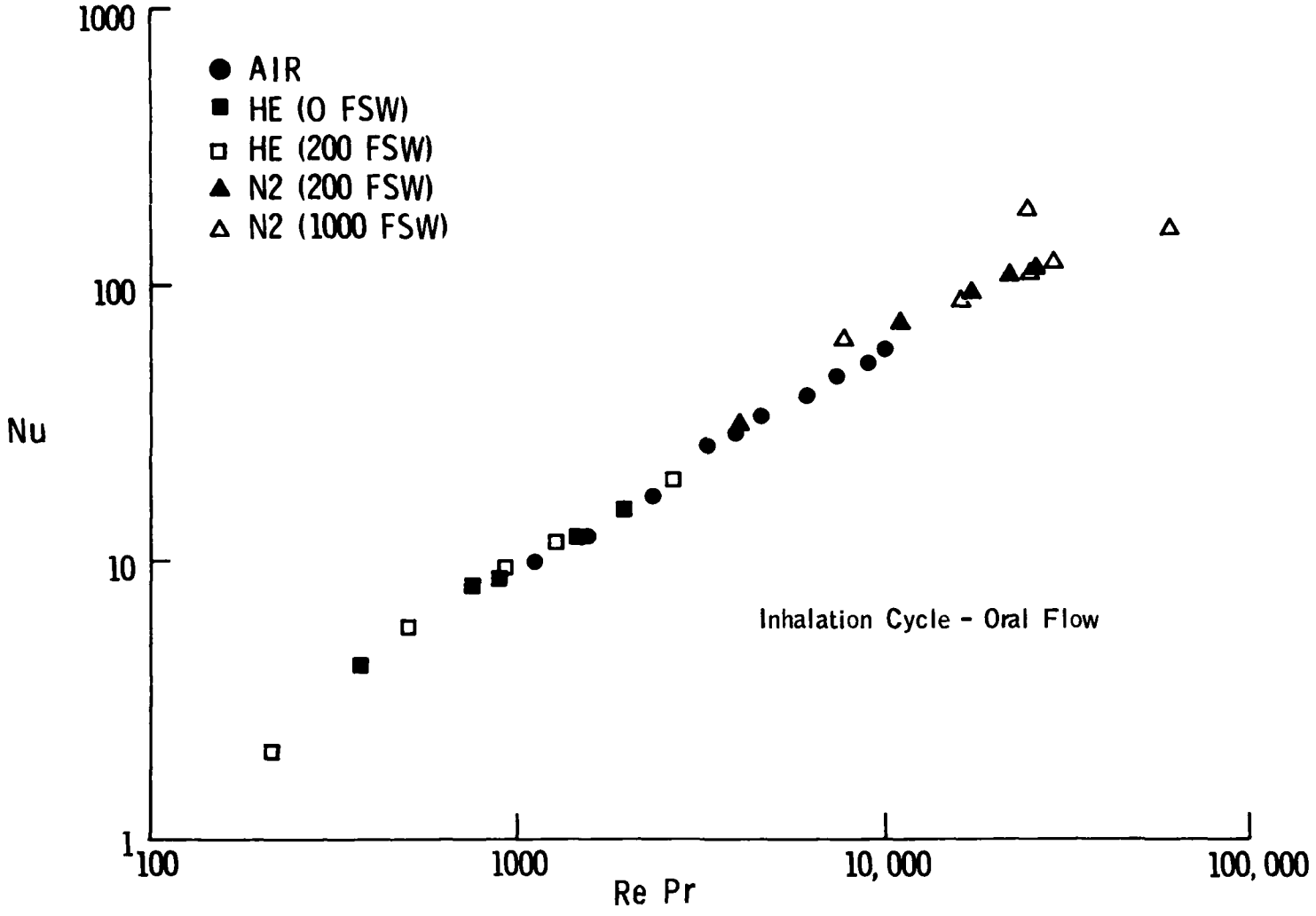

FIGURE 37: HEAT TRANSFER CHARACTERISTICS - UPPER RESPIRATORY TRACT

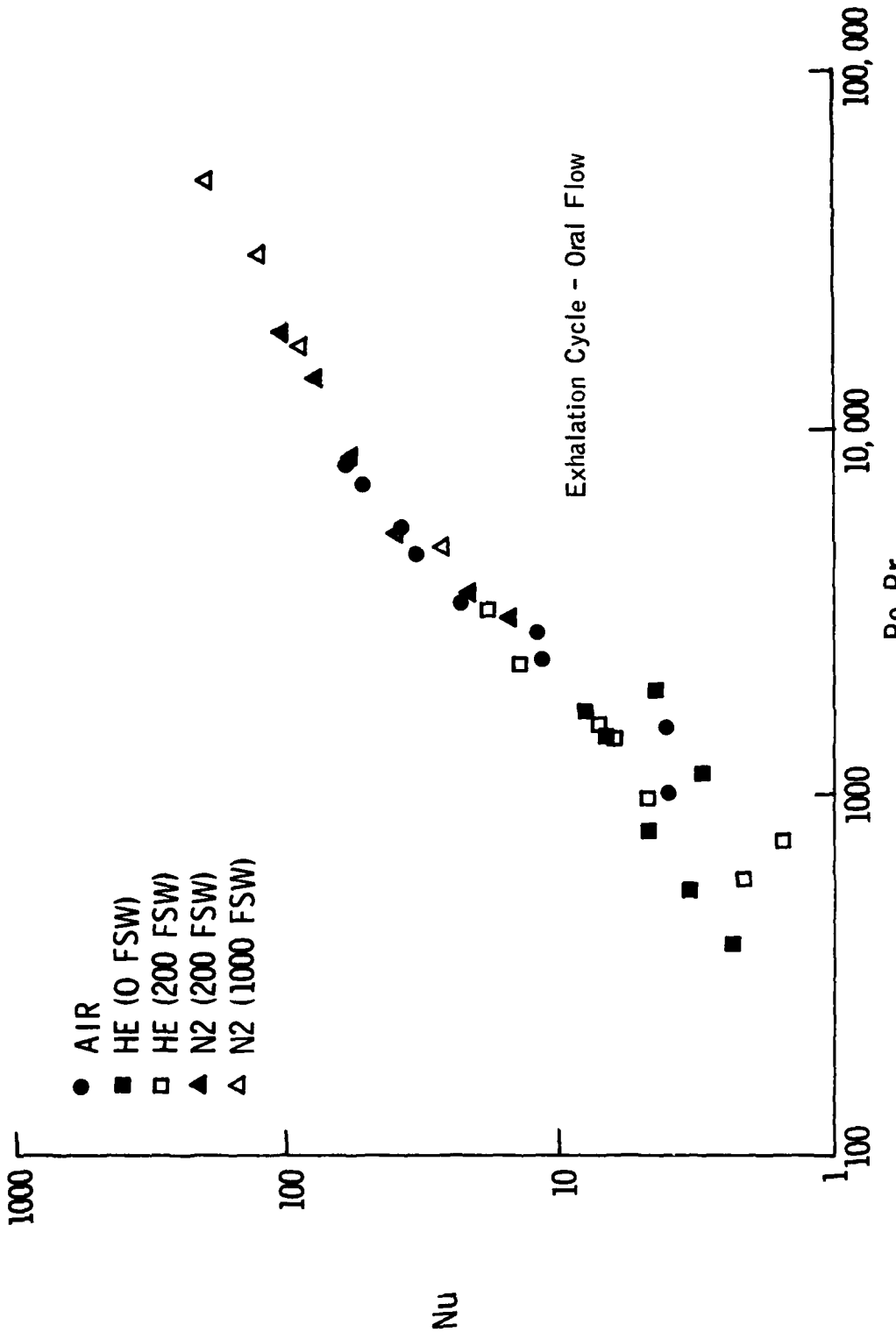

FIGURE 38: HEAT TRANSFER CHARACTERISTICS - UPPER RESPIRATORY TRACT

$$\underline{\text{Oral Breathing}}\ \underline{\text{Exhalation}}: \quad \overline{Nu} = 0.0006\ (RePr)^{1.269} \quad \text{for } Re \leq 12{,}000 \tag{14a}$$

$$\overline{Nu} = 0.094\ (RePr)^{0.704} \quad \text{for } Re > 12{,}000 \tag{14b}$$

The above relationships are based on the physical dimensions and gas flow properties in the trachea and are applicable for Reynolds number values up to 70,000. A composite of the above relationships is shown in Figure 39 for comparison. As a rule the heat transfer characteristics of the nasal tract exceed those of the oral tract during both inhalation and exhalation at comparable values of Re. During exhalation, the slopes of the curves appear to decrease at the higher values of Re·Pr for both oral and nasal breathing. No explanation is offered for this apparent trend.

Comparative Conditioning Capabilities of Oral and Nasal Passageways

It is universally accepted that the nasal airways are more suitable for heating and humidifying inspired gases than the oral airway. Without repeating a detailed discussion of the anatomies of these two passageways, it is sufficient to explain this superior conditioning capability as being due to the relatively large surface area-to-cross sectional area ratio that exists in the nasal passageway. A relatively large cross-sectional area in the main nasal passage is broken into narrow widths by the nasal septum, dividing the nasal airway into two, and further by the folds of the turbinates. With the derived heat transfer relationships found in this investigation, we are now able to quantify these relative conditioning efficiencies.

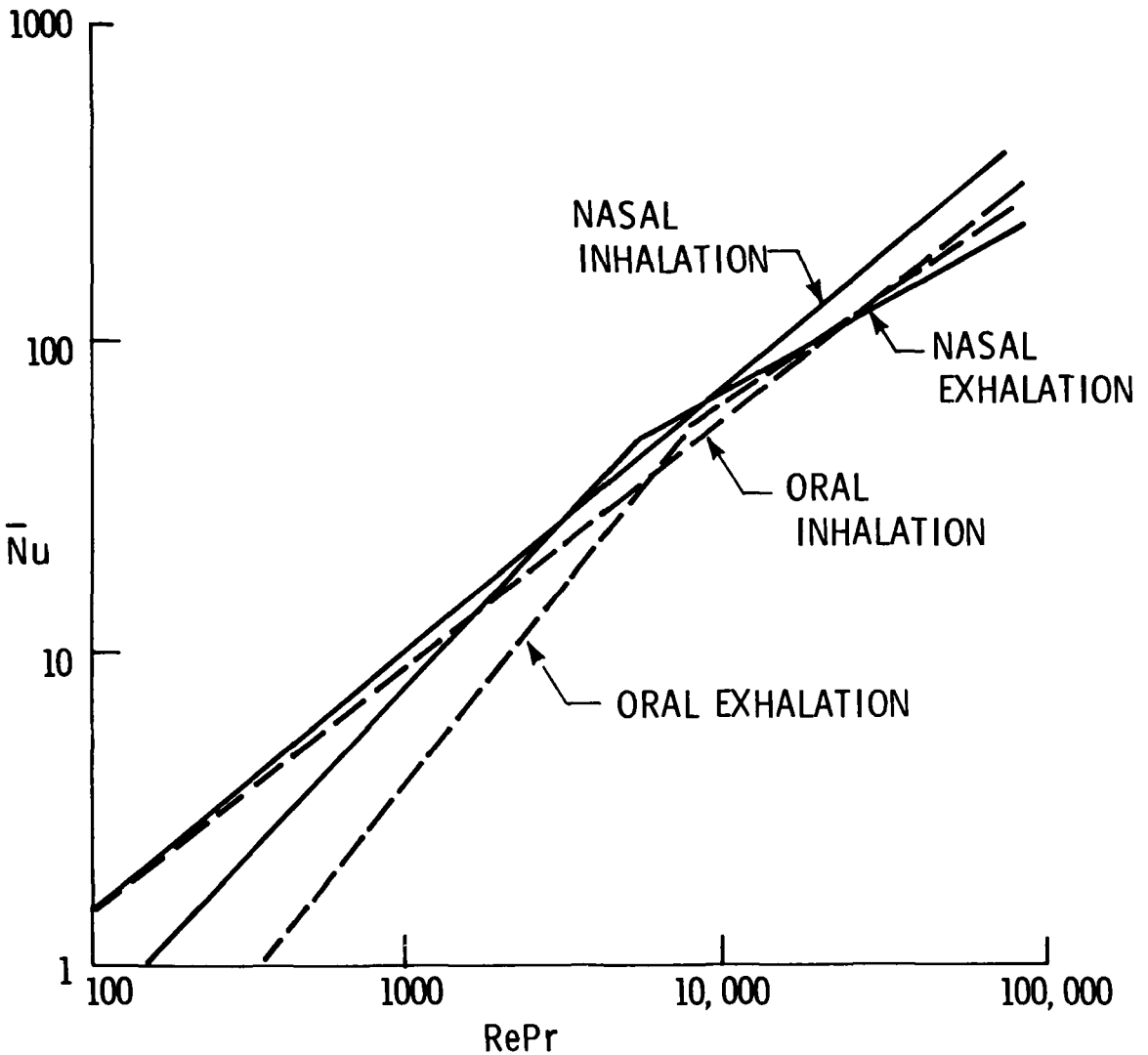

FIGURE 39: COMPARISON OF HEAT TRANSFER CHARACTERISTICS IN VARIOUS BREATHING MODES

In the following analysis a relative conditioning efficiency factor for the nasal and oral passageways will be defined and evaluated. While this analysis is based strictly on the results of the previous heat transfer characterizations and does not consider the effects of insensible heat transfer, as we will see in the next chapter the insensible heat transport process parallels closely this sensible heat transport. Thus, the relative conditioning efficiencies presented here should be indicative of the overall energy exchange process in the upper airways.

Recall that these relationships were derived by defining a characteristic diameter (trachea) and passageway length, with an overall heat transfer coefficient calculated as follows (Equation 5):

$$\bar{h} = \rho C_p \left(\frac{\Delta T}{\Delta T_w}\right) \left(\frac{\bar{V}D}{4L}\right)$$

where:

ρ, C_p are gas properties

L, D are characteristic length and diameter of passageway

$\bar{V}$ = mean flow velocity at diameter D

ΔT = Differential gas temperature across passageway

ΔT_w = Temperature differential between passageway wall and entering gas temperature

By rearranging the above expression we get

$$\Delta T = \frac{4\bar{h}\ L\ \Delta T_w}{\rho C_p\ \bar{V}D}$$

where:

$\bar{h} = \overline{Nu}\ \frac{K}{D}$ K = gas thermal conductivity

Therefore

$$\Delta T = \frac{4\ \overline{Nu}\ K\ L\ \Delta T_w}{\rho C_p\ \bar{V}\ D^2}\ .$$

A conditioning efficiency term can be defined for each passageway as

$$\eta = \frac{\Delta T}{\Delta T_w} = \frac{4\ \bar{N}_u\ K\ L}{\rho C_p\ \bar{V}\ D^2} \qquad (15)$$

This efficiency term, ranging in value from 0 to 1, indicates how closely the heat exchange process used in heating the inhaled gas approaches the maximum temperature differential possible, ΔT_w. The above expression can be used to compare the conditioning efficiencies of the oral and nasal passageways. During inhalation, the following heat transfer relationships were found for the upper passageways as

$$\overline{Nu} = 0.028\ (RePr)^{0.854} \qquad \text{[Nasal]} \qquad (11)$$

$$\overline{Nu} = 0.035\ (RePr)^{0.804} \qquad \text{[Oral]} \qquad (13)$$

Their relative conditioning capabilities can be evaluated by looking at the ratio η_{oral}/η_{nasal} at similar flow conditions.

$$\frac{\eta_{oral}}{\eta_{nasal}} = \frac{\dfrac{4\ \overline{Nu}_{oral}\ K\ L_{oral}}{\rho C_p\ \bar{V}\ D^2}}{\dfrac{4\ \overline{Nu}_{nasal}\ K\ L_{nasal}}{\rho C_p\ \bar{V}\ D^2}}$$

Since equal gas properties, flow velocities, and incoming gas temperatures for both passageways are present for similar flows we can reduce the above to

$$\frac{\eta_{oral}}{\eta_{nasal}} = \frac{\overline{Nu}_{oral}\, L_{oral}}{\overline{Nu}_{nasal}\, L_{nasal}} = \frac{0.035\ (Re\ Pr)^{0.804}}{0.028\ (Re\ Pr)^{0.854}} \left(\frac{19.7}{24.1}\right)$$

or reducing further

$$\frac{\eta_{oral}}{\eta_{nasal}} = 1.022\ (Re\ Pr)^{-0.05}$$

and for $Pr \tilde{\simeq} 0.7$ (for respirable gases considered)

$$\frac{\eta_{oral}}{\eta_{nasal}} = 1.04\ (Re)^{-0.05} \qquad (16)$$

A tabulation of these results is shown below:

Re	η_{oral}/η_{nasal}
500	0.762
1000	0.736
2000	0.711
5000	0.679
10,000	0.656
50,000	0.605
100,000	0.585

During exhalation, a similar ratio can be derived as

$$\frac{\eta_{oral}}{\eta_{nasal}} = \frac{0.094\ (Re\ Pr)^{0.704}}{0.310\ (Re\ Pr)^{0.585}}\ \left(\frac{19.7}{24.1}\right) \qquad \text{for } Re > 12{,}000$$

$$= 0.248\ (Re\ Pr)^{0.119}$$

or

$$\frac{\eta_{oral}}{\eta_{nasal}} = 0.238\ Re^{0.119} \quad \text{for the respirable gases.} \tag{17a}$$

For $Re < 7800$

$$\frac{\eta_{oral}}{\eta_{nasal}} = \frac{0.0006\ (Re\ Pr)^{1.269}}{0.0045\ (Re\ Pr)^{1.080}}\ \left(\frac{19.7}{24.1}\right)$$

$$= 0.1090\ (Re\ Pr)^{0.189}$$

or for $Pr \simeq 0.7$

$$\frac{\eta_{oral}}{\eta_{nasal}} = 0.1019\ Re^{0.189} \tag{17b}$$

A tablulation of these relative efficiency values follow:

Re	η_{oral}/η_{nasal}
100	0.243
500	0.330
1000	0.376
2000	0.429
5000	0.5097
7500	0.5503
12,000	0.728
50,000	0.862
100,000	0.937

Figure 40 shows the relative conditioning efficiencies of the oral and nasal passageways during inhalation. As expected, the oral passageway is a less efficient gas conditioner than the nasal passageway (ratio less than 1) across the entire range of tracheal Reynolds numbers. In addition, the oral conditioning capability is seen to be progressively worsened with higher Re (resulting from respiration in hyperbaric environments). Unfortunately, beyond an Re of approximately 15,000 (peak nasal resistances of 6 to 9 cm H_2O for all respirable mixes), mouth breathing was seen previously to be mandatory due to the high nasal resistance. One is thus forced to breathe through the mouth when its relative efficiency is seen to be lowest (0.6).

It should be noted that the derived relationships for oral breathing are applicable only for the configurations of the model tested. It is conceivable that variable conditioning capabilities can be obtained through the oral cavity by varying the position of the tongue relative to the roof of the mouth. The sensitivity of this variable configuration to heat transfer processes is left for future investigations.

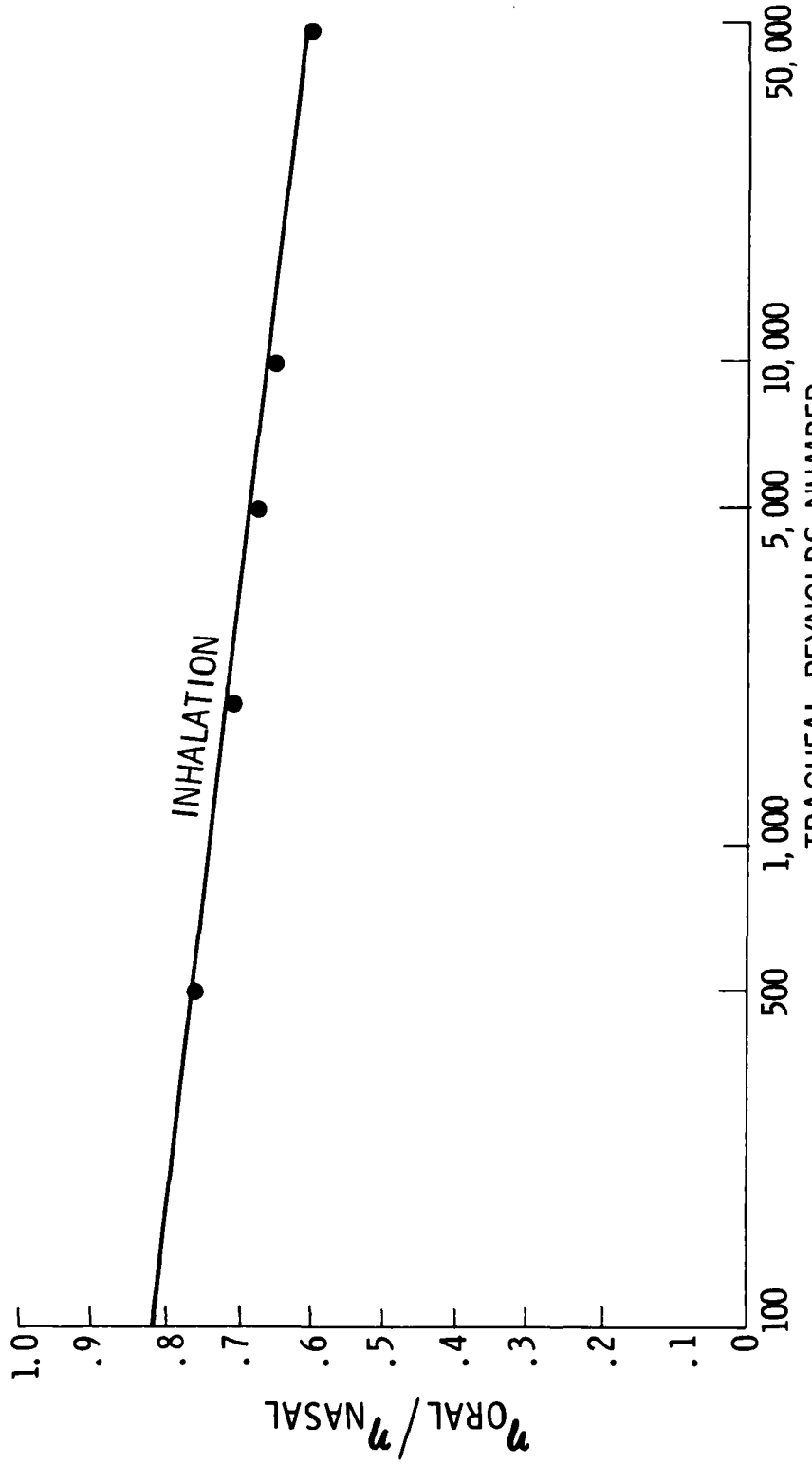

FIGURE 40: RELATIVE CONDITIONING CAPABILITIES OF ORAL AND NASAL PASSAGEWAYS

CHAPTER V

SIMILARITY RELATIONS FOR CONVECTIVE MASS TRANSFER

The determination of heat transfer relationships in the previous two chapters has satisfied only half the necessary requirements for our understanding of the conditioning capability of the human respiratory system. Humidification processes must also be characterized.

Heat transfer coefficients have been determined experimentally for a number of different flow geometries [60] by other investigators. As in the case of the models used in this investigation, these coefficients can be determined relatively easy over a wide range of flow conditions. On the other hand, data on mass transfer are relatively sparse [64] due to the complexity of experiments required to produce mass transfer coefficients. Fortunately, however, previous investigators [61, 62, 63] have recognized that there is an analogy between heat and mass, as well as, momentum transfer processes. They have been able to use heat transfer data in predicting mass transfer coefficients quite reliably at low mass transfer rates, situations not unlike the humidification process which takes place in the respiratory system. The following discussion will develop this analogy between heat and mass transfer in the human respiratory tract, and apply this analogy to derive mass transfer coefficients from the experimentally determined heat transfer data. The development of this analogy will be made for steady, fully developed flow and later modified to cover the special flow in the respiratory system.

Consider the steady isothermal flow of a gas, B, containing water vapor, A, in a segment of a tube (representative of the human airway) shown in Figure 41. We assume that the velocity distribution at plane "1" is known, and that the fluid concentration is constant at X_{A1} in the region $Z < 0$ where

X_A = mole fraction of water vapor; i.e., molar concentration of A divided by total molar density of mixture.

From $Z = 0$ to $Z = L$, the wall is coated with a thin layer of liquid water (mucus was reported earlier to be 95% water [38]) which dissolves slowly and maintains the liquid interface composition, X_{AO}, constant along the dissolving surface. The physical properties of the gas and liquid are also assumed constant along this tube section.

The rate of heat transfer by conduction, Q, through the tube walls between "1" and "2" can be written.

$$Q = \int_o^L \int_o^{2\pi} \left(K \frac{\partial T}{\partial r}_{r=R}\right) R \, d\theta \, dz$$

where

K = thermal conductivity of tube wall, $\frac{\text{watts}}{\text{cm-}^\circ\text{C}}$

R = tube radius, cm

$d\theta$, dz = elemental angle and length, respectively.

Additionally, this heat is transferred to gas B convectively as

$$Q = h_1 \pi 2RL (T_w - T_1)$$

where

T_w = tube wall temperature, °C

T_1 = bulk gas temperature at "1", °C

h_1 = heat transfer coefficient based on the initial temperature difference $(T_w - T_1)$, $\frac{\text{watts}}{\text{cm}^2\text{-°C}}$

For this tube segment, we can equate the conduction and convection heat flows at the wall to get

$$h_1 = \frac{1}{2\pi RL (T_w - T_1)} \int_o^L \int_o^{2\pi} \left(K \frac{\partial T}{\partial r}_{r=R}\right) R \, d\theta \, dz \qquad (18)$$

Note that this expression is valid for either laminar or turbulent flow, as long as all turbulent profiles are time smoothed.

Likewise, an expression for the mass transfer rate of water vapor to gas B in this tube section is shown by Bird, Stewart, and Lightfoot [61] to be

$$K_{X1} = \frac{1}{2\pi RL (X_{A0} - X_{A1})} \int_o^L \int_o^{2\pi} \left(CD_v \frac{\partial X_A}{\partial r}_{r=R}\right) R \, d\theta \, dz \qquad (19)$$

where

K_{X1} = mass transfer coefficient, $\frac{\text{gm - moles}}{\text{sec - m}^2}$

X_{A1} = mole fraction of water vapor at "1"

C = mix molar density = $\frac{\text{gm - moles}}{\text{m}^3}$

D_v = mass diffusivity coefficient of water vapor to gas, $\frac{\text{m}^2}{\text{sec}}$

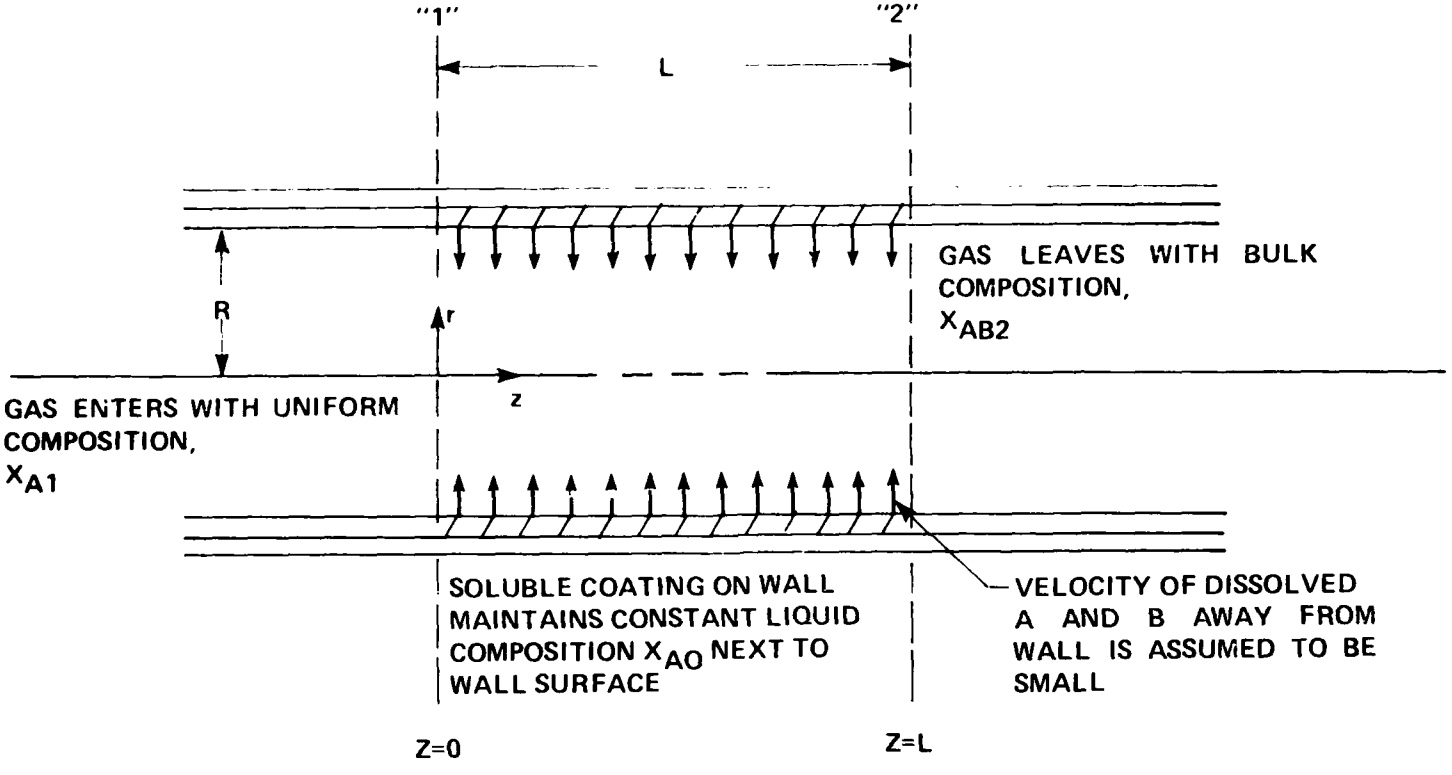

FIGURE 41: SEGMENT OF AIRWAY

Equations (18) and (19) are similar in form, with only a variation in constants and quantities of gradient. The similarities between equations (18) and (19) can be further highlighted by normalizing them with the following dimensionless quantities:

$$\bar{r} = \frac{r}{D}, \quad D = \text{tube diameter}$$

$$\bar{Z} = \frac{z}{D}$$

$$\bar{T} = \frac{T-T_w}{T_1-T_w}$$

$$\bar{X}_A = \frac{X_A - X_{A0}}{X_{A1}-X_{A0}}$$

Following normalization of equations (18) and (19),

$$\frac{h_1 D}{K} = \frac{1}{2\,\pi\,L/D}\int_0^{L/D}\int_0^{2\pi}\left(-\frac{\partial\bar{T}}{\partial\bar{r}}\right)_{\bar{r}=\frac{1}{2}} \overline{d\theta}\;\overline{dz} \tag{18a}$$

$$\frac{K_{X1} D}{C\,D_v} = \frac{1}{2\,\pi\,L/D}\int_0^{L/D}\int_0^{2\pi}\left(-\frac{\partial\bar{X}_A}{\partial\bar{r}}\right)_{\bar{r}=\frac{1}{2}} \overline{d\theta}\;\overline{dz} \tag{19a}$$

The close resemblance between the right side of equations (18a) and (19a) is seen to differ by only the quantity of gradient at the tube wall interface; i.e., temperature gradient for heat transfer and mole fraction gradient for mass transfer.

The group of terms on the left of equation (18a) is recognized as the dimensionless Nusselt number, Nu. This number is a dimensionless expression for the heat transfer coefficient. Similarly, the dimensionless mass transfer coefficient seen on the right side of equation (19a) is the Sherwood number, Sh; i.e.,

$$Nu \equiv \frac{h_1 D}{K}$$ can be interpreted as the ratio of the temperature gradient at wall to the overall stream temperature difference [65].

and

$$Sh \equiv \frac{K_{X1} D}{C\, D_v}$$ can be interpreted as the ratio of mass diffusivity to molecular diffusivity [65].

Bird, Stewart, and Lightfoot [61] have additionally shown that this resemblance can be further highlighted by observing the normalized equations of change for heat and mass transfer in this tube section. When viscous dissipation is ignored the energy equation for this system is written

$$\frac{D\bar{T}}{D\bar{t}} = \frac{1}{RePr}\, \bar{\nabla}^2\, \bar{T} \tag{20}$$

where

Re = Reynolds number, $\rho VD/\mu$

Pr = Prandtl number, $C_p\mu/K$

and the motion equation for mass transfer is

$$\frac{D\bar{X}_A}{D\,\bar{t}} = \frac{1}{ReSc}\, \bar{\nabla}^2\, \bar{X}_A \tag{21}$$

where Sc = Schmidt number, $\mu/\rho D_v$.

These equations are seen to be analogous. In fact, we can see that provided Pr = Sc the dimensionless temperature and water vapor mole fraction profiles must be identical. Under these conditions the solutions to equations (18a) and (19a) would be exactly the same, and we could equate

$$\frac{h_1 D}{K} = \frac{K_{X1} D}{C\, D_v}$$

or

$$Nu = Sh. \tag{22}$$

Although, it is shown in Appendix E that Pr is in fact approximately equal to Sc for the respirable gases evaluated in this study, in general we can derive expressions to handle unequal values of Sc and Pr. (This development will follow shortly.)

By going through a similar analysis as above, see Appendix H, the dimensionless velocity profiles for certain fully developed flow problems can be shown to be identical to the temperature profiles provided the molecular Prandtl number, Pr, is unity [60].

Note: For turbulent flow, $Pr = Pr_t = 1.0$ must apply [65]

where

$$Pr_t = \frac{\varepsilon_m}{\varepsilon_H} = \frac{\text{Eddy Diffisivity of Momentum}}{\text{Eddy Diffisivity of Heat}}$$
$$= \text{Turbulent Prandtl Number}$$

Under this condition

$$\frac{h_1 D}{K} = \frac{f}{2}\, Re \tag{23}$$

where

f = tube friction factor.

Equation 23 is the well known Reynolds analogy [65], see Appendix H, which has been used for years to reliably correlate convective heat transfer with friction factors for fully developed flow systems with Prandtl numbers of approximately one.

A closer look at the physical meaning of the dimensionless groups discussed above gives added insight into these analogous heat, mass, and momentum processes. By definition

$$\text{Prandtl number} = Pr = \frac{\upsilon, \text{ kinematic viscosity (momentum diffusivity)}}{\alpha, \text{ thermal diffusivity}}$$

$$= \frac{\upsilon}{\alpha} = \left(\frac{\mu}{\rho}\right)\left(\frac{C_p \rho}{K}\right) = \frac{C_p \mu}{K} .$$

Note that if the momentum diffusivity equals the thermal diffusivity (molecular and eddy), one would expect similar temperature and velocity profiles within the tube section. Although data on eddy diffusivities, ε, are rare, it has been observed that $\varepsilon_H = \varepsilon_m$ is a good approximation, except for liquid metals [65]. (This is the fundamental postulate for Reynolds analogy in turbulent flow.)

Similarly, the molecular Schmidt number is defined as

$$Sc = \frac{\upsilon, \text{ momentum diffusivity}}{D_v, \text{ mass diffusivity}}$$

$$= \left(\frac{\mu}{\rho}\right)\frac{1}{D_v} = \frac{\mu}{\rho D_v}$$

while the turbulent Schmidt number is

$$Sc_t = \frac{\varepsilon_m}{\varepsilon_D} = \frac{\text{Eddy Diffusivity of Momentum}}{\text{Eddy Mass Diffusivity}}$$

Here again, Sc = Pr and $Sc_t = Pr_t$ implies that mass diffusivity equals thermal diffusivity, giving similar temperature and water vapor mole fraction profiles. In the case of Sc = Pr = 1 (molecular and turbulent), or $D_v = \alpha = \upsilon$, the dimensionless mole fraction, temperature, and velocity profiles must be identical for the fully developed flow system in Figure 41. This permits us to equate equations (22) and (23) to give

$$Nu = Sh = \frac{f}{2} Re \qquad \text{for } Pr = Sc = 1.$$

Or since Sc = Pr = 1, we can rewrite the above to give

$$\frac{Nu}{Re\ Pr} = \frac{Sh}{Re\ Sc} = \frac{f}{2} \tag{24}$$

or after substitution

$$\frac{h_1}{\rho C_p V} = \frac{K_{X1}}{CV} = \frac{f}{2} \tag{24a}$$

The above relationships have been found to give reliable correlations of heat, mass, and friction factor data for fully developed flow systems having moderate temperature, low mass transfer rate flows with gases having Pr = Sc ≈ 1 [60]. Chilton and Colburn [62] showed empirically that the above relationships could be applied as well to gases with Prandtl and Schmidt numbers other than unity (they showed satisfactory correlations over range of 0.7 < Pr < 1000) by substituting $Pr^{1/3}$ for Pr and $Sc^{1/3}$ for Sc in equation (24) to give

$$j_H \equiv \frac{Nu}{RePr^{1/3}} = \left(\frac{h_1}{\rho C_p V}\right) (Pr)^{2/3} = \frac{f}{2} \tag{25}$$

and

$$j_D \equiv \frac{Sh}{ReSc^{1/3}} = \left(\frac{K_{X1}}{CV}\right) (Sc)^{2/3} = \frac{f}{2} \tag{26}$$

Due to the identical equalities displayed on the right hand sides of Equations (25) and (26), a direct result of the above relationships makes $j_H = j_D$. Equations (25) and (26) are known as the Chilton-Colburns j- factor analogy. They can be used to predict heat and mass transfer coefficients from friction factor data for fully developed flow over flat plates and straight tubes. Unfortunately, the complex flow through the respiratory system cannot be considered fully developed. For flow across bluff bodies or curved conduits as in the respiratory system the drag coefficients based on total drag are seen to be much greater than the j- factors. (See Appendix F). This discrepancy is due to the drag coefficients for bluff bodies are based on the drag due to skin friction, and the additional form drag component. The form drag has no counterpart in heat or mass transfer [61]. However, $j_H = j_D$ has been observed to still hold for flow systems not fully developed [78]. By equating the left hand side of equations (25) and (26) to each other, we are then able to predict mass transfer coefficients from known heat transfer data, even for complex flow systems.

Parker, Boggs, and Blick [65] have shown that by defining $\frac{K_{X1}}{C}$ as h_D, the above form of Chilton-Colburn j- factor equation becomes

$$j_D = \frac{h_D}{V} (Sc)^{2/3} \tag{27}$$

Here h_D has the units $\frac{m}{sec}$.

The Chilton-Colburn j- factor analogy can now be applied to the heat transfer data obtained from the models of the human respiratory tract. For the branching pipe model, heat transfer was characterized during both inspiration and expiration as

$$Nu = 0.0733\ (RePr)^{0.731} \qquad \text{(for } 195 < Re < 62{,}000\text{)}$$

From this relationship, the appropriate j- factor can be calculated as

$$j_H = \frac{Nu}{RePr^{1/3}} = \frac{0.0733\ Re^{0.731}\ Pr^{0.731}}{RePr^{.33}}$$

$$j_H = 0.0733\ Re^{-.269}\ Pr^{.401} \tag{28}$$

This relationship is shown in Figure 42 for the branching model of the human respiratory tract as plotted from actual test data.

The corresponding mass transfer j- factor can now be derived by equating it to j_H with Prandtl number replaced by Schmidt number; i.e.,

$$j_D = 0.0733\ Re^{-.269}\ Sc^{.401} \quad . \tag{29}$$

This analogy can likewise be applied to the other heat transfer relationships derived experimentally in this study to obtain expressions of mass transfer in the upper respiratory tract. These derived j- factor relationships are shown in Figures 43-46 and summarized in Table 11.

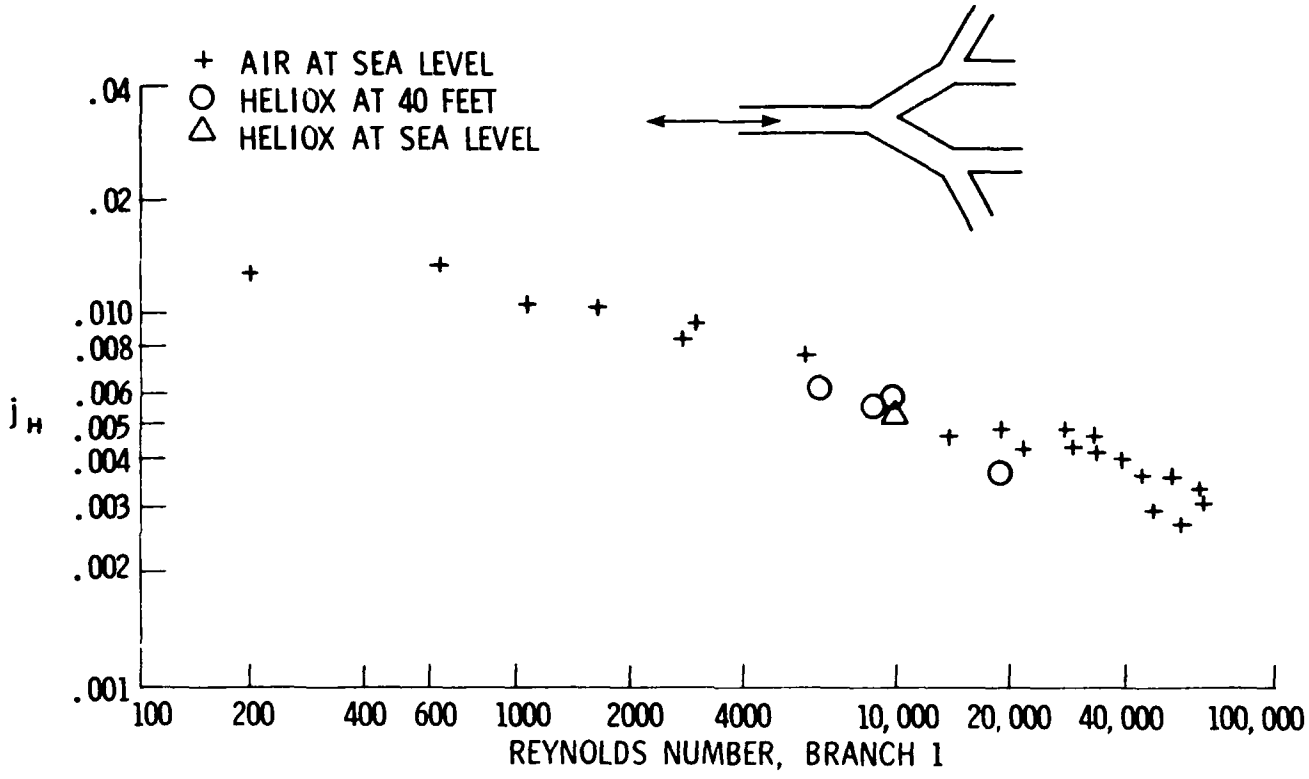

FIGURE 42: CHILTON-COLBURN j-FACTORS FOR FLOW IN THE LOWER RESPIRATORY TRACT

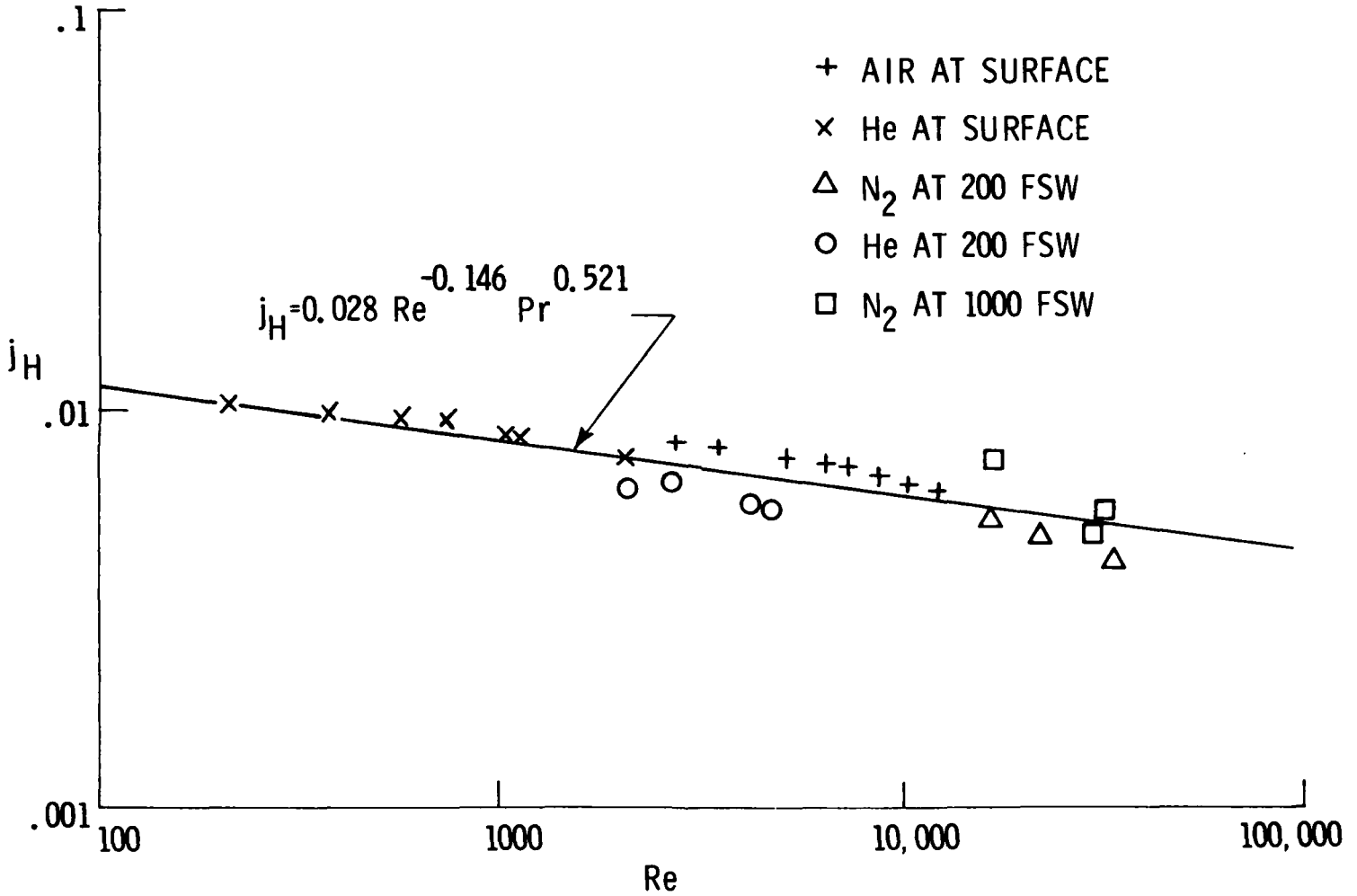

FIGURE 43: CHILTON-COLBURN j-FACTORS FOR INHALATION FLOW THROUGH THE HUMAN NASAL TRACT

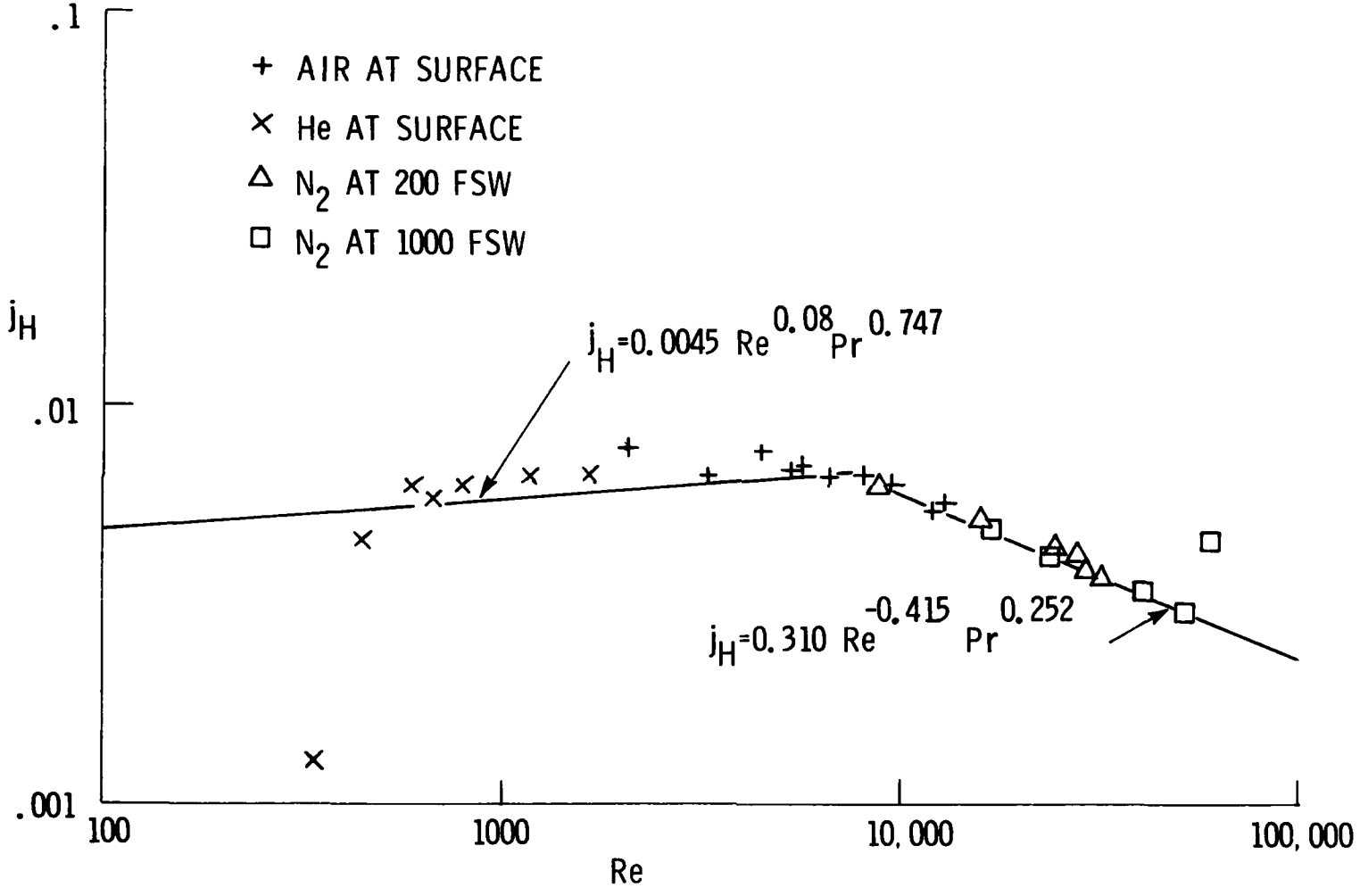

FIGURE 44: CHILTON-COLBURN j-FACTORS FOR EXHALATION FLOW THROUGH THE HUMAN NASAL TRACT

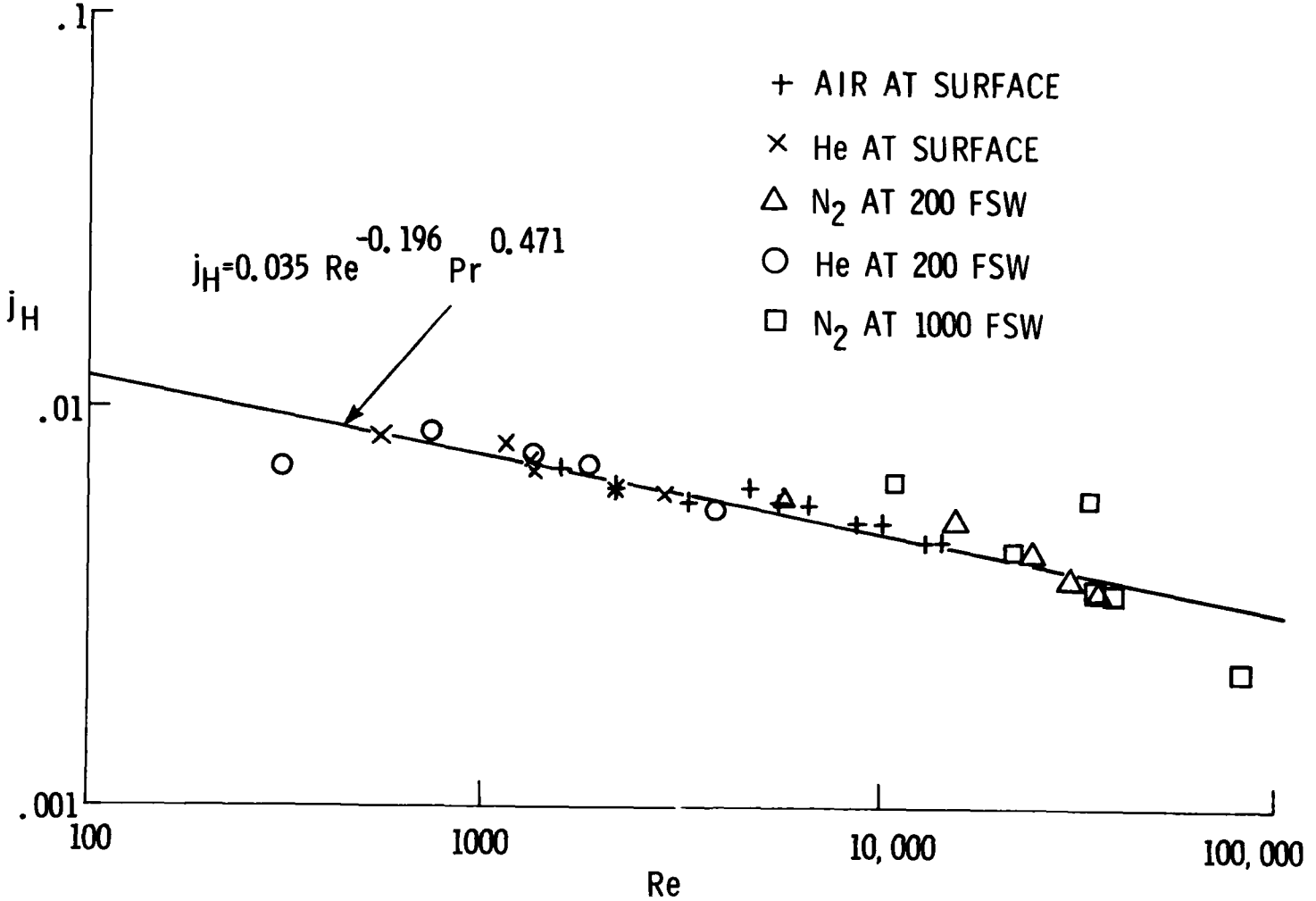

FIGURE 45: CHILTON COLBURN j-FACTORS FOR INHALATION FLOW THROUGH THE HUMAN ORAL TRACT

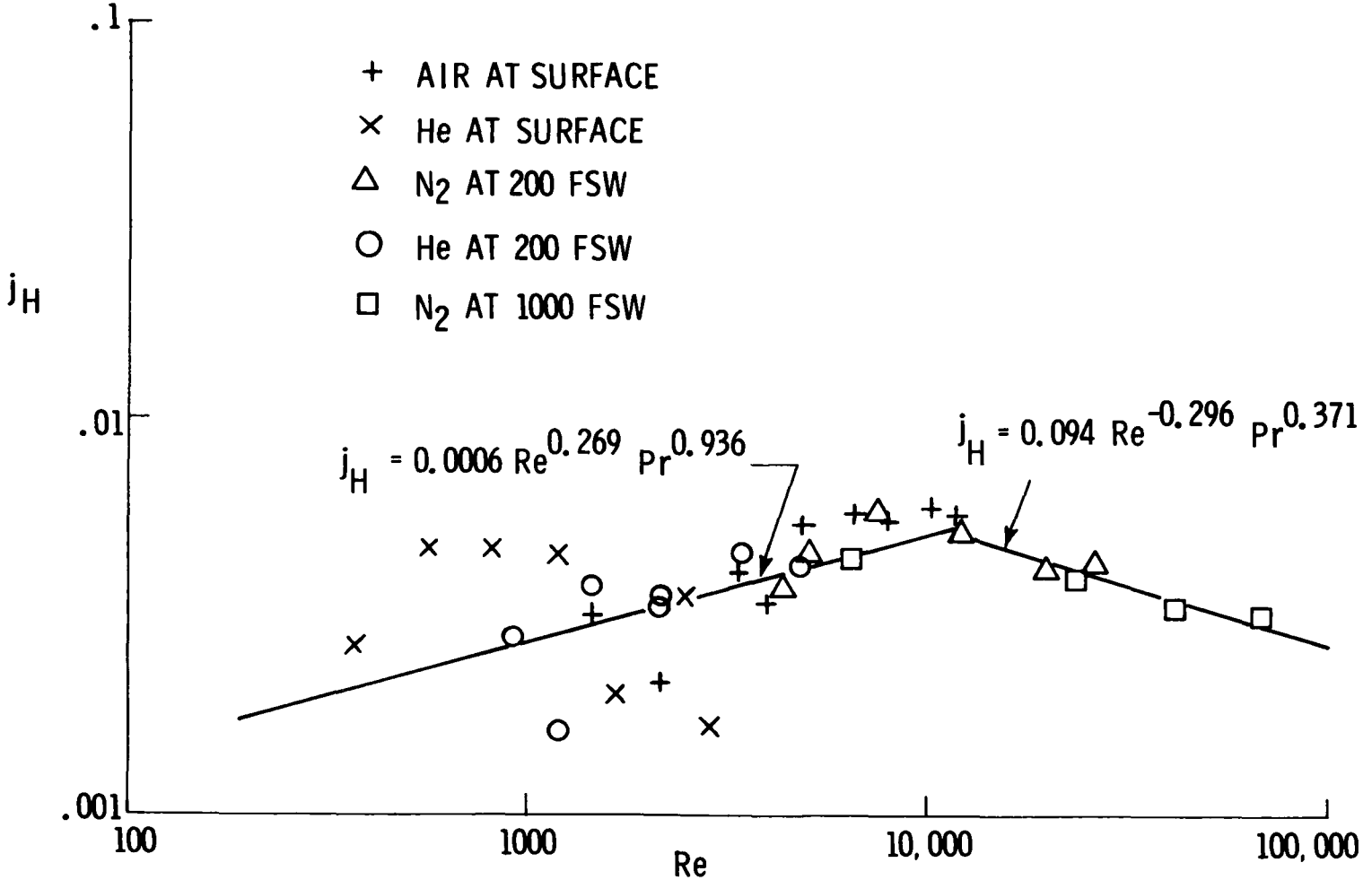

FIGURE 46: CHILTON-COLBURN j-FACTORS FOR EXHALATION FLOW THROUGH THE HUMAN ORAL TRACT

TABLE 11: SUMMARY OF J- FACTOR RELATIONSHIPS FOR THE HUMAN RESPIRATORY SYSTEM

$$j_H \equiv \frac{Nu}{Re\ Pr}1/3 \qquad j_D \equiv \frac{Sh}{Re\ Sc}1/3$$

	HEAT TRANSFER	MASS TRANSFER	
Lower Tract			
Inspiration and Expiration	$j_H = 0.0733\ Re^{-.269}\ Pr^{.401}$	$J_D = 0.0733\ Re^{-.269}\ Sc^{.401}$	
Upper Tract			
Nasal Breathing/Inhalation	$j_H = 0.028\ Re^{-.146}\ Pr^{.521}$	$j_D = 0.028\ Re^{-.146}\ Sc^{.521}$	
/Exhalation	$j_H = 0.0045\ Re^{0.08}\ Pr^{.747}$	$j_D = 0.0045\ Re^{0.08}\ Sc^{.747}$	$Re \leq 7800$
	$j_H = 0.310\ Re^{-.415}\ Pr^{.252}$	$j_D = 0.310\ Re^{-.415}\ Sc^{.252}$	$Re > 7800$
Oral Breathing/Inhalation	$j_H = 0.035\ Re^{-.196}\ Pr^{.471}$	$j_D = 0.035\ Re^{-.196}\ Sc^{.471}$	
/Exhalation	$j_H = 0.0006\ Re^{.269}\ Pr^{.936}$	$j_D = 0.0006\ Re^{.269}\ Sc^{.936}$	$Re \leq 12000$
	$j_H = 0.094\ Re^{-.296}\ Pr^{.371}$	$j_D = 0.094\ Re^{-.296}\ Sc^{.371}$	$Re > 12000$

The following example demonstrates the usefulness of the above j- factor relationships to finding heat and mass transfer coefficients for the respiratory tract.

Example

Air at 30°C is flowing at a mean velocity of 9.144 m/sec through the main bronchus of the lower respiratory tract. A thin mucus layer covers the entire surface of airway passage. What are the heat and mass transfer coefficients for the first three branches of the lower respiratory tract?

Solution

Using the gas properties for air at approximately 30 °C [46] $\rho = 1.202$ Kg/m^3; $\mu = 0.0649$ Kgm/m-hr; $K = 0.0220$ Kcal/hr-m-°C; $C_p = 0.2402$ cal/gm-°C. From Weibel morphological dimensions [27], the diameter of the main bronchus is approximately 1.27 cm.

From these conditions

$$Re = \frac{\rho VD}{\mu} = 7{,}743$$

$$Pr = \frac{C_p \mu}{K} = 0.708$$

From Figure 42, $j_H \cong 0.006$ for Re = 7743. This agrees with Equation (28) where j_H is found to be 0.0057.

Therefore,

$$h_1 = j_H \rho C_p V/Pr^{2/3}$$

$$= .0057\ (1.202)\frac{Kg}{m^3}\ (0.2402)\ \frac{Cal}{gm\text{-}^\circ C}\ \ (9.144)\ \frac{\frac{m}{sec}}{(0.708)^{2/3}}$$

$$h_1 = 0.01897\ Kcal/m^2\text{-}sec\text{-}^\circ C$$

$$h_1 = 68.28\ Kcal/m^2\text{-}hr\text{-}^\circ C.$$

And assuming that $j_D = j_H = 0.0057$, then

$$h_D = j_D\ V/Sc^{2/3}$$

where

$$Sc = \frac{\mu}{\rho D_v}$$

Spaulding [9] gives an empirical relationship for the mass diffusivity, D_v, of water vapor in air as

$$D_v = \frac{0.000146}{P_T} \cdot \frac{T^{2.5}}{T+441} \qquad (30)$$

where

P_T = total pressure, atmospheres

T = temperature, °R

D_v has units of ft^2/hr.

For the above conditions, $D_v = 0.972\ ft^2/hr$ or $D_v = 0.0903\ m^2/hr$

and

$$Sc = \frac{0.0649\ Kg/m\text{-}hr}{1.202\ \frac{Kg}{m^3}\ \times\ 0.0903\ \frac{m^2}{hr}} = 0.598.$$

Therefore,

$$h_D = \frac{0.0057\ (9.144)\ \frac{m}{sec}}{(0.598)^{2/3}} = 0.0736\ \frac{m}{sec}$$

or

$$h_D = 265\ \frac{m}{hr}$$

These heat and mass transfer coefficients can now be utilized to solve for the heat and mass exchange in the first three branches of the lower respiratory tree. The application of these derived transport data and similarly derived data from the experimentally obtained upper tract characteristics will be discussed in the next chapter.

CHAPTER VI

APPLICATION OF EXPERIMENTAL RESULTS

In order to investigate the local heat and water vapor transports in the respiratory system it is necessary to first develop a theoretical model of this system in which the experimentally derived heat and mass transfer coefficients can be utilized. Two models are proposed for this application.

The first approach, and the more rigorous of the two, has been proposed by Scherer and Hanna of the University of Pennsylvania [85]. In their model, shown schematically in Figure 47, anatomical details of the airway wall are neglected and the distance between wall blood supply (capillaries and venous plexae) and the gas-mucous interface (Δy) is considered to be occupied by a homogeneous medium of constant thermal conductivity, K_{tis} (a good first approximation). Heat is assumed to be transported across this medium from the blood, at temperature $T_B(x)$, to the mucous-gas interface temperatures, $T_M(x)$, as given by

$$q_B = - \frac{K_{tis}}{\Delta y} \left[T_M - T_B\right]$$

Under steady-state conditions a heat balance at the mucous-gas interface at any location in the respiratory system would be

$$q_B = q_{conv} + q_L$$

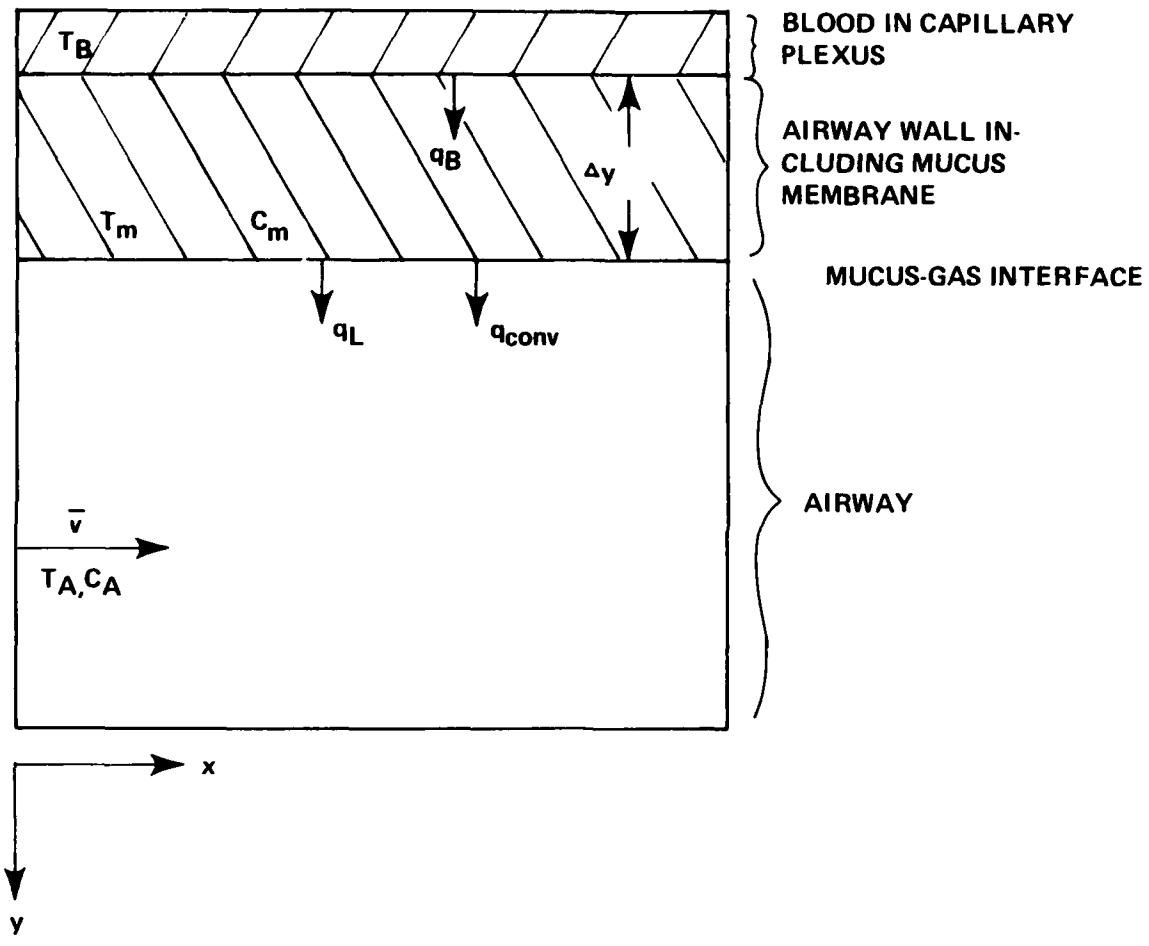

FIGURE 47: SCHEMATIC REPRESENTATION OF A STEADY STATE AIRWAY HEAT AND WATER VAPOR TRANSPORT MODEL

where q_{conv} is the convective heat flux between the mucous-gas interface and the gas stream, and q_L is the latent heat exchange with the gas stream.

With the experimentally derived local heat transfer coefficients, h(x), we can write the convective heat flux as

$$q_{conv} = -h(x)\ [T_A - T_M].$$

Additionally, the latent heat exchange can be written as

$$q_L = NM_w \cdot h_{fg} \text{ where:}$$

N = mass flux of water vapor, $\frac{\text{moles } H_2O}{M^2\text{-sec}}$

M_w = molecular weight of water, $\frac{gm}{mole}$

h_{fg} = latent heat of vaporization, cal/gm

The above heat balance can now be written as

$$\frac{K_{tis}}{\Delta y}\ (T_B - T_M) = h(x)\ (T_M - T_A) + NM_w \cdot h_{fg}\ . \tag{31}$$

However, the convective mass flux, N, at the gas-mucous interface can be derived from the average water vapor contents of the mucous layer and the air stream once a knowledge of the local mass transfer coefficients, $h_D(x)$, is obtained:

$$N = h_D(x)\ [C_m - C_A] \tag{32}$$

where: C_A and C_M are the molar water vapor contents of the gas stream and mucous-gas interface, respective, $\frac{\text{moles } H_2O}{M^3}$

The above expressions for heat and water vapor transfer at the mucous-gas interface are seen to be coupled at equilibrium since

$$C_M = f(T_M). \tag{33}$$

Neglecting axial vapor diffusion, Scherer and Hanna go on to show that the water vapor mass balance on a differential slice of the total airway cross-section can be written as

$$V(x) \frac{dC_A}{dx} = \frac{P(x)}{A(x)} h_D(x) [C_M - C_A] \tag{34}$$

where:

V(x) is the local mean airstream velocity

P(x) is the local total airway perimeter

A(x) is the local total airway cross-sectional area.

Also, the energy balance on this differential slice of the airway can be written

$$V(x) \frac{dT_A}{dx} = \frac{P(x)}{A(x)} \frac{1}{\rho C_{pA}} h(x) [T_M - T_A] + \frac{P(x)}{A(x)} \frac{C_{pw} M_w N}{\rho C_{pA}} [T_M - T_A] \tag{35}$$

The above equations, Equations (31)-(35), make up a system of coupled, non-linear ordinary differential and algebraic equations for the solution of local mass flux of water vapor, N; mucous-gas interface and mean local gas temperatures, T_M and T_A; and mucous-gas interface and mean local gas water vapor contents, C_M and C_A. Although specific solutions to this system are beyond the scope of this investigation, this system of five equations can

be solved numerically to determine the steady state temperatures, humidities and heat and water vapor fluxes along the human respiratory tract.

A second and more simplistic approach looks at the heat and water vapor transport systems independently, and assumes that the capillary and venous plexae are capable of maintaining the heat load requirements of both mechanisms, thereby maintaining constant local mucous-gas interface temperatures.

The experimentally derived heat and mass transport characteristics for the upper and lower respiratory tracts can then be used to calculate the heat and water vapor additions to the respiratory gases as they progress inward to the alveoli. Such calculations can be made in a stepwise manner from segment to segment in the respiratory tract while having the option to vary wall temperature as we progress inward.

Treating the heat and mass transfer mechanisms within the respiratory tract independently, we can write:

HEAT TRANSFER

Energy of gas entering segment	+	Convective heat addition within segment	=	Energy of gas leaving segment

or

$$\rho V_1 \pi \frac{D^2}{4} C_p T_i + \pi D L \bar{h} (T_w - T_i) = \rho V_1 \frac{\pi D^2}{4} C_p T_{i+1}$$

where D and V_l are the characteristic diameter and flow velocity in the airway segment respectively, and L is the total flow path length within the respiratory system segment.

Upon rearranging, we can calculate the downstream temperature of each segment as

$$T_{i+1} = T_i + \frac{4\,\bar{h}\,L}{\rho V_l C_p D}(T_w - T_i) \tag{36}$$

and

MASS TRANSFER

Mass of water vapor entering segment + mass of water vapor added to gas in segment = mass of water vapor leaving segment

By definition [60] the mass of water vapor entering through convective diffusion into the airway segment is

$$\dot{m} = h_D A\,(\rho_w - \rho_i)$$

where $\dot{m}$ = mass transfer rate, gm/sec

h_D = mass transfer coefficient determined experimentally, cm/sec

A = mass transfer surface area, cm^2

ρ_w, ρ_i = partial mass density of water vapor at wall interface and airway segment entrance, respectively, gm/cm^3.

Assuming that the water vapor behaves as an ideal gas, we can write

$$\frac{P_v}{\rho} = R_v T$$

and we can approximate the mass transfer rate as

$$\dot{m} = \frac{h_D A}{R_v T} (P_{v_w} - P_{v_i})$$

where

R_v = gas constant for water

= universal gas constant/molecular weight of water

= 8314.3 joules/Kg-mole-°K÷18.016 Kg/Kg mole = 461.5 joules/Kg-°K

$T = T_w + 273$, °K

P_{v_w}, P_{v_i} = vapor pressure at wall interface and entrance, respectively, N/m^2 (pascal).

With the above definitions, we can rewrite the mass balance as

$$\rho V_1 \frac{\pi D^2}{4} W_i + \frac{h_D \pi D L}{R_v T} (P_{v_w} - P_{v_i}) = \rho V_1 \frac{\pi D^2}{4} W_{i+1}.$$

However,

W_i = humidity ratio, gm water vapor per gm dry air. The humidity ratios can be calculated from the vapor pressure as [66]

$$W_i = \frac{P_{v_i}}{P_t - P_{v_i}} \frac{R_g}{R_v}$$

and

$$W_{i+1} = \frac{P_{v_{i+1}}}{P_t - P_{v_{i+1}}} \frac{R_g}{R_v}$$

where

R_g = gas constant of dry gas, joules/Kg-°K

P_t = total pressure, N/M^2

The above mass balance can now be written

$$\rho V_1 \frac{\pi D^2}{4} \frac{R_g}{R_v} \frac{P_{v_i}}{P_t - P_{v_i}} + \frac{h_D \pi D L}{R_v T} (P_{v_w} - P_{v_i})$$

$$= \rho V_1 \frac{\pi D^2}{4} \frac{R_g}{R_v} \frac{P_{v_{i+1}}}{P_t - P_{v_{i+1}}}$$

Upon rearranging and simplification, we can solve for the downstream vapor pressure of each segment as

$$P_{v_{i+1}} = P_t \frac{\left[R_g \cdot B + \frac{4 h_D L}{\rho V_1 D T} \cdot C \right]}{\left[R_g + R_g \cdot B + \frac{4 h_D L}{\rho V_1 D T} \cdot C \right]} \tag{37}$$

where

$$B = \frac{P_{v_i}}{P_t - P_{v_i}}$$

and

$$C = P_{v_w} - P_{v_i}.$$

Equations (36) and (37) can be utilized in a stepwise matter to calculate the mean gas stream temperature and vapor pressure in each location of the respiratory airway. Once these values have been obtained, the various contributions of energy addition to the respiratory mixture as it progresses through the airways can be determined as outlined in Appendix G.

During expiration, the energy and water vapor conservation features of the airways can be shown by performing these stepwise calculations in the reverse direction. However, it should be noted that the exhalation gas stream, having been previously saturated with water vapor during inhalation, will remain saturated (i.e., ρ_i = saturated mass density at T_i). Any condensate from the gas stream onto the airway walls will result due to the reduction in ρw as the wall temperature progressively decreases axially.

The above calculations were made for typical inlet and ambient conditions using the program "Application" listed in Appendix I. Examples of these predicted gas stream temperatures are shown in Figure 48 during inhalation studies. These examples show a moderate effect of respiratory flow rates on the depth of penetration of the gas stream prior to reaching body temperature. At similar flow rates, ambient gas temperature is seen to have only a minor effect on the depth of penetration prior to reaching body temperature. However, it will be emphasized again that the use of this simplified model in which heat and water vapor transport are handled independently allows chances for significant errors to occur in these predictions. The use of the coupled model presented earlier, in conjunction with the experimentally derived heat and mass transfer coefficients from this research, should provide a better predictive capability for the gas stream conditions and mucosa conditions throughout the respiratory system.

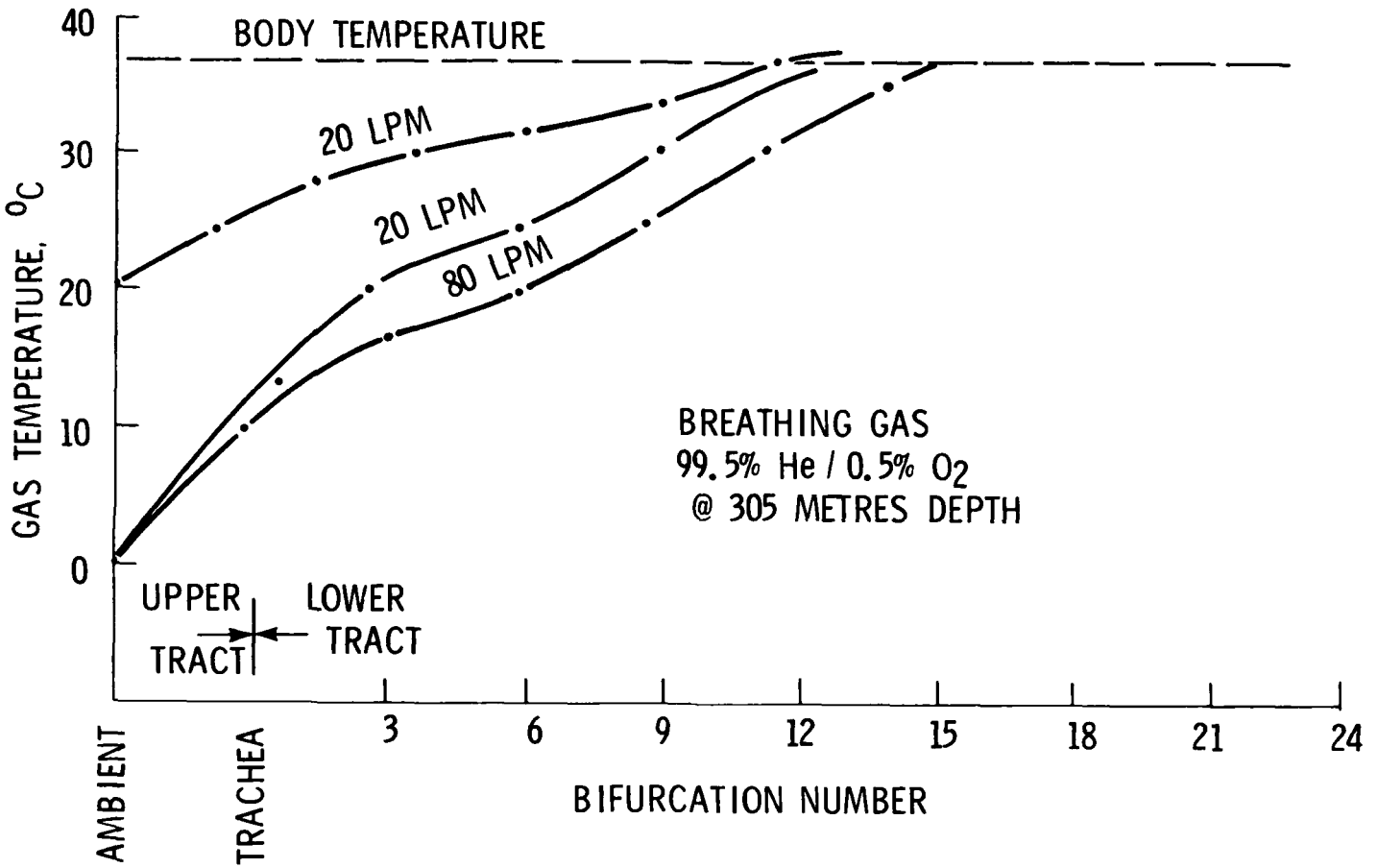

FIGURE 48: GAS CONDITIONING IN THE HUMAN RESPIRATORY SYSTEM DURING INHALATION

CHAPTER VII

SUMMARY - FINDINGS AND RECOMMENDATIONS

Heat transfer mechanisms have been characterized in physical models of the upper and lower respiratory tracts of humans over a wide range of environmental pressures and gas mixtures. Characterizations were made using quasi-steady gas flow representations for inhalation and exhalation phases for both oral and nasal breathing modes.

A single heat transfer relationship was found to well represent both inhalatory and exhalatory flow modes for the lower respiratory tract. On the other hand, unique relationships were found necessary for the upper respiratory tracts during inhalation and exhalation. However, characterizations of both test models were found to behave independently with depth, so that testing at 1 ATA yielded data representative of that recorded at depth.

From the above characterizations a convenient analysis of the comparative conditioning efficiencies of the oral and nasal cavities was possible. It was observed with the model configuration used in this investigation that the oral cavity was a less efficient gas conditioner than the nasal cavity across the entire spectrum of ambient conditions tested. It was additionally observed that the conditioning capability of the oral cavity decreased

relative to the nasal cavity as the respiratory rates and/or ambient pressures increased.

It should be noted that the above results pertaining to the oral cavity heat transfer characteristics and the relative conditioning capabilities of the oral and nasal cavities can be quite sensitive to the positioning of the tongue. Proctor and Swift [38] note that the oral airway has a highly variable size and shape. They point out that it is conceivable that a narrow airway produced by approximation of tongue and palate is nearly as effective as the nose in conditioning inspired gases. On the other hand, a wide oropharyngeal airway will almost certainly give negligible heat exchange to inspired gases before they reach the trachea.

To a lesser extent, the conditioning capability of the nasal cavity will be somewhat variable. The "nasal cycle", the observed phenomena in which flow resistance in the left and right nasal passages appear to follow cyclic patterns out of phase with one another, will have a potential effect on the overall conditioning capability of the nasal tract. The significance of the "nasal cycle" and tongue positioning in the oral tract on the conditioning capabilities of these air passageways should be explored. The inherent difficulty in constructing a physical model of these passageways having variable geometrics can be avoided by evaluating several different rigid models, each with a unique flow passageway geometry.

Analogous mass transfer relationships have additionally been found for each respiratory flow mode. Efforts to relate the heat and mass transfer j-factors (Chilton-Colburn) with corresponding friction factors, as derived

from pressure drop recordings in the upper respiratory tract model, showed consistently $j < f/2$. This finding is consistent with other flow systems having curved streamlines rather than fully developed flow due mainly to form drag. This form drag as described by Bird, Stewart, and Lightfoot [61] has no counterpart in heat transfer, and thus its added contribution to f is expected.

In the last portion of this study a mathematical model was introduced to apply the experimentally obtained heat transfer relationships and derived mass transfer relationships to an evaluation of heat and mass transfer in the human respiratory tract. It is emphasized that such a model, which couples these two transport processes, is important as each mechanism will directly effect the magnitude of the other. Independent utilization of the heat and mass transfer relationships can only be expected to give erroneous results. Such a coupled system model should be developed to adequately utilize the data from this investigation. Following its development the results of its utilization should be compared with available physiological data of local gas stream and passageway wall temperatures in the human lung. These validation efforts can lead to refinements in the mathematical model until satisfactory agreements are observed between predictions and experimental recordings. The successful development of such a model will offer a valuable tool in the investigation of the effects of breathing cold, dense gases on the local conditions of respiratory passageways. It can further be utilized in the continuing investigations of cold induced asthma, cystic fibrosis, and numerous other respiratory ailments which plague humans daily.

APPENDICES

APPENDIX A

ASSUMPTIONS USED DURING EXPERIMENTAL RECORDINGS

In the process of the experimental analyses, several fundamental assumptions were necessarily made including,

a. The thermocouple probes used in the experimental procedure, described for the lower tract testing, are recording true gas stream temperatures which are insignificantly effected by radiant heat exchange with the tube walls or gas medium, or heat conduction through the thermocouple probes,

b. Constant model wall temperatures can be assumed in both test setups and

c. Steady state flow experiments are respresentative of the actual variable flow situation in the respiratory tract.

At this time arguments will be made which justify the above assumptions.

a. Error Analysis for Thermocouple Probes

According the McAdams [47], the following heat balance equation is applicable in steady state for a gas sensor when considering errors induced by *radiation*, *convection*, and conduction heat transfer:

$$Q_{gr} + Q_c + Q_r + Q_k = 0$$

(145)

where

Q_{gr} = heat flux by gas radiation between the gas and the sensor.

Q_c = heat flux by convection between the gas and the sensor.

Q_r = heat flux by radiation between the sensor and surface that it "sees."

Q_k = heat flux by conduction between the sensor and the surrounding walls.

Heat flux, Q_{gr} , by gas radiation between the gas and the sensor will be ignored in this experimental effort. Siegel and Howell [48] point out that heat exchange through this medium becomes significant only when evaluating such unsymmetrical gas molecules as carbon dioxide or water vapor. For all but extremely high gas temperatures (several thousand degrees) insignificant radiant energy is transferred between gases with symmetrical molecules through emission, absorption, and scattering.

Heat flux, Q_k , by conduction between the sensor and the surrounding wall can be expressed as

$$Q_k = \frac{(T_w - T_s)}{\frac{L_p}{K_p A_p} + \frac{L_t}{K_t A_t}}$$

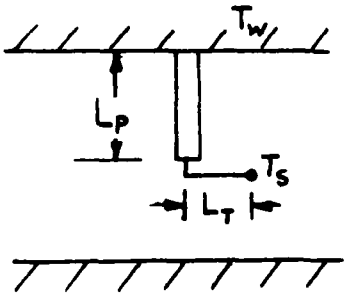

where

K_p, K_t = thermal conductivity of thermal probe material and thermocouple leads, respectively (watts/cm - °K)

A_p, A_t = cross sectional area of thermal probe and thermocouple leads, respectively (cm^2)

L_p, L_t = probe length and thermocouple lead length, respectively (cm)

T_w = wall temperature, °K

T_s = sensor temperature, °K

For the thermoprobes used, L_t is approximately 2 cm, K_t is approximately 4.04 watts/cm - °K, and the cross sectional area, A_t, of two 30-gauge wire leads is 0.001 cm^2. Thus, the resistance to heat flow due to the thermocouple lead is

$$R_t = \frac{L_t}{K_t A_t} = 495.1 \text{ °K/watt} \quad .$$

This resistance, in addition to the added variable resistance of the thermal probe as it traverses the lower tract model radially, is sufficient to prevent a heat exchange between the sensor and the surrounding walls in excess of 0.04 watts for a typical temperature differential (T_w - T_s) of 20°C. This low heat exchange can thus be ignored in this steady state analysis.

Following the exclusion of Q_{gr} and Q_k we are left with the expression $Q_c + Q_r = 0$. For example, under steady state conditions, the rate of heat flow by radiation from the thermocouple junction to the walls equals the rate of heat flow by convection from the gas to the couple. The effect of the radiant exchange between the sensor and the surrounding walls on the recorded

temperature can thus be estimated by looking at the above heat balance in an expanded form during steady state conditions:

$$\bar{h}\, A(T_g - T_s) = AF_{sw}\, \varepsilon\sigma\, (T_s^4 - T_w^4)$$

where

T_g = true gas stream temperature

A = surface area of the thermocouple bead

ε = emissivity of the thermocouple surface

σ = Stefan-Boltzmann constant = 5.672×10^{-8} W/m^2K^4 [50]

$\bar{h}$ = mean convective coefficient between sensor and gas.

F_{sw} = shape factor between thermocouple bead and surrounding walls (assumed to be 1.0)

Under a typical experimental measurement in this study, T_w was 45°C (318°K), T_s (minimum) is 25°C (298°K), and $\bar{h}$ can be approximated as 0.142 w/cm^2 °C [49]. Using an emissivity of 0.1 for the soldered, highly reflective, thermocouple surface [48] we have for radiant heat exchange

$$\frac{Q}{A} = 0.1 \times 5.672 \left[\left(\frac{318}{100}\right)^4 - \left(\frac{298}{100}\right)^4\right] \frac{w}{m^2}$$

$$= 13.27 \frac{w}{m^2} .$$

The true gas temperature, T_g, can now be calculated as

$$T_g = \frac{Q}{\bar{h}} + T_s = \frac{13.27 \frac{w}{m^2} \times \frac{m^2}{10000\ cm^2}}{0.0142 \frac{w}{cm^2}\,°C} + 25°C$$

$$= 25.09°C$$

It is obvious from this example that radiant heat exchange between the surrounding walls and the thermocouple bead have an insignificant effect (less than 0.1°C) on the temperature recorded by the thermocouple.

b. Constant Model Wall Temperture

It is universally accepted that the temperature of the mucosal lining of the respiratory tract varies to some extent with axial position in the airways. However, Johnson [26] has given evidence which suggests that nearly steady state conditions are set up fairly rapidly during inspiration and expiration, with minimal mucosa temperature fluctuations occurring over the respiratory cycle. For the segmental model used in this investigation, it was assumed that constant surface wall temperatures were adequate for representing the heat transfer characteristics of the respiratory tract. This was found to be necessary due to the extreme difficulty that was anticipated in matching the thermal properties of the model with that of human tissue. It should be noted, however, that this constant wall temperature assumption holds only for the upper tract segment and the three branch segment represented by the lower tract model, and does not prevent a stepwise axial temperature gradient along the airway passages. By thinking of the respiratory tract as an assembly of the upper tract and consecutively scaled segmental models of the lower tract, each with its own mean wall temperature, we are able to analyze the heat transfer characteristics of the respiratory tract with axially varying wall temperatures.

Johnson [51] confirmed the axial temperature gradient in an anesthesized dog's lung even while breathing temperate air at surface conditions. However, he found that the local wall temperatures in the upper and lower trachea

remained constant during rapid periodic respiration, even while being ventilated with cold, dense air at a simulated depth of 58 metres of seawater. This observation gives supporting evidence that the airway walls may display an insignificant transient temperature variation with the respiratory cycle. The assumption of constant wall surface temperature thus appears to be reasonable, provided the time interval used in analyzing the respiratory heat transfer is relatively short, and periodic updating of the wall temperature is made.

c. Steady State Versus Reciprocating Flow Systems

The experimental heat transfer characterizations derived from the two models were obtained from steady flow processes. This approach of using steady flow characterizations as being representative of the respiratory process had previously been used by numerous investigators [17, 52, 53]. The primary justifications for the use of such models in engineering analysis have been summarized by Johnson [51] from the papers of Schroter and Sudlow [53] and Pedley, Schroter, and Sudlow [54, 55, 56] and is quoted below:

> "A quasi-steady flow analysis of gas flow through the respiratory airways was considered to closely approximate the unsteady flow state of cyclic breathing and superimposed heart-beat pulsations. The Imperial College of London research group argued that the boundary layers of the airways were constantly being reformed because of the very short airway lengths (less than 4 diameters) between junctions. Since the boundary layer (δ) was always developing it was therefore considered to be thin and basically laminar in nature. As a result of

this, δ was considered to be somewhat independent of the axial velocity (u) at or near the core of the stream flow. Pedley, Schroter, and Sudlow further argued that although secondary flows were induced at the junctions of the airways and did operate on the axial velocity gradients observed in the cross section, the radial and tangential components of velocity were considered to be very much less than the axial component. This argument enabled them to apply the basic concepts of classical boundary layer theory to their perspex (plexiglas) model. Now, Womersley [57] had shown analytically that oscillations superimposed on a parabolic pipe flow would not grossly disturb the boundary layer velocity profile of a quasi-steady flow if α is less than one (1), where

$$\alpha = R\sqrt{\frac{\omega}{\upsilon}}$$

R = Radius of pipe or tube

ω = Angular frequency in radians

υ = Kinematic viscosity

"This statement is similar to Schlichting's [58] comment that for $R\sqrt{\frac{\omega}{\upsilon}}$ very small; i.e., very slow oscillations, the velocity distribution near the wall is in phase with the existing pressure distribution forcing the flow. Since the boundary layer growth is a function of the local velocity, then it is assumed that for $\alpha < 1$ the developed boundary layer at some instant of time for a periodic flow will be the same as the boundary layer associated with a quasi-steady flow of an equivalent velocity."

"Sudlow, Olson, and Schroter [59] noted in flow visualizations of both ideal models and casting of the bronical tree that the boundary layer thickness of an airway was very much less than the tube radius. They note that

for the normal range of respiratory frequencies of 0.2 to 0.83 cycles per second (cps) [5] with 1 ata air that α is very much less than one even in regions of anticipated turbulent flow if the boundary layer thickness (δ) is substituted for the airway radius (R) in the previous equation. α would be greater than one during normal quiet respiration of twelve breaths per minute (0.2 cps) for airways of greater than 0.7 centimeters (0.28 in.) diameter using the originally stated equation of Womersley. This hypothesis of Sudlow, Olson, and Schroter [59] as yet has not been experimentally evaluated."

"With respect to parabolic flow alone, α may be considered to be an idealization of the relative magnitude of oscillating disturbances created in the boundary layer to the magnitude of the steady flow boundary layer. For nonparabolic flow profiles, Womersley defined the following relationship to estimate the effect on the boundary layer of superimposed flow oscillations."

$$\beta = \frac{\delta}{\left(\frac{\omega}{\nu}\right)^{1/2}}$$

If β is greater than one ($\beta > 1$) then the oscillations of angular frequency ω will affect the flow profile, and if β is less than one ($\beta < 1$), then the quasi-steady state may be assumed to be appropriately representative of a periodic flow state. For a normal respiration rate of twelve breaths per minute (0.2 cps) the maximum boundary layer thickness without perturbation from the periodic flow would be 3.5 millimeters (0.14 in.). The maximum

boundary layer thickness at the maximum respiratory rate of fifty breaths per minute (0.83 cps) is estimated to be one 1.7 millimeters (0.07 in.).

"It shold be again remembered that these are idealizations of the boundary layer effects on models of branching airways. The developments are based on ideal flows, both fully developed laminar (Poiseuille) and fully developed turbulent, in smooth cylindrical pipe. The application is to symmetrical dichotomous branching airways that are cylindrical in nature. The actual bronchial tree is neither symmetric nor dichotomous in its branching, and the cross-sectional shapes deviate considerably from the idealistic circular cross section. However, the boundary layer concepts that have been set forth provide the researcher a relevant perspective concerning the applicability of the result of quasi-steady flow studies in bronchial tree models." Likewise, the applicability of the quasi-steady flow studies in the upper tract model can be similarly argued.

APPENDIX B

TESTING OF ELECTRONIC ICE POINT REFERENCE JUNCTIONS FOR USE IN HYPERBARIC ENVIRONMENTS

Prior to using thermocouples in a hyperbaric environment, it was necessary to determine the effect of elevated pressures on the electronic ice point reference junctions (Omega MCJ) being utilized in this research, Figure B-1. Since all electrical penetrations through the hyperbaric chamber wall have copper conductors, it will be necessary for the electronic ice point to be positioned inside the chamber, fully exposed to the high pressure environment.

To investigate this condition, a copper/constantan thermocouple junction, constructed of 30-gauge wire with nylon insulation, was placed in a beaker of ambient temperature water. In series with this thermocouple circuit was placed an electronic ice point junction (Omega Model MCJ). Additionally, a thermistor (Yellow Springs, Inc., YSI 701) was placed in the same beaker of water to be compared with the thermocouple readout. DeBoer, Stetzner, and O'Brien [34] have previously found that this type of thermistor was little affected by pressures up to 71 ata. Thus, it serves as a good reference for comparison with the thermocouple circuit.

This entire assembly was positioned in a small hyperbaric chamber (rated to 6890 kPa), and the temperature monitor leads were attached to the

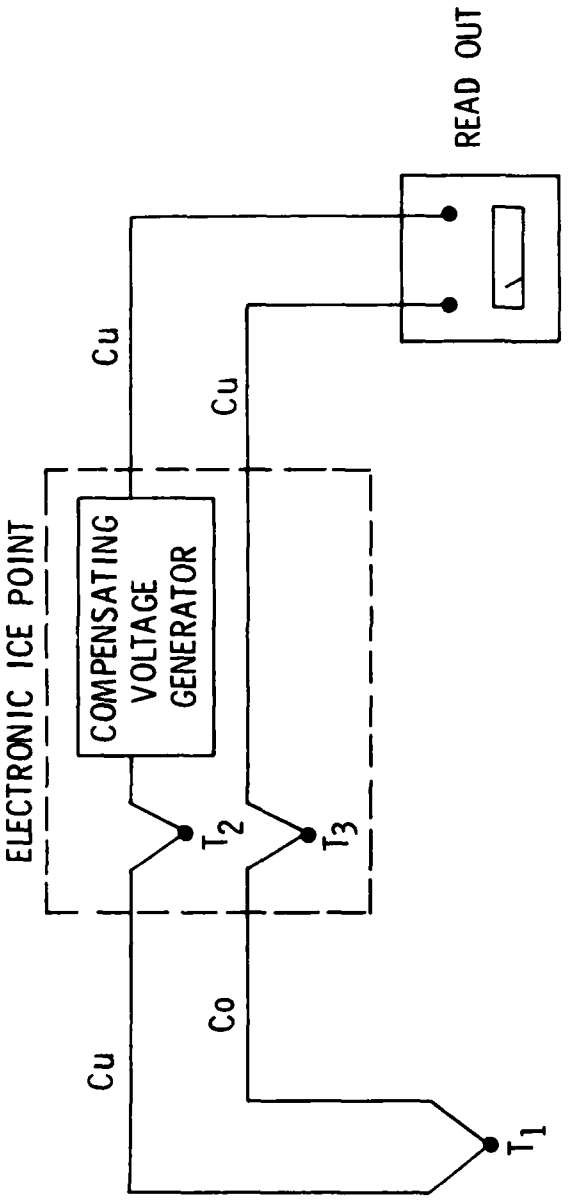

FIGURE B-1: ELECTRONIC ICE POINT REFERENCE JUNCTION

chamber electrical penetration connectors. Outside the chamber, the leads from the thermocouple connectors were monitored by a Hewlett-Packard 3466A Digital Multimeter while the thermistor was monitored by its appropriate YSI signal conditioner. See Figure B-2 for a schematic of this test setup. At this point, the chamber was sealed and initial temperature readings were recorded for the thermocouple and thermistor.

The chamber was then successively pressurized at a rate of 60 feet/minute using nitrogen to depths of 100, 200, 300, 400, 500, 750, 1000, and 1150 feet of seawater. Following a 10-minute waiting interval at each depth, temperature readings were recorded for both temperature transducers. Figure B-3 shows the results of these measurements in elevated pressure environments.

Although both temperature probes showed a slight upward trend in temperature as depth increased (due to temperature build-up in the chamber during pressurization), the copper/constantan thermocouple tracked the thermistor throughout the test. A maximum variation of 0.4°C was seen between the two transducers during approximately 90 minutes at depth.

Following these recordings, the chamber was decompressed to the surface at a rate of 60 feet/minute. The thermocouple circuit was then taken from the chamber and a calibration check made using the test setup shown in Figure B-4. A hot plate/magnetic stirrer (Cole Parmer Model #4817) used in conjunction with a water-filled beaker provided a boiling water source for this calibration check (barometric pressure was 30.00 inches Hg). The signal relayed from the water immersed junction through the electronic ice point was monitored by an HP 3466A digital multimeter. During vigorous

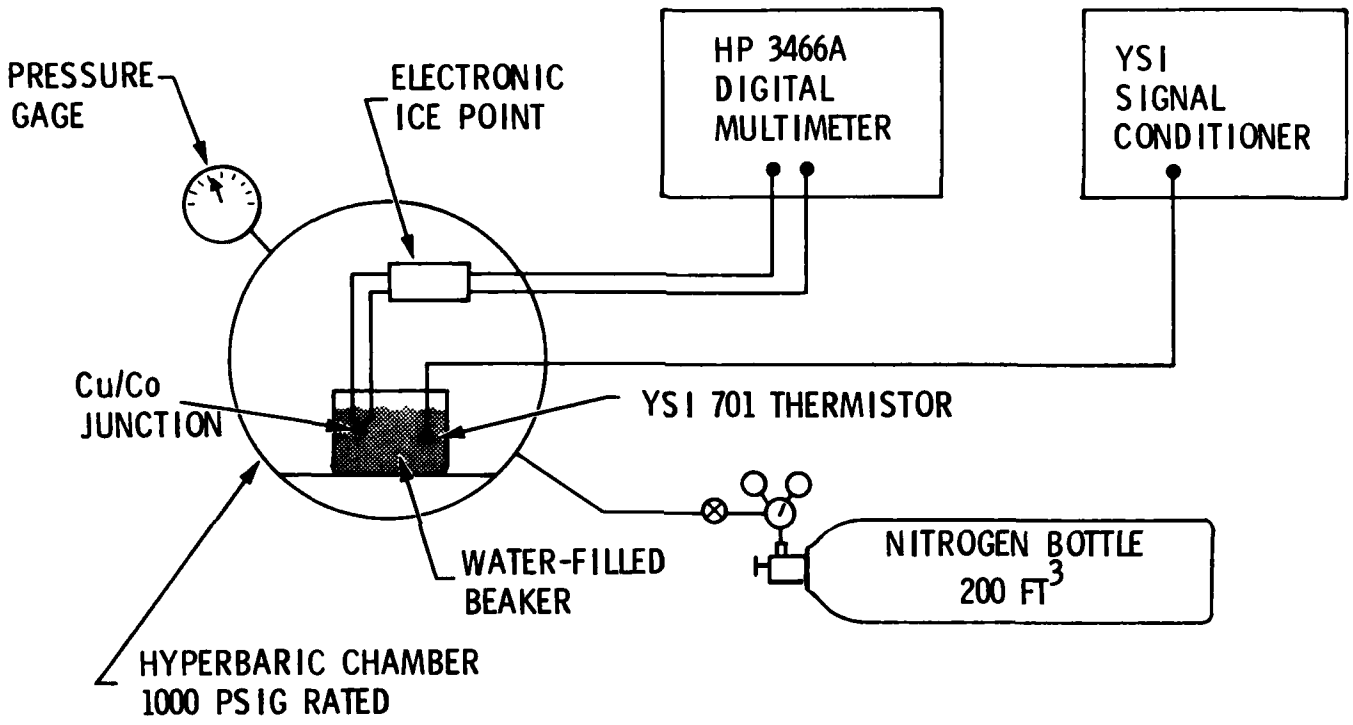

FIGURE B-2: TEST SETUP TO OBSERVE EFFECTS OF ELEVATED PRESSURES ON ELECTRONIC ICE POINT PERFORMANCE

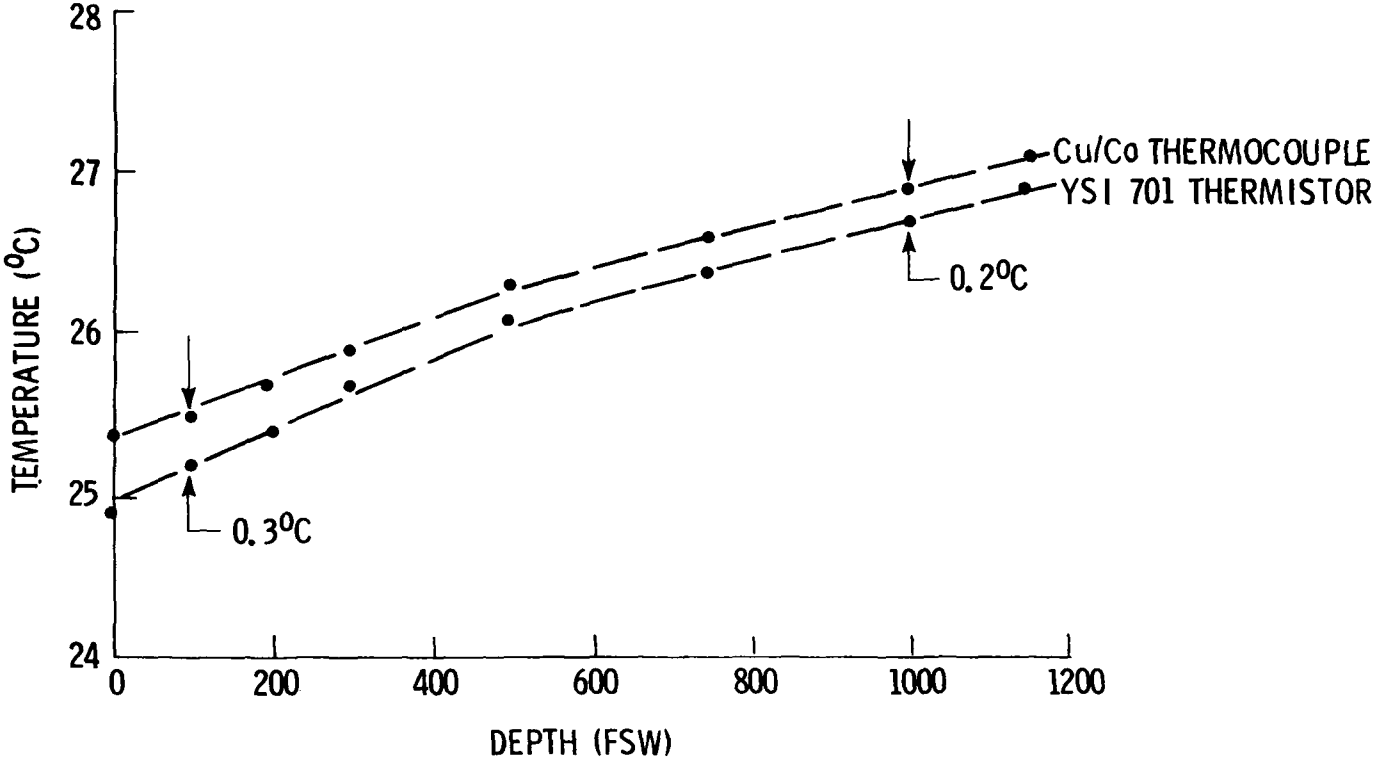

FIGURE B-3: COMPARISON OF TEMPERATURE RECORDINGS OBTAINED FROM A YSI 701 THERMISTOR AND COPPER/CONSTANTAN THERMOCOUPLE

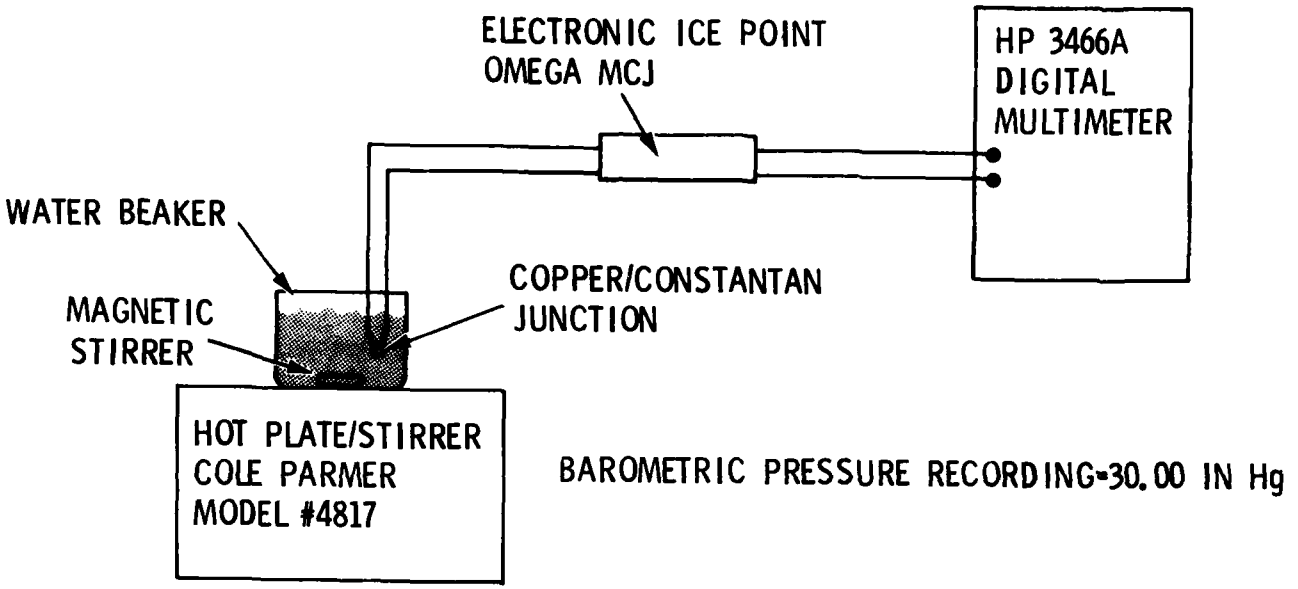

FIGURE B-4: TEST SETUP FOR CALIBRATION CHECK ON ELECTRONIC ICE POINT JUNCTION FOLLOWING HYPERBARIC EXPOSURE

water boiling, the copper/ constantan junction developed an emf of 4.245 ±0.025 millivolts, which corresponds to a temperature reading of 99.5°C [35]. A similar check with the thermocouple immersed in a well-stirred ice bath showed an EMF corresponding to a temperature reading of 0.1 °C. This 0.5°C maximum variation with the boiling point is within the stated accuracy of 0.5 °C of the electronic ice point junction [33].

These tests have shown no ill effects of elevated pressures on the electronic ice point junction, either during compression or decompression at moderate travel rates. These results would indicate that the use of thermocouples, in conjunction with an electronic ice point, is an acceptable temperature transducer for hyperbaric use to 1150 feet of seawater.

APPENDIX C

LAMINAR FLOW ELEMENT VISCOSITY CORRECTION

The Meriam Laminar Flow Element is factory calibrated for flow with air at 70°F (viscosity is 181.78 μ poise). The LFE works on the principle of a gas flowing through many small, parallel flow channels in the laminar regime while establishing a pressure drop across the flow channels which is proportional to the flow rate. For incompressible viscous flow (a good assumption in this case due to the small pressure drop encountered), this pressure drop can be shown to be the following for laminar flow in a pipe (Poiseuille flow) [69]:

$$\Delta P = \frac{128\ qL\mu}{\pi D^4}$$

where:

ΔP = pressure drop across pipe

q = volumetric gas flow

L, D = length and diameter of pipe, respectively

μ = gas viscosity.

That is, since D and L are fixed for any particular device the pressure drop across any pipe is directly related to only flow rate and viscosity.

When using the LFE to record flow of gases other than air at the calibrated conditions, the LFE can either be recalibrated with the gas to be measured or a viscosity correction can be applied to the calibration curve found with air as follows:

1. The differential pressure transducer records the pressure drop across the LFE; for this application, the transducer output was calibrated to give a 10-volt output at a full scale pressure of 0.5 psid.

2. The LFE calibration curve supplied by the factory for air flow can be described by the following relationship through a least square curve fitting routine:

$$\text{†CFM (actual cubic feet of air @70°F)} = -0.029004 * \Delta P^2(\text{in}H_2O) + 3.058701 * \Delta P(\text{in}H_2O) - 0.008485.$$

3. The above calibration is based on air at 70°F (viscosity = 181.87 μ poise). The following calculates the actual gas viscosity.

i) temperature correction of gas constituents based on US Navy Diving Gas Manual [46].

<u>viscosity of O_2 (μ poise)</u>

$$\mu_{O_2} \text{ @ temperature T (°F)} = 203.29 * \left(\frac{459.67+T}{529.67}\right)^{0.79}$$

---

†This curve is unique for each LFE. Complete linearity is not achieved due to the dynamic losses seen on entry to and exit from the resistance element.

viscosity of He (μ poise)

$$\mu_{H_e} \text{ @ temperature } T = 195.80 * \left(\frac{459.67+T}{529.67}\right)^{0.646}$$

Note: The above relationships were derived by curve fitting data from the Navy Diving-Gas Maunual

ii) the viscosity of the gas mix can now be calculated as follows [61]

$$\mu_{mix} = \sum_{i=1}^{n} \frac{X_i \mu_i}{\sum_{j=1}^{n} X_j \Phi_{ij}}$$

where:

X = mole fraction of gas mix

$$\Phi_{ij} = \frac{1}{\sqrt{8}} \left(1 + \frac{M_i}{M_j}\right)^{-\frac{1}{2}} \left[1 + \left(\frac{\mu_i}{\mu_j}\right)^{\frac{1}{2}} \left(\frac{M_j}{M_i}\right)^{\frac{1}{4}}\right]^2$$

M = gas molecular weight.

For a two constituent gas, HeO_2, we have

$$\mu_{HeO_2} = \frac{X_{He} \mu_{He}}{X_{He} \Phi_{HeHe} + X_{O_2} \Phi_{HeO_2}} + \frac{X_{O_2} \mu_{O_2}}{X_{He} \Phi_{O_2He} + X_{O_2} \Phi_{O_2O_2}}$$

where:

$$\Phi_{HeO_2} = \frac{1}{\sqrt{8}} \left(1 + \frac{M_{He}}{M_{O_2}}\right)^{-\frac{1}{2}} \left[1 + \left(\frac{\mu_{He}}{\mu_{O_2}}\right)^{\frac{1}{2}} \left(\frac{M_{O_2}}{M_{He}}\right)^{\frac{1}{4}}\right]^2$$

$$\Phi_{O_2He} = \frac{1}{\sqrt{8}} \left(1 + \frac{M_{O_2}}{M_{He}}\right)^{-\frac{1}{2}} \left[1 + \left(\frac{\mu_{O_2}}{\mu_{He}}\right)^{\frac{1}{2}} \left(\frac{M_{He}}{M_{O_2}}\right)^{\frac{1}{4}}\right]^2$$

$$\Phi_{HeHe} = 1$$

$$I_{O_2O_2} = 1.$$

4. A corrected flow based on the actual gas viscosity can now be calculated as (flow inverse to viscosity):

$$\text{CFM (actual)} = \text{CFM (air @70°F)} \times \frac{181.87\ \mu\text{ poise}}{\mu_{HeO_2}} .$$

5. This flow can then be converted to litres/minutes

$$\text{LPM (actual)} = \text{CFM (actual)} \times 28.32\ \frac{\text{litres}}{\text{cu ft}} .$$

The above viscosity correction routine was incorporated in the computer program "Data Acquisition - Upper Tract" shown in Appendix I for recording model flow rates in the chamber testing.

APPENDIX D

FINITE DIFFERENCE SOLUTION OF UPPER TRACT MODEL WALL

The derivation of heat transfer coefficients from the upper tract model requires an accurate knowledge of the model wall temperature during data collection. The polyester resin used in the fabrication of the upper tract model does not exhibit the thermal properties (Table D-1) necessary for a lumped-system (Biot number <0.1) assumption, as was used in the pipe model of the lower tract. It was thus felt worthwhile to observe analytically the wall's responses to exposures of cold, dense gases prior to physical experimentation in the laboratory.

TABLE D-1

APPROXIMATE THERMAL PROPERTIES OF POLYESTER CASTING MATERIAL [40]

Thermal Conductivity, K	$4 \times 10^{-4} \frac{\text{cal - cm}}{\text{sec - cm}^2 \text{ - } ^\circ\text{C}}$
Specific Heat, C_p	$0.25 \frac{\text{cal}}{\text{gm - } ^\circ\text{C}}$
Density, ρ	$1.10 - 1.46 \frac{\text{gm}}{\text{cc}}$

A small element of the model wall was first portrayed as a plane wall, for simplicity, having one-dimensional heat flow as seen in Figure D-1).

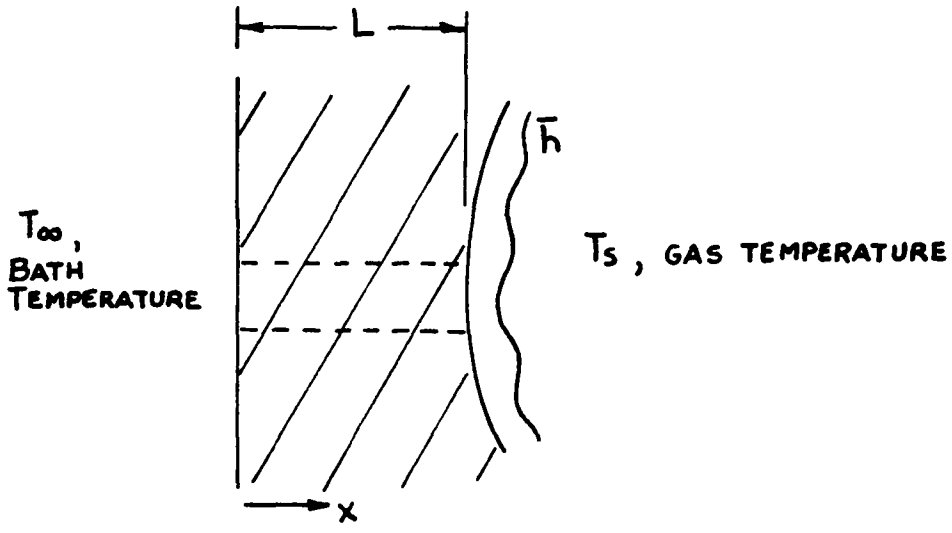

FIGURE D-1. IDEALIZATION OF UPPER TRACT MODEL WALL

The heat equation in one-dimensional form is [70]

$$\frac{\partial^2 t}{\partial x^2} = \frac{1}{\alpha} \frac{\partial t}{\partial \theta}$$

where:

$\alpha = \frac{K}{\rho C_p}$ = thermal diffusivity

x, t, θ are the space, temperature, and time variables, respectively.

The boundary conditions can be written

at $x = 0$ $\quad t = T_\infty$

at $x = L$ $\quad \bar{h} (t - T_s) = -K \frac{\partial t}{\partial x}$

The initial condition can be written

at $\theta = 0$ $\quad t = T_\infty$.

By defining the following dimensionless variables

$$\bar{x} = \frac{x}{L},\ \bar{\theta} = \frac{\theta\alpha}{L^2},\ u = \frac{t - T_s}{T_\infty - T_s}$$

and substituting into the original problem statement we can rewrite the problem as follows:

$$u_{\bar{x}\bar{x}} = u_{\bar{\theta}}$$

$$u = 1 \quad @\ \bar{x} = 0$$

$$u_{\bar{x}} = -\,Hu\ @\ \bar{x} = 1 \quad \text{where:} \quad H = \frac{\bar{h}L}{K}$$

$$u = 1 \quad @\ \bar{\theta} = 0.$$

Using a separation of variables technique [70] the analytical solution for the above problem was found to be

$$u(\bar{x}, \bar{\theta}) = \sum_{N=1}^{\infty} \left[\frac{\sin \lambda_N}{\frac{\lambda_N}{2} + \frac{\sin 2\lambda_N}{4}}\right] \cos \lambda_N \bar{x}\ e^{-\lambda_N^2 \bar{\theta}}$$

where:

$$\lambda_N \tan \lambda_N = H$$

The first five roots of the equation for H = 2 are found in Table C-1 of Reference 70 to be

N	λ_N
1	1.0769
2	3.6436
3	6.5783
4	9.6296
5	12.7223

A series expansion of the above solution using the first five terms proved unsatisfactory in meeting the boundary conditions due to the slow damping observed in the later terms of this series. For a more accurate solution a further expansion of this series appears to be necessary. Rather than continuing this series solution approach, a finite difference solution was developed under the assumption that the model wall could be approximated by a thin rectangular slab with 1-dimensional heat transfer (a nodal representation of this problem is shown in the figure below).

Finite Difference Solution

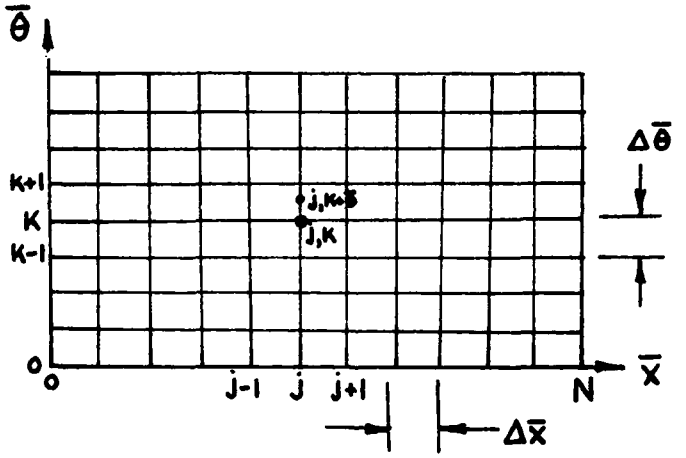

The computational form of the above problem statement is [71]

$$(u_{\bar{\theta}})_{j,k} = (u_{\bar{x}\bar{x}})_{j,k}$$

where: j is the spatial locator in the model wall and k is the time indicator.

Using an implicit solution method (Crank Nicolson) we can say that the time derivative of u at some incremental time k+Θ can be approximated by the average time derivatives at k and k+1, or

$$(u_{\bar{\theta}})_{j,k+\Theta} = \frac{(u_{\bar{\theta}})_{j,k+1} + (u_{\bar{\theta}})_{j,k}}{2} .$$

Substituting for $(u_{\bar{\theta}})_{j,k+1}$ and $(u_{\bar{\theta}})_{j,k}$ in the above equation gives

$$(u_{\bar{\theta}})_{j,k+\theta} = \frac{(u_{\bar{x}\bar{x}})_{j,k+1} \quad (u_{\bar{x}\bar{x}})_{j,k}}{2} \tag{D-0}$$

But, from Crandall [71] the computational molecules for $(u_{\bar{x}\bar{x}})_{j,k}$ and $(u_{\bar{x}\bar{x}})_{j,k+1}$ can be written

$$(u_{\bar{x}\bar{x}})_{j,k} = \frac{u_{j-1,k} - 2u_{j,k} + u_{j+1,k}}{(\Delta\bar{x})^2} \tag{D-1}$$

and

$$(u_{\bar{x}\bar{x}})_{j,k+1} = \frac{u_{j-1,k+1} - 2u_{j,k+1} + u_{j+1,k+1}}{(\Delta\bar{x})^2} \tag{D-2}$$

Substituting Equations D-1 and D-2 into Equation D-0 and noting also that

$$(u_{\bar{\theta}})_{j,k+\theta} = \frac{u_{j,k+1} - u_{j,k}}{\Delta\bar{\theta}}$$

gives

$$\frac{u_{j,k+1} - u_{j,k}}{\Delta\bar{\theta}} = \frac{u_{j-1,k+1} - 2u_{j,k+1} + u_{j+1,k+1} + u_{j-1,k} - 2u_{j,k} + u_{j+1,k}}{2\,(\Delta\bar{x})^2}$$

By defining $P = \frac{\Delta\bar{\theta}}{(\Delta\bar{x})^2}$, the general nodal equation can be written,

following rearrangement as

$$(1 + P)\, u_{j,k+1} - \frac{P}{2}\, u_{j-1,k+1} - \frac{P}{2}\, u_{j+1,k+1} = (1 - P)\, u_{j,k} + \frac{P}{2}\, u_{j-1,k} + \frac{P}{2}\, u_{j+1,k}$$

GENERAL NODAL EQUATION

In a similar manner the boundary conditions can be written in nodal form as follows:

$$\underline{\text{at } \bar{x} = 1} \qquad (u_{\bar{x}})_{j,k} = - Hu_{j,k}$$

where $j = N$.

The computational molecules are (from Crandall)

$$\frac{-u_{N-1,k} + u_{N+1,k}}{2\,\Delta\bar{x}} = - Hu_{N,k}$$

and

$$\frac{-u_{N-1,k+1} + u_{N+1,k+1}}{2\,\Delta\bar{x}} = - Hu_{N,k+1}$$

Solving for $u_{N+1,k}$ and $u_{N+1,k+1}$ from above and substituting into the general nodal equation for $j = N$, we get

$$- P\, u_{N-1,k+1} + (1 + P + P\Delta\bar{x}H)\, u_{N,k+1} = (1 - P - P\Delta\bar{x}H)\, u_{N,k} + P\, u_{N-1,k}$$

NODAL EQUATION AT $\bar{x} = 1$

$$\underline{\text{at } \bar{x} = 0} \qquad u_{0,k} = 1$$

NODAL EQUATION AT $\bar{x} = 0$

The above nodal equations can be expanded in matrix format as shown in Figure D-2 with $N = 10$.

A Burroughs B7000/B6000 series computer was programmed to solve this problem for values of H varying from 0.1 to 40.0 (range of values expected over the hyperbaric conditions under investigation). Solutions to this problem are shown in Figures D-3 and D-4 at various times after the initiation of gas flow adjacent to the model wall. All solutions were seen to be stable with no oscillations. As can be seen in these figures, the wall surface adjacent to the gas stream cools quite rapidly for values of H in excess of 2 (estimated value of H for air flow at surface conditions). These findings emphasize the need to have temperature monitors on the inside wall surface during testing with the upper track model so actual wall temperatures can be recorded. On the other hand, these finding demonstrate the acceptability of the assumption made during lower tract testing (pipe model) that wall temperature is equal to bath temperature (H was less than 0.05).

$$
\begin{bmatrix}
1 & -P & & & & & & & & \\
-\frac{P}{2} & 1+P & -\frac{P}{2} & & & & & & & \\
 & -\frac{P}{2} & 1+P & -\frac{P}{2} & & & & & & \\
 & & -\frac{P}{2} & 1+P & -\frac{P}{2} & & & & & \\
 & & & -\frac{P}{2} & 1+P & -\frac{P}{2} & & & & \\
 & & & & -\frac{P}{2} & 1+P & -\frac{P}{2} & & & \\
 & & & & & -\frac{P}{2} & 1+P & -\frac{P}{2} & & \\
 & & & & & & -\frac{P}{2} & 1+P & -\frac{P}{2} & \\
 & & & & & & & -\frac{P}{2} & 1+P & -\frac{P}{2} \\
 & & & & & & & & -P & 1+P+P\Delta\bar{x}H
\end{bmatrix}
\begin{bmatrix} U_{0,\ k+1} \\ U_{1,\ k+1} \\ U_{2,\ k+1} \\ U_{3,\ k+1} \\ U_{4,\ k+1} \\ U_{5,\ k+1} \\ U_{6,\ k+1} \\ U_{7,\ k+1} \\ U_{8,\ k+1} \\ U_{9,\ k+1} \\ U_{10,\ k+1} \end{bmatrix}
=
\begin{bmatrix}
1 & -P & & & & & & & & \\
\frac{P}{2} & 1-P & \frac{P}{2} & & & & & & & \\
 & \frac{P}{2} & 1-P & \frac{P}{2} & & & & & & \\
 & & \frac{P}{2} & 1-P & \frac{P}{2} & & & & & \\
 & & & \frac{P}{2} & 1-P & \frac{P}{2} & & & & \\
 & & & & \frac{P}{2} & 1-P & \frac{P}{2} & & & \\
 & & & & & \frac{P}{2} & 1-P & \frac{P}{2} & & \\
 & & & & & & \frac{P}{2} & 1-P & \frac{P}{2} & \\
 & & & & & & & \frac{P}{2} & 1-P & \frac{P}{2} \\
 & & & & & & & & P & 1-P-P\Delta\bar{x}H
\end{bmatrix}
\begin{bmatrix} U_{0,\ k} \\ U_{1,\ k} \\ U_{2,\ k} \\ U_{3,\ k} \\ U_{4,\ k} \\ U_{5,\ k} \\ U_{6,\ k} \\ U_{7,\ k} \\ U_{8,\ k} \\ U_{9,\ k} \\ U_{10,\ k} \end{bmatrix}
$$

Figure D-2: EXPANDED MATRIX FORMAT OF TEN INCREMENT NODAL EQUATIONS

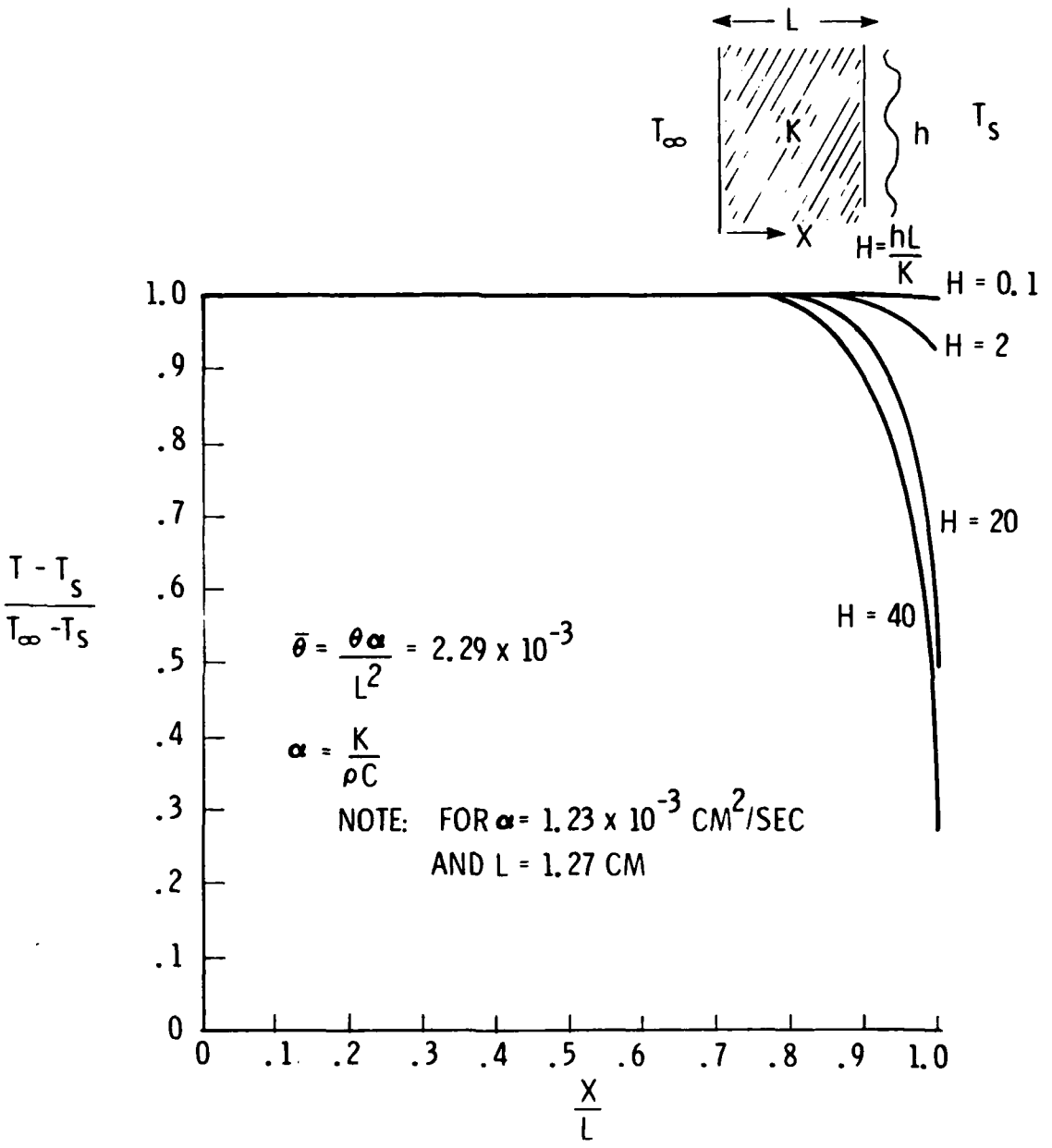

FIGURE D-3: TEMPERATURE DISTRIBUTION IN WALL WITH VARIOUS VALUES OF CONVECTIVE COEFFICIENTS AT ONE WALL (0=3 SEC)

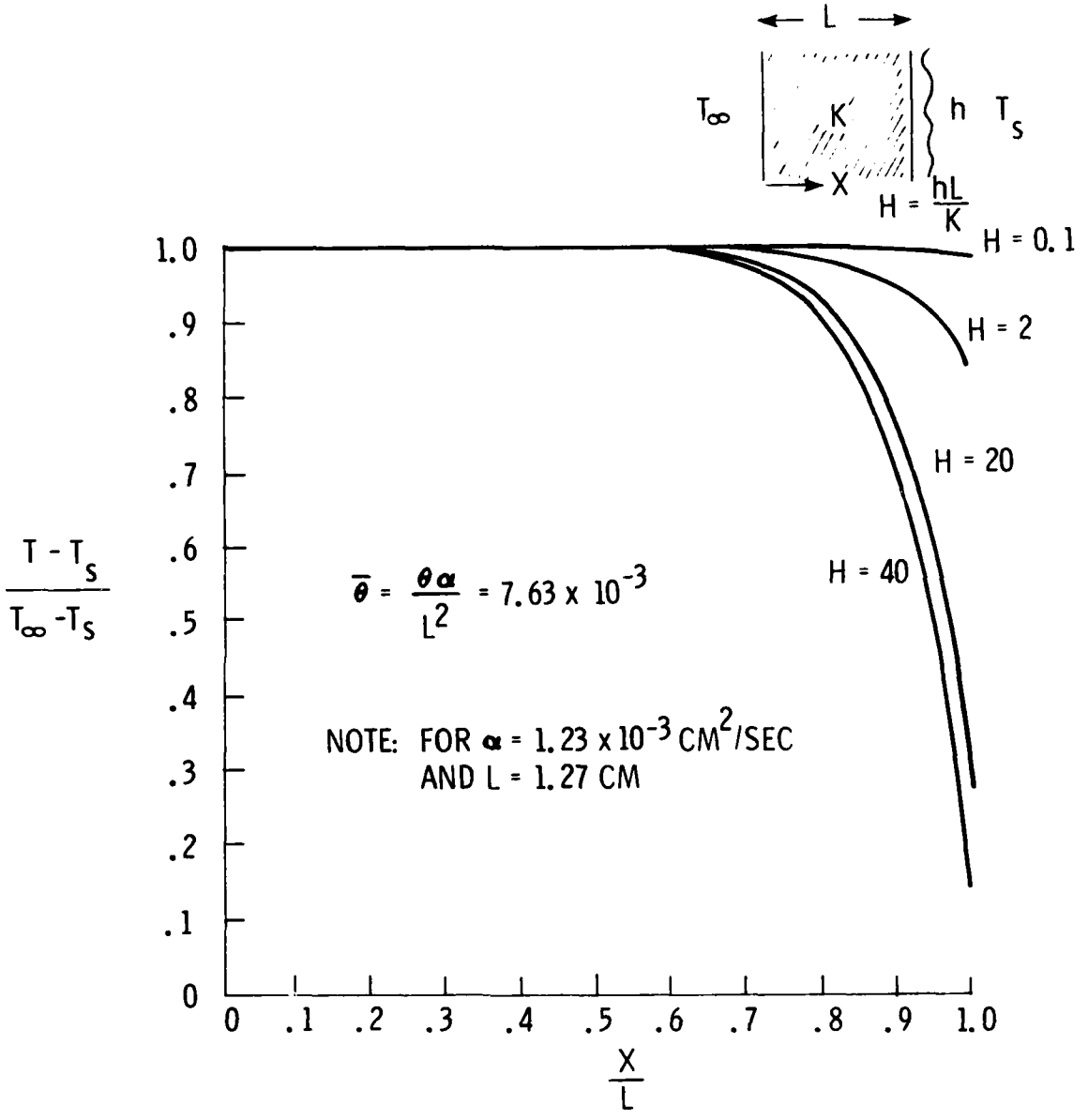

FIGURE D-4: TEMPERATURE DISTRIBUTION IN PLANE WALL WITH VARIOUS VALUES OF CONVECTIVE COEFFICIENTS AT ONE WALL (θ=10 SEC)

APPENDIX E

EVALUATION OF SCHMIDT NUMBERS FOR HIGH PRESSURE GASES

In order to obtain approximate values for the dimensionless Schmidt number ($Sc = \frac{\mu}{\rho D_v}$) it will be necessary to determine the diffusion coefficient for binary mixtures, D_v, as a function of temperature, pressure, and composition. Since experimental measurements of D_v are quite limited it will be necessary to calculate values from equations developed primarily from theory with constants adjusted from limited experimental data. Slattery and Bird [75] have developed the following equation for estimation of D_v at low pressures from a combination of kinetic theory and corresponding-states arguments:

$$\frac{P_t \; D_v}{(P_{C1}P_{C2})^{1/3} \; (T_{C1}T_{C2})^{5/12} \; (\frac{1}{M_1} + \frac{1}{M_2})^{1/2}} = a \left(\frac{T}{\sqrt{T_{C1}T_{C2}}} \right)^b$$

where:

P_{C1}, P_{C2} are the critical pressures of components 1 and 2, respectively (ATM)

T_{C1}, T_{C2} are the critical temperatures of components 1 and 2, respectively (°K)

M_1, M_2 are the molecular weights of components 1 and 2, respectively (gm/gm-mole)

P_t total ambient pressure (ATM)

T ambient temperature (°K)

D_v diffusion coefficient, (cm^2/sec)

For H_2O with a nonpolar gas, a and b were found to be the following

$$a = 3.640 \times 10^{-4}$$

$$b = 2.334 .$$

This equation has been found to agree with experimental data at atmospheric conditions to within 8 percent [75]. It shows that D_v is inversely proportional to pressure and increases with temperature. Experimental data has shown that at high pressures D_v no longer varies inversely with pressure. However, due to a lack of other data sources, we will assume that the above relationship holds for pressures encountered to 610 metres of seawater (2000 feet) for these estimates.

Table E-1 tabulates the needed properties for the above calculations for gases normally encountered in diving. An estimate for the diffusion coefficient for water vapor-air at 1 ATM and 25°C can be made as follows:

$$(P_{C1}P_{C2})^{1/3} = (218.4 \times 36.4)^{1/3} = 19.96$$

$$(T_{C1}T_{C2})^{5/12} = (647 \times 132)^{5/12} = 113.44$$

$$\left(\frac{1}{M_1} + \frac{1}{M}_2\right)^{1/2} = \left(\frac{1}{18.01} + \frac{1}{28.97}\right)^{1/2} = 0.3001$$

$$a\left(\frac{T}{\sqrt{T_{C1}T_{C2}}}\right)^{b} = 3.640 \times 10^{-4} \left(\frac{25 + 273}{\sqrt{647 \times 132}}\right)^{2.334} = 3.81 \times 10^{-4}$$

therefore:

$$(1.0)D_v = (3.81 \times 10^{-4})(19.96)(113.44)(0.3001)$$

$$D_v = 0.259 \frac{cm^2}{sec} \quad (1.003 \frac{ft^2}{hr})$$

TABLE E-1

CRITICAL GAS PROPERTIES [61, 76]

Substance	Molecular Weight	Tc, °K	Pc, ATM
H_2O	18.01	647	218.4
He	4.00	5.26	2.26
O_2	32.00	154.4	49.7
Air	28.97	132	36.4

This value agrees nicely with an empirical equation for the diffusivity of water vapor in air developed by Spaulding [77]. For temperatures up to 1093°C (2000°F) he found the following expression for mass diffusion for water vapor in air as

$$D_v = \frac{0.000146}{P_t} \cdot \frac{T^{2.5}}{T + 441}$$

where

D_v has units $\frac{ft^2}{hr}$

T has units °R

P_t has units atmospheres

For 1 ATM and 25°C (537°R)

$$D_v = 0.000146 \frac{(537)^{2.5}}{978} = 0.998 \frac{ft^2}{hr} \quad (0.258 \frac{cm^2}{sec})$$

Similar estimates can be made for the diffusion coefficients of water vapor in other gases and ambient conditions using the critical properties in Table E-1. Several of these estimates and the corresponding Schmidt numbers are shown in Table E-2.

TABLE E-2

ESTIMATES OF DIFFUSION COEFFICIENTS AND SCHMIDT NUMBERS FOR VARIOUS WATER VAPOR/GAS MIXES

Air @ 25.0°C (77°F) $\mu = 1.83 \times 10^{-4}$ gm/cm-sec

P, ATM	Density, gm/cm^3	D_v, cm^2/sec	Sc
1	1.178×10^{-3}	0.259	0.60
4	4.742×10^{-3}	0.065	0.59
8	9.388×10^{-3}	0.032	0.61

Helium @ 25.0°C (77°F) $\mu = 1.997 \times 10^{-4}$ gm/cm-sec

P, ATM	Density, gm/cm^3	D_v, cm^2/sec	Sc
1	1.63×10^{-4}	2.12	0.58
4	6.54×10^{-4}	0.53	0.58
8	1.21×10^{-3}	0.27	0.62

From this investigation, based on the assumption that the inverse relationship of the mass diffusion coefficient to pressure applies throughout the pressure range of interest, we can see that the Schmidt number is fairly constant at a value of 0.6 for the gases normally encountered in diving. This value is pleasingly close to the Prandtl numbers for these gases, Pr $\simeq$ 0.7; a condition which supports the similarity between the temperature and partial pressure profiles.

AD-A104 992 NAVAL COASTAL SYSTEMS CENTER PANAMA CITY FL F/G 6/19
HEAT AND WATER VAPOR TRANSFER IN THE HUMAN RESPIRATORY SYSTEM A--ETC(U)
SEP 81 M L NUCKOLS
UNCLASSIFIED NCSC-TR-364-81 SBIE-AD-F200 009 NL

3 OF 4
AD
A104992

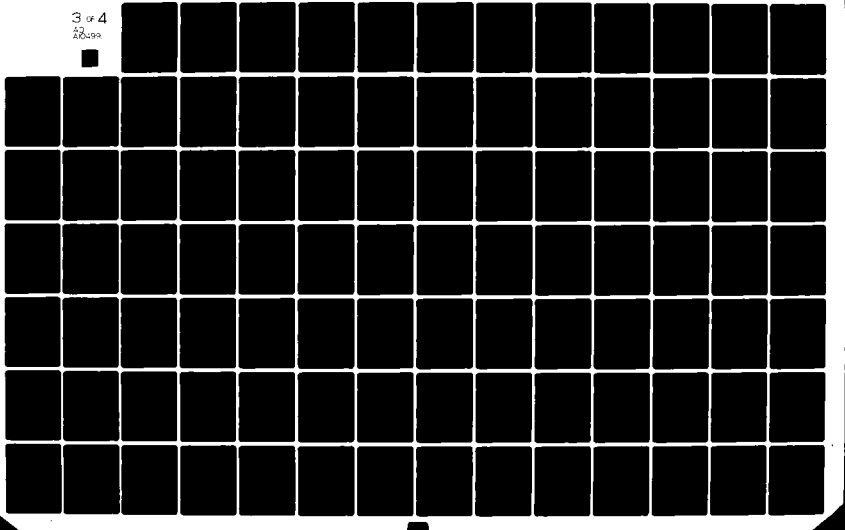

APPENDIX F

CALCULATION OF FRICTION FACTORS IN UPPER TRACT MODEL

A convenient method of relating pressure drop in a flowing fluid system to mass flow is through a dimensionless quantity called the friction factor, f. This friction factor is actually a dimensionless pressure gradient as defined as follows [65]

$$f = \frac{-\frac{dp}{dz} D}{\frac{1}{2}\rho V^2_{avg}}$$

For steady, fully developed flow systems such as conduits, theoretical values of f can be determined by calculating the pressure gradient in such systems from the known velocity profile. For systems in which fully developed flow may not be present, as in flow around objects or through curved passageways, we can define an analogous factor as

$$f = \frac{\Delta P}{L} \frac{D_t}{\frac{1}{2}\rho V^2_{avg}}$$

where

ΔP is the measured pressure drop across the system.

L is the flow length across the system.

D_t is the characteristic diameter (trachea).

In these non-developed systems there are contributions to f owing to both friction drag, as in the case of fully developed tube flow, and "form drag" [61] owing to the dynamic effects of flow around bluff objects. Under these conditions in the Chilton-Colburn j- factors, j_H and j_D, will be less than f/2 due to the additional component of f owing to form drag. This is aptly demonstrated by calculating friction factors from the data collected on the model of the upper respiratory tract and comparing these values with the corresponding j- factors.

From measured data of head loss through the upper tract model, Figure F-1, corresponding friction factors are calculated for the model as defined by the following [69]:

$$f = h_L \left(\frac{D_t}{L}\right) \left(\frac{2}{V^2}\right)$$

where:

$$h_L = \frac{\Delta P}{\rho} \; g_o = \text{head loss, } (ft^2/sec^2)$$

D_t,L = diameter and length (characteristic), (ft)

V = mean velocity at diameter D_t, (ft/sec)

$$\therefore \quad g_o = 32.2 \; \frac{lbm - ft}{lbf - sec^2}$$

$$f = \frac{\Delta P}{\rho} \; g_o \left(\frac{D_t}{L}\right) \left(\frac{2}{V^2}\right)$$

The above calculation was performed for data collected during nasal breathing/exhalation as seen in Table F-1 and compared with the Chilton-Colburn j- factors in Figure F-2. As anticipated, the quantity f/2 is significantly higher across the range of Re than either j_H or j_D. This is due to the added component of form drag to the calculated drag coefficient, which has no counterpart in heat or mass transfer. The contribution of this form drag component can theoretically be determined by subtracting j_H from the calculated f/2 value since

$$f/2_{\text{form}} + f/2_{\text{friction}} = f/2_{\text{total}}$$

But

$$f/2_{\text{friction}} = j_H = j_D.$$

The results of this comparison emphasize that $j_H < f/2$ for any system which flows in curved, rather than straight, streamlines due to form drag. Under these conditions the Reynolds Analogy, i.e.

$$\frac{Nu}{RePr} = \frac{f}{2}$$

will not hold. This has also been shown to be the case for flow around long circular cylinders [61, 78]. However, as in the case of the circular cylinder the equality of the Chilton-Colburn j- factors, $j_H = j_D$, would still hold for the respiratory system.

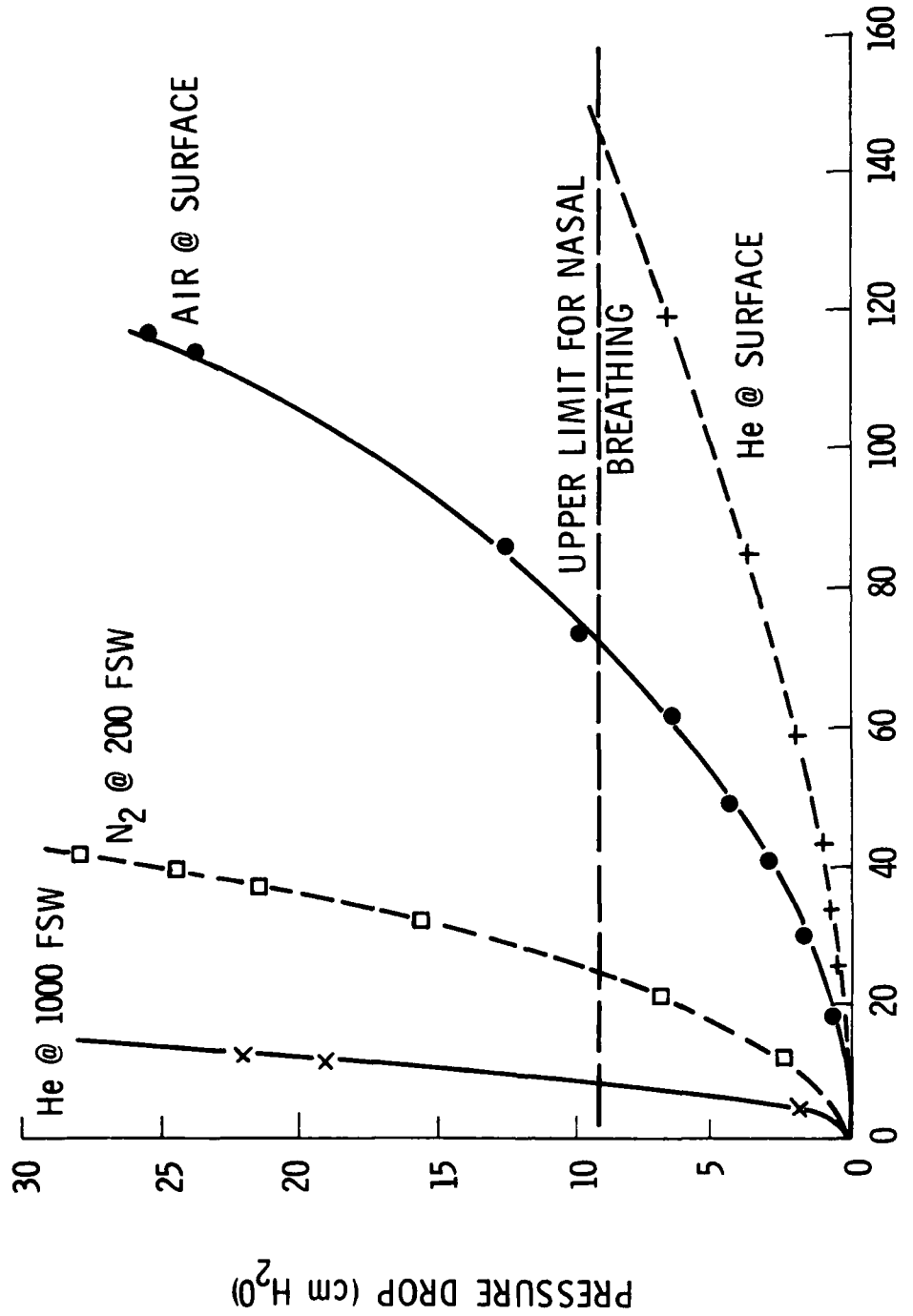

FIGURE F-1: PRESSURE DROP THROUGH NASAL TRACT WITH VARIOUS GASES

TABLE F-1

CALCULATED FRICTION FACTORS FOR HUMAN NASAL TRACT

Test	Pressure Drop lb/ft^2	Flow Velocity ft/sec	Calculated f	Re	
0.	0.2046	8.2251	0.1396	2051.8523	
1.	5.9334	17.6969	0.8744	4414.7152	
2.	9.2070	22.1752	0.8641	5531.8985	
3.	13.0944	26.4370	0.8647	6595.0640	
4.	25.5750	37.0702	0.8589	9247.6580	Air
5.	48.4902	49.1273	0.9273	12255.4590	Surface
6.	9.0024	21.2270	0.9221	5295.3666	
7.	3.4782	12.9593	0.9558	3232.8745	
8.	20.0508	31.8602	0.9116	7947.9606	
9.	1.4322	7.8346	1.0768	1954.4568	
10.	51.9684	50.2887	0.9484	12545.1900	
27.	3.6828	25.2723	1.9232	799.4052	
28.	7.1610	36.6404	1.7791	1158.9975	
29.	13.2990	51.3648	1.6813	1624.7551	
30.	0.8184	10.9350	2.2828	345.8935	He
31.	2.4552	20.6234	1.9254	652.3512	Surface
32.	1.2276	14.5112	1.9445	459.0120	
33.	2.0460	18.5991	1.9727	588.3199	
34.	4.5012	5.1673	1.1404	8926.4002	
35.	13.9128	9.2585	1.0979	15993.8421	
36.	31.9176	13.9501	1.1095	24098.4467	N_2
37.	43.7844	16.1450	1.1363	27890.0414	
38.	49.7178	17.2638	1.1284	29822.6779	200 ft
39.	57.0834	18.2546	1.1588	31534.2797	
54.	3.6828	2.1522	8.6278	2092.4787	
56.	19.6416	13.9928	1.0886	13604.3015	He
57.	88.1826	31.7749	0.9478	30892.7691	1000 ft

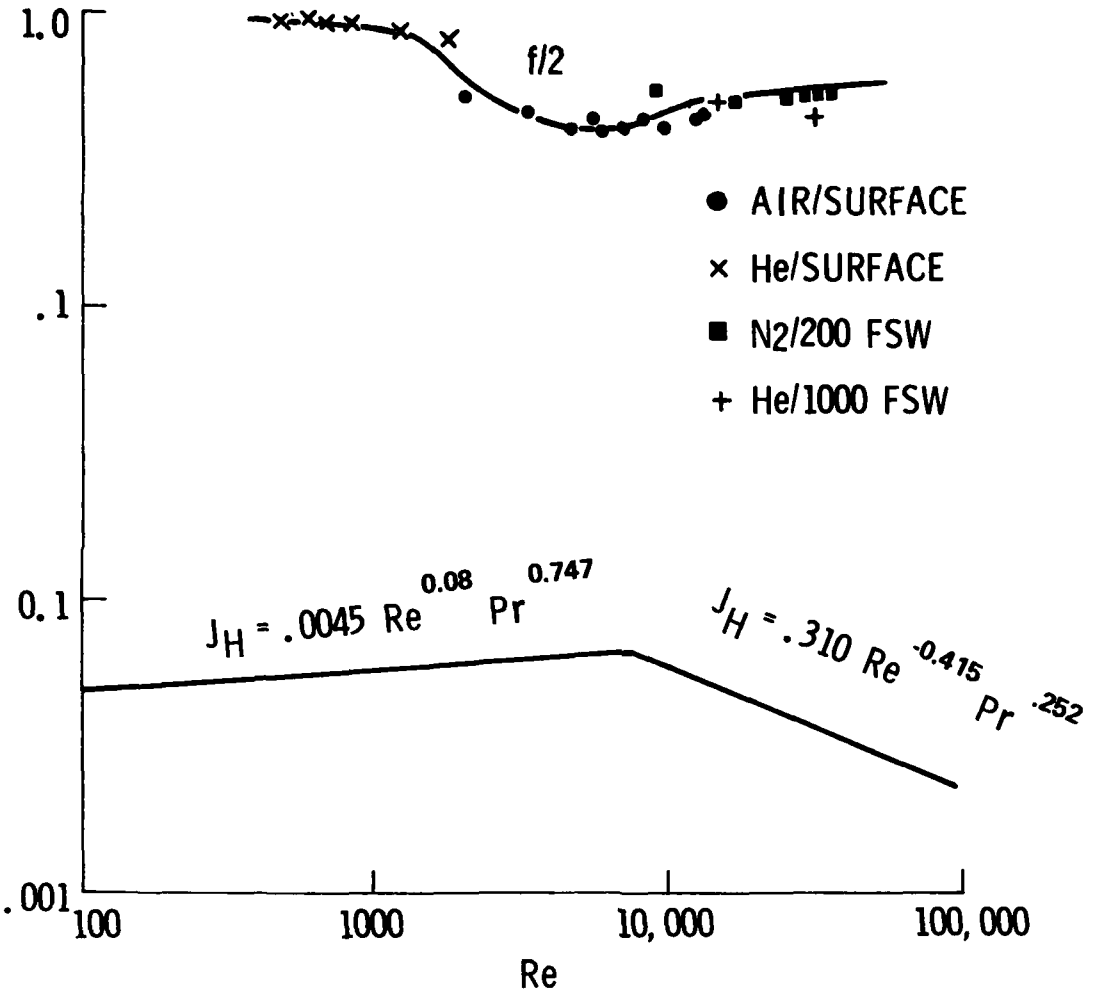

FIGURE F-2: COMPARISON OF CHILTON-COLBURN j-FACTORS WITH CALCULATED FRICTION FACTORS FOR THE UPPER RESPIRATORY TRACT DURING NASAL BREATHING/EXHALATION

APPENDIX G

RESPIRATORY HEAT LOSS CALCULATIONS

In the classical method, heat and moisture transfer from the respiratory tract are calculated from a simple energy and mass balance between inspiratory and expiratory gas conditions. Although such an analysis gives no information concerning the heating and humidification of the breathing gas as it progresses through the respiratory tract, it does give an overall assessment of the heat drain on the body through this exchange mode.

Three components must be considered when performing this energy and mass balance as indicated by Figure G-1:

a. Sensible heat associated with the temperature conditioning of the dry breathing gas.

b. Sensible heat associated with raising the temperature of the entering water vapor to body temperature.

c. Latent or insensible heat associated with the vaporization of added water during gas humidification.

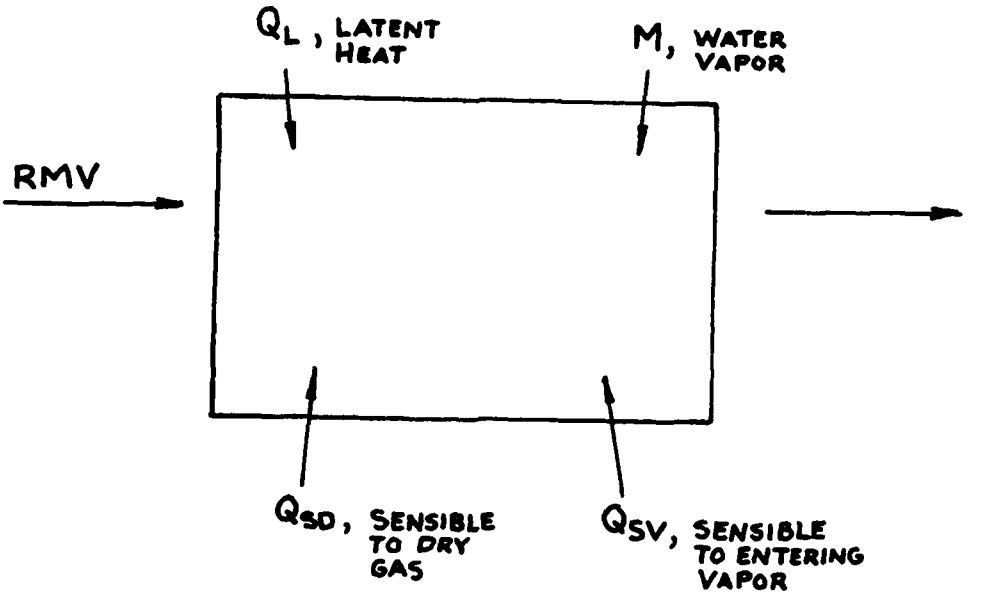

FIGURE G-1. HEATING AND HUMIDIFICATION OF RESPIRATORY GASES

a. Sensible Heat Added to Dry Gas

$$Q_{SD} = RMV \cdot \rho_{ge}\ Cp_{ge}\ Te - RMV \cdot \rho_{gi}\ Cp_{gi}\ Ti$$

Where

$$\rho_g = \frac{(P_A - P_{H_2O}) \cdot 144}{T \cdot R}\ , \text{lbm/ft}^3$$

C_p = gas specific heat, BTU/lbm-°F

T = gas temperature, °R

RMV = flow rate, ft^3/min

P = partial pressure, lb_f/in^2

R = gas constant, ft-lb_f/lbm-°R

e,i = exit and inlet conditions, respectively

b. Sensible Heat Added to Entering Water Vapor

$$Q_{SV} = RMV \cdot \rho_{gi} \cdot W_i \cdot Cp_{H_2O} \quad (Te - Ti)$$

Where

$$W = \frac{\text{mass of water vapor}}{\text{mass of dry gas}} = \text{humidity ratio}$$

Assuming that both the dry breathing gas and the water vapor behave as ideal gases, we can express the humidity ratio, W, as

$$W = \frac{P_{H_2O}\ V}{R_{H_2O}\ T} \cdot \frac{R_g\ T}{P_g\ V} = \frac{P_{H_2O}}{P_g} \cdot \frac{R_g}{R_{H_2O}}$$

However, since

$$R = Ru/M \text{ and } P_{H_2O} = \phi P_v$$

where

M = molecular weight, lbm/mole

Ru = universal gas constant, ft-lb_f/mole - °R

ϕ = relative humidity

the humidity ratio can be written as

$$W = \frac{\phi P_v}{P_A - \phi P_v} \cdot \frac{M_{H_2O}}{M_g}$$

c. Latent Heat of Vaporization

As the respiratory gas is being humidified, latent heat is being added according to the expression

$$Q_L = RMV \cdot \rho_g \cdot (We - Wi) \cdot h_{fg}$$

where

h_{fg} = latent heat of vaporization, BTU/lbm

As previously shown, this expression can be simplified by using the definition of the humidity ratio to give

$$Q_L = RMV \cdot \rho_g \cdot \frac{M_{H_2O}}{M_g} \cdot h_{fg} \frac{\phi P_{v_e} - \phi P_{v_i}}{P_A - \phi P_{v_i}}$$

It was assumed above that the expiration gas was saturated with water vapor.

Gas Properties

It should be noted from the above expressions that it is necessary to be able to measure or predict the following quantities in order to calculate the total respiratory heat losses at given inspired temperature and respiratory minute volumes:

1. Expiration temperature.

2. Vapor pressure at inspiration and expiration temperatures.

3. Gas mixture properties (molecular weights, specific heats, gas constants, etc.).

a. Expiration Temperature

Several investigators [3, 4, 6] have proposed empirical relationships to predict expired temperatures as a function of inspired temperature. Among others, the following have been proposed:

$$Te = 24.4 + 0.32\ Ti \qquad \text{(Goodman [4])}$$

$$Te = 29.3 + 0.09\ Ti + 0.004\ Ti^2 \qquad \text{(Hoke [6])}$$

$$Te = 29.0 + 0.2\ Ti \qquad \text{(Webb [3])}$$

Each of these expressions was derived from similar experimental trials in which Te and Ti were continually monitored at various hyperbaric environments. During each of these investigations the results at preset conditions were evaluated and their results extrapolated over the range of operational conditions that a diver might see. It is interesting to note that each of these investigators observed no significant variation in expired temperature over varying depths of exposures, respiratory minute volumes, or exercise levels.

b. Vapor Pressure

Values for water vapor pressures at varying ambient temperatures are found tabulated in any table which presents the properties of saturated and super-heated steam. However, for calculation purposes it is desirable to be able to express vapor pressure as some known function of temperature. Smith, Keyes and Gerry [67] offer one such expression as

$$\log_{10} \frac{218.167}{P_v} = \frac{X}{T} \frac{3.2437814 + 5.86826 \cdot 10^{-3} X + 1.1702379 \cdot 10^{-8} X^3}{1 + 2.1878462 \cdot 10^{-3} X}$$

where

$$X = (647.27 - T)$$

T has units of degree Kelvin and P_v has units of atmospheres

This expression can be solved iteratively for P_v at any temperature for use in the respiratory heat loss calculations above. As shown below, this above expression shows close agreement with tabulated values of P_v.

	Saturated Vapor Pressure, PSIA	
Temperature, °F	Steam Tables [68]	Smith, Keyes, and Gerry [67]
35	0.099	0.099
40	0.122	0.126
50	0.178	0.179
60	0.256	0.259
70	0.363	0.365
80	0.507	0.506
90	0.698	0.699
100	0.949	0.947

c. Gas Properties

Due to the narcotic effects of nitrogen and the toxic behavior of oxygen as depth increases, it is necessary to alter the respiratory gas mix of divers at varying depths. This mix variation will affect significantly the pertinent gas properties which are necessary to calculate respiratory heat loss such as specific heats, gas constants, and the apparent gas molecular weight.

The specific heat of a mixed gas can be calculated as weighted average (weighted by component molecular weight and percentage of mix volume) of the specific heats of each component [66].

$$C_{p_{mix}} = \frac{Xa \cdot M_a \cdot C_{p_a} + Xb \cdot M_b \cdot C_{p_b} + \cdots}{Xa \cdot M_a + Xb \cdot M_b + \cdots}$$

Where: a, b, etc., are the components of the gas mix, and X is each components mole fraction.

In a similar manner the gas constant of a gas mix is calculated as: [66]

$$R_{mix} = \frac{Xa \cdot M_a \cdot R_a + Xb \cdot M_b \cdot R_b + \cdots}{Xa \cdot M_a + Xb \cdot M_b + \cdots}$$

And finally, the apparent molecular weight of the gas mix is calculated as:

$$M_{mix} = Xa \cdot M_a + Xb \cdot M_b + \cdots$$

Using the above methods and expressions for the mix gas properties at inspiration and expiration, the total respiratory heat losses can be calculated for various depths, inspiration temperatures, humidity levels, and gas mixtures as:

$$Q_{TOT} = Q_{SD} + Q_{SV} + Q_L.$$

A Hewlett-Packard 9830 Desk Computer was programmed to calculate respiratory heat losses using the above methods (a program listing called "RHL" is given in Appendix I). A plot of typical results from this analysis is seen in Figure G-2.

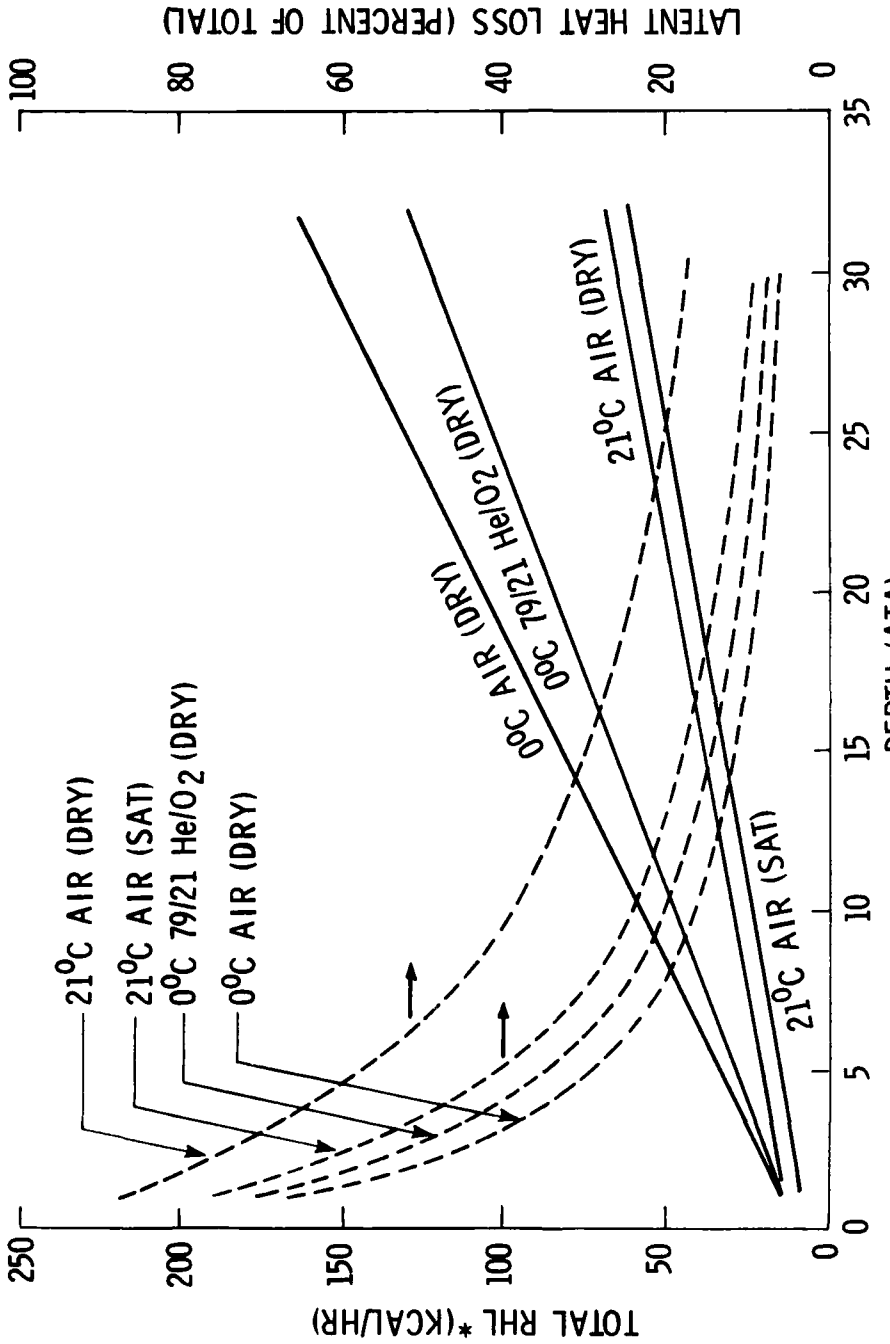

*BASED ON RMV OF 10 LPM

FIGURE G-2: RESPIRATORY HEAT LOSS AT HYPERBARIC CONDITIONS

Observations

As previously known, respiratory heat loss increases nearly linearly with pressure due to the increased gas density. It can also be seen that latent heat, although approximately constant with depth, plays a rapidly diminishing role in total heat loss as pressure increases (latent heat 70 to 90 percent of total at the surface compared to 6 to 18 percent at 30 ata).

The humidity level of the inspired gas plays a relatively minor role in the total respiratory heat loss at low inspiration temperatures. Conversely, the humidity level of the inspired gas shows a significant inverse relationship with respiratory heat loss as the diver's gas temperature is elevated.

A comparison of the products of gas density and specific heat for air and a 79 percent He/21 percent O_2 mixture shows that air would consistently cause a higher heat drain on the respiratory tract than its He/O_2 counterpart. The high heat losses associated with heliox mixtures at elevated pressures would in fact be surpassed by air, if air were a breathable mix at high pressures.

APPENDIX H

REYNOLDS ANALOGY

The transport of momentum and the transport of heat in a fluid can be shown to have similarities under many conditions. This observation has led to a useful means of determining the heat transfer characteristics of many fully developed flow systems from available friction factor data, a method referred to as the Reynolds Analogy. The following gives a brief derivation of this analogy.

As a first example in this derivation, we can look at the simple case of flow over a flat plate (assume constant properties, no viscous dissipation, and no buoyancy forces). Under these conditions, the momentum and energy equations for laminar flow can be written [65] as

$$\bar{u}\frac{\partial\bar{u}}{\partial\bar{x}} + \bar{v}\frac{\partial\bar{u}}{\partial\bar{y}} = \frac{1}{Re}\frac{\partial^2\bar{u}}{\partial\bar{y}^2} \qquad \text{(H-1)}$$

and

$$\bar{u}\frac{\partial\bar{T}}{\partial\bar{x}} + \bar{v}\frac{\partial\bar{T}}{\partial\bar{y}} = \frac{1}{PrRe}\frac{\partial^2\bar{T}}{\partial\bar{y}^2} \qquad \text{(H-2)}$$

where

$$\bar{u} = \frac{u}{V_\infty} \quad , \quad \bar{T} = \frac{T-T_w}{T_\infty-T_w}, \quad \bar{x} = \frac{x}{L}$$

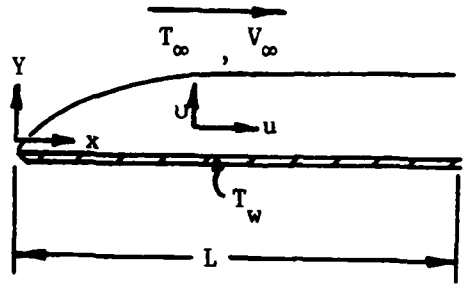

At the wall ($y = 0$), $\bar{u} = \bar{T} = 0$; and in the free stream ($y = \infty$), $\bar{u} = \bar{T} = 1$.

The above two equations, having the same boundary conditions, will have identical solutions for the dimensionless temperature and velocity profiles provided that Pr = 1 in Equation (H-2). Under this condition we can equate these dimensionless profiles at the wall to get

$$\left.\frac{\partial \bar{T}}{\partial \bar{y}}\right)_{wall} = \left.\frac{\partial \bar{u}}{\partial \bar{y}}\right)_{wall}$$

or in dimensional terms

$$\frac{L}{T_\infty - T_w}\left.\frac{\partial T}{\partial y}\right)_{wall} = \frac{L}{V_\infty}\left.\frac{\partial u}{\partial y}\right)_{wall} . \qquad \text{(H-3)}$$

But we know also that the heat flux and shear stress at the wall can be written as

$$\dot{q}/A = h(T_w - T_\infty) = -K\left.\frac{\partial T}{\partial y}\right)_{wall} \qquad \text{(H-4)}$$

and

$$\tau_{wall} = \mu \left(\frac{\partial u}{\partial y} \right)_{wall} \quad . \tag{H-5}$$

By substituting the temperature and velocity profiles at the wall from Equations (H-4) and (H-5) into Equation (H-3) we obtain

$$\frac{L}{T_\infty - T_w} \left[- \frac{h(T_w - T_\infty)}{K} \right] = \frac{L}{V_\infty} \left[\frac{\tau_{wall}}{\mu} \right]$$

or

$$\frac{h}{K} = \frac{\tau_w}{\mu V_\infty} \quad . \tag{H-6}$$

A dimensionless coefficient of drag is defined in Reference [69] as

$$C_f = \frac{\text{Drag/Area}}{\frac{1}{2}\rho V_\infty^2} = \frac{\tau_w}{\frac{1}{2}\rho V_\infty^2} \quad .$$

Substituting this coefficient into Equation (H-6) and solving for the convective heat transfer coefficient, h, we can obtain

$$h = \frac{C_f}{2} (\rho V_\infty C_p) \quad \frac{K}{\mu C_p}$$

However, since $\mu C_p/K$ is the dimensionless Prandtl number which we initially set equal to 1, we obtain the form of Reynolds Analogy

$$\frac{h}{\rho V_\infty C_p} = \frac{C_f}{2} \tag{H-7}$$

where the dimensionless group, $h/\rho V_\infty C_p$, is the Stanton number.

In the case of turbulent flow over the same flat plate the Reynolds Analogy can be shown to also be valid provided certain other conditions are met. Under turbulent flow conditions the total shear stress on the fluid is made up of the molecular stress shown in Equation (H-5) and an additional stress due to eddy currents [65]

$$\frac{\tau_{eddy}}{\rho} = \varepsilon_M \frac{\partial u}{\partial y}$$

where: ε_M is the eddy diffusivity of momentum

u is time-smoothed velocity

The total stress can thus be written as

$$\frac{\tau_{total}}{\rho} = (\nu + \varepsilon_M) \frac{\partial u}{\partial y} \tag{H-8}$$

where $\nu = \frac{\mu}{\rho}$ = kinematic viscosity or the molecular diffusivity of momentum.

Similarly, the heat transfer relationship given in Equation (H-4) must be modified to include the additional turbulent flow component as

$$(\dot{q}/A)_{total} = - (K + \rho C_P \varepsilon_H) \frac{\partial T}{\partial y}$$

or

$$\frac{(\dot{q}/A)_{total}}{\rho C_P} = - (\alpha + \varepsilon_H) \frac{\partial T}{\partial y} \qquad \text{(H-9)}$$

where: $\alpha = \frac{K}{\rho C_P}$ = the thermal diffusivity of heat (molecular)

ε_H = eddy diffusivity of heat

T is time smoothed temperature.

Kays [64] notes that, with the exception of near the wall where the flow will be laminar, the eddy diffusivities (ε_M and ε_H) will be much greater than their molecular counterparts. Also, unlike the molecular diffusivities, the eddy diffusivities are not fluid properties, but they vary with the flow parameters and from point to point in the flow stream. However, the fundamental assumption made by Reynolds was that these turbulent diffusivities are equal at each point in the flow, or

$$\varepsilon_M = \varepsilon_H .$$

By defining an analogous turbulent Prandtl number, Pr_t as

$$Pr_t = \frac{\varepsilon_M}{\varepsilon_H}$$

we see that $Pr_t = 1$ in all cases based on Reynolds postulation. Thus, as long as $\nu = \alpha$ (Pr = 1)

$$\nu + \varepsilon_M = \alpha + \varepsilon_H$$

and the dimensionless, time smoothed temperature and velocity profiles will be identical. Under these conditions the equality given in Equation (H-3) for laminar flow can be made at any point in the turbulent flow stream and the previous results, $St = C_f/2$, will still apply.

APPENDIX I

PROGRAM LISTINGS

Program	Language
Data Acquisition - Lower Tract	Basic
Data Reduction - Lower Tract	Basic
Data Acquisition - Upper Tract	HP
Application	Basic
Finite Difference	Fortran
RHL	Basic

```
10 [illegible] [illegible]I[20],X[80],[illegible]Z[16],G$[5],[illegible]$[8],M[20],F[6],[illegible][9]
20 [illegible] [illegible]
30 DISP "DO YOU WANT TO SCAN?";
40 INPUT G$
50 IF POS(G$,"N")=1 THEN 120
60 DISP "WHAT SCAN POINT?";
70 INPUT A
80 FORMAT F3.0
90 CMD "[illegible]"
100 OUTPUT (13,80)A
110 GOTO 30
120 CMD "?U"
130 FORMAT B
140 OUTPUT (13,130)76
150 CMD "?U1"
160 OUTPUT (13,80)8
170 CMD "?U7","F1R7A1H1M3T1","?U5"
180 ENTER (13,*)T[9]
190 T[9]=80
200 CMD "?"
210 DISP "TEST NUMBER";
220 INPUT N1
230 DISP "MODEL TYPE";
240 INPUT Z$
250 DISP "OTHER COMMENTS?: IF NO,HIT N-EXECUTE";
260 INPUT X$
270 DISP "NUMBER OF DATA CHANNELS USED";
280 INPUT N
290 DISP "DESIRED INTERVAL OF DATA(MIN)";
300 INPUT T1
310 PRINT
320 PRINT TAB10,"RESPIRATORY HEAT TRANSFER EVALUATION"
330 PRINT TAB10,"MODEL TYPE:   "Z$
340 PRINT TAB10,"OTHER COMMENTS:   "X$
350 REM****INITIAL TIME IS RECORDED BEFORE TEST IS INITIATED
360 CMD "?U3"
370 CMD "?U5"
380 ENTER (13,*)T$
390 PRINT TAB10,"DATE:"T$[3,4]"/"T$[5,6]"/80"
400 PRINT TAB55,"TIME:"T$[7,8]":"T$[9,10]":"T$[11,12]
410 PRINT TAB10,"AMB TEMP:";T[9],"FILE NUMBER"N1
420 PRINT
430 PRINT "TAP      1       2       3       4       5       6       7       8       9"
440 PRINT
450 FOR I=1 TO N
460 D9=I
470 CMD "?U7"
480 OUTPUT (13,80)I-1
490 CMD "?U7","F1R7A1H1M3T1","?U5"
500 D[illegible] [illegible]9+D9
510 ENTER (13,*)M[D9]
515 CMD "?"
520 M[D9]=M[D9]*1000
530 M[D9]=32.1594[illegible] [illegible]M[D9][illegible]
535 [illegible]
536 [illegible]
540 [illegible]
541 [illegible]
550 [illegible]
560 [illegible]
```

```
[illegible] HEN [illegible]
[illegible]
[illegible] ENTER [illegible] T$
[illegible] VAL(T$[7,8])+[illegible]00+VAL(T$[9,10])+[illegible]VAL(T$[11,12])
[illegible] 60
620 IF [illegible] THEN 580
630 D9=D9+1
640 GOTO 440
650 C1=(I-1)*9+1
651 C2=(I-1)*9+2
652 C3=(I-1)*9+3
653 C4=(I-1)*9+4
654 C5=(I-1)*9+5
655 C6=(I-1)*9+6
656 C7=(I-1)*9+7
657 C8=(I-1)*9+8
658 C9=(I-1)*9+9
680 [illegible] M[C1],M[C2],M[C3],M[C4],M[C5],M[C6],M[C7],M[C8],M[C9]
690 FORMAT F5.0,9F[illegible]
700 CMD "?U"
710 OUTPUT 13;8026
720 CMD "?U7","F1R7[illegible]1[illegible]","N5"
730 ENTER 13;F[I]
735 F[I]=F[I]*10
740 CMD "?U"
750 OUTPUT 13;8037
760 CMD "?U7","F1R7[illegible]","N5"
770 ENTER 13;T[I]
775 CMD "?"
780 T[I]=T[I]*100
782 T[I]=T[I]*1.8+32
790 FIXED 1
800 PRINT TAB10,"BATH TEMPERATURE(F)= ";T[I],"FLOW RATE(CFM)= ";F[I]
805 WAIT 10000
810 NEXT I
820 M[55]=(F[1]+F[2]+F[3]+F[4]+F[5]+F[6])/6
830 M[56]=(T[1]+T[2]+T[3]+T[4]+T[5]+T[6])/6
840 STORE DATA #5,N1,M
850 DISP "***TEST COMPLETE***"
860 END
```

```
10 DIM ME(44)
20 DISP "FILE NUMBER"
30 INPUT N1
40 PRINT TAB10"TEST NUMBER N1
50 PRINT
60 PRINT "TAP     1       2       3       4       5       6       7       8       "
70 LOAD  DATA #5,N1,M
80 I=0
90 C1=I*9+1
100 C2=I*9+2
110 C3=I*9+3
120 C4=I*9+4
130 C5=I*9+5
140 C6=I*9+6
150 C7=I*9+7
160 C8=I*9+8
170 C9=I*9+9
180 WRITE #15,190,I,ME(C1),ME(C2),ME(C3),ME(C4),ME(C5),ME(C6),ME(C7),ME(C8),ME(C9)
190 FORMAT F3.0,10F7.1
200 IF I=5 THEN 230
210 I=I+1
220 GOTO 80
230 ME(1)=ME(1)+ME(2)+ME(3)+ME(4)+ME(5)+ME(6)+ME(7)+ME(8)+ME(9)+ME(10)
240 ME(2)=ME(11)+ME(12)+ME(13)+ME(14)+ME(15)+ME(16)+ME(17)+ME(18)+ME(19)
250 ME(3)=ME(20)+ME(21)+ME(22)+ME(23)+ME(24)+ME(25)+ME(26)+ME(27)+ME(28)
260 ME(4)=ME(29)+ME(30)+ME(31)+ME(32)+ME(33)+ME(34)+ME(35)+ME(36)+ME(37)
270 ME(5)=ME(38)+ME(39)+ME(40)+ME(41)+ME(42)+ME(43)+ME(44)+ME(45)+ME(46)
280 ME(6)=ME(47)+ME(48)+ME(49)+ME(50)+ME(51)+ME(52)+ME(53)+ME(54)+ME(55)
290 T1=(ME(5)+ME(6))/2
300 T3=(ME(3)+ME(4))/2
310 T4=(ME(1)+ME(2))/2
320 WRITE #15,330,ME(1),ME(2),ME(3),ME(4),ME(5),ME(6)
330 FORMAT /,"AVG TAP TEMP F=",6F8.1,
340 WRITE #15,350,T4,T3,T1
350 FORMAT "T4=",F8.1,5X,"T3=",F8.1,5X,"T1=",F8.1
355 PRINT
360 REM******VELOCITY CALCULATIONS FOLLOW******
370 DISP "FLOW TEMP F";
380 INPUT T9
390 P1=14.5
400 D3=0.042
410 T4=0.242
420 P2=
430 D1=
440 
450 
460 
470 
480 
490 
500 
510 
520 
530 
540 
550 
560 
570 
580 
590 
600 
```

```
560 REM*****GAS PROPERTIES*****
570 REM*****SPECIFIC HEAT,C1(B/LB-F)*****
580 REM*****THERMAL CONDUCTIVITY,K(B/HR-FT-F)
590 REM*****VISCOSITY,V(LB/FT-SEC)
600 REM*****PRANDTL NO.,P
610 REM DENSITY,R0(LB/CUFT)
620 C1=0.24
630 K=0.015
640 V=0.00001/12
650 P=0.7
660 R0=0.075
670 R1=R0*V1*D1/V
680 T5=(V3*T3+V4*T4)/(V3+V4)
690 REM*****CONVECTIVE COEF BASED ON VELOCITY IN BRANCH 1
700 REM*****L=TOTAL LENGTH OF MODEL (L1+L2+L3 OR L4)
710 L=((10.4-3.1)+4.1+1.64)/12
720 D5=T1-T5
730 D6=M[56]-T5
740 H0=R0*V1*D1*C1*D5*3600/(4*L*D6)
750 N0=H0*D1/K
760 Z0=R1*P
770 PRINT
780 PRINT TAB(10)"OVERALL FILM COEF (B/HR-FT-F)=";H0
785 PRINT TAB(10)"BRANCH 1 REYNOLDS NO=";R1
790 PRINT TAB(10)"PRODUCT OF REYNOLDS NO AND PRANDTL NO=";Z0
800 PRINT TAB(10)"OVERALL NUSSELT NO=";N0
805 PRINT
806 PRINT
807 PRINT "**************************************************"
810 END
```

```
0: "(RHT3(RESPIRATORY HEAT TRANSFER TEST (N2O2)- RD:  ":
1: dim D[8,15],M[8,9],F[7],B[3],N[4],H$[12],T$[16],A$[65],F$[10],A[2],B$[3]
2: dim G$[6],L$[3,50],C$[65],Z$[6],E[3],V[2],W[2],X[2],Y[2],P[50],Y$[80]
3: "RESPIRATORY HEAT TRANSFER TEST"→A$;1.27→F[1];1.27→F[2];20→F[3]
4: "20 CFM-#L-37961":-.008485→E[1];3.058701→E[2];-.029004→E[3]
5: 1→W
6: fxd 0;setk "PRG1K";wrt 9,"U1=I2";wrt 9,"U1G"
7: ent "Specific Heat Cp?",F[4]
8: ent "Density p?",F[5];ent "Viscosity u?",F[6]
9: ent "Thermal Conductivity K?",F[7]
10: ent "Depth?",B[1],"N2O2 Gas Mix in % (79.0/21.0)",H$;val(H$[6,9])→B[3]
11: ent "Flow Direction?, Inhalation or Exhalation",F$
12: (B[1]*.444439+14.696)/14.696→B[2];fmt 1;wrt 722,"F1R7A1H0M3T1"
13: "SCAN":ent "Want To Check Scan Points?",G$
14: if cap(G$[1,1])="N";sto "STATIC"
15: fmt 1,f3.0;ent "What Scan Point?",X;wrt 709,"C";wrt 709.1,X;sto "SCAN"
16: "STATIC":fxd 3;ent "Want To Record Static Run?",B$
17: fmt 1;wrt 722,"R4T1";if cap(B$[1,1])="N";sto "?"
18: for I=1 to 2;fmt 1,f3.0;wrt 709.1,I-1;fmt 1;wrt 722,"T2T3";trg 722
19: red 722,A[I];fxd 3;prt A[I];next I;spc 2;sto "STATIC"
20: "?":fxd 0;ent "File Number",F;str(F)→Z$;"b"→Z$[1,1]
21: "START":fmt 1;wrt 709,"00E";wrt 722,"T1R3";wrt 9,"R";red 9,T$;esb "LBL"
22: dsp "Start Gas Flow and Press Cont.";stp
23: "ST":for J=1 to 3;wrt 722,"R7T2T3";wrt 709,"00E";trg 722;red 722,D[J,1]
24: wrt 709,"02E";trg 722;red 722,D[J,3];D[J,3]*100→D[J,3];D[J,3]→T
25: (D[J,1]-A[1])*1.385→D[J,1];E[3]*D[J,1]↑2+E[2]*D[J,1]+E[1]→D[J,1]
26: cll 'VIS';D[J,1]*S*28.32→D[J,1];fxd 2;dsp "FLOW=",D[J,1]
27: if not fla1;sto "ST"
28: dsp "*********TEST IN PROGRESS***********"
29: "X":cfg 1;fmt 1;wait 1000;wrt 9,"U1C"
30: "LOOP":for W=1 to 2;fxd 6
31: wrt 9,"U1V";red 9,D[W,14];wrt 722,"T2T2";for I=1 to 2;fmt 1,f3.0
32: wrt 709.1,I-1;fmt 1;trg 722;red 722,D[W,I];next I;for I=3 to 13
33: fmt 1,f3.0;wrt 709.1,I-1;fmt 1;trg 722;red 722,D[W,I];next I
34: for I=1 to 2;D[W,I]-A[I]→D[W,I];next I
35: D[W,1]*1.385→D[W,1];D[W,2]*1.385*2.54→D[W,2];D[W,3]*100→D[W,3]
36: (D[W,4]*100-32)/1.8→D[W,4];for I=5 to 7
37: D[W,I]*100→D[W,I];next I
38: for I=5 to 7;deg;sin(9.73*(D[W,I]-5))→M[W,9]
39: D[W,I]+.3*M[W,9]→D[W,I];next I
40: for I=8 to 13;D[W,I]*1000→D[W,I]
41: 32.15943+D[W,I]*46.39959-D[W,I]↑2*1.10315→D[W,I]
42: (D[W,I]-32)/1.8→D[W,I];next I
43: E[3]→Y;for K=2 to 1 by -1;Y*D[W,1]+E[K]→Y;next K;Y→D[W,1]
44: D[W,3]→T;cll 'VIS';D[W,1]*S*28.32→D[W,1]
45: F[5]*(D[W,1]/F[1])*(1000/60)*F[2]/F[6]→M[W,1]
46: (D[W,10]+D[W,11]+D[W,12])/3→M[W,2]
47: (D[W,5]+D[W,6])/2→M[W,3];(D[W,7]+D[W,13])/2→M[W,4]
48: if cap(F$[1,1])="I";M[W,2]-M[W,3]→M[W,5];M[W,4]-M[W,3]→M[W,6]
49: if cap(F$[1,1])="E";M[W,2]-M[W,4]→M[W,5];M[W,3]-M[W,4]→M[W,6]
50: F[5]*F[4]*(M[W,6]/M[W,5])*(D[W,1]/F[1]*(1000/60)*F[2])/(4*F[3])→M[W,7]
51: M[W,7]*F[2]/F[7]→M[W,8];fxd 3
52: for I=1 to 14;D[W,I]→r[I];next I;r14/1000/60→r14
53: fmt 1,13f5.1,1f5.2
54: wrt 6.1,r1,r2,r3,r4,r5,r6,r7,r8,r9,r10,r11,r12,r13,r14;fmt 1;wrt 6
55: M[W,1]→r15;M[W,8]→r16
56: fxd 10;fmt 3,2f10.2;wrt 6.3,"          Re=",r15,"          Nu=",r16;wrt 6
```

```
57: wrt 9,"U1V";red 9,r0;if r0<D[W,14]+15000;jmp 0
58: r0→D[W,14];next W;fmt 3/;wrt 6;fmt
59: for I=1 to 4;beep;dsp "*****TEST COMPLETE*****";wait 500;next I
60: ent "Want to Record Data?",G$;if cap(G$[1,1])="N";jmp 2
61: open Z$,13;0→Z;asgn Z$,1,0,Z;sprt 1,D[*],B[*],H$,T$,A$,F$,M[*],"end"
62: gto "?"
63: "VIS":
64: 203.29*((459.67+T)/529.67)↑.79→V[1];175.88*((459.67+T)/529.67)↑.746→V[2]
65: 32→W[1];28.0134→W[2];val(H$[6,9])→X[1];100-val(H$[6,9])→X[2]
66: 0→S;1/√(8(1+W[2]/W[1]))*(1+√V[2]*(W[2]/W[1])↑.25)↑2→Y[1]
67: 1/√(8(1+W[2]/W[1]))*(1+√(V[2]/V[1])*(W[1]/W[2])↑.25)↑2→Y[2]
68: X[1]*V[1]/(Y[1]*X[2]+X[1])+X[2]*V[2]/(Y[2]*X[1]+X[2])→S
69: 181.87/S→S;ret
70: "RED":fmt ;wrt 722,"R7A0T2T3";for K=1 to 50;trg 722;red 722,P[K];next K
71: wrt 722,"A1";ret
72: "LBL":fxd 0;fmt 3/;wrt 6;fmt ;if cap(F$[1,1])="I";0→D[W,2]
73: ""→Y$;"              Gas Mix=N2O2 "→Y$[1,23];H$→Y$[24,39]
74: ""→Y$[len(Y$)+1,80];"Temperature in Deg. "→Y$[40,59];"C"→Y$[60,60]
75: fmt ;wrt 6,Y$;fxd 0
76: "            Data File No.="→Y$[1,24]
77: fxd 0;Z$→Y$[25,39];""→Y$[len(Y$)+1,80];"FSW="→Y$[40,43]
78: str(B[1])→Y$[44,48];fmt ;wrt 6,Y$
79: ""→Y$;"              D1= Supply Flow(Alpm)          "→Y$[1,39]
80: ""→Y$[len(Y$)+1,80];"D2= Model press.(cm H2O)"→Y$[40,64];fmt ;wrt 6,Y$
81: ""→Y$;"              D3= Supply Gas Temp.'F"→Y$[1,39]
82: ""→Y$[len(Y$)+1,80];"D4= Bath Temp. "→Y$[40,69];fmt
83: wrt 6,Y$;""→Y$;"              D5= Oral  #1 GAS Temp.       "→Y$[1,39]
84: ""→Y$[len(Y$)+1,80];"D6= Oral  #2 Gas Temp."→Y$[40,60];fmt ;wrt 6,Y$
85: ""→Y$;"              D7= Trachea Temp.#1          "→Y$[1,39]
86: ""→Y$[len(Y$)+1,80];"D8= Wall #1Temp."→Y$[40,60];fmt ;wrt 6,Y$
87: ""→Y$;"              D9= Wall #2 Temp.       "→Y$[1,39]
88: ""→Y$[len(Y$)+1,80];"D10= Wall #3 Temp."→Y$[40,64]
89: fmt ;wrt 6,Y$
90: ""→Y$;"              D11=Wall #4 Temp.          "→Y$[1,39]
91: ""→Y$[len(Y$)+1,80]
92: "D12= Wall#5 Temp."→Y$[40,67];fmt ;wrt 6,Y$
93: ""→Y$;"              D13= Trachea Temp. #2        "→Y$[1,39]
94: ""→Y$[len(Y$)+1,80];"D14= Time into Test(min)"→Y$[40,65];fmt ;wrt 6,Y$
95: ""→Y$
96: ""→Y$;""→Y$[1,10];T$[1,2]→Y$[11,12];"/"→Y$[13,13]
97: T$[4,5]→Y$[14,15];"/"→Y$[16,16];"81"→Y$[17,39]
98: F$→Y$[40,50];"Cycle"→Y$[51,80];wrt 6,Y$;fmt ;wrt 6;""→Y$
99: "    D1"→Y$[1,5];"    D2"→Y$[6,10];"    D3"→Y$[11,15];"    D4"→Y$[16,20]
100: "    D5"→Y$[21,25];"    D6"→Y$[26,30];"    D7"→Y$[31,35]
101: "    D8"→Y$[36,40];"    D9"→Y$[41,45];"   D10"→Y$[46,50]
102: "   D11"→Y$[51,55];"   D12"→Y$[56,60];"   D13"→Y$[61,65]
103: "   D14"→Y$[66,70];fmt ;wrt 6,Y$
104: wrt 6;ret
105: "?":ent "Want to Continue Data Collection?",G$;if cap(G$[1,1])="N";gto "
106: F+1→F;str(F)→Z$;"a"→Z$[1,1];cll 'LBL';gto "X"
107: end
*31143
```

```
10 DIM N$[80]
20 DIM D[25],L[25],P[25],N[25],V[25],M[25],S[25]
30 DIM H[25],W[25],T[25],C[5],F[25],R[25]
40 REM*****************************************************************
50 FOR I=1 TO 24
60 REM W( )=WALL TEMPERATURE
70 REM  VALUES ARE READ IN METRIC UNITS; D IN CM, L IN CM, W IN DEG C
80 READ D[I],L[I],W[I]
90 NEXT I
100 REM*****************************************************************
110 DISP "INLET TEMPERATURE(C)";
120 INPUT T0
130 DISP "INLET RH(%)=";
140 INPUT H1
150 DISP "NUMBER OF RUNS";
160 INPUT N
170 REM*****************************************************************
180 REM  THE FOLLOWING CALCULATES SAT VAPOR PRESS OF INLET GAS
190 T3=T0+273
200 X=647.27-T3
210 Y=3.2437814+5.86826E-03*X+1.1702379E-08*X↑3
220 Y=(Y/(1+2.1878462E-03*X))*X/T3
230 P2=0.005
240 Y1=LGT(218.167/P2)
250 IF Y1>Y THEN 270
260 GOTO 290
270 P2=P2+0.0006
280 GOTO 240
290 P2=P2*14.7
300 REM  P4 IS THE VAPOR PRESS OF INLET GAS IN PSI
310 P4=P2*H1/100
320 REM*****************************************************************
330 REM THE FOLLOWING CALCULATES SAT VAPOR PRESS AT MEAN NASOPHARYNX WALL TEMP
340 DISP "MEAN NASOPHARYNX WALL TEMP(C)";
350 INPUT W3
360 T3=W3+273
370 X=647.27-T3
380 Y=3.2437814+5.86826E-03*X+1.1702379E-08*X↑3
390 Y=(Y/(1+2.1878462E-03*X))*X/T3
400 P3=0.005
410 Y1=LGT(218.167/P3)
420 IF Y1>Y THEN 440
430 GOTO 460
440 P3=P3+0.0006
450 GOTO 410
460 P3=P3*14.7
470 REM P3 IS THE SAT VAPOR PRESS AT MEAN NASOPHARYNX WALL TEMP(PSI)
480 REM*****************************************************************
490 P1=3.14159
500 FOR I=1 TO N
510 DISP "DEPTH (FSW)";
520 INPUT A1
530 A1=A1*14.7/33
540 DISP "GAS MIX,DEPTH";
550 INPUT N$
560 PRINT TAB10,"RESPIRATORY HEAT & MASS TRANSFER:";N$
570 PRINT TAB10,"-----------------------------------"
580 PRINT
590 PRINT
600 FOR L 1 TO 25 STEP 3
```

```
610 T[L]=37
620 V[L]=0.90258
630 NEXT L
640 REM  H5=LATENT HEAT OF VAPORIZATION AT 90F (CAL/GM)
650 H5=578.6
660 REM  R0=DENSITY (KG/M↑3)
670 REM  M1=VISCOSITY (KG/M-SEC)
680 REM  P9=PRANTL NUMBER
690 REM  K1=THERMAL CONDUCTIVITY (KCAL/SEC-M-C)
700 REM  C2=SPECIFIC HEAT (CAL/GM-C)
710 READ R0,M1,P9,K1,C2
720 DISP "GAS MIX:%HE,%O2,%N2,%CO2";
730 INPUT G1,G2,G3,G4
740 PRINT TAB5,"INSPIRATION GAS:  %HE="G1,"TEMP(C)="T0
750 PRINT TAB5,"                  %O2="G2,"RH%    ="H1
760 PRINT TAB5,"                  %N2="G3,"VP(PSIA)="P4
770 M2=(G1/100)*4.003+(G2/100)*32+(G3/100)*28.016+(G4/100)*44.011
780 REM  R2 IS THE GAS CONSTANT OF GAS MIX (FT-LBF/LBM-R)
790 R2=1544/M2
800 W0=18.016*P4/(M2*(A1-P4))
810 PRINT TAB5,"                  %CO2="G4,"H RATIO(GM/GM)="W0
820 PRINT
830 PRINT
840 M1=M1*0.00001
850 K1=K1*0.00001
860 REM R1 IS IN LITERS PER MIN
870 R1=20
880 REM Q0=SENSIBLE HEAT LOSS OF GAS(CAL/SEC)
890 REM  Q1=SENSIBLE HEAT LOSS OF ENTERING H2O(CAL/SEC)
900 REM  Q2=LATENT HEAT LOSS OF ADDED H2O(CAL/SEC)
910 REM*************************************************************************
920 FOR J=1 TO 5
930 PRINT TAB5,"RMV (LPM)=";R1
940 PRINT TAB5,"----------"
950 REM*************************************************************************
960 REM  THE FOLLOWING CALCULATES HEAT & MASS TRANS COEF OF UPPER TRACT
970 DISP "UPPER TRACT CHARACTERISTIC DIA,LENGTH (CM)";
980 INPUT X1,X2
990 X3=(R1/60)*4*1000/(P1*X1*X1)
1000 X4=R0*X3*X1/(M1*10000)
1010 X5=X4*P9
1020 J0=0.0733*P9↑0.401/X4↑0.269
1030 X6=J0*R0*C2*X3/(P9↑0.667*100)
1040 X7=2*X6*X2*100/(R0*X3*C2*X1)
1050 PRINT
1060 Z1=T0*1.8+32+460
1070 Z2=0.000146*Z1↑2.5/((A1/14.7)*(Z1+441))
1080 Z2=Z2+0.00002581
1090 Z3=M1/(R0*Z2)
1100 Z4=J0*X3/Z3↑0.667
1110 Z5=4+Z4*X2*(16.02/1.8)/(R0*X3*X1*T3)
1120 Z6=P4/(A1-P4)
1130 Z7=(P3-P4)*144
1140 REM*************************************************************************
1150 REM C1 IS RESPIRATORY MINUTE VOLUME IN LITERS PER SEC
1160 C1=P1/60
1170 REM THE TEMP,VP,& HEAT TRANSFER UP TO TRACHEA FOLLOW
1180 T[1]=T0+2*X7*(W3-T0)
1190 V[1]=A1*(R2*Z6+Z5+Z7)/(P2+R2*Z6+Z5+Z7)
1200 T[1]=18.016*V[1]*M2/(A1-V[1]))
1210 Q0=P0*C2*C1*(T[1]-T0)
1220 Q1=P0*C1*W0*1*(T[1]-T0)
1230 Q2=P0*C1*(S[1]-W0)*H5
1240 Q=Q0+Q1+Q2
1250 PRINT TAB5,"UPPER TRACT TRANSPORT CHARACTERISTICS"
```

```
1260 PRINT
1270 PRINT TAB7,"RE        H          HD        T(1)        V(1)        Q3"
1280 PRINT TAB7,"    KCAL/M↑2-SEC-C CM/SEC     (C)         PSIA      CAL/SEC"
1290 PRINT
1300 WRITE (15,1310)X4,X6,Z4,T(1),V(1),Q3
1310 FORMAT F10.1,2F10.3,F10.2,2F10.3
1320 PRINT
1330 PRINT
1340 PRINT TAB7,"LOWER TRACT TRANSPORT CHARACTERISTICS"
1350 PRINT
1360 A=0
1370 PRINT TAB7,"BRANCH   RE          H            HD       BTU TO POINT
1380 PRINT TAB7,"NUMBER NUMBER   KCAL M↑2-SEC-C CM/SEC     FT↑3/SEC"
1390 PRINT
1400 FOR K=4 TO 25 STEP 3
1410 K3=K-3
1420 REM*************************************************************
1430 REM  THE FOLLOWING CALCULATES SAT VAPOR PRESSURE AT WALL TEMP
1440 T3=W(K3)+273
1450 X=647.27-T3
1460 Y=3.2437814+5.86826E-03*X+1.1702379E-08*X↑3
1470 Y=(Y/(1+2.1878462E-03*X))*X/T3
1480 P5=0.005
1490 Y1=LGT(218.167/P5)
1500 IF Y1>Y THEN 1520
1510 GOTO 1540
1520 P5=P5+0.0006
1530 GOTO 1490
1540 P5=P5+14.7
1550 C(J)=C1/8↑A
1560 REM  F( ) IS IN CM SEC
1570 REM*************************************************************
1580 REM  THE FOLLOWING CALCULATES HEAT TRANSFER COEFFICIENT IN LOWER TRACT
1590 F(K3)=C(J)*4*1000/(P1*D(K3)*D(K3))
1600 R(K3)=R0*F(K3)*D(K3)/(M1*10000)
1610 P(K3)=R(K3)*P9
1620 J1=0.0733*P9↑0.401/R(K3)↑0.269
1630 H(K3)=J1*R0*C2*F(K3)/(P9↑0.667*100)
1640 IF P(K3) <= 100 THEN 1670
1650 N(K3)=0.0733*P(K3)↑0.731
1660 GOTO 1690
1670 N(K3)=3.66
1680 H(K3)=N(K3)*K1*100/D(K3)
1690 REM*************************************************************
1700 REM THE FOLLOWING CALCULATES MASS TRANSFER COEFFICIENT IN LOWER TRACT
1710 REM  CONVERT T(K3) TO RANKINE AND USE SPAULDING
1720 T5=T(K3)*1.8+32+460
1730 D5=0.000146*T5↑2.5/((A1/14.7)*(T5+441))
1740 REM  CONVERT D5 FROM FT↑2/HR TO M↑2/SEC
1750 D5=D5*0.00002581
1760 S5=M1/(R0*D5)
1770 M(K3)=J1*F(K3)/S5↑0.667
1780 REM  M( ) IS MASS TRANSFER COFFICIENT(GM/SEC-C) S5 IS SCHMIDT NUMBER
1790 REM*************************************************************
1800 REM  THE FOLLOWING CALCULATES DOWNSTREAM TEMPERATURE
1810 L9=L(K-1)+L(K-2)+L(K-3)
1820 S9=H(K3)*100/(R0*C2*F(K3))
1830 D8=S9*L9/(D(K3)/2)
1840 T(K)=2*D8*(W(K3)-T(K3))+T(K3)
1850 REM  T(K) IS THE DOWNSTREAM TEMPERATURE
1860 REM*************************************************************
1870 REM  THE FOLLOWING CALCULATES DOWNSTREAM VAPOR PRESSURE
1880 P(K)=4.(K)-3)+L9*(1.02/1.8)/(R0*F(K-3)*D(K-3)*T5)
1890 REM P  HAS UNITS FT↑3/LBM-R
1900 P(K)=V(K-3)*(M1-V(K-3))
```

```
1910 P7=(P5-V[K3])*144
1920 V[K]=A1*(P2+P6+D6+P7)-(R2+R2*P6+D6+P7)
1930 REM  V(P) IS DOWNSTREAM VAPOR PRESSURE (PSI)
1940 REM*****************************************************
1950 D7=T[I]-T[K3]
1960 D0=D0+R0*C2*D7*I
1970 S[K]=18.016*V[K]*(M2*(A1-V[K]))
1980 Q1=R0*C1*W0*1*(T[K]-T0)
1990 Q2=Q2+R0*C1*(S[K]-S[K3])*H5
2000 Q3=D0+Q1+Q2
2010 FIXED 2
2020 WRITE (15,2030)K3,R[K3],H[K3],M[K3],Q3
2030 FORMAT F10.0,F10.1,F10.4,3X,F10.4,F10.2
2040 A=A+1
2050 T9=W[K3]-T[K]
2060 IF T[K] >= 37 THEN 2090
2070 IF T9 <= 0.1 THEN 2090
2080 GOTO 2130
2090 T[K]=37
2100 IF V[K] >= P5 THEN 2140
2110 V9=P5-V[K]
2120 IF V9 <= 0.01 THEN 2140
2130 NEXT K
2140 PRINT
2150 PRINT "T IN    T 3     T 6     T 9     T 12    T 15    T 18    T 21    T 24
2160 WRITE (15,2170)T[1],T[4],T[7],T[10],T[13],T[16],T[19],T[22],T[25]
2170 FORMAT F5.1,F7.1,7F8.1
2180 PRINT
2190 PRINT "P IN    P 3     P 6     P 9     P 12    P 15    P 18    P 21    P24"
2200 WRITE (15,2210)V[1],V[4],V[7],V[10],V[13],V[16],V[19],V[22],V[25]
2210 FORMAT F6.3,F7.3,7F8.3
2220 PRINT
2230 PRINT
2240 R1=R1+20
2250 NEXT J
2260 NEXT I
2270 DATA 1.8,12,37
2280 DATA 1.22,4.76,37
2290 DATA 0.83,1.9,37
2300 DATA 0.56,0.76,37
2310 DATA 0.45,1.27,37
2320 DATA 0.35,1.07,37
2330 DATA 0.28,0.9,37
2340 DATA 0.23,0.76,37
2350 DATA 0.186,0.64,37
2360 DATA 0.154,0.54,37
2370 DATA 0.13,0.46,37
2380 DATA 0.109,0.39,37
2390 DATA 0.095,0.33,37
2400 DATA 0.082,0.27,37
2410 DATA 0.074,0.23,37
2420 DATA 0.066,0.2,37
2430 DATA 0.06,0.165,37
2440 DATA 0.054,0.141,37
2450 DATA 0.05,0.117,37
2460 DATA 0.047,0.099,37
2470 DATA 0.045,0.083,37
2480 DATA 0.043,0.07,37
2490 DATA 0.041,0.059,37
2500 DATA 0.041,0.05,37
2510 DATA 5.18439,2.0[illegible]2,0.68,3.601,1.706
2520 END
```

FINITE DIFFERENCE SOLUTION

```
$RESET FREE
FILE  5=RHLDATA,UNIT=DISK,RECORD=14,BLOCKING=30
FILE  6=P,UNIT=PRINTER
      DIMENSION A(11,11),T(11),IR(11),JC(11),B(11)
      READ/,DTHETA,H,TMAX,N,IND,EPS
      N1=N+1
      READ(5,/) (T(I),I=1,N1)
      DUMN=N
      DELTAX=1.0/DUMN
      P=DTHETA/DELTAX**2
      NCOUNT=1
      COUNT=0.0
       WRITE(6,2)
    2  FORMAT(1H1,20X,'SOLUTION OF 1-DIMENSIONAL, TRANSIENT HEAT TRANSFER
     1 PROBLEM'///)
       WRITE(6,3) H,DTHETA,TMAX,DELTAX
    3  FORMAT(20X,'H=',F5.1,5X,'DELTA THETA=',F7.3,5X,'TMAX=',F5.2,5X,'DE
     1LTA X=',F6.3,//)
       WRITE(6,60)
   60  FORMAT(7X,'TAU',8X,'T(1)',8X,'T(2)',6X,'T(3)',6X,'T(4)',6X,'T(5)',
     16X,'T(6)',6X,'T(7)',6X,'T(8)',6X,'T(9)',6X,'T(10)',6X,'T(11)')
      DO 50 I=1,N1
      DO 50 J=1,N1
      A(I,J)=0.0
   50  CONTINUE
       A(1,1)=1.0
      N2=N
      DO 100 I=2,N2
      IM1=I-1
      IP1=I+1
      DIM1=IM1
      DIP1=IP1
       A(I,IM1)=-P/2.0
      A(I,I)=1.+P
       A(I,IP1)=-P/2.0
  100  CONTINUE
      A(N1,N)=-P
       A(N1,N1)=1.0+P+P*DELTAX*H
  108  CALL ELIM(A,N1,N1,IR,JC,IND,EPS)
      WRITE(6,110) COUNT,(T(I),I=1,N1)
  110  FORMAT(/,5X,F8.3,5X,11F10.6)
  125  COUNT=COUNT+DTHETA
      NCOUNT=NCOUNT+1
      NSTORE=NCOUNT-1
       B(1)=T(1)
      DO 150 I=2,N2
      IM1=I-1
```

```
5400         DIM1=IM1
5500         IP1=I+1
5600         DIP1=IP1
5700          B(I)=(P/2.)*T(IM1)+(1.-P)*T(I)+(P/2.0)*T(IP1)
5900   150   CONTINUE
6100          B(N1)=P*T(N)+(1.-P-P*DELTAX*H)*T(N1)
6600   170   CALL FORW(A,N1,IR,JC,B)
6700         CALL BACW(A,N1,IR,JC,B)
6800         DO 200 I=1,N1
6900         T(I)=B(I)
7000   200   CONTINUE
7100         WRITE(6,110) COUNT,(T(I),I=1,N1)
7200         IF(COUNT.GT.TMAX) GO TO 500
7300         GO TO 125
7400   500   WRITE(6,1000)
7500   1000  FORMAT(1H1)
7600         STOP
7700         END
7800  C
7900  C      SUBROUTINE ELIM FOLLOWS
8000  C
8100         SUBROUTINE ELIM(A,P,N,IR,JC,IND,EPS)
8200         INTEGER N,P,IR(N),JC(P),X,Z,IND
8300         REAL A(N,P),EPS,M
8400         DO 10 J=1,N
8500         IR(J)=J
8600     10  CONTINUE
8700         DO 15 J=1,P
8800         JC(J)=J
8900    15   CONTINUE
9000         L=P-1
*
9100         IF(P.LT.N)L=P
9200    20   DO 500 K=1,L
9300    42   IF(IND.EQ.0) GO TO 450
9400         IF(IND.EQ.2) GO TO 150
9500  C
9600  C      IND=1;  THE FOLLOWING IS A PARTIAL PIVOTING SEARCH ON THE COLUMNS
9700  C
9800         X=K+1
9900         DO 75 J=X,N
10000         IF(ABS(A(IR(K),K)).GE.ABS(A(IR(J),K))) GO TO 75
10100         IMP=IR(K)
10200         IR(K)=IR(J)
10300         IR(J)=IMP
10400    75   CONTINUE
10500         IF(ABS(A(IR(K),K)).LT.EPS) GO TO 500
10600         GO TO 450
10700 C
10800 C       IND=2;  THE FOLLOWING IS A TOTAL SEARCH ROUTINE
10900 C
```

```
11000   150   X=K+1
11100         ITR=K
11200         J=K
11300   151   DO 200 I=K,P
11400         IF(ABS(A(IR(ITR),JC(K))).GE.ABS(A(IR(J),JC(I)))) GO TO 200
11500         ITR=J
11600         IMP=JC(K)
11700         JC(K)=JC(I)
11800         JC(I)=IMP
11900   200   CONTINUE
12000         J=J+1
12100         IF(J.GT.N) GO TO 350
12200         GO TO 151
12300   350   IMN=IR(K)
12400         IR(K)=IR(ITR)
12500         IR(ITR)=IMN
12600         IF(ABS(A(IR(ITR),JC(K))).LT.EPS) GO TO 500
12700 C
12800 C       THE FOLLOWING CALCULATES COEFFICIENT MULTIPLIERS FOR THE REDUCTION
12900 C
13000   450   IF(K.EQ.P) GO TO 500
13100         X=K+1
13200         DO 480 Z=X,N
13300         M=A(IR(Z),JC(K))/A(IR(K),JC(K))
13400         IF(ABS(M).LE.EPS) M=0.0
13500         A(IR(Z),JC(K))=M
13600         DO 470 J=X,P
13700         A(IR(Z),JC(J))=A(IR(Z),JC(J))-M*A(IR(K),JC(J))
13800         IF(ABS(A(IR(Z),JC(J))).LE.EPS) A(IR(Z),JC(J))=0.0
13900   470   CONTINUE
14000   480   CONTINUE
14100    500  CONTINUE
14200         IND=0
14300         DO 600 K=1,P
14400         IF(ABS(A(IR(K),JC(K))).GT.EPS) IND=IND-1
14500   600   CONTINUE
14600   1500  RETURN
14700         END
14800 C
14900 C       SUBROUTINE FORW FOLLOWS
15000 C
15100         SUBROUTINE FORW(A,N,IR,JC,B)
15200         INTEGER N,IR(N),JC(N),X
15300         REAL A(N,N),B(N)
15400         DO 40 I=2,N
15500         SUM=0.0
15600         L=I-1
15700         DO 30 K=1,L
15800         SUM=SUM+A(IR(I),JC(K))*B(IR(K))
15900    30   CONTINUE
16000         B(IR(I))=B(IR(I))-SUM
```

```
16100    40  CONTINUE
16200        RETURN
16300        END
16400 C
16500 C      SUBROUTINE BACW FOLLOWS
16600 C
16700        SUBROUTINE BACW(A,N,IR,JC,Y)
16800        INTEGER N,IR(N),JC(N),X
16900        REAL A(N,N),Y(N)
17000        K=N
17100        X=N+1
17200   650  L=K+1
17300        SUM=0.0
17400   680  IF(L.GT.N) GO TO 700
17500        SUM=SUM+A(IR(K),JC(L))*Y(IR(L))
17600        L=L+1
17700        GO TO 680
17800   700  Y(IR(K))=(Y(IR(K))-SUM)/A(IR(K),JC(K))
17900        K=K-1
18000        IF(K.LE.0) GO TO 750
18100        GO TO 650
18200   750  RETURN
18300        END
*
```

```
10 PRINT
20 PRINT TAB(5,"RESPIRATORY HEAT LOSS PER 10 LITER RMV"
30 PRINT
40 PRINT
50 DISP "INSPIRATION TEMPERATURE(C)=";
60 INPUT T
70 DISP "INSPIRATION GAS RH(%)=";
80 INPUT H
90 DISP "GAS MIX: %HE,%O2,%N2,%CO2";
100 INPUT G1,G2,G3,G4
110 REM    T1 IS EXPIRATION TEMPERATURE BASED ON HOKE
120 T1=29.3+0.09*T+0.004*T↑2
130 REM   THE FOLLOWING CALCULATES THE SAT VAPOR PRESS OF INSPIRED GAS
140 T3=T+273
150 X=647.27-T3
160 Y=3.2437814+5.86826E-03*X+1.1702379E-08*X↑3
170 Y=(Y/(1+2.1878462E-03*X))*X/T3
180 P2=0.005
190 Y1=LGT(218.167/P2)
200 IF Y1>Y THEN 220
210 GOTO 240
220 P2=P2+0.0006
230 GOTO 190
240 P2=P2*14.7
250 REM   P4 IS THE VAPOR PRESS OF INSPIRED GAS
260 P4=P2*H/100
270 T2=T1*1.8+32+460
280 T4=T*1.8+32+460
290 REM    THE FOLLOWING CALCULATES THE SAT VAPOR PRESS OF EXPIRED GAS
300 T3=T1+273
310 X=647.27-T3
320 Y=3.2437814+5.86826E-03*X+1.1702379E-08*X↑3
330 Y=(Y/(1+2.1878462E-03*X))*X/T3
340 P3=0.005
350 Y1=LGT(218.167/P3)
360 IF Y1>Y THEN 380
370 GOTO 410
380 P3=P3+0.0006
390 GOTO 350
400 REM  P3 IS THE SAT VAPOR PRESS OF EXPIRED GAS
410 P3=P3*14.7
420 REM   H1 IS THE LATENT HEAT OF VAPORIZATION OF WATER AT 85F(B/LB)
430 H1=1045
440 REM   V IS THE RESPIRATORY MINUTE VOLUME (LPM)
450 V=10
460 REM   R IS THE GAS CONSTANT OF THE GAS MIX(FT-LBF/LBM-R)
470 R=G1*4.003*386.2+G2*32*48.29+G3*28.016*55.16+G4*44.011*35.11
480 R=R/(G1*4.003+G2*32+G3*28.016+G4*44.011)
490 REM  C IS THE SPECIFIC HEAT OF THE GAS MIX (B/LB-F)
500 C=G1*4.003*1.24+G2*32*0.22+G3*28.016*0.247+G4*44.011*0.2
510 C=C/(G1*4.003+G2*32+G3*28.016+G4*44.011)
520 WRITE (15,530)G1,R
530 FORMAT 5X,"GAS MIX:",F5.1,"% HE",20X,"GAS CONSTANT (FT-LBF/LBM-R)=",F8.2
540 WRITE (15,550)G2,C
550 FORMAT 13X,F5.1,"% O2",20X,"GAS SPECIFIC HEAT (B/LB-F)=",F8.3
560 WRITE (15,570)G3,T
570 FORMAT 13X,F5.1,"% N2",20X,"INSPIRATION TEMP (C)=",F5.1
580 WRITE (15,590)G4,T1
590 FORMAT 13X,F5.1,"% CO2",19X,"EXPIRATION TEMP (C)=",F5.1
600 WRITE (15,610)H
```

```
[illegible]
620 PRINT
630 PRINT
640 WRITE [illegible]
650 FORMAT [illegible]
660 WRITE (15,620)
670 FORMAT [illegible]
680 PRINT
690 FOR P 1 TO 3[illegible]
700 REM P1 IS AMBIE[illegible]
710 P1 P-14.7
720 REM    R0 IS THE [illegible]
730 REM    R1 IS THE [illegible]
740 R1 [illegible] P4 [illegible] 144 [illegible]
750 R0 [illegible] P1 P3 [illegible] 144 [illegible]
760 REM    Q1 IS THE SENSIBLE [illegible]
770 Q1 [illegible] V [illegible] C*(R0*T1 R1 [illegible] 1.[illegible]
780 M1 [illegible] G1 100 [illegible] 4.00 [illegible] G2 100 [illegible]
790 H1 13.016*P4 [illegible] M1 [illegible] P1-P4 [illegible]
800 [illegible] 19.86-597 SQR [illegible] 12 [illegible] 7500 T [illegible]
810 [illegible] V*R1*W1*C1*(T1 T)*1.0 [illegible]
820 [illegible] R0*18.016*H1*(P3 P4 [illegible] M [illegible]
830 REM    Q2 IS THE SENSIBLE HEAT OF THE WATER VAPOR [illegible]
840 REM    Q3 IS THE LATENT HEAT LOSS OF THE WATER VAPOR [illegible]
850 Q4=Q1+Q2+Q3
855 Q5 [illegible] Q4 [illegible] 100
858 REM    W2 IS THE WEIGHT (LB/HR) OF WATER ADDED TO RESPIRATORY GAS
859 W2 [illegible] H1 [illegible] 3.9685
860 WRITE (15,870)P,R1,Q1,Q2,Q3,Q4,Q5,W2
870 FORMAT 3F8.3,5F10.3
880 NEXT P
890 END
```

APPENDIX J

TEST DATA

LOWER RESPIRATORY TRACT

EXHALATION

T NUMBER 4

TAP	1	2	3	4	5	6	7	8	9	TW
1	111.4	[illegible]	91.9	92.0	91.2	90.9	93.1	87.6	89.0	115.6
2	108.9	104.2	94.8	90.4	88.6	88.3	93.2	87.9	97.3	115.6
3	95.1	91.6	90.7	90.0	89.2	88.4	87.4	88.6	102.9	115.6
4	139.1	93.7	93.8	91.9	90.7	89.5	89.3	88.1	89.7	115.6
5	131.5	99.8	98.4	97.6	97.2	97.4	96.9	97.1	97.7	115.6
6	136.6	104.5	100.8	99.3	98.7	98.4	98.1	98.4	99.9	115.6

AVG TAP TEMP(F) 96.9 97.0 96.3 96.9 101.3 103.3

T4= 96.9 T3= 96.6 T1= 102.3

AVERAGE BRANCH VELOCITIES(FT/SEC)

BRANCH 1	BRANCH 2	BRANCH 3	BRANCH 4
2.37	2.42	2.14	2.70

OVERALL FILM COEF (B/SQFT-HR-F)= 1.29
BRANCH 1 REYNOLDS NO= 1930.50
PRODUCT OF REYNOLDS NO AND PRANDTL NO= 1281.35
OVERALL NUSSELT NO= 10.79

****

TEST NUMBER 1

TAP	1	2	3	4	5	6	7	8	9	TW
1	84.8	82.1	81.4	80.1	80.1	79.6	79.8	81.6	81.8	113.1
2	85.6	81.6	80.5	80.2	80.2	79.9	79.2	79.2	78.9	113.1
3	81.7	81.1	79.5	79.3	78.9	78.7	78.7	85.2	91.0	113.1
4	90.4	82.0	79.9	78.9	78.2	78.5	78.4	79.1	81.9	113.1
5	87.7	87.2	85.1	84.5	84.9	84.7	85.2	85.2	84.9	113.1
6	91.9	89.5	87.6	86.5	85.7	85.5	85.5	86.3	87.3	113.1

AVG TAP TEMP(F) 87.0 86.5 87.3 86.7 90.5 92.0

T4= 86.9 T3= 87.0 T1= 91.2

AVERAGE BRANCH VELOCITIES(FT/SEC)

BRANCH 1	BRANCH 2	BRANCH 3	BRANCH 4
44.47	45.49	40.23	50.69

OVERALL FILM COEF (B/SQFT-HR-F)= 13.83
BRANCH 1 REYNOLDS NO= 34415.32
PRODUCT OF REYNOLDS NO AND PRANDTL NO= 24030.72
OVERALL NUSSELT NO= 115.27

****

TEST NUMBER 2

TAP	1	2	3	4	5	6	7	8	9	TW
1	89.3	83.1	81.2	80.6	90.0	79.4	79.0	79.4	82.0	113.9
2	87.3	82.7	81.6	80.7	80.5	80.3	80.5	80.2	80.4	113.9
3	83.2	81.7	81.6	80.9	80.9	80.3	80.7	80.9	89.2	113.9
4	84.8	82.2	81.0	80.6	80.5	80.7	80.7	81.6	86.5	113.9
5	89.6	87.5	86.6	86.9	86.6	86.8	86.9	87.3	87.3	113.9
6	93.5	90.3	89.4	87.6	86.6	86.5	86.3	86.7	87.4	113.9

AVG TAP TEMP(F) 87.4 87.5 88.0 87.9 92.1 93.1

T4= 87.4 T3= 87.9 T1= 91.6

AVERAGE BRANCH VELOCITIES(FT/SEC)

BRANCH 1	BRANCH 2	BRANCH 3	BRANCH 4
35.69	37.51	33.18	41.80

OVERALL FILM COEF (B/SQFT-HR-F)= 12.93
BRANCH 1 REYNOLDS NO= 28383.13
PRODUCT OF REYNOLDS NO AND PRANDTL NO= 19868.19
OVERALL NUSSELT NO= 107.75

****

TEST NUMBER 3

TAP	1	2	3	4	5	6	7	8	9	TW
1	102.8	98.2	84.3	82.7	83.8	81.9	81.5	81.3	82.5	113.9
2	94.6	88.0	85.5	84.5	83.7	83.9	84.1	83.1	84.8	113.9
3	87.3	87.4	84.5	84.4	83.8	83.4	82.8	84.0	96.6	113.9
4	94.7	85.7	83.2	83.3	82.5	82.6	84.3	92.4	92.1	113.9
5	94.9	91.9	90.7	90.5	90.3	90.7	90.6	90.5	91.2	113.9
6	97.9	96.3	93.5	91.3	90.4	90.7	90.4	90.4	91.5	113.9

AVG TAP TEMP(F) 90.6 90.9 91.1 91.7 95.4 96.4

T4= 90.7 T3= 91.4 T1= 95.9

AVERAGE BRANCH VELOCITIES(FT/SEC)

BRANCH 1	BRANCH 2	BRANCH 3	BRANCH 4
23.58	24.11	21.32	26.87

OVERALL FILM COEF (B/SQFT-HR-F)= 9.31
BRANCH 1 REYNOLDS NO= 18243.00
PRODUCT OF REYNOLDS NO AND PRANDTL NO= 12770.10
OVERALL NUSSELT NO= 77.58

****

TEST NUMBER 4

TAP	1	2	3	4	5	6	7	8	9	TW
1	93.8	82.9	80.8	80.5	80.0	79.1	78.6	78.8	79.3	113.5
2	86.3	81.1	80.1	80.1	79.5	79.9	79.3	78.6	79.7	113.5
3	80.5	79.5	78.8	78.5	78.2	78.7	78.4	78.3	78.6	113.5
4	79.8	78.5	77.8	77.6	77.5	78.2	77.5	82.6	83.1	113.5
5	86.7	83.5	83.1	83.3	83.2	84.0	84.2	83.6	84.0	113.5
6	90.3	88.6	86.0	84.8	83.8	83.2	83.9	84.4	85.4	113.5

AVG TAP TEMP(F) 87.3 86.4 85.1 85.4 89.1 90.7

T4= 86.9 T3= 85.3 T1= 89.9

AVERAGE BRANCH VELOCITIES(FT/SEC)

BRANCH 1	BRANCH 2	BRANCH 3	BRANCH 4
79.82	81.61	72.17	90.93

OVERALL FILM COEF (B/SQFT-HR-F)= 20.35
BRANCH 1 REYNOLDS NO= 61743.81
PRODUCT OF REYNOLDS NO AND PRANDTL NO= 42220.10
OVERALL NUSSELT NO= 169.57

TEST NUMBER 5

TAP	1	2	3	4	5	6	7	8	9	TW
1	92.7	82.9	81.1	81.2	80.4	79.5	79.3	78.9	79.1	113.0
2	84.1	81.8	80.2	79.4	79.5	79.1	78.6	78.8	79.2	113.0
3	85.6	82.0	80.9	79.4	79.7	79.2	80.3	80.4	80.1	113.0
4	83.3	80.5	79.2	78.4	78.0	77.5	78.2	77.9	77.9	113.0
5	86.6	83.4	83.3	83.6	83.0	83.4	83.3	83.8	86.4	113.0
6	91.0	88.5	87.1	85.8	84.5	84.6	84.8	85.6	86.6	113.0

AVG TAP TEMP(F) 87.4 86.1 86.7 85.2 89.3 91.3

T4= 86.7 T3= 85.9 T1= 90.3

AVERAGE BRANCH VELOCITIES(FT/SEC)

BRANCH 1	BRANCH 2	BRANCH 3	BRANCH 4
80.10	81.89	72.42	91.25

OVERALL FILM COEF (B/SQFT-HR-F)= 22.22
BRANCH 1 REYNOLDS NO= 61959.57
PRODUCT OF REYNOLDS NO AND PRANDTL NO= 43371.70
OVERALL NUSSELT NO= 185.17

TEST NUMBER 6

TAP	1	2	3	4	5	6	7	8	9	TW
1	103.1	89.5	87.0	85.3	82.9	83.0	82.7	81.7	82.0	113.1
2	90.6	86.4	83.8	83.5	82.5	81.6	82.1	83.7	89.9	113.1
3	94.6	86.6	86.2	86.3	85.6	85.8	86.2	87.2	88.2	113.1
4	94.0	87.2	84.9	83.9	83.1	82.5	81.8	82.8	82.5	113.1
5	94.1	91.4	89.9	89.3	89.4	89.0	89.4	89.4	90.4	113.1
6	97.8	96.1	93.4	91.6	90.6	90.4	90.1	90.8	91.8	113.1

AVG TAP TEMP(F) 91.2 90.0 92.1 89.9 94.4 96.3

T4= 90.6 T3= 91.0 T1= 95.

AVERAGE BRANCH VELOCITIES(FT/SEC)

BRANCH 1	BRANCH 2	BRANCH 3	BRANCH 4
17.34	17.72	15.67	19.75

OVERALL FILM COEF (B/SQFT-HR-F)= 6.57
BRANCH 1 REYNOLDS NO= 13409.69
PRODUCT OF REYNOLDS NO AND PRANDTL NO= 9386.78
OVERALL NUSSELT NO= 54.73

TEST NUMBER 7

TAP	1	2	3	4	5	6	7	8	9	TW
1	97.6	86.4	82.8	81.7	81.3	81.3	80.0	79.8	80.3	113.0
2	86.6	82.8	81.0	80.5	80.3	79.8	79.9	79.5	80.2	113.0
3	91.5	85.2	83.0	83.5	82.8	82.7	83.1	84.5	82.7	113.0
4	90.6	85.0	82.9	81.8	80.5	79.7	79.4	79.5	79.7	113.0
5	88.7	85.5	84.9	85.0	84.9	85.0	85.0	85.2	86.3	113.0
6	93.4	89.8	88.3	86.7	85.4	85.3	85.5	87.2	87.7	113.0

AVG TAP TEMP(F) 88.8 86.0 89.5 87.7 90.6 92.3

T4= 87.9 T3= 88.6 T1= 91.4

AVERAGE BRANCH VELOCITIES(FT/SEC)

BRANCH 1	BRANCH 2	BRANCH 3	BRANCH 4
59.64	60.47	53.02	67.94

OVERALL FILM COEF (B/SQFT-HR-F)= 14.40
BRANCH 1 REYNOLDS NO= 46133.04
PRODUCT OF REYNOLDS NO AND PRANDTL NO= 32293.13
OVERALL NUSSELT NO= 120.02

TEST NUMBER 8

TAP	1	2	3	4	5	6	7	8	9	TW
1	[illegible]	[illegible]	86.9	85.9	84.5	[illegible]	[illegible]	[illegible]	[illegible]	[illegible]
2	[illegible]	[illegible]	84.5	84.8	[illegible]	[illegible]	[illegible]	[illegible]	[illegible]	[illegible]
3	[illegible]	[illegible]	[illegible]	90.4	[illegible]	[illegible]	[illegible]	[illegible]	[illegible]	[illegible]
4	[illegible]	[illegible]	91.0	88.1	[illegible]	[illegible]	[illegible]	[illegible]	[illegible]	[illegible]
5	[illegible]	[illegible]	91.1	[illegible]	90.7	[illegible]	[illegible]	[illegible]	[illegible]	[illegible]
6	[illegible]	[illegible]	93.9	92.7	[illegible]	[illegible]	[illegible]	[illegible]	[illegible]	[illegible]

AVG TAP TEMP(F) 91.9 90.8 [illegible] [illegible] [illegible] [illegible]

T4= [illegible] T3= 94.5 T1= [illegible]

AVERAGE BRANCH VELOCITIES(FT/SEC)

BRANCH 1	BRANCH 2	BRANCH 3	BRANCH 4
15.84	16.20	14.32	[illegible].05

OVERALL FILM COEF (B/SQFT-HR-F)= [illegible]
BRANCH 1 REYNOLDS NO= [illegible]
PRODUCT OF REYNOLDS NO AND PRANDTL NO= [illegible]
OVERALL NUSSELT NO= [illegible]

****

TEST NUMBER 9

TAP	1	2	3	4	5	6	7	8	9	TW
1	88.8	85.0	84.0	82.8	82.3	80.3	80.5	80.7	81.0	111.8
2	98.7	84.8	83.2	82.3	81.7	81.9	81.6	81.8	82.0	111.8
3	95.0	89.3	88.1	87.2	87.3	88.5	87.5	87.5	87.0	111.8
4	91.7	91.6	85.2	84.1	83.4	82.8	82.3	82.0	82.9	111.8
5	90.5	90.0	88.8	88.7	88.5	88.1	88.6	89.0	89.8	111.8
6	97.2	92.8	91.9	90.6	89.5	88.7	89.1	89.7	89.5	111.8

AVG TAP TEMP(F) 88.1 89.3 92.8 90.0 93.2 94.8

T4= 88.7 T3= 91.4 T1= 94.0

AVERAGE BRANCH VELOCITIES(FT/SEC)

BRANCH 1	BRANCH 2	BRANCH 3	BRANCH 4
27.42	28.03	24.79	31.24

OVERALL FILM COEF (B/SQFT-HR-F)= 9.62
BRANCH 1 REYNOLDS NO= 21209.94
PRODUCT OF REYNOLDS NO AND PRANDTL NO= 14846.96
OVERALL NUSSELT NO= 80.14

****

TEST NUMBER 10

TAP	1	2	3	4	5	6	7	8	9	TM
1	96.0	82.8	81.6	80.4	80.2	74.5	78.9	79.3	79.3	111.7
2	86.7	82.0	82.1	81.1	80.5	80.5	79.4	79.1	78.6	111.7
3	94.0	90.0	86.0	83.4	83.2	85.1	84.4	84.9	84.9	111.7
4	88.4	89.3	83.1	82.3	81.6	81.1	80.7	80.5	84.5	111.7
5	89.5	88.0	86.3	86.0	86.0	86.1	86.3	86.4	87.6	111.7
6	94.2	93.7	88.7	87.7	87.2	87.0	86.9	88.3	91.7	111.7

AVG TAP TEMP(F) 87.4 85.7 91.1 88.3 91.4 90.5

T4= 87.0 T2= 89.9 T1= 91.5

AVERAGE BRANCH VELOCITIES(FT/SEC)

BRANCH 1	BRANCH 2	BRANCH 3	BRANCH 4
49.17	50.27	44.46	56.01

OVERALL FILM COEF (B/SQFT-HR-F = 15.37
BRANCH 1 REYNOLDS NO= 38032.36
PRODUCT OF REYNOLDS NO AND PRANDTL NO= 26622.65
OVERALL NUSSELT NO= 136.44

TEST NUMBER 11

TAP	1	2	3	4	5	6	7	8	9	TM
1	93.4	83.4	82.7	80.2	79.6	79.1	79.7	78.5	79.6	111.5
2	87.3	81.3	80.0	79.0	78.5	78.2	78.4	78.9	79.3	111.5
3	92.5	84.2	82.9	83.5	85.1	84.1	82.0	82.8	84.5	111.5
4	88.2	86.9	83.3	82.1	80.3	80.1	79.7	79.6	84.9	111.5
5	86.6	85.6	85.5	85.5	85.2	85.2	85.4	85.6	85.9	111.5
6	92.3	90.4	88.2	87.2	86.5	86.4	86.4	86.7	88.6	111.5

AVG TAP TEMP(F) 87.1 85.9 89.6 85.1 90.2 92.3

T4= 86.5 T3= 88.9 T1= 9 .5

AVERAGE BRANCH VELOCITIES(FT/SEC)

BRANCH 1	BRANCH 2	BRANCH 3	BRANCH 4
48.85	49.35	40.45	56.16

OVERALL FILM COEF (B/SQFT-HR-F = 19.70
BRANCH 1 REYNOLDS NO= 51712.23
PRODUCT OF REYNOLDS NO AND PRANDTL NO= 36149.13
OVERALL NUSSELT NO= 184.87

TEST NUMBER 12

TAP	1	2	3	4	5	6	7	8	9	TW
1	82.0	81.8	81.2	81.0	79.9	80.1	79.0	78.9	78.0	111.4
2	86.1	82.3	80.5	80.1	79.7	79.2	78.4	78.2	78.2	111.4
3	91.5	86.4	82.2	83.9	83.7	83.0	83.1	82.7	82.3	111.4
4	85.1	86.4	82.7	81.6	80.2	79.0	78.5	77.7	82.7	111.4
5	86.7	86.4	82.8	82.9	83.6	83.1	83.4	83.7	84.1	111.4
6	90.4	89.3	87.2	85.4	84.8	84.5	84.6	85.4	86.0	111.4

AVG TAP TEMP(F) 86.0 86.4 89.5 87.0 89.0 91.0

T4= 86.2 T3= 88.2 T1= 90.0

AVERAGE BRANCH VELOCITIES(FT/SEC)

BRANCH 1	BRANCH 2	BRANCH 3	BRANCH 4
73.52	75.17	66.48	83.76

OVERALL FILM COEF (B/SQFT-HR-F)= 16.46
BRANCH 1 REYNOLDS NO= 56977.50
PRODUCT OF REYNOLDS NO AND PRANDTL NO= 39810.75
OVERALL NUSSELT NO= 137.18

TEST NUMBER 13

TAP	1	2	3	4	5	6	7	8	9	TW
1	98.9	86.2	86.0	82.5	82.0	81.6	81.1	81.3	87.2	125.3
2	96.6	97.3	84.3	82.1	81.2	81.1	81.1	81.2	82.1	125.3
3	98.0	99.1	88.0	87.3	89.4	90.2	90.6	88.7	89.2	125.3
4	93.6	90.1	85.7	84.1	83.0	82.9	82.5	82.3	91.4	125.3
5	92.4	91.0	90.2	90.0	90.3	90.5	90.4	91.0	94.1	125.3
6	100.7	97.4	94.9	93.2	91.9	91.0	90.5	91.9	93.3	125.3

AVG TAP TEMP(F) 92.7 90.7 97.4 93.3 97.3 99.6

T4= 91.7 T3= 95.3 T1= 98.5

AVERAGE BRANCH VELOCITIES(FT/SEC)

BRANCH 1	BRANCH 2	BRANCH 3	BRANCH 4
56.20	57.46	50.81	64.02

OVERALL FILM COEF (B/SQFT-HR-F)= 16.81
BRANCH 1 REYNOLDS NO= 43471.34
PRODUCT OF REYNOLDS NO AND PRANDTL NO= 30429.84
OVERALL NUSSELT NO= 140.35

TEST NUMBER 14

TAP	1	2	3	4	5	6	7	8	9	TW
1	86.9	84.5	80.4	80.8	80.9	80.2	79.8	82.9	85.4	115.9
2	85.7	85.2	89.6	81.2	80.5	79.9	79.8	80.1	82.0	115.9
3	89.9	90.8	90.8	85.6	88.3	88.6	86.4	85.8	85.4	115.9
4	88.6	87.6	85.2	84.1	83.7	82.6	81.2	81.2	82.3	115.9
5	90.6	92.3	87.1	86.9	87.5	87.2	87.2	87.0	87.2	115.9
6	94.7	94.8	90.9	89.3	88.7	87.0	86.4	86.3	86.6	115.9

AVG AIR TEMP(F) 89.7 89.7 93.0 89.9 92.9 94.2

T4= 89.7 T3= 91.4 T1= 90.6

AVERAGE BRANCH VELOCITIES(FT/SEC)

BRANCH 1	BRANCH 2	BRANCH 3	BRANCH 4
78.35	71.92	63.61	80.14

OVERALL FILM COEF (B/SQFT-HR-F)= 15.93
BRANCH 1 REYNOLDS NO= 54417.31
PRODUCT OF REYNOLDS NO AND PRANDTL NO= 38092.12
OVERALL NUSSELT NO= 132.72

TEST NUMBER 15

TAP	1	2	3	4	5	6	7	8	9	TW
1	83.1	83.1	82.3	81.0	80.2	80.1	79.2	79.1	79.6	111.1
2	85.7	81.9	80.3	80.1	79.8	79.7	80.4	80.5	80.4	111.1
3	82.3	81.3	81.2	80.6	80.4	80.3	80.5	80.6	93.2	111.1
4	86.0	83.8	82.0	81.7	81.5	81.1	81.1	81.6	81.7	111.1
5	86.8	86.8	86.6	86.7	86.1	85.9	85.9	85.9	86.9	111.1
6	93.2	90.4	88.2	87.0	86.9	86.7	86.3	86.2	87.2	111.1

AVG TAP TEMP(F) 87.3 86.5 87.5 87.5 90.9 92.2

T4= 86.9 T3= 87.5 T1= 91.5

AVERAGE BRANCH VELOCITIES(FT/SEC)

BRANCH 1	BRANCH 2	BRANCH 3	BRANCH 4
74.56	66.00	58.37	78.55

OVERALL FILM COEF (B/SQFT-HR-F)= 21.90
BRANCH 1 REYNOLDS NO= 49907.04
PRODUCT OF REYNOLDS NO AND PRANDTL NO= 34955.93
OVERALL NUSSELT NO= 182.57

TEST NUMBER 16

TAP	1	2	3	4	5	6	7	8	9	TW
1	[illegible]	[illegible]	81.7	81.1	80.3	79.8	80.[illegible]	80.6	80.9	112.3
2	91.4	90.6	81.9	80.9	80.5	79.8	80.1	81.0	80.7	112.3
3	82.5	83.9	81.9	80.9	81.0	81.6	81.3	95.[illegible]	94.8	112.3
4	87.3	87.0	83.4	82.5	81.7	81.9	83.1	82.1	83.7	112.3
5	91.6	91.4	88.4	87.9	87.9	87.5	87.8	88.5	89.4	112.3
6	96.[illegible]	92.9	90.3	89.9	88.7	88.[illegible]	88.5	88.5	89.1	112.3

AVG TAP TEMP(F) 88.0 88.3 89.[illegible] [illegible] 93.[illegible] 94.3

T[illegible]= 88.2 TO= 89.3 TI= [illegible]

AVERAGE BRANCH VELOCITIES(FT/SEC)

BRANCH 1	BRANCH 2	BRANCH 3	BRANCH 4
35.69	36.48	32.27	40.65

OVERALL FILM COEF (B/SQFT-HR-F)= 14.15
BRANCH 1 REYNOLDS NO= 27603.75
PRODUCT OF REYNOLDS NO AND PRANDTL NO= 19822.63
OVERALL NUSSELT NO= 117.91

****

TEST NUMBER 17

TAP	1	2	3	4	5	6	7	8	9	TW
1	[illegible]	[illegible]	83.1	82.9	81.7	80.9	80.2	80.1	80.5	112.8
2	91.9	[illegible]	81.0	80.9	80.2	80.6	80.1	80.7	81.0	112.8
3	[illegible]	[illegible]	81.3	81.2	80.4	80.6	79.7	80.7	91.6	112.8
4	8[illegible].0	[illegible]	81.1	81.2	80.5	79.8	80.3	80.8	80.6	112.8
5	8[illegible].4	87.5	86.6	86.6	86.6	86.5	86.5	87.0	88.0	112.8
6	95.[illegible]	[illegible]	89.8	89.0	88.3	87.7	88.1	89.0	90.2	112.8

AVG TAP TEMP(F) 88.3 87.8 88.0 87.4 91.7 94.2

T[illegible]= [illegible] TO= 87.7 TI= 93.0

AVERAGE BRANCH VELOCITIES(FT/SEC)

BRANCH 1	BRANCH 2	BRANCH 3	BRANCH 4
[illegible]	43.20	38.21	48.14

OVERALL FILM COEF (B/SQFT-HR-F)= 16.04
BRANCH 1 REYNOLDS NO= 32688.5[illegible]
PRODUCT OF REYNOLDS NO AND PRANDTL NO= 22861.97
OVERALL NUSSELT NO= 133.6[illegible]

****

[illegible] NUMBER 18

TAP	1	2	3	4	5	6	7	8	[illegible]	TW
[illegible]	[illegible]	[illegible]	9[illegible]	83.3	86.6	87.1	[illegible]	8[illegible]	[illegible]	11[illegible]
[illegible]	[illegible]	[illegible].6	81.9	8[illegible].7	87.0	86.[illegible]	[illegible]	85.2	[illegible].5	113.[illegible]
[illegible]	[illegible]	94.8	96.4	96.[illegible]	96.0	95.0	94.[illegible]	94.4	104.6	11[illegible]
[illegible]	[illegible]	[illegible]	[illegible]	87.0	85.7	85.4	95.2	94.5	92.6	113.2
[illegible]	[illegible]	93.2	96.[illegible]	9[illegible]	95.[illegible]	95.2	95.0	95.3	95.1	113.2
[illegible]	[illegible]	101.5	99.[illegible]	98.[illegible]	98.[illegible]	97.2	96.7	96.9	97.5	11[illegible]

[illegible] TEMP [illegible] 9[illegible] 9[illegible] 94.2 96.5 99.6 101.8

[illegible]4 94.2 [illegible] 94.5 TI= 100.7

AVERAGE BRANCH VELOCITIES (FT/SEC)

BRANCH 1	BRANCH 2	BRANCH 3	BRANCH 4
[illegible].41	7.58	6.70	8.49

OVERALL FILM COEF B/SQFT HR-F = 4.35
BRANCH 1 REYNOLDS NO= 5[illegible]2.60
PRODUCT OF REYNOLDS NO AND PRANDTL NO= 4012.82
OVERALL NUSSELT NO= [illegible]8.77

[illegible] NUMBER [illegible]

[illegible]	1	2	3	4	5	6	7	8	9	TW
[illegible]	[illegible]	[illegible]	[illegible]	90.[illegible]	86.[illegible]	[illegible]	[illegible].4	[illegible]	91.4	11[illegible]
[illegible]	[illegible]	[illegible].4	89.8	88.2	87.4	86.2	[illegible] 2	87.5	100.6	11[illegible]
[illegible]	[illegible]	[illegible]	92.6	91.7	89.7	[illegible]	[illegible].9	9[illegible]	100.[illegible]	113.4
4	[illegible]	99.4	[illegible].9	85.6	88.2	[illegible].9	89.[illegible]	[illegible].6	[illegible]1.2	113.4
[illegible]	[illegible]	100.[illegible]	100.1	99.5	98.9	9[illegible]	98.4	97.8	[illegible].7	113.4
[illegible]	[illegible]	[illegible]05.5	103.5	101.6	[illegible]00.7	99.[illegible]	100.0	100.5	101.9	113.4

AVG [illegible] TEMP [illegible] 95.[illegible] 96.[illegible] 98.0 9[illegible] 102.[illegible] 104.6

[illegible] [illegible] 97.0 TI= 10[illegible]

[illegible] BRANCH VELOCITIES [illegible]

[illegible]	BRANCH [illegible]	BRANCH [illegible]	[illegible]
[illegible]	[illegible]	[illegible]	[illegible]

[illegible] FILM COEF [illegible]
[illegible] REYNOLDS NO= [illegible]
[illegible] OF [illegible] REYNOLDS NO AND PRANDTL [illegible] [illegible]
[illegible] NUSSELT NO= [illegible]

[illegible] NUMBER 20

[illegible]	1	2	3	4	5	6	7	8	9	10
1	[illegible]	98.8	90.7	90.9	92.4	89.[illegible]	[illegible]	[illegible]	[illegible]	[illegible]
2	106.[illegible]	96.5	93.4	92.9	94.4	90.[illegible]	90.[illegible]	90.[illegible]	89.4	115.[illegible]
3	10[illegible]	100.8	94.2	91.0	91.0	[illegible]	[illegible]	89.5	108.1	115.[illegible]
4	105.0	100.1	94.7	91.9	91.5	89.[illegible]	90.4	90.5	91.5	115.[illegible]
5	105.5	[illegible]	100.5	100.0	100.0	99.[illegible]	99.4	99.0	99.1	115.[illegible]
6	108.2	[illegible]	104.0	101.8	101.4	100.[illegible]	101.0	101.[illegible]	101.[illegible]	115.[illegible]

AVG [illegible] TEMP(F) 97.4 97.8 98.8 [illegible] [illegible] [illegible]

T4= [illegible] T3= 98.4 T1= 104.3

AVERAGE BRANCH VELOCITIES(FT/SEC)

BRANCH 1	BRANCH 2	BRANCH 3	BRANCH 4
1.14	1.16	1.0[illegible]	1.[illegible]

OVERALL FILM COEF (B/SQFT-HR-F) [illegible]
BRANCH 1 REYNOLDS NO= [illegible].09
PRODUCT OF REYNOLDS NO AND PRANDTL NO= [illegible]
OVERALL NUSSELT NO= 6.[illegible]

****

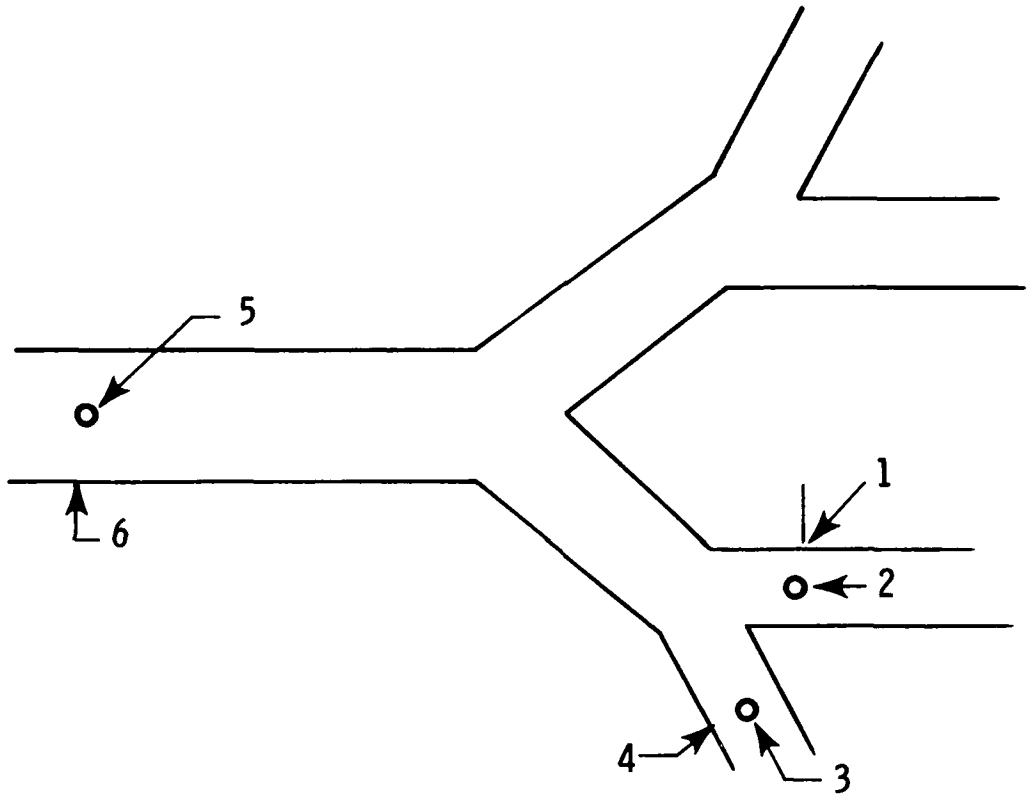

DATA TAP LOCATIONS

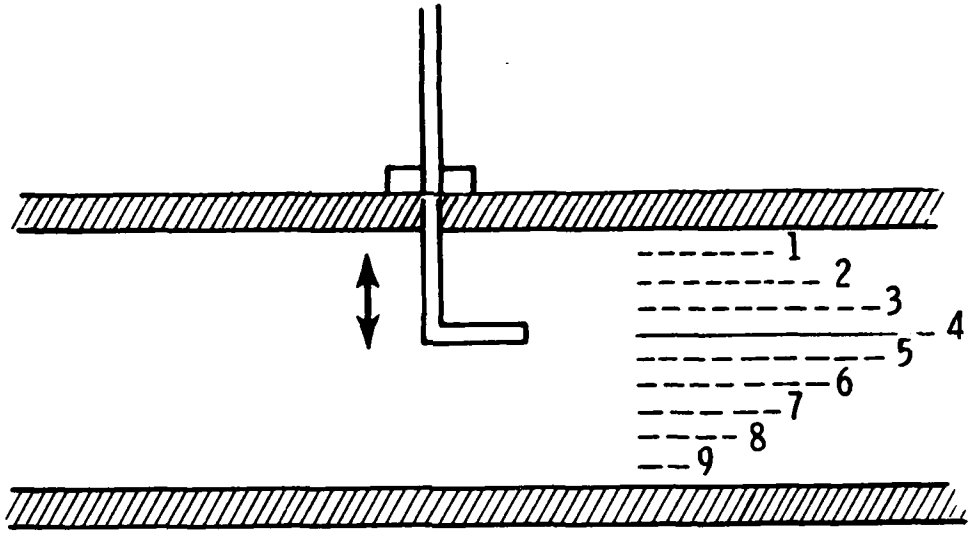

THERMOCOUPLE TIP LOCATION

UPPER RESPIRATORY TRACT

INDEX TO TEST DATA

TEST MODE	DEPTH,FT	GAS	TEST FILES
Nasal/Exhalation	0	Air	0-10
"	0	He	27-33
"	200	N_2	34-39
"	1000	He	54-57
"	1000	N_2	58-62
Nasal/Inhalation	0	Air	11-19
"	0	He	20-26
"	200	N_2	40-43
"	200	He	44-47
"	1000	He	48-50
"	1000	N_2	51-53
Oral/Exhalation	0	Air	63-71
"	0	He	72-77
			124-128
"	200	N_2	104-109
"	200	He	110-116
"	1000	He	117-119
"	1000	N_2	120-123
Oral/Inhalation	0	He	78-83
"	0	Air	84-93
"	200	N_2	94-98
"	200	He	99-103
"	1000	N_2	129-134
"	1000	He	135-137

UPPER RESPIRATORY TRACT

NASAL/EXHALATION

```
TEST NO 0              NASAL              EXHALATION
GAS:AIR                DEPTH (FSW): 0.0      FLOW (LPM): 19.1
BATH TEMPERATURE(C): 44.2                 PRESSURE DROP(CM H2O): 0.1
TWALL1    TWALL2    TWALL3    TWALL4    TWALL5    MEAN
 41.9      43.0      43.0      43.3      44.1      43.1

TNASAL1              TNASAL2              MEAN
 41.9                  42.2                42.1

TTRACHEA1            TTRACHEA2            MEAN
 38.8                  37.2                38.8

MEAN VELOCITY(CM/SEC): 250.7              REYNOLDS NO: 2049.2

DTWALL(C): 4.3       DT(C): 3.3           NUSSELT NO: 14.4

++++++++++++++++++++++++++++++++++++++++++++++++++++++++++++++++++++++++


TEST NO 1              NASAL              EXHALATION
GAS:AIR                DEPTH (FSW): 0.0      FLOW (LPM): 41.1
BATH TEMPERATURE(C): 44.5                 PRESSURE DROP(CM H2O): 2.4
TWALL1    TWALL2    TWALL3    TWALL4    TWALL5    MEAN
 40.6      43.5      43.5      43.8      44.3      43.1

TNASAL1              TNASAL2              MEAN
 40.5                  41.1                40.8

TTRACHEA1            TTRACHEA2            MEAN
 34.1                  34.1                34.1

MEAN VELOCITY(CM/SEC): 539.4              REYNOLDS NO: 4409.5

DTWALL(C): 9.0       DT(C): 6.7           NUSSELT NO: 30.1

++++++++++++++++++++++++++++++++++++++++++++++++++++++++++++++++++++++++


TEST NO 2              NASAL              EXHALATION
GAS:AIR                DEPTH (FSW): 0.0      FLOW (LPM): 51.5
BATH TEMPERATURE(C): 44.8                 PRESSURE DROP(CM H2O): 4.5
TWALL1    TWALL2    TWALL3    TWALL4    TWALL5    MEAN
 39.4      43.7      43.5      43.9      44.0      42.5

TNASAL1              TNASAL2              MEAN
 39.4                  40.0                39.7

TTRACHEA1            TTRACHEA2            MEAN
 33.0                  33.7                33.0

MEAN VELOCITY(CM/SEC): 675.9              REYNOLDS NO: 5525.2

DTWALL(C): 9.9       DT(C): 6.7           NUSSELT NO: 34.4

++++++++++++++++++++++++++++++++++++++++++++++++++++++++++++++++++++++++
```

TEST NO 3 NASAL EXHALATION
GAS:AIR DEPTH (FSW): 0.0 FLOW (LPM): 61.4
BATH TEMPERATURE(C): 45.4 PRESSURE DROP(CM H2O): 6.4

TWALL1	TWALL2	TWALL3	TWALL4	TWALL5	MEAN
38.7	43.9	43.7	44.2	44.4	43.0

TNASAL1	TNASAL2	MEAN
38.8	39.5	39.2

TTRACHEA1	TTRACHEA2	MEAN
32.0	33.3	32.0

MEAN VELOCITY(CM/SEC): 805.8 REYNOLDS NO: 6587.4

DTWALL(C): 11.0 DT(C): 7.2 NUSSELT NO: 39.4

++

TEST NO 4 NASAL EXHALATION
GAS:AIR DEPTH (FSW): 0.0 FLOW (LPM): 86.1
BATH TEMPERATURE(C): 46.0 PRESSURE DROP(CM H2O): 12.5

TWALL1	TWALL2	TWALL3	TWALL4	TWALL5	MEAN
38.0	44.2	44.1	44.6	44.5	43.1

TNASAL1	TNASAL2	MEAN
38.2	38.8	38.5

TTRACHEA1	TTRACHEA2	MEAN
31.1	32.2	31.1

MEAN VELOCITY(CM/SEC): 1129.9 REYNOLDS NO: 9237.3

DTWALL(C): 12.0 DT(C): 7.4 NUSSELT NO: 52.5

++

TEST NO 5 NASAL EXHALATION
GAS:AIR DEPTH (FSW): 0.0 FLOW (LPM): 114.1
BATH TEMPERATURE(C): 46.5 PRESSURE DROP(CM H2O): 23.7

TWALL1	TWALL2	TWALL3	TWALL4	TWALL5	MEAN
37.6	44.7	44.5	45.2	45.0	43.4

TNASAL1	TNASAL2	MEAN
37.1	38.0	37.6

TTRACHEA1	TTRACHEA2	MEAN
31.1	32.0	31.1

MEAN VELOCITY(CM/SEC): 1497.4 REYNOLDS NO: 12241.3

DTWALL(C): 12.7 DT(C): 7.6 NUSSELT NO: 59.5

++

TEST NO 6 NASAL EXHALATION
GAS:AIR DEPTH (FSW): 0.0 FLOW (LPM): 49.3
BATH TEMPERATURE(C): 47.1 PRESSURE DROP(CM H2O): 4.4

TWALL1	TWALL2	TWALL3	TWALL4	TWALL5	MEAN
41.2	44.9	44.7	45.8	45.8	44.9

TNASAL1	TNASAL2	MEAN
41.1	41.4	41.3

TTRACHEA1	TTRACHEA2	MEAN
34.9	35.4	34.9

MEAN VELOCITY(CM SEC): 647.0 REYNOLDS NO: 5,89.2

DTWALL(C): 9.6 DT(C): 6.4 NUSSELT NO: 22.2

++

TEST NO 7 NASAL EXHALATION
GAS:AIR DEPTH (FSW): 0.0 FLOW (LPM): 30.1
BATH TEMPERATURE(C): 47.0 PRESSURE DROP(CM H2O): 1.7

TWALL1	TWALL2	TWALL3	TWALL4	TWALL5	MEAN
42.4	45.3	45.1	45.8	45.8	44.9

TNASAL1	TNASAL2	MEAN
42.4	42.6	42.5

TTRACHEA1	TTRACHEA2	MEAN
38.3	38.3	38.3

MEAN VELOCITY(CM SEC): 395.0 REYNOLDS NO: 3,29.3

DTWALL(C): 6.6 DT(C): 4.7 NUSSELT NO: 19.0

++

TEST NO 8 NASAL EXHALATION
GAS:AIR DEPTH (FSW): 0.0 FLOW (LPM): 74.0
BATH TEMPERATURE(C): 47.2 PRESSURE DROP(CM H2O): 9.8

TWALL1	TWALL2	TWALL3	TWALL4	TWALL5	MEAN
40.0	45.5	45.2	45.8	46.0	44.5

TNASAL1	TNASAL2	MEAN
40.0	40.7	40.4

TTRACHEA1	TTRACHEA2	MEAN
32.4	33.7	32.4

MEAN VELOCITY(CM SEC): 971.1 REYNOLDS NO: [illegible]

DTWALL(C): 12.1 DT(C): 8.0 NUSSELT NO: [illegible]

++

```
TEST NO 9              NASAL              EXHALATION
GAS:AIR                DEPTH (FSW): 0.0      FLOW (LPM): 18.2
BATH TEMPERATURE(C): 47.7                 PRESSURE DROP(CM H20): 0.7
TWALL1    TWALL2    TWALL3    TWALL4    TWALL5    MEAN
 43.9      45.7      45.4      46.4      46.4      45.6

TNASAL1                TNASAL2            MEAN
 44.0                    43.9              44.0

TTRACHEA1              TTRACHEA2          MEAN
 42.7                    41.1              42.7

MEAN VELOCITY(CM/SEC): 238.8              REYNOLDS NO: 1952.6

DTWALL(C): 2.9         DT(C): 1.3         NUSSELT NO: 7.8

++++++++++++++++++++++++++++++++++++++++++++++++++++++++++++++++++++++++


TEST NO 10             NASAL              EXHALATION
GAS:AIR                DEPTH (FSW): 0.0      FLOW (LPM): 116.8
BATH TEMPERATURE(C): 48.0                 PRESSURE DROP(CM H20): 25.4
TWALL1    TWALL2    TWALL3    TWALL4    TWALL5    MEAN
 39.0      46.5      46.3      46.8      46.9      45.1

TNASAL1                TNASAL2            MEAN
 38.5                    39.6              39.1

TTRACHEA1              TTRACHEA2          MEAN
 31.6                    32.6              31.6

MEAN VELOCITY(CM/SEC): 1532.8             REYNOLDS NO: 12531.0

DTWALL(C): 13.5        DT(C): 7.5         NUSSELT NO: 63.6

++++++++++++++++++++++++++++++++++++++++++++++++++++++++++++++++++++++++


TEST NO 27             NASAL              EXHALATION
GAS:HELIUM             DEPTH (FSW): 0.0      FLOW (LPM): 58.7
BATH TEMPERATURE(C): 52.3                 PRESSURE DROP(CM H20): 1.0
TWALL1    TWALL2    TWALL3    TWALL4    TWALL5    MEAN
 49.8      51.2      51.4      51.4      53.2      51.4

TNASAL1                TNASAL2            MEAN
 48.2                    49.4              48.8

TTRACHEA1              TTRACHEA2          MEAN
 42.8                    43.5              43.2

MEAN VELOCITY(CM/SEC): 1770.1             REYNOLDS NO:  23.5

DTWALL(C): 5.0         DT(C): 2.7         NUSSELT NO: 4.5

++++++++++++++++++++++++++++++++++++++++++++++++++++++++++++++++++++++++
```

TEST NO 28 NASAL EXHALATION
GAS:HELIUM DEPTH (FSW): 0.0 FLOW (LPM): 85.1
BATH TEMPERATURE(C): 52.3 PRESSURE DROP(CM H2O): 3.5

TWALL1	TWALL2	TWALL3	TWALL4	TWALL5	MEAN
48.7	51.2	51.3	51.3	52.9	51.1

TNASAL1	TNASAL2	MEAN
48.0	48.7	48.4

TTRACHEA1	TTRACHEA2	MEAN
43.1	39.4	43.1

MEAN VELOCITY(CM/SEC): 1116.8 REYNOLDS NO: 1157.7

DTWALL(C): 8.0 DT(C): 5.3 NUSSELT NO: 6.9

++

TEST NO 29 NASAL EXHALATION
GAS:HELIUM DEPTH (FSW): 0.0 FLOW (LPM): 119.3
BATH TEMPERATURE(C): 52.3 PRESSURE DROP(CM H2O): 6.5

TWALL1	TWALL2	TWALL3	TWALL4	TWALL5	MEAN
47.7	51.2	51.3	51.3	52.8	50.9

TNASAL1	TNASAL2	MEAN
47.1	48.0	47.6

TTRACHEA1	TTRACHEA2	MEAN
41.4	36.4	41.4

MEAN VELOCITY(CM/SEC): 1565.6 REYNOLDS NO: 1622.9

DTWALL(C): 9.5 DT(C): 6.2 NUSSELT NO: 9.6

++

TEST NO 30 NASAL EXHALATION
GAS:HELIUM DEPTH (FSW): 0.0 FLOW (LPM): 25.4
BATH TEMPERATURE(C): 52.3 PRESSURE DROP(CM H2O): 0.4

TWALL1	TWALL2	TWALL3	TWALL4	TWALL5	MEAN
49.5	51.1	51.2	51.3	52.4	51.1

TNASAL1	TNASAL2	MEAN
49.1	49.2	49.2

TTRACHEA1	TTRACHEA2	MEAN
48.9	48.9	48.9

MEAN VELOCITY(CM/SEC): 333.8 REYNOLDS NO: 343.5

DTWALL(C): 2.2 DT(C): 0.3 NUSSELT NO: 0.4

++

TEST NO 31 NASAL EXHALATION
GAS:HELIUM DEPTH (FSW): 0.0 FLOW (LPM): 47.9
BATH TEMPERATURE(C): 52.3 PRESSURE DROP(CM H2O): 1.2

TWALL1	TWALL2	TWALL3	TWALL4	TWALL5	MEAN
49.5	51.2	51.3	51.4	52.5	51.2

TNASAL1	TNASAL2	MEAN
49.0	49.0	49.0

TTRACHEA1	TTRACHEA2	MEAN
46.0	44.3	46.0

MEAN VELOCITY(CM/SEC): 628.6 REYNOLDS NO: 651.6

DTWALL(C): 5.2 DT(C): 3.0 NUSSELT NO: 3.4

++

TEST NO 32 NASAL EXHALATION
GAS:HELIUM DEPTH (FSW): 0.0 FLOW (LPM): 33.7
BATH TEMPERATURE(C): 52.3 PRESSURE DROP(CM H2O): 0.6

TWALL1	TWALL2	TWALL3	TWALL4	TWALL5	MEAN
50.1	51.3	51.3	51.4	52.7	51.4

TNASAL1	TNASAL2	MEAN
49.5	49.6	49.6

TTRACHEA1	TTRACHEA2	MEAN
48.0	47.3	48.0

MEAN VELOCITY(CM/SEC): 442.3 REYNOLDS NO: 458.4

DTWALL(C): 3.4 DT(C): 1.6 NUSSELT NO: 1.9

++

TEST NO 33 NASAL EXHALATION
GAS:HELIUM DEPTH (FSW): 0.0 FLOW (LPM): 43.2
BATH TEMPERATURE(C): 52.3 PRESSURE DROP(CM H2O): 1.0

TWALL1	TWALL2	TWALL3	TWALL4	TWALL5	MEAN
49.8	51.2	51.3	51.4	52.5	51.2

TNASAL1	TNASAL2	MEAN
49.3	49.4	49.4

TTRACHEA1	TTRACHEA2	MEAN
46.4	45.0	46.4

MEAN VELOCITY(CM/SEC): 566.1 REYNOLDS NO: 587.7

DTWALL(C): 4.8 DT(C): 3.0 NUSSELT NO: 3.2

++

```
TEST NO 34          NASAL          EXHALATION
GAS:NITROGEN        DEPTH (FSW): 200.0      FLOW (LPM): 12.0
BATH TEMPERATURE(C): 51.3          PRESSURE DROP(CM H2O): 2.2
TWALL1   TWALL2   TWALL3   TWALL4   TWALL5   MEAN
 45.1     50.0     49.4     50.1     51.1     49.1

TNASAL1             TNASAL2          MEAN
 44.0                 44.9            44.5

TTRACHEA1           TTRACHEA2        MEAN
 37.0                 38.0            37.0

MEAN VELOCITY(CM/SEC): 157.5        REYNOLDS NO: 8915.1

DTWALL(C): 12.1     DT(C): 7.5      NUSSELT NO: 51.4

++++++++++++++++++++++++++++++++++++++++++++++++++++++++++++++++++++++++


TEST NO 35          NASAL          EXHALATION
GAS:NITROGEN        DEPTH (FSW): 200.0      FLOW (LPM): 21.5
BATH TEMPERATURE(C): 51.3          PRESSURE DROP(CM H2O): 6.8
TWALL1   TWALL2   TWALL3   TWALL4   TWALL5   MEAN
 41.2     50.1     49.6     50.1     51.1     48.4

TNASAL1             TNASAL2          MEAN
 40.5                 42.1            41.3

TTRACHEA1           TTRACHEA2        MEAN
 34.2                 34.8            34.2

MEAN VELOCITY(CM/SEC): 282.2        REYNOLDS NO: 15973.0

DTWALL(C): 14.2     DT(C): 7.1      NUSSELT NO: 74.9

++++++++++++++++++++++++++++++++++++++++++++++++++++++++++++++++++++++++


TEST NO 36          NASAL          EXHALATION
GAS:NITROGEN        DEPTH (FSW): 200.0      FLOW (LPM): 32.4
BATH TEMPERATURE(C): 51.4          PRESSURE DROP(CM H2O): 15.6
TWALL1   TWALL2   TWALL3   TWALL4   TWALL5   MEAN
 39.2     50.2     49.6     49.9     51.0     48.0

TNASAL1             TNASAL2          MEAN
 38.3                 40.1            39.2

TTRACHEA1           TTRACHEA2        MEAN
 32.9                 33.1            32.9

MEAN VELOCITY(CM/SEC): 425.2        REYNOLDS NO: 24070.9

DTWALL(C): 15.1     DT(C): 6.3      NUSSELT NO: 94.4

++++++++++++++++++++++++++++++++++++++++++++++++++++++++++++++++++++++++
```

TEST NO 37 NASAL EXHALATION
GAS:NITROGEN DEPTH (FSW): 200.0 FLOW (LPM): 37.5
BATH TEMPERATURE(C): 51.5 PRESSURE DROP (M H20): 21.4

TWALL1	TWALL2	TWALL3	TWALL4	TWALL5	MEAN
40.0	50.3	49.7	50.1	51.2	48..

TNASAL1	TNASAL2	MEAN
38.9	40.6	39.8

TTRACHEA1	TTRACHEA2	MEAN
33.7	33.5	33.7

MEAN VELOCITY(CM/SEC): 492.1 REYNOLDS NO: 27859.8

DTWALL(C): 14.6 DT(C): 6.1 NUSSELT NO: 108.7

++

TEST NO 38 NASAL EXHALATION
GAS:NITROGEN DEPTH (FSW): 200.0 FLOW (LPM): 40.1
BATH TEMPERATURE(C): 51.6 PRESSURE DROP(CM H20): 24.9

TWALL1	TWALL2	TWALL3	TWALL4	TWALL5	MEAN
37.9	50.2	49.9	50.2	51.3	47.9

TNASAL1	TNASAL2	MEAN
37.2	38.9	38.1

TTRACHEA1	TTRACHEA2	MEAN
32.2	32.6	32.2

MEAN VELOCITY(CM/SEC): 526.. REYNOLDS NO: 29791.4

DTWALL(C): 15.7 DT(C): 5.9 NUSSELT NO: 104.3

++

TEST NO 39 NASAL EXHALATION
GAS:NITROGEN DEPTH (FSW): 200.0 FLOW (LPM): 42.4
BATH TEMPERATURE(C): 51.8 PRESSURE DROP(CM H20): 27.9

TWALL1	TWALL2	TWALL3	TWALL4	TWALL5	MEAN
39.2	50.3	49.7	50.2	51.4	48.2

TNASAL1	TNASAL2	MEAN
38.0	39.8	38.9

TTRACHEA1	TTRACHEA2	MEAN
33.5	33.5	33.5

MEAN VELOCITY(CM/SEC): 556.4 REYNOLDS NO: 31500.2

DTWALL(C): 14.7 DT(C): 6.4 NUSSELT NO: 109.0

++

TEST NO 54 NASAL EXHALATION
GAS:HELIUM DEPTH (FSW): 1000.0 FLOW (LPM): 5.0
BATH TEMPERATURE(C): 53.6 PRESSURE DROP(CM H2O): 1.8

TWALL1	TWALL2	TWALL3	TWALL4	TWALL5	MEAN
53.7	53.7	53.7	53.5	55.7	54.1

TNASAL1	TNASAL2	MEAN
45.8	47.4	46.6

TTRACHEA1	TTRACHEA2	MEAN
39.6	39.7	39.6

MEAN VELOCITY(CM/SEC): 65.6 REYNOLDS NO: 2090.6

DTWALL(C): 14.5 DT(C): 7.0 NUSSELT NO: 9.0

++

TEST NO 55 NASAL EXHALATION
GAS:HELIUM DEPTH (FSW): 1000.0 FLOW (LPM): 12.7
BATH TEMPERATURE(C): 52.5 PRESSURE DROP(CM H2O): 22.0

TWALL1	TWALL2	TWALL3	TWALL4	TWALL5	MEAN
44.3	53.3	52.7	52.5	54.4	51.4

TNASAL1	TNASAL2	MEAN
42.1	43.8	43.0

TTRACHEA1	TTRACHEA2	MEAN
37.8	37.1	37.8

MEAN VELOCITY(CM/SEC): 166.7 REYNOLDS NO: 5810.2

DTWALL(C): 13.6 DT(C): 5.2 NUSSELT NO: 17.9

++

TEST NO 56 NASAL EXHALATION
GAS:HELIUM DEPTH (FSW): 1000.0 FLOW (LPM): 32.5
BATH TEMPERATURE(C): 52.3 PRESSURE DROP(CM H2O): 9.6

TWALL1	TWALL2	TWALL3	TWALL4	TWALL5	MEAN
37.4	52.6	51.6	51.0	53.3	49.2

TNASAL1	TNASAL2	MEAN
36.9	38.7	37.8

TTRACHEA1	TTRACHEA2	MEAN
32.6	32.2	32.6

MEAN VELOCITY(CM/SEC): 426.5 REYNOLDS NO: 13589.1

DTWALL(C): 16.6 DT(C): 5.2 NUSSELT NO: 38.1

++

TEST NO 57 NASAL EXHALATION
GAS:HELIUM DEPTH (FSW): 1000.0 FLOW (LPM): 73.8
BATH TEMPERATURE(C): 52.0 PRESSURE DROP(CM H2O): 43.1

TWALL1	TWALL2	TWALL3	TWALL4	TWALL5	MEAN
32.7	51.7	50.8	49.6	52.6	47.5

TNASAL1	TNASAL2	MEAN
31.8	33.1	32.5

TTRACHEA1	TTRACHEA2	MEAN
30.0	29.9	30.0

MEAN VELOCITY(CM/SEC): 968.5 REYNOLDS NO: 30857.8

DTWALL(C): 17.5 DT(C): 2.5 NUSSELT NO: 38.6

++

TEST NO 58 NASAL EXHALATION
GAS:NITROGEN DEPTH (FSW): 1000.0 FLOW (LPM): 5.0
BATH TEMPERATURE(C): 51.6 PRESSURE DROP(CM H2O): 0.1

TWALL1	TWALL2	TWALL3	TWALL4	TWALL5	MEAN
47.1	51.0	50.2	50.3	52.1	50.1

TNASAL1	TNASAL2	MEAN
45.3	46.4	45.9

TTRACHEA1	TTRACHEA2	MEAN
42.1	38.2	42.1

MEAN VELOCITY(CM/SEC): 65.6 REYNOLDS NO: 16352.1

DTWALL(C): 8.0 DT(C): 3.8 NUSSELT NO: 70.4

++

TEST NO 59 NASAL EXHALATION
GAS:NITROGEN DEPTH (FSW): 1000.0 FLOW (LPM): 18.6
BATH TEMPERATURE(C): 51.5 PRESSURE DROP(CM H2O): 3.5

TWALL1	TWALL2	TWALL3	TWALL4	TWALL5	MEAN
42.2	51.2	50.3	49.9	52.1	49.1

TNASAL1	TNASAL2	MEAN
41.4	43.1	42.3

TTRACHEA1	TTRACHEA2	MEAN
36.6	35.7	36.6

MEAN VELOCITY(CM/SEC): 244.1 REYNOLDS NO: 60829.8

DTWALL(C): 12.5 DT(C): 5.7 NUSSELT NO: 253.1

++

TEST NO 60 NASAL EXHALATION
GAS:NITROGEN DEPTH (FSW): 1000.0 FLOW (LPM): 7.4
BATH TEMPERATURE(C): 51.3 PRESSURE DROP(CM H2O): 3.5

TWALL1	TWALL2	TWALL3	TWALL4	TWALL5	MEAN
44.0	51.0	50.0	50.3	52.0	49.5

TNASAL1	TNASAL2	MEAN
42.0	43.3	42.7

TTRACHEA1	TTRACHEA2	MEAN
37.8	37.7	37.8

MEAN VELOCITY(CM/SEC): 97.1 REYNOLDS NO: 24201.1

DTWALL(C): 11.7 DT(C): 4.9 NUSSELT NO: 93.0

++

TEST NO 61 NASAL EXHALATION
GAS:NITROGEN DEPTH (FSW): 1000.0 FLOW (LPM): 15.9
BATH TEMPERATURE(C): 51.2 PRESSURE DROP(CM H2O): 15.2

TWALL1	TWALL2	TWALL3	TWALL4	TWALL5	MEAN
39.8	50.9	50.1	50.1	51.8	48.5

TNASAL1	TNASAL2	MEAN
38.4	39.9	39.2

TTRACHEA1	TTRACHEA2	MEAN
35.2	35.2	35.2

MEAN VELOCITY(CM/SEC): 208.7 REYNOLDS NO: 51999.7

DTWALL(C): 13.3 DT(C): 4.0 NUSSELT NO: 142.2

++

TEST NO 62 NASAL EXHALATION
GAS:NITROGEN DEPTH (FSW): 1000.0 FLOW (LPM): 12.
BATH TEMPERATURE(C): 51.0 PRESSURE DROP(CM H2O): 9.

TWALL1	TWALL2	TWALL3	TWALL4	TWALL5	MEAN
41.4	50.6	49.7	49.8	51.4	48.

TNASAL1	TNASAL2	MEAN
39.7	41.1	40.4

TTRACHEA1	TTRACHEA2	MEAN
36.4	36.4	36.4

MEAN VELOCITY(CM/SEC): 160.1 REYNOLDS NO: 40899.1

DTWALL(C): 12. DT(C): 4.0 NUSSELT NO: 1.1.0

++

UPPER RESPIRATORY TRACT

NASAL/INHALATION

TEST NO 11 NASAL INHALATION
GAS:AIR DEPTH (FSW): 0.0 FLOW (LPM): 29.4
BATH TEMPERATURE(C): 50.6 PRESSURE DROP(CM H20): 0.
TWALL1 TWALL2 TWALL3 TWALL4 TWALL5 MEAN
44.9 49.9 49.9 49.9 51.6 49.

TNASAL1 TNASAL2 MEAN
39.6 40.0 39.8

TTRACHEA1 TTRACHEA2 MEAN
47.5 48.6 47.5

MEAN VELOCITY(CM/SEC): 333.3 REYNOLDS NO: 2725.1

DTWALL(C): 9.4 DT(C): 7.7 NUSSELT NO: 20.4

++

TEST NO 12 NASAL INHALATION
GAS:AIR DEPTH (FSW): 0.0 FLOW (LPM): 31.9
BATH TEMPERATURE(C): 50.7 PRESSURE DROP(CM H20): 0.2
TWALL1 TWALL2 TWALL3 TWALL4 TWALL5 MEAN
43.5 50.0 50.0 50.1 51.9 49.1

TNASAL1 TNASAL2 MEAN
37.7 38.6 38.2

TTRACHEA1 TTRACHEA2 MEAN
46.6 48.2 46.6

MEAN VELOCITY(CM/SEC): 418.6 REYNOLDS NO: 3[illegible].4

DTWALL(C): 11.0 DT(C): 8.5 NUSSELT NO: 24.

++

TEST NO 13 NASAL INHALATION
GAS:AIR DEPTH (FSW): 0.0 FLOW (LPM): 47.4
BATH TEMPERATURE(C): 50.8 PRESSURE DROP(CM H20): 0.4
TWALL1 TWALL2 TWALL3 TWALL4 TWALL5 MEAN
42.0 49.7 49.7 49.9 51.[illegible] 48.

TNASAL1 TNASAL2 MEAN
37.2 37.6 37.4

TTRACHEA1 TTRACHEA2 MEAN
45.8 47.[illegible] 46.[illegible]

MEAN VELOCITY(CM/SEC): [illegible] REYNOLDS NO: [illegible]

DTWALL(C): [illegible] DT(C): [illegible] NUSSELT NO: [illegible]

++

TEST NO 14 NASAL INHALATION
GAS:AIR DEPTH (FSW): 0.0 FLOW (LPM): 59.1
BATH TEMPERATURE(C): 50.9 PRESSURE DROP(CM H2O): 0.5

TWALL1	TWALL2	TWALL3	TWALL4	TWALL5	MEAN
42.3	49.6	49.6	49.9	51.5	48.6

TNASAL1	TNASAL2	MEAN
36.8	36.4	36.6

TTRACHEA1	TTRACHEA2	MEAN
45.1	46.6	45.1

MEAN VELOCITY(CM/SEC): 775.6 REYNOLDS NO: 6340.6

DTWALL(C): 12.0 DT(C): 8.5 NUSSELT NO: 41.4

++

TEST NO 15 NASAL INHALATION
GAS:AIR DEPTH (FSW): 0.0 FLOW (LPM): 79.5
BATH TEMPERATURE(C): 51.0 PRESSURE DROP(CM H2O): 0.9

TWALL1	TWALL2	TWALL3	TWALL4	TWALL5	MEAN
41.3	49.6	49.7	49.9	51.6	48.4

TNASAL1	TNASAL2	MEAN
35.5	34.9	35.2

TTRACHEA1	TTRACHEA2	MEAN
44.0	45.6	44.0

MEAN VELOCITY(CM/SEC): 1044.3 REYNOLDS NO: 8529.2

DTWALL(C): 13.2 DT(C): 8.8 NUSSELT NO: 52.2

++

TEST NO 16 NASAL INHALATION
GAS:AIR DEPTH (FSW): 0.0 FLOW (LPM): 96.8
BATH TEMPERATURE(C): 51.1 PRESSURE DROP(CM H2O): 1.2

TWALL1	TWALL2	TWALL3	TWALL4	TWALL5	MEAN
43.1	49.6	49.7	50.0	51.7	48.5

TNASAL1	TNASAL2	MEAN
35.5	34.4	35.0

TTRACHEA1	TTRACHEA2	MEAN
43.5	45.4	43.5

MEAN VELOCITY(CM/SEC): 1261.3 REYNOLDS NO: 10385.3

DTWALL(C): 13.1 DT(C): 8.6 NUSSELT NO: 60.4

++

TEST NO 17 NASAL INHALATION
GAS:AIR DEPTH (FSW): 0.0 FLOW (LPM): 35.0
BATH TEMPERATURE (C): 51.2 PRESSURE DROP (IN H20): 1.0
TWALL1 TWALL2 TWALL3 TWALL4 TWALL5 MEAN
41.3 49.8 49.7 50.0 51.7 48.5

TNASAL1 TNASAL2 MEAN
34.9 34.7 34.8

TTRACHEA1 TTRACHEA2 MEAN
43.2 44.8 43.2

MEAN VELOCITY (CM/SEC): 1490.1 REYNOLDS NO: 1748.4

DTWALL (C): 13.7 DT (C): 8.4 NUSSELT NO: 55.2

++

TEST NO 18 NASAL INHALATION
GAS:AIR DEPTH (FSW): 0.0 FLOW (LPM): 35.0
BATH TEMPERATURE (C): 51.3 PRESSURE DROP (IN H20): 1.0
TWALL1 TWALL2 TWALL3 TWALL4 TWALL5 MEAN
42.1 50.0 50.0 50.2 51.8 48.5

TNASAL1 TNASAL2 MEAN
36.1 35.7 35.9

TTRACHEA1 TTRACHEA2 MEAN
44.2 46.1 44.2

MEAN VELOCITY (CM/SEC): 1154.9 REYNOLDS NO: 1441.2

DTWALL (C): 12.9 DT (C): 8.3 NUSSELT NO: 55.3

++

TEST NO 19 NASAL INHALATION
GAS:AIR DEPTH (FSW): 0.0 FLOW (LPM): 60.7
BATH TEMPERATURE (C): 51.3 PRESSURE DROP (IN H20): 0.5
TWALL1 TWALL2 TWALL3 TWALL4 TWALL5 MEAN
43.3 49.0 49.8 50.3 51.9 49.1

TNASAL1 TNASAL2 MEAN
37.8 37.4 37.6

TTRACHEA1 TTRACHEA2 MEAN
45.5 46.9 45.5

MEAN VELOCITY (CM/SEC): 2574.3 REYNOLDS NO: 3116.0

DTWALL (C): 11.3 DT (C): 7.7 NUSSELT NO: 45.5

++

TEST NO 20 NASAL INHALATION
GAS:HELIUM DEPTH (FSW): 0.0 FLOW (LPM): 40.1
BATH TEMPERATURE(C): 51.9 PRESSURE DROP(CM H2O): 0.2

TWALL1	TWALL2	TWALL3	TWALL4	TWALL5	MEAN
41.7	51.4	51.5	51.3	53.1	49.8

TNASAL1	TNASAL2	MEAN
37.2	35.8	36.5

TTRACHEA1	TTRACHEA2	MEAN
49.1	50.0	49.1

MEAN VELOCITY(CM/SEC): 526.2 REYNOLDS NO: 545.5

DTWALL(C): 13.3 DT(C): 12.6 NUSSELT NO: 4.7

++

TEST NO 21 NASAL INHALATION
GAS:HELIUM DEPTH (FSW): 0.0 FLOW (LPM): 81.8
BATH TEMPERATURE(C): 52.0 PRESSURE DROP(CM H2O): 0.5

TWALL1	TWALL2	TWALL3	TWALL4	TWALL5	MEAN
40.7	51.3	51.6	51.4	53.2	49.6

TNASAL1	TNASAL2	MEAN
33.2	34.3	33.8

TTRACHEA1	TTRACHEA2	MEAN
47.1	48.0	47.1

MEAN VELOCITY(CM/SEC): 1073.5 REYNOLDS NO: 1112.8

DTWALL(C): 15.9 DT(C): 13.4 NUSSELT NO: 8.5

++

TEST NO 22 NASAL INHALATION
GAS:HELIUM DEPTH (FSW): 0.0 FLOW (LPM): 150.4
BATH TEMPERATURE(C): 52.0 PRESSURE DROP(CM H2O): 1.2

TWALL1	TWALL2	TWALL3	TWALL4	TWALL5	MEAN
41.0	50.9	51.1	51.0	52.9	49.4

TNASAL1	TNASAL2	MEAN
30.4	32.1	31.3

TTRACHEA1	TTRACHEA2	MEAN
44.5	45.3	44.5

MEAN VELOCITY(CM/SEC): 1973.8 REYNOLDS NO: 2046.0

DTWALL(C): 18.1 DT(C): 13.3 NUSSELT NO: 15.6

++

TEST NO 23 NASAL INHALATION
GAS:HELIUM DEPTH (FSW): 0.0 FLOW (LPM): 76.0
BATH TEMPERATURE(C): 52.1 PRESSURE DROP(CM H20): 0.4

TWALL1	TWALL2	TWALL3	TWALL4	TWALL5	MEAN
40.4	50.8	51.0	51.2	52.8	49.2

TNASAL1	TNASAL2	MEAN
33.7	34.5	34.1

TTRACHEA1	TTRACHEA2	MEAN
47.1	47.9	47.1

MEAN VELOCITY(CM/SEC): 997.4 REYNOLDS NO: 1033.9

DTWALL(C): 15.1 DT(C): 13.0 NUSSELT NO: 8.1

++

TEST NO 24 NASAL INHALATION
GAS:HELIUM DEPTH (FSW): 0.0 FLOW (LPM): 52.7
BATH TEMPERATURE(C): 52.1 PRESSURE DROP(CM H20): 0.3

TWALL1	TWALL2	TWALL3	TWALL4	TWALL5	MEAN
41.2	50.8	51.0	51.1	52.8	49.4

TNASAL1	TNASAL2	MEAN
36.0	36.1	36.1

TTRACHEA1	TTRACHEA2	MEAN
48.3	49.1	48.3

MEAN VELOCITY(CM/SEC): 691.6 REYNOLDS NO: 716.9

DTWALL(C): 13.3 DT(C): 12.3 NUSSELT NO: 6.0

++

TEST NO 25 NASAL INHALATION
GAS:HELIUM DEPTH (FSW): 0.0 FLOW (LPM): 15.2
BATH TEMPERATURE(C): 52.2 PRESSURE DROP(CM H20): 0.0

TWALL1	TWALL2	TWALL3	TWALL4	TWALL5	MEAN
45.2	51.0	51.1	51.2	52.9	50.3

TNASAL1	TNASAL2	MEAN
45.8	38.2	42.0

TTRACHEA1	TTRACHEA2	MEAN
50.2	51.0	50.2

MEAN VELOCITY(CM/SEC): 199.5 REYNOLDS NO: 206.8

DTWALL(C): 8.3 DT(C): 8.2 NUSSELT NO: 1.9

++

TEST NO 26 NASAL INHALATION
GAS:HELIUM DEPTH (FSW): 0.0 FLOW (LPM): 27.2
BATH TEMPERATURE(C): 52.2 PRESSURE DROP(CM H2O): 0.1

TWALL1	TWALL2	TWALL3	TWALL4	TWALL5	MEAN
42.7	51.1	51.3	51.3	53.1	49.9

TNASAL1	TNASAL2	MEAN
42.8	35.9	39.4

TTRACHEA1	TTRACHEA2	MEAN
49.7	50.7	49.7

MEAN VELOCITY(CM/SEC): 357.0 REYNOLDS NO: 370.0

DTWALL(C): 10.6 DT(C): 10.4 NUSSELT NO: 3.3

++

TEST NO 40 NASAL INHALATION
GAS:NITROGEN DEPTH (FSW): 200.0 FLOW (LPM): 12.5
BATH TEMPERATURE(C): 52.0 PRESSURE DROP(CM H2O): 0.2

TWALL1	TWALL2	TWALL3	TWALL4	TWALL5	MEAN
43.4	51.0	50.8	51.0	52.3	49.7

TNASAL1	TNASAL2	MEAN
40.0	40.3	40.2

TTRACHEA1	TTRACHEA2	MEAN
46.1	47.8	46.1

MEAN VELOCITY(CM/SEC): 164.0 REYNOLDS NO: 9286.6

DTWALL(C): 9.6 DT(C): 6.0 NUSSELT NO: 54.3

++

TEST NO 41 NASAL INHALATION
GAS:NITROGEN DEPTH (FSW): 200.0 FLOW (LPM): 22.4
BATH TEMPERATURE(C): 52.1 PRESSURE DROP(CM H2O): 0.5

TWALL1	TWALL2	TWALL3	TWALL4	TWALL5	MEAN
39.3	51.2	50.8	51.0	52.3	48.9

TNASAL1	TNASAL2	MEAN
35.5	36.4	36.0

TTRACHEA1	TTRACHEA2	MEAN
42.7	44.6	42.7

MEAN VELOCITY(CM/SEC): 294.0 REYNOLDS NO: 16641.6

DTWALL(C): 13.0 DT(C): 6.8 NUSSELT NO: 81.3

++

TEST NO 42 NASAL INHALATION
GAS:NITROGEN DEPTH (FSW): 200.0 FLOW (LPM): 28.8
BATH TEMPERATURE(C): 52.2 PRESSURE DROP(CM H2O): 0.9

TWALL1	TWALL2	TWALL3	TWALL4	TWALL5	MEAN
37.4	51.0	50.6	50.9	52.3	48.4

TNASAL1	TNASAL2	MEAN
33.4	34.2	33.8

TTRACHEA1	TTRACHEA2	MEAN
40.5	42.7	40.5

MEAN VELOCITY(CM/SEC): 378.0 REYNOLDS NO: 21396.3

DTWALL(C): 14.6 DT(C): 6.7 NUSSELT NO: 92.0

++

TEST NO 43 NASAL INHALATION
GAS:NITROGEN DEPTH (FSW): 200.0 FLOW (LPM): 45.6
BATH TEMPERATURE(C): 52.3 PRESSURE DROP(CM H2O): 1.8

TWALL1	TWALL2	TWALL3	TWALL4	TWALL5	MEAN
36.3	50.8	50.5	50.8	52.2	48.1

TNASAL1	TNASAL2	MEAN
31.7	32.6	32.2

TTRACHEA1	TTRACHEA2	MEAN
38.6	40.6	38.6

MEAN VELOCITY(CM/SEC): 598.4 REYNOLDS NO: 33877.5

DTWALL(C): 16.0 DT(C): 6.5 NUSSELT NO: 128.5

++

TEST NO 44 NASAL INHALATION
GAS:HELIUM DEPTH (FSW): 200.0 FLOW (LPM): 23.1
BATH TEMPERATURE(C): 52.8 PRESSURE DROP(CM H2O): 0.6

TWALL1	TWALL2	TWALL3	TWALL4	TWALL5	MEAN
42.0	52.6	52.1	52.1	54.0	50.6

TNASAL1	TNASAL2	MEAN
36.7	38.0	37.4

TTRACHEA1	TTRACHEA2	MEAN
45.4	47.0	45.4

MEAN VELOCITY(CM/SEC): 303.1 REYNOLDS NO: 2703.6

DTWALL(C): 13.2 DT(C): 8.1 NUSSELT NO: 12.2

++

```
TEST NO 45          NASAL          INHALATION
GAS:HELIUM          DEPTH (FSW): 200.0      FLOW (LPM): 28.2
BATH TEMPERATURE(C): 52.9          PRESSURE DROP(CM H2O): 0.3
TWALL1   TWALL2   TWALL3   TWALL4   TWALL5   MEAN
 42.5     52.2     51.9     51.9     53.7     50.4

TNASAL1             TNASAL2          MEAN
 35.9                 36.1            36.0

TTRACHEA1           TTRACHEA2        MEAN
 45.3                 46.7            45.3

MEAN VELOCITY(CM/SEC): 370.1        REYNOLDS NO: 2690.1

DTWALL(C): 14.4     DT(C): 9.3      NUSSELT NO: 15.7

++++++++++++++++++++++++++++++++++++++++++++++++++++++++++++++++++++++++++++++++
```

```
TEST NO 46          NASAL          INHALATION
GAS:HELIUM          DEPTH (FSW): 200.0      FLOW (LPM): 49.1
BATH TEMPERATURE(C): 53.1          PRESSURE DROP(CM H2O): 0.5
TWALL1   TWALL2   TWALL3   TWALL4   TWALL5   MEAN
 41.0     52.1     51.9     51.8     53.5     50.1

TNASAL1             TNASAL2          MEAN
 34.1                 34.9            34.5

TTRACHEA1           TTRACHEA2        MEAN
 43.0                 44.4            43.0

MEAN VELOCITY(CM/SEC): 644.4        REYNOLDS NO: 4683.8

DTWALL(C): 15.6     DT(C): 8.5      NUSSELT NO: 23.2

++++++++++++++++++++++++++++++++++++++++++++++++++++++++++++++++++++++++++++++++
```

```
TEST NO 47          NASAL          INHALATION
GAS:HELIUM          DEPTH (FSW): 200.0      FLOW (LPM): 44.8
BATH TEMPERATURE(C): 53.1          PRESSURE DROP(CM H2O): 0.4
TWALL1   TWALL2   TWALL3   TWALL4   TWALL5   MEAN
 41.2     51.7     51.5     51.5     53.1     49.8

TNASAL1             TNASAL2          MEAN
 34.5                 35.3            34.9

TTRACHEA1           TTRACHEA2        MEAN
 43.3                 44.7            43.3

MEAN VELOCITY(CM/SEC): 587.7        REYNOLDS NO: 4267.6

DTWALL(C): 14.7     DT(C): 8.4      NUSSELT NO: 21.7

++++++++++++++++++++++++++++++++++++++++++++++++++++++++++++++++++++++++++++++++
```

TEST NO 45 RUN# INHALATION
GAS=HELIUM DEPTH (FSW): 1000.0 FLOW (LPM): 4.3
PATH TEMPERATURE (C): 53.5 PRESSURE DROP (IN H2O): 11.1

TWALL1	TWALL2	TWALL3	TWALL4	TWALL5	MEAN
43.9	52.6	52.7	52.9	54.8	51.4

TNASAL1	TNASAL2	MEAN
40.1	40.0	40.1

TTRACHEA1	TTRACHEA2	MEAN
46.4	48.4	46.4

MEAN VELOCITY (FPS): 56.4 REYNOLDS NO: 1747.9

DTWALL (C): 11.3 DT (C): 6.4 NUSSELT NO: 5.0

TEST NO 46 RUN# INHALATION
GAS=HELIUM DEPTH (FSW): 1000.0 FLOW (LPM): 60.6
PATH TEMPERATURE (C): 53.1 PRESSURE DROP (IN H2O): 2.0

TWALL1	TWALL2	TWALL3	TWALL4	TWALL5	MEAN
36.4	52.3	52.7	51.2	54.3	49.4

TNASAL1	TNASAL2	MEAN
33.0	33.4	33.2

TTRACHEA1	TTRACHEA2	MEAN
36.9	37.3	36.9

MEAN VELOCITY (FPS): 75.4 REYNOLDS NO: 24182.5

DTWALL (C): 13.2 DT (C): 6.7 NUSSELT NO: 50.1

TEST NO 47 RUN# INHALATION
GAS=HELIUM DEPTH (FSW): 1000.0 FLOW (LPM): 23.9
PATH TEMPERATURE (C): 52.9 PRESSURE DROP (IN H2O): 0.8

TWALL1	TWALL2	TWALL3	TWALL4	TWALL5	MEAN
39.5	52.3	52.7	52.5	53.4	49.5

TNASAL1	TNASAL2	MEAN
35.	35.4	35.1

TTRACHEA1	TTRACHEA2	MEAN
40.	41.0	40.5

MEAN VELOCITY (FPS): 19.3 REYNOLDS NO: 6733.2

DTWALL (C): 12.9 DT (C): 6.7 NUSSELT NO: 21.7

TEST NO 51 NASAL INHALATION
GAS:NITROGEN DEPTH (FSW): 1000.0 FLOW (LPM): 5.1
BATH TEMPERATURE(C): 52.6 PRESSURE DROP(CM H2O): 0.0

TWALL1	TWALL2	TWALL3	TWALL4	TWALL5	MEAN
44.4	51.5	51.5	51.7	53.5	50.5

TNASAL1	TNASAL2	MEAN
37.4	38.6	38.0

TTRACHEA1	TTRACHEA2	MEAN
47.0	48.7	47.0

MEAN VELOCITY(CM/SEC): 66.9 REYNOLDS NO: 1067[illegible]

DTWALL(C): 12.5 DT(C): 9.0 NUSSELT NO: 11[illegible]

++

TEST NO 52 NASAL INHALATION
GAS:NITROGEN DEPTH (FSW): 1000.0 FLOW (LPM): 9.6
BATH TEMPERATURE(C): 52.5 PRESSURE DROP(CM H2O): 0.1

TWALL1	TWALL2	TWALL3	TWALL4	TWALL5	MEAN
41.7	51.4	51.4	51.4	53.4	49.9

TNASAL1	TNASAL2	MEAN
37.2	37.9	37.6

TTRACHEA1	TTRACHEA2	MEAN
43.8	45.3	43.8

MEAN VELOCITY(CM/SEC): 126.0 REYNOLDS NO: [illegible]1396.0

DTWALL(C): 12.3 DT(C): 6.2 NUSSELT NO: 14[illegible].2

++

TEST NO 53 NASAL INHALATION
GAS:NITROGEN DEPTH (FSW): 1000.0 FLOW (LPM): 9.[illegible]
BATH TEMPERATURE(C): 52.4 PRESSURE DROP(CM H2O): 0.[illegible]

TWALL1	TWALL2	TWALL3	[illegible]	[illegible]	MEAN
40.9	[illegible]1.2	51.2	[illegible]	[illegible]	[illegible]

[illegible]	[illegible]	MEAN
37.0	37.6	37.

[illegible]	[illegible]	MEAN
43.0	44.8	43.0

MEAN VELOCITY(CM/SEC): 128.7 REYNOLDS NO: [illegible]087.9

DTWALL(C): 12.3 DT(C): 5.7 NUSSELT NO: 1[illegible].0

++

UPPER RESPIRATORY TRACT

ORAL/EXHALATION

TEST NO 63 ORAL EXHALATION
GAS:AIR DEPTH (FSW): 0.0 FLOW (LPM): 13.3
BATH TEMPERATURE(C): 51.3 PRESSURE DROP(CM H20): 0.0

TWALL1	TWALL2	TWALL3	TWALL4	TWALL5	MEAN
50.9	51.1	50.2	50.1	51.5	50.6

TNASAL1	TNASAL2	MEAN
47.1	45.9	46.5

TTRACHEA1	TTRACHEA2	MEAN
45.1	46.5	45.1

MEAN VELOCITY(CM/SEC): 174.5 REYNOLDS NO: 1426.9

DTWALL(C): 5.5 DT(C): 1.4 NUSSELT NO: 4.1

++

TEST NO 64 ORAL EXHALATION
GAS:AIR DEPTH (FSW): 0.0 FLOW (LPM): 20.4
BATH TEMPERATURE(C): 51.2 PRESSURE DROP(CM H20): 0.0

TWALL1	TWALL2	TWALL3	TWALL4	TWALL5	MEAN
50.6	51.0	50.1	49.9	50.9	50.3

TNASAL1	TNASAL2	MEAN
46.5	45.8	46.2

TTRACHEA1	TTRACHEA2	MEAN
45.3	42.9	45.3

MEAN VELOCITY(CM/SEC): 267.7 REYNOLDS NO: 2188.6

DTWALL(C): 5.0 DT(C): 0.9 NUSSELT NO: 4.2

++

TEST NO 65 ORAL EXHALATION
GAS:AIR DEPTH (FSW): 0.0 FLOW (LPM): 31.1
BATH TEMPERATURE(C): 51.2 PRESSURE DROP(CM H20): 0.0

TWALL1	TWALL2	TWALL3	TWALL4	TWALL5	MEAN
50.7	51.0	50.1	49.8	50.4	50.1

TNASAL1	TNASAL2	MEAN
45.6	44.7	45.2

TTRACHEA1	TTRACHEA2	MEAN
42.8	40.2	42.8

MEAN VELOCITY(CM/SEC): 408.1 REYNOLDS NO: 3336.6

DTWALL(C): 7.3 DT(C): 2.4 NUSSELT NO: 4.1

++

TEST NO 66 ORAL EXHALATION
GAS:AIR DEPTH (FSW): 0.0 FLOW (LPM): 37.1
BATH TEMPERATURE(C): 51.2 PRESSURE DROP(CM H2O): 0.1

TWALL1	TWALL2	TWALL3	TWALL4	TWALL5	MEAN
50.7	51.2	50.3	50.0	49.9	50.1

TNASAL1	TNASAL2	MEAN
44.6	43.7	44.2

TTRACHEA1	TTRACHEA2	MEAN
41.9	39.6	41.9

MEAN VELOCITY(CM/SEC): 486.9 REYNOLDS NO: 3980.3

DTWALL(C): 8.2 DT(C): 2.3 NUSSELT NO: 12.3

++

TEST NO 67 ORAL EXHALATION
GAS:AIR DEPTH (FSW): 0.0 FLOW (LPM): 44.8
BATH TEMPERATURE(C): 51.2 PRESSURE DROP(CM H2O): 0.2

TWALL1	TWALL2	TWALL3	TWALL4	TWALL5	MEAN
50.6	51.1	50.0	49.9	49.6	49.8

TNASAL1	TNASAL2	MEAN
44.4	43.9	44.2

TTRACHEA1	TTRACHEA2	MEAN
39.9	40.9	39.9

MEAN VELOCITY(CM/SEC): 587.9 REYNOLDS NO: 4806.4

DTWALL(C): 9.9 DT(C): 4.3 NUSSELT NO: 23.1

++

TEST NO 68 ORAL EXHALATION
GAS:AIR DEPTH (FSW): 0.0 FLOW (LPM): 72.8
BATH TEMPERATURE(C): 51.2 PRESSURE DROP(CM H2O): 0.3

TWALL1	TWALL2	TWALL3	TWALL4	TWALL5	MEAN
50.6	51.1	49.8	49.9	49.3	49.7

TNASAL1	TNASAL2	MEAN
42.8	42.5	42.7

TTRACHEA1	TTRACHEA2	MEAN
37.3	38.6	37.3

MEAN VELOCITY(CM/SEC): 955.4 REYNOLDS NO: 7810.4

DTWALL(C): 7.4 DT(C): 5.4 NUSSELT NO: 38.0

++

TEST NO 69 ORAL EXHALATION
GAS:AIR DEPTH (FSW): 0.0 FLOW (LPM): 61.4
BATH TEMPERATURE(C): 51.2 PRESSURE DROP(CM H20): 0.3

TWALL1	TWALL2	TWALL3	TWALL4	TWALL5	MEAN
50.5	51.1	49.7	50.0	49.5	49.7

TNASAL1	TNASAL2	MEAN
43.8	43.6	43.7

TTRACHEA1	TTRACHEA2	MEAN
38.6	39.0	38.6

MEAN VELOCITY(CM/SEC): 805.8 REYNOLDS NO: 6587.4

DTWALL(C): 11.1 DT(C): 5.1 NUSSELT NO: 33.9

++

TEST NO 70 ORAL EXHALATION
GAS:AIR DEPTH (FSW): 0.0 FLOW (LPM): 95.0
BATH TEMPERATURE(C): 51.2 PRESSURE DROP(CM H20): 0.8

TWALL1	TWALL2	TWALL3	TWALL4	TWALL5	MEAN
50.6	51.2	49.7	50.1	49.8	49.9

TNASAL1	TNASAL2	MEAN
43.9	42.7	42.8

TTRACHEA1	TTRACHEA2	MEAN
36.6	37.3	36.6

MEAN VELOCITY(CM/SEC): 1246.7 REYNOLDS NO: 10192.2

DTWALL(C): 13.9 DT(C): 6.7 NUSSELT NO: 53.6

++

TEST NO 71 ORAL EXHALATION
GAS:AIR DEPTH (FSW): 0.0 FLOW (LPM): 108.7
BATH TEMPERATURE(C): 51.2 PRESSURE DROP(CM H20): 1.2

TWALL1	TWALL2	TWALL3	TWALL4	TWALL5	MEAN
50.5	51.1	49.6	49.9	49.5	49.7

TNASAL1	TNASAL2	MEAN
42.3	42.7	42.5

TTRACHEA1	TTRACHEA2	MEAN
36.4	36.7	36.4

MEAN VELOCITY(CM/SEC): 1420.5 REYNOLDS NO: 11662.0

DTWALL(C): 14.5 DT(C): 7.1 NUSSELT NO: 60.3

++

TEST NO 72 ORAL EXHALATION
GAS:HELIUM DEPTH (FSW): 0.0 FLOW (LPM): 88.6
BATH TEMPERATURE(C): 50.7 PRESSURE DROP(CM H2O): 0.1

TWALL1	TWALL2	TWALL3	TWALL4	TWALL5	MEAN
49.1	49.6	48.7	49.0	48.6	48.5

TNASAL1	TNASAL2	MEAN
40.9	41.8	41.4

TTRACHEA1	TTRACHEA2	MEAN
41.9	39.0	41.9

MEAN VELOCITY(CM/SEC): 1162.7 REYNOLDS NO: 3365.3

DTWALL(C): 7.4 DT(C): 0.6 NUSSELT NO: 1.0

++

TEST NO 73 ORAL EXHALATION
GAS:HELIUM DEPTH (FSW): 0.0 FLOW (LPM): 27.8
BATH TEMPERATURE(C): 50.7 PRESSURE DROP(CM H2O): 0.0

TWALL1	TWALL2	TWALL3	TWALL4	TWALL5	MEAN
49.2	49.8	48.8	49.2	48.7	48.9

TNASAL1	TNASAL2	MEAN
45.1	44.9	45.0

TTRACHEA1	TTRACHEA2	MEAN
45.8	36.7	45.8

MEAN VELOCITY(CM/SEC): 364.8 REYNOLDS NO: 378.2

DTWALL(C): 3.9 DT(C): 0.8 NUSSELT NO: 0.9

++

TEST NO 74 ORAL EXHALATION
GAS:HELIUM DEPTH (FSW): 0.0 FLOW (LPM): 124.3
BATH TEMPERATURE(C): 50.6 PRESSURE DROP(CM H2O): 0.2

TWALL1	TWALL2	TWALL3	TWALL4	TWALL5	MEAN
48.8	49.8	48.7	49.0	48.7	48.8

TNASAL1	TNASAL2	MEAN
40.1	41.0	40.6

TTRACHEA1	TTRACHEA2	MEAN
39.0	29.6	39.0

MEAN VELOCITY(CM/SEC): 1631.2 REYNOLDS NO: 1690.9

DTWALL(C): 4.8 DT(C): 1.4 NUSSELT NO: 1.0

++

```
TEST NO 75              ORAL              EXHALATION
GAS:HELIUM              DEPTH (FSW): 0.0      FLOW (LPM): 211.7
BATH TEMPERATURE(C): 50.6                 PRESSURE DROP(CM H20): 0.4
TWALL1    TWALL2    TWALL3    TWALL4    TWALL5    MEAN
 47.6      49.9      48.5      48.5      48.3      48.4

TNASAL1                 TNASAL2           MEAN
 37.4                     39.0             38.2

TTRACHEA1               TTRACHEA2         MEAN
 36.6                     27.8             36.6

MEAN VELOCITY(CM/SEC): 2778.2             REYNOLDS NO: 3879.9

DTWALL(C): 11.8      DT(C): 1.6           NUSSELT NO: 4.3

++++++++++++++++++++++++++++++++++++++++++++++++++++++++++++++++++++++++++++++++


TEST NO 76              ORAL              EXHALATION
GAS:HELIUM              DEPTH (FSW): 0.0      FLOW (LPM): 106.9
BATH TEMPERATURE(C): 50.6                 PRESSURE DROP(CM H20): 0.2
TWALL1    TWALL2    TWALL3    TWALL4    TWALL5    MEAN
 48.3      50.0      48.4      48.5      47.7      48.2

TNASAL1                 TNASAL2           MEAN
 40.5                     41.4             41.0

TTRACHEA1               TTRACHEA2         MEAN
 41.2                     37.2             41.2

MEAN VELOCITY(CM/SEC): 1402.9             REYNOLDS NO: 1454.2

DTWALL(C): 7.3       DT(C): 0.3           NUSSELT NO: 0.6

++++++++++++++++++++++++++++++++++++++++++++++++++++++++++++++++++++++++++++++++


TEST NO 77              ORAL              EXHALATION
GAS:HELIUM              DEPTH (FSW): 0.0      FLOW (LPM): 41.0
BATH TEMPERATURE(C): 50.6                 PRESSURE DROP(CM H20): 0.0
TWALL1    TWALL2    TWALL3    TWALL4    TWALL5    MEAN
 48.7      50.0      48.4      48.8      48.1      48.4

TNASAL1                 TNASAL2           MEAN
 44.6                     44.8             44.7

TTRACHEA1               TTRACHEA2         MEAN
 44.6                     43.3             44.6

MEAN VELOCITY(CM/SEC): 538.1              REYNOLDS NO: 557.8

DTWALL(C): 3.8       DT(C): 0.1           NUSSELT NO: 0.2

++++++++++++++++++++++++++++++++++++++++++++++++++++++++++++++++++++++++++++++++
```

TEST NO 104 ORAL EXHALATION
GAS:NITROGEN DEPTH (FSW): 200.0 FLOW (LPM): 5.8
BATH TEMPERATURE(C): 54.5 PRESSURE DROP(CM H2O): 0.0

TWALL1	TWALL2	TWALL3	TWALL4	TWALL5	MEAN
54.0	54.9	53.7	53.0	55.2	54.0

TNASAL1	TNASAL2	MEAN
48.0	48.7	48.4

TTRACHEA1	TTRACHEA2	MEAN
45.9	47.2	45.9

MEAN VELOCITY(CM/SEC): 76.1 REYNOLDS NO: 4309.0

DTWALL(C): 8.1 DT(C): 2.5 NUSSELT NO: 15.0

++

TEST NO 105 ORAL EXHALATION
GAS:NITROGEN DEPTH (FSW): 200.0 FLOW (LPM): 26.9
BATH TEMPERATURE(C): 54.5 PRESSURE DROP(CM H2O): 0.0

TWALL1	TWALL2	TWALL3	TWALL4	TWALL5	MEAN
53.5	54.8	53.3	52.9	55.0	53.7

TNASAL1	TNASAL2	MEAN
45.6	46.8	46.2

TTRACHEA1	TTRACHEA2	MEAN
42.5	42.6	42.5

MEAN VELOCITY(CM/SEC): 358.0 REYNOLDS NO: 19984.8

DTWALL(C): 11.2 DT(C): 3.7 NUSSELT NO: 75.6

++

TEST NO 106 ORAL EXHALATION
GAS:NITROGEN DEPTH (FSW): 200.0 FLOW (LPM): 6.8
BATH TEMPERATURE(C): 54.6 PRESSURE DROP(CM H2O): 0.0

TWALL1	TWALL2	TWALL3	TWALL4	TWALL5	MEAN
53.6	54.8	53.6	53.2	55.1	54.0

TNASAL1	TNASAL2	MEAN
48.7	48.7	48.7

TTRACHEA1	TTRACHEA2	MEAN
45.8	47.4	45.8

MEAN VELOCITY(CM/SEC): 89.2 REYNOLDS NO: 5051.9

DTWALL(C): 8.2 DT(C): 2.9 NUSSELT NO: 20.6

++

```
TEST NO 107          ORAL              EXHALATION
GAS:NITROGEN         DEPTH (FSW): 200.0      FLOW (LPM): 10.0
BATH TEMPERATURE(C): 54.6              PRESSURE DROP(CM H2O): 0.0
TWALL1    TWALL2    TWALL3    TWALL4    TWALL5    MEAN
 53.7      55.0      53.6      53.1      55.3      54.0

TNASAL1              TNASAL2           MEAN
 46.3                  47.1             46.7

TTRACHEA1            TTRACHEA2         MEAN
 40.7                  43.6             40.7

MEAN VELOCITY(CM/SEC): 131.2          REYNOLDS NO: 7429.3

DTWALL(C): 13.3      DT(C): 6.0       NUSSELT NO: 38.5

++++++++++++++++++++++++++++++++++++++++++++++++++++++++++++++++++++++++++++++


TEST NO 108          ORAL              EXHALATION
GAS:NITROGEN         DEPTH (FSW): 200.0      FLOW (LPM): 16.2
BATH TEMPERATURE(C): 54.6              PRESSURE DROP(CM H2O): 0.1
TWALL1    TWALL2    TWALL3    TWALL4    TWALL5    MEAN
 53.6      55.1      53.7      52.8      55.1      53.9

TNASAL1              TNASAL2           MEAN
 44.3                  45.3             44.8

TTRACHEA1            TTRACHEA2         MEAN
 38.6                  41.9             38.6

MEAN VELOCITY(CM/SEC): 212.6          REYNOLDS NO: 12035.4

DTWALL(C): 15.3      DT(C): 6.2       NUSSELT NO: 56.2

++++++++++++++++++++++++++++++++++++++++++++++++++++++++++++++++++++++++++++++


TEST NO 109          ORAL              EXHALATION
GAS:NITROGEN         DEPTH (FSW): 200.0      FLOW (LPM): 35.5
BATH TEMPERATURE(C): 54.6              PRESSURE DROP(CM H2O): 0.3
TWALL1    TWALL2    TWALL3    TWALL4    TWALL5    MEAN
 53.4      55.2      53.6      52.2      55.3      53.7

TNASAL1              TNASAL2           MEAN
 41.1                  42.5             41.8

TTRACHEA1            TTRACHEA2         MEAN
 35.7                  38.8             35.7

MEAN VELOCITY(CM/SEC): 465.9          REYNOLDS NO: 26374.0

DTWALL(C): 18.0      DT(C): 6.1       NUSSELT NO: 102.7

++++++++++++++++++++++++++++++++++++++++++++++++++++++++++++++++++++++++++++++
```

TEST NO 110 ORAL EXHALATION
GAS:HELIUM DEPTH (FSW): 200.0 FLOW (LPM): 11.6
BATH TEMPERATURE(C): 54.7 PRESSURE DROP(CM H2O): 0.0

TWALL1	TWALL2	TWALL3	TWALL4	TWALL5	MEAN
53.6	55.1	53.7	53.0	55.1	53.9

TNASAL1	TNASAL2	MEAN
46.9	46.8	46.9

TTRACHEA1	TTRACHEA2	MEAN
45.8	47.1	45.8

MEAN VELOCITY(CM/SEC): 152.2 REYNOLDS NO: 1,0[illegible]6

DTWALL(C): 8.1 DT(C): 1.1 NUSSELT NO: 1.6

++

TEST NO 111 ORAL EXHALATION
GAS:HELIUM DEPTH (FSW): 200.0 FLOW (LPM): 35.6
BATH TEMPERATURE(C): 54.7 PRESSURE DROP(CM H2O): 0.0

TWALL1	TWALL2	TWALL3	TWALL4	TWALL5	MEAN
53.5	55.2	53.7	53.7	55.0	54.1

TNASAL1	TNASAL2	MEAN
44.0	44.5	44.3

TTRACHEA1	TTRACHEA2	MEAN
38.5	40.0	38.5

MEAN VELOCITY(CM/SEC): 467.[illegible] REYNOLDS NO: 3896.0

DTWALL(C): 15.6 DT(C): 5.[illegible] NUSSELT NO: 13.9

++

TEST NO 112 ORAL EXHALATION
GAS:HELIUM DEPTH (FSW): 200.0 FLOW (LPM): 15.2
BATH TEMPERATURE(C): 54.8 PRESSURE DROP(CM H2O): 0.0

TWALL1	TWALL2	TWALL3	TWALL4	TWALL5	MEAN
53.6	55.2	53.6	53.0	55.2	53.[illegible]

TNASAL1	TNASAL2	MEAN
47.7	48.0	47.[illegible]

TTRACHEA1	TTRACHEA2	MEAN
45.3	46.2	45.[illegible]

MEAN VELOCITY(CM/SEC): 199.[illegible] REYNOLDS NO: 1,650.0

DTWALL(C): [illegible] DT(C): [illegible] NUSSELT NO: 4.[illegible]

++

TEST NO 113 ORAL EXHALATION
GAS:HELIUM DEPTH (FSW): 200.0 FLOW (LPM): 24.5
BATH TEMPERATURE(C): 54.8 PRESSURE DROP(CM H2O): 0.0

TWALL1	TWALL2	TWALL3	TWALL4	TWALL5	MEAN
53.7	55.3	53.7	52.7	55.1	53.8

TNASAL1	TNASAL2	MEAN
46.1	46.1	46.1

TTRACHEA1	TTRACHEA2	MEAN
43.1	43.1	43.1

MEAN VELOCITY(CM/SEC): 321.5 REYNOLDS NO: 2337.1

DTWALL(C): 10.7 DT(C): 3.0 NUSSELT NO: 7.3

++

TEST NO 114 ORAL EXHALATION
GAS:HELIUM DEPTH (FSW): 200.0 FLOW (LPM): 9.1
BATH TEMPERATURE(C): 54.9 PRESSURE DROP(CM H2O): 0.0

TWALL1	TWALL2	TWALL3	TWALL4	TWALL5	MEAN
53.6	55.3	53.6	53.1	55.0	53.9

TNASAL1	TNASAL2	MEAN
48.9	49.0	49.0

TTRACHEA1	TTRACHEA2	MEAN
47.6	49.0	47.6

MEAN VELOCITY(CM/SEC): 119.4 REYNOLDS NO: 868.1

DTWALL(C): 6.3 DT(C): 1.4 NUSSELT NO: 2.1

++

TEST NO 115 ORAL EXHALATION
GAS:HELIUM DEPTH (FSW): 200.0 FLOW (LPM): 22.5
BATH TEMPERATURE(C): 54.9 PRESSURE DROP(CM H2O): 0.0

TWALL1	TWALL2	TWALL3	TWALL4	TWALL5	MEAN
53.8	55.5	53.8	53.0	54.9	53.9

TNASAL1	TNASAL2	MEAN
46.2	46.7	46.5

TTRACHEA1	TTRACHEA2	MEAN
43.7	44.3	43.7

MEAN VELOCITY(CM/SEC): 295.3 REYNOLDS NO: 2146.3

DTWALL(C): 10.2 DT(C): 2.1 NUSSELT NO: 6.4

++

TEST NO 116 ORAL EXHALATION
GAS:HELIUM DEPTH (FSW): 100.0 FLOW (LPM): 50.7
BATH TEMPERATURE(C): 54.9 PRESSURE DROP(CM H2O): 0.1

TWALL1	TWALL2	TWALL3	TWALL4	TWALL5	MEAN
53.4	55.4	53.7	52.3	54.7	53.6

TNASAL1	TNASAL2	MEAN
42.4	43.0	42.7

TTRACHEA1	TTRACHEA2	MEAN
37.1	38.6	37.1

MEAN VELOCITY(CM/SEC): 665.4 REYNOLDS NO: 4836.4

DTWALL(C): 16.5 DT(C): 5.6 NUSSELT NO: 18.3

++

TEST NO 117 ORAL EXHALATION
GAS:HELIUM DEPTH (FSW): 1000.0 FLOW (LPM): 4.5
BATH TEMPERATURE(C): 54.7 PRESSURE DROP(CM H2O): 0.1

TWALL1	TWALL2	TWALL3	TWALL4	TWALL5	MEAN
54.4	55.7	54.2	52.9	56.0	54.4

TNASAL1	TNASAL2	MEAN
46.2	47.5	46.9

TTRACHEA1	TTRACHEA2	MEAN
41.9	44.1	41.9

MEAN VELOCITY(CM/SEC): 59.1 REYNOLDS NO: 1081.6

DTWALL(C): 12.5 DT(C): 5.0 NUSSELT NO: 8.2

++

TEST NO 118 ORAL EXHALATION
GAS:HELIUM DEPTH (FSW): 1000.0 FLOW (LPM): 11.2
BATH TEMPERATURE(C): 54.6 PRESSURE DROP(CM H2O): 0.0

TWALL1	TWALL2	TWALL3	TWALL4	TWALL5	MEAN
53.2	55.4	53.9	52.7	55.4	53.9

TNASAL1	TNASAL2	MEAN
43.7	44.8	44.3

TTRACHEA1	TTRACHEA2	MEAN
39.3	41.1	39.3

MEAN VELOCITY(CM/SEC): 147.0 REYNOLDS NO: 4683.0

DTWALL(C): 14.6 DT(C): 5.0 NUSSELT NO: 17.4

++

TEST NO 119 ORAL EXHALATION
GAS:HELIUM DEPTH (FSW): 1000.0 FLOW (LPM): 44.4
BATH TEMPERATURE(C): 54.6 PRESSURE DROP(CM H20): 0.0

TWALL1	TWALL2	TWALL3	TWALL4	TWALL5	MEAN
51.9	55.4	53.7	49.4	54.8	52.6

TNASAL1	TNASAL2	MEAN
37.8	39.3	38.6

TTRACHEA1	TTRACHEA2	MEAN
34.6	35.8	34.6

MEAN VELOCITY(CM/SEC): 582.7 REYNOLDS NO: 18564.8

DTWALL(C): 18.0 DT(C): 4.0 NUSSELT NO: 44.4

++

TEST NO 120 ORAL EXHALATION
GAS:NITROGEN DEPTH (FSW): 1000.0 FLOW (LPM): 2.0
BATH TEMPERATURE(C): 54.2 PRESSURE DROP(CM H20): 0.6

TWALL1	TWALL2	TWALL3	TWALL4	TWALL5	MEAN
53.4	54.8	53.1	52.3	54.7	53.4

TNASAL1	TNASAL2	MEAN
47.5	48.0	47.8

TTRACHEA1	TTRACHEA2	MEAN
44.7	46.7	44.7

MEAN VELOCITY(CM/SEC): 26.2 REYNOLDS NO: [illegible]44.8

DTWALL(C): 8.7 DT(C): 3.1 NUSSELT NO: 26.0

++

TEST NO 121 ORAL EXHALATION
GAS:NITROGEN DEPTH (FSW): 1000.0 FLOW (LPM): 20.9
BATH TEMPERATURE(C): 54.2 PRESSURE DROP(CM H20): 0.6

TWALL1	TWALL2	TWALL3	TWALL4	TWALL5	MEAN
53.0	54.8	53.2	50.9	54.4	52.8

TNASAL1	TNASAL2	MEAN
40.7	41.4	41.1

TTRACHEA1	TTRACHEA2	MEAN
37.1	39.0	37.1

MEAN VELOCITY(CM/SEC): 274.3 REYNOLDS NO: 68851.8

DTWALL(C): 15.7 DT(C): 4.0 NUSSELT NO: 193.9

++

TEST NO 122 ORAL EXHALATION
GAS:NITROGEN DEPTH (FSW): 1000.0 FLOW (LPM): 13.1
BATH TEMPERATURE(C): 54.2 PRESSURE DROP(CM H20): 0.1

TWALL1	TWALL2	TWALL3	TWALL4	TWALL5	MEAN
53.0	54.5	52.0	51.2	54.3	52.6

TNASAL1	TNASAL2	MEAN
41.7	42.8	42.3

TTRACHEA1	TTRACHEA2	MEAN
38.5	40.9	38.5

MEAN VELOCITY(CM/SEC): 171.9 REYNOLDS NO: 4,842.5

DTWALL(C): 14.3 DT(C): 3.8 NUSSELT NO: 126.6

++

TEST NO 123 ORAL EXHALATION
GAS:NITROGEN DEPTH (FSW): 1000.0 FLOW (LPM): 7.3
BATH TEMPERATURE(C): 54.1 PRESSURE DROP(CM H20): 0.1

TWALL1	TWALL2	TWALL3	TWALL4	TWALL5	MEAN
53.1	54.4	52.9	51.7	54.2	52.9

TNASAL1	TNASAL2	MEAN
44.2	45.0	44.6

TTRACHEA1	TTRACHEA2	MEAN
40.7	42.9	40.7

MEAN VELOCITY(CM/SEC): 95.3 REYNOLDS NO: 23874.1

DTWALL(C): 14.2 DT(C): 3.9 NUSSELT NO: 86.0

++

TEST NO 124 ORAL EXHALATION
GAS:HELIUM DEPTH (FSW): 0.0 FLOW (LPM): 185.1
BATH TEMPERATURE(C): 53.7 PRESSURE DROP(CM H20): 0.3

TWALL1	TWALL2	TWALL3	TWALL4	TWALL5	MEAN
52.6	54.0	52.0	51.4	52.7	52.5

TNASAL1	TNASAL2	MEAN
43.3	45.2	44.3

TTRACHEA1	TTRACHEA2	MEAN
40.9	41.4	40.9

MEAN VELOCITY(CM/SEC): 2424.1 REYNOLDS NO: 2518.1

DTWALL(C): 11.6 DT(C): 3.4 NUSSELT NO: 8.1

++

TEST NO 125 ORAL EXHALATION
GAS:HELIUM DEPTH (FSW): 0.0 FLOW (LPM): 60.0
BATH TEMPERATURE(C): 53.7 PRESSURE DROP(CM H2O): 0.1

TWALL1	TWALL2	TWALL3	TWALL4	TWALL5	MEAN
52.8	53.0	53.2	52.0	52.3	52.5

TNASAL1	TNASAL2	MEAN
47.9	48.4	48.2

TTRACHEA1	TTRACHEA2	MEAN
45.6	47.9	45.6

MEAN VELOCITY(CM/SEC): 787.4 REYNOLDS NO: 816.2

DTWALL(C): 6.9 DT(C): 2.6 NUSSELT NO: 3.4

++

TEST NO 126 ORAL EXHALATION
GAS:HELIUM DEPTH (FSW): 0.0 FLOW (LPM): 42.1
BATH TEMPERATURE(C): 53.7 PRESSURE DROP(CM H2O): 0.0

TWALL1	TWALL2	TWALL3	TWALL4	TWALL5	MEAN
53.0	53.1	53.1	52.1	52.1	52.4

TNASAL1	TNASAL2	MEAN
48.5	49.0	48.8

TTRACHEA1	TTRACHEA2	MEAN
46.5	49.3	46.5

MEAN VELOCITY(CM/SEC): 552.5 REYNOLDS NO: 572.7

DTWALL(C): 5.9 DT(C): 2.3 NUSSELT NO: 2.4

++

TEST NO 127 ORAL EXHALATION
GAS:HELIUM DEPTH (FSW): 0.0 FLOW (LPM): 87.2
BATH TEMPERATURE(C): 53.7 PRESSURE DROP(CM H2O): 0.1

TWALL1	TWALL2	TWALL3	TWALL4	TWALL5	MEAN
53.0	53.1	53.0	52.1	52.3	52.5

TNASAL1	TNASAL2	MEAN
46.2	47.2	46.7

TTRACHEA1	TTRACHEA2	MEAN
43.5	45.1	43.5

MEAN VELOCITY(CM/SEC): 1144.4 REYNOLDS NO: 1186.2

DTWALL(C): 9.0 DT(C): 3.2 NUSSELT NO: 4.7

++

TEST NO 128 ORAL EXHALATION
GAS:HELIUM DEPTH (FSW): 0.0 FLOW (LPM): 157.6
BATH TEMPERATURE(C): 53.7 PRESSURE DROP(CM H2O): 0.3

TWALL1	TWALL2	TWALL3	TWALL4	TWALL5	MEAN
52.9	53.0	53.2	51.9	52.1	52.4

TNASAL1	TNASAL2	MEAN
43.0	44.6	43.8

TTRACHEA1	TTRACHEA2	MEAN
40.5	41.2	40.5

MEAN VELOCITY(CM/SEC): 2068.2 REYNOLDS NO: 2143.9

DTWALL(C): 11.9 DT(C): 3.3 NUSSELT NO: 6.6

++

UPPER RESPIRATORY TRACT

ORAL/INHALATION

TEST NO 78 ORAL INHALATION
GAS:HELIUM DEPTH (FSW): 0.0 FLOW (LPM): 40.8
BATH TEMPERATURE(C): 50.6 PRESSURE DROP(CM H20): 0.2

TWALL1	TWALL2	TWALL3	TWALL4	TWALL5	MEAN
48.7	49.9	48.5	48.7	48.6	48.6

TNASAL1	TNASAL2	MEAN
32.0	31.9	32.0

TTRACHEA1	TTRACHEA2	MEAN
43.4	45.7	43.4

MEAN VELOCITY(CM/SEC): 1035.4 REYNOLDS NO: 5545.0

DTWALL(C): 16.7 DT(C): 11.5 NUSSELT NO: 4.1

++

TEST NO 79 ORAL INHALATION
GAS:HELIUM DEPTH (FSW): 0.0 FLOW (LPM): 90.0
BATH TEMPERATURE(C): 50.6 PRESSURE DROP(CM H20): 0.7

TWALL1	TWALL2	TWALL3	TWALL4	TWALL5	MEAN
48.1	50.0	48.6	47.7	48.5	48.3

TNASAL1	TNASAL2	MEAN
28.5	29.2	28.9

TTRACHEA1	TTRACHEA2	MEAN
40.8	42.5	40.8

MEAN VELOCITY(CM/SEC): 1286.1 REYNOLDS NO: [illegible]

DTWALL(C): 19.4 DT(C): 12.0 NUSSELT NO: [illegible]

++

TEST NO 80 ORAL INHALATION
GAS:HELIUM DEPTH (FSW): 0.0 FLOW (LPM): [illegible]
BATH TEMPERATURE(C): 50.5 PRESSURE DROP(CM H20): [illegible]

TWALL1	TWALL2	TWALL3	TWALL4	TWALL5	MEAN
47.4	[illegible]	[illegible]	[illegible]	48.1	47.

TNASAL1	TNASAL2	MEAN
[illegible]	[illegible]	[illegible]

TTRACHEA1	TTRACHEA2	MEAN
[illegible]	[illegible]	[illegible]

MEAN VELOCITY(CM/SEC): [illegible] REYNOLDS NO: [illegible]

DTWALL(C): [illegible] DT(C): [illegible] NUSSELT NO: [illegible]

++++++++++ [illegible]

TEST NO =1 ORAL INHALATION
GAS=HELIUM DEPTH (FSW): 0.0 FLOW (LPM): 210.6
BATH TEMPERATURE(C): 50.5 PRESSURE DROP(CM H2O): 2.1

TWALL1	TWALL2	TWALL3	TWALL4	TWALL5	MEAN
47.8	50.1	48.8	46.3	48.5	47.9

TMASAL1	TMASAL2	MEAN
25.2	26.4	25.8

TTRACHEA1	TTRACHEA2	MEAN
34.5	38.4	36.5

MEAN VELOCITY(CM/SEC): 2763.8 REYNOLDS NO: 2864.9

DTWALL(C): 32.1 DT(C): 18.2 NUSSELT NO: 15.5

TEST NO 8 ORAL INHALATION
GAS=HELIUM DEPTH (FSW): 0.0 FLOW (LPM): 97.3
BATH TEMPERATURE(C): 50.5 PRESSURE DROP(CM H2O): 0.7

TWALL1	TWALL2	TWALL3	TWALL4	TWALL5	MEAN
47.8	50.1	48.4	46.3	48.2	48.0

TMASAL1	TMASAL2	MEAN
28.4	29.7	29.1

TTRACHEA1	TTRACHEA2	MEAN
40.3	36.4	38.3

MEAN VELOCITY(CM/SEC): 1275.9 REYNOLDS NO: 1323.6

DTWALL(C): 29.9 DT(C): 17.4 NUSSELT NO: 8.8

TEST NO 5 ORAL INHALATION
GAS=HELIUM DEPTH (FSW): 0.0 FLOW (LPM): 81.7
BATH TEMPERATURE(C): 50.5 PRESSURE DROP(CM H2O): 0.6

TWALL1	TWALL2	TWALL3	TWALL4	TWALL5	MEAN
47.8	50.1	48.8	46.3	48.3	48.3

TMASAL1	TMASAL2	MEAN
28.4	31.4	29.9

TTRACHEA1	TTRACHEA2	MEAN
42.5	44.5	43.5

MEAN VELOCITY(CM/SEC): 1061.7 REYNOLDS NO: 1111.4

DTWALL(C): 31.4 DT(C): 19.1 NUSSELT NO: 8.3

TEST NO: [illegible] ORAL INHALATION
GAS: AIR DEPTH (CM): [illegible] FLOW (LPM): 14.7
BATH TEMPERATURE (C): 50.5 PRESSURE DROP(CM H2O): 0.1

TWALL1	TWALL2	TWALL3	TWALL4	TWALL5	MEAN
[illegible]	50.1	[illegible]	[illegible]	49.9	48.6

TNASAL1	TNASAL2	MEAN
[illegible]	40.3	39.7

TTRACHEA1	TTRACHEA2	MEAN
[illegible]	4[illegible]	44.9

MEAN VELOCITY (CM/SEC): [illegible] REYNOLDS NO: [illegible]7.1

DTRACHEA(CM): [illegible] [illegible] NUSSELT NO: [illegible]

++

TEST NO: [illegible] ORAL INHALATION
GAS: AIR DEPTH (CM): 0.0 FLOW (LPM): 20.5
BATH TEMPERATURE (C): 50.5 PRESSURE DROP(CM H2O): 0.1

TWALL1	TWALL2	TWALL3	TWALL4	TWALL5	MEAN
[illegible]	50.0	[illegible]	[illegible]	49.1	48.9

TNASAL1	TNASAL2	MEAN
[illegible]	[illegible]	[illegible]9.2

TTRACHEA1	TTRACHEA2	MEAN
4[illegible].1	4[illegible]	44.1

MEAN VELOCITY (CM/SEC): [illegible] REYNOLDS NO: 2[illegible]99.4

DTRACHEA(CM): [illegible] [illegible] NUSSELT NO: 12.6

++

TEST NO: [illegible] ORAL INHALATION
GAS: AIR DEPTH (CM): 0.0 FLOW (LPM): 30.9
BATH TEMPERATURE (C): 50.5 PRESSURE DROP(CM H2O): 0.3

TWALL1	TWALL2	TWALL3	TWALL4	TWALL5	MEAN
[illegible]	[illegible].1	4[illegible]	48.[illegible]	49.4	49.1

TNASAL1	TNASAL2	MEAN
[illegible]	[illegible]	38.0

TTRACHEA1	TTRACHEA2	MEAN
[illegible]	4[illegible].0	43.1

MEAN VELOCITY (CM/SEC): [illegible] REYNOLDS NO: [illegible].1

DTRACHEA(CM): [illegible] [illegible] NUSSELT NO: [illegible]

++

AD-A104 992 NAVAL COASTAL SYSTEMS CENTER PANAMA CITY FL F/G 6/19
HEAT AND WATER VAPOR TRANSFER IN THE HUMAN RESPIRATORY SYSTEM A--ETC(U)
SEP 81 M L NUCKOLS
UNCLASSIFIED NCSC-TR-364-81 SBIE-AD-F200 009 NL

4 of 4
AD
A104992

END
DATE FILMED
10-81
DTIC

TEST NO 5. ORAL INHALATION
GAS:AIR DEPTH (FSW): 33.0 FLOW (LPM): 5.5
BATH TEMPERATURE(C): 50.5 PRESSURE DROP: 0.0 IN H20 0.0
TWALL1 TWALL2 TWALL3 TWALL4 TWALL5 MEAN
48.7 50.0 49.3 48.5 49.3 49.4

TNASAL1 TNASAL2 MEAN
35.7 37.3 36.5

TTRACHEA1 TTRACHEA2 MEAN
42.0 44.0 43.0

MEAN VELOCITY(CM/SEC): 0.0 REYNOLDS NO: 0.0

DTWALL(C): 12.7 DT(C): 0.0 NUSSELT NO: 0.0

TEST NO 88 ORAL INHALATION
GAS:AIR DEPTH (FSW): 0.0 FLOW (LPM): 51.7
BATH TEMPERATURE(C): 50.4 PRESSURE DROP: 0.0 IN H20: 0.0
TWALL1 TWALL2 TWALL3 TWALL4 TWALL5 MEAN
47.7 50.2 49.5 48.4 49.5 49.

TNASAL1 TNASAL2 MEAN
35.1 37.5 36.3

TTRACHEA1 TTRACHEA2 MEAN
42.4 45.1 43.4

MEAN VELOCITY(CM/SEC): 694.9 REYNOLDS NO: 49.7

DTWALL(C): 12.9 DT(C): 0.1 NUSSELT NO: 29.5

TEST NO 89 ORAL INHALATION
GAS:AIR DEPTH (FSW): 0.0 FLOW (LPM): 60.6
BATH TEMPERATURE(C): 50.4 PRESSURE DROP: 0.0 IN H20: 0.0
TWALL1 TWALL2 TWALL3 TWALL4 TWALL5 MEAN
48.8 50.0 49.3 48.5 49.6 49.1

TNASAL1 TNASAL2 MEAN
34.5 36.7 35.6

TTRACHEA1 TTRACHEA2 MEAN
41.9 44.8 41.9

MEAN VELOCITY(CM/SEC): 795.3 REYNOLDS NO: 56.5

DTWALL(C): 12.5 DT(C): 0.1 NUSSELT NO: 34.0

TEST NO 90 ORAL INHALATION
GAS:AIR DEPTH (FSW): 0.0 FLOW (LPM): 80.7
BATH TEMPERATURE(C): 50.4 PRESSURE DROP(CM H2O): 1.0

TWALL1	TWALL2	TWALL3	TWALL4	TWALL5	MEAN
48.7	50.1	49.4	48.2	49.6	49.1

TNASAL1	TNASAL2	MEAN
32.3	35.5	33.9

TTRACHEA1	TTRACHEA2	MEAN
40.1	42.9	40.1

MEAN VELOCITY(CM/SEC): 1059.1 REYNOLDS NO: 8658.0

DTWALL(C): 15.2 DT(C): 6.2 NUSSELT NO: 39.8

++

TEST NO 91 ORAL INHALATION
GAS:AIR DEPTH (FSW): 0.0 FLOW (LPM): 119.4
BATH TEMPERATURE(C): 50.4 PRESSURE DROP(CM H2O): 1.8

TWALL1	TWALL2	TWALL3	TWALL4	TWALL5	MEAN
48.6	50.1	49.4	47.9	49.5	48.9

TNASAL1	TNASAL2	MEAN
30.3	33.6	32.0

TTRACHEA1	TTRACHEA2	MEAN
38.2	41.1	38.2

MEAN VELOCITY(CM/SEC): 1566.9 REYNOLDS NO: 12809.9

DTWALL(C): 17.0 DT(C): 6.3 NUSSELT NO: 53.0

++

TEST NO 92 ORAL INHALATION
GAS:AIR DEPTH (FSW): 0.0 FLOW (LPM): 97.3
BATH TEMPERATURE(C): 50.4 PRESSURE DROP(CM H2O): 1.4

TWALL1	TWALL2	TWALL3	TWALL4	TWALL5	MEAN
48.7	50.3	49.5	48.3	49.7	49.2

TNASAL1	TNASAL2	MEAN
31.7	35.1	33.4

TTRACHEA1	TTRACHEA2	MEAN
39.8	43.2	39.8

MEAN VELOCITY(CM/SEC): 1276.9 REYNOLDS NO: 10438.9

DTWALL(C): 15.8 DT(C): 6.4 NUSSELT NO: 47.7

++

TEST NO 93 ORAL INHALATION
GAS:AIR DEPTH (FSW): 0.0 FLOW (LPM): 132.6
BATH TEMPERATURE(C): 50.4 PRESSURE DROP(CM H2O): 2.1

TWALL1	TWALL2	TWALL3	TWALL4	TWALL5	MEAN
48.7	50.1	49.4	48.0	49.5	49.0

TNASAL1	TNASAL2	MEAN
30.7	34.3	32.5

TTRACHEA1	TTRACHEA2	MEAN
38.6	43.6	38.6

MEAN VELOCITY(CM/SEC): 1740.2 REYNOLDS NO: 14226.1

DTWALL(C): 16.5 DT(C): 6.1 NUSSELT NO: 59.3

++

TEST NO 94 ORAL INHALATION
GAS:NITROGEN DEPTH (FSW): 200.0 FLOW (LPM): 7.7
BATH TEMPERATURE(C): 56.6 PRESSURE DROP(CM H2O): 0.0

TWALL1	TWALL2	TWALL3	TWALL4	TWALL5	MEAN
57.1	58.4	57.4	56.1	58.6	57.4

TNASAL1	TNASAL2	MEAN
39.0	41.3	40.2

TTRACHEA1	TTRACHEA2	MEAN
48.2	51.0	48.2

MEAN VELOCITY(CM/SEC): 101.0 REYNOLDS NO: 5720.5

DTWALL(C): 17.2 DT(C): 8.1 NUSSELT NO: 30.7

++

TEST NO 95 ORAL INHALATION
GAS:NITROGEN DEPTH (FSW): 200.0 FLOW (LPM): 20.7
BATH TEMPERATURE(C): 56.5 PRESSURE DROP(CM H2O): 0.4

TWALL1	TWALL2	TWALL3	TWALL4	TWALL5	MEAN
57.0	58.3	57.4	54.7	58.2	56.8

TNASAL1	TNASAL2	MEAN
33.3	36.6	35.0

TTRACHEA1	TTRACHEA2	MEAN
43.7	46.5	43.7

MEAN VELOCITY(CM/SEC): 271.7 REYNOLDS NO: 15378.6

DTWALL(C): 21.8 DT(C): 8.8 NUSSELT NO: 70.9

++

TEST NO 96 ORAL INHALATION
GAS:NITROGEN DEPTH (FSW): 200.0 FLOW (LPM): 32.2
BATH TEMPERATURE(C): 56.3 PRESSURE DROP(CM H20): 1.0

TWALL1	TWALL2	TWALL3	TWALL4	TWALL5	MEAN
56.7	58.2	57.1	53.5	57.7	56.1

TNASAL1	TNASAL2	MEAN
31.2	33.9	32.6

TTRACHEA1	TTRACHEA2	MEAN
40.5	43.3	40.5

MEAN VELOCITY(CM/SEC): 422.6 REYNOLDS NO: 23922.3

PTWALL(C): 23.6 DT(C): 8.0 NUSSELT NO: 92.8

++

TEST NO 97 ORAL INHALATION
GAS:NITROGEN DEPTH (FSW): 200.0 FLOW (LPM): 41.1
BATH TEMPERATURE(C): 55.8 PRESSURE DROP(CM H20): 1.4

TWALL1	TWALL2	TWALL3	TWALL4	TWALL5	MEAN
56.1	57.8	56.5	53.0	57.4	55.6

TNASAL1	TNASAL2	MEAN
30.8	33.5	32.2

TTRACHEA1	TTRACHEA2	MEAN
39.3	41.8	39.3

MEAN VELOCITY(CM/SEC): 539.4 REYNOLDS NO: 30534.4

DTWALL(C): 23.5 DT(C): 7.2 NUSSELT NO: 106.8

++

TEST NO 98 ORAL INHALATION
GAS:NITROGEN DEPTH (FSW): 200.0 FLOW (LPM): 48.4
BATH TEMPERATURE(C): 55.5 PRESSURE DROP(CM H20): 2.0

TWALL1	TWALL2	TWALL3	TWALL4	TWALL5	MEAN
55.5	57.5	56.1	52.1	56.9	55.0

TNASAL1	TNASAL2	MEAN
30.3	32.8	31.6

TTRACHEA1	TTRACHEA2	MEAN
37.9	40.3	37.9

MEAN VELOCITY(CM/SEC): 635.2 REYNOLDS NO: 35957.7

DTWALL(C): 23.5 DT(C): 6.4 NUSSELT NO: 111.7

++

TEST NO 99 ORAL INHALATION
GAS:HELIUM DEPTH (FSW): 200.0 FLOW (LPM): 3.3
BATH TEMPERATURE(C): 55.1 PRESSURE DROP(CM H2O): 0.0

TWALL1	TWALL2	TWALL3	TWALL4	TWALL5	MEAN
55.4	57.1	55.6	54.2	56.4	55.4

TNASAL1	TNASAL2	MEAN
40.6	41.8	41.2

TTRACHEA1	TTRACHEA2	MEAN
49.4	52.0	49.4

MEAN VELOCITY(CM/SEC): 43.3 REYNOLDS NO: 314.8

DTWALL(C): 14.2 DT(C): 8.2 NUSSELT NO: 2.0

++

TEST NO 100 ORAL INHALATION
GAS:HELIUM DEPTH (FSW): 200.0 FLOW (LPM): 41.2
BATH TEMPERATURE(C): 55.0 PRESSURE DROP(CM H2O): 0.4

TWALL1	TWALL2	TWALL3	TWALL4	TWALL5	MEAN
55.1	56.9	55.5	52.2	56.3	54.7

TNASAL1	TNASAL2	MEAN
32.0	32.9	32.5

TTRACHEA1	TTRACHEA2	MEAN
42.5	44.3	42.5

MEAN VELOCITY(CM/SEC): 540.7 REYNOLDS NO: 3930.2

DTWALL(C): 22.2 DT(C): 10.1 NUSSELT NO: 19.7

++

TEST NO 101 ORAL INHALATION
GAS:HELIUM DEPTH (FSW): 200.0 FLOW (LPM): 19.6
BATH TEMPERATURE(C): 54.7 PRESSURE DROP(CM H2O): 0.1

TWALL1	TWALL2	TWALL3	TWALL4	TWALL5	MEAN
54.8	56.7	55.3	53.1	55.9	54.8

TNASAL1	TNASAL2	MEAN
34.0	35.2	34.6

TTRACHEA1	TTRACHEA2	MEAN
46.1	48.3	46.1

MEAN VELOCITY(CM SEC): 257.2 REYNOLDS NO: 1869.7

DTWALL(C): 20.2 DT(C): 11.5 NUSSELT NO: 11.8

++

TEST NO 102 ORAL INHALATION
GAS:HELIUM DEPTH (FSW): 200.0 FLOW (LPM): 14.3
BATH TEMPERATURE(C): 54.4 PRESSURE DROP(CM H2O): 0.0

TWALL1	TWALL2	TWALL3	TWALL4	TWALL5	MEAN
54.8	56.5	55.1	53.5	56.1	54.9

TNASAL1	TNASAL2	MEAN
35.6	36.5	36.1

TTRACHEA1	TTRACHEA2	MEAN
47.7	49.8	47.7

MEAN VELOCITY(CM/SEC): 187.7 REYNOLDS NO: 1364.1

DTWALL(C): 18.9 DT(C): 11.7 NUSSELT NO: 9.4

++

TEST NO 103 ORAL INHALATION
GAS:HELIUM DEPTH (FSW): 200.0 FLOW (LPM): 7.8
BATH TEMPERATURE(C): 54.3 PRESSURE DROP(CM H2O): 0.0

TWALL1	TWALL2	TWALL3	TWALL4	TWALL5	MEAN
54.5	56.2	54.9	53.5	55.6	54.7

TNASAL1	TNASAL2	MEAN
36.7	38.6	37.7

TTRACHEA1	TTRACHEA2	MEAN
49.4	51.3	49.4

MEAN VELOCITY(CM/SEC): 102.4 REYNOLDS NO: 744.1

DTWALL(C): 17.0 DT(C): 11.8 NUSSELT NO: 5.7

++

TEST NO 129 ORAL INHALATION
GAS:NITROGEN DEPTH (FSW): 1000.0 FLOW (LPM): 8.3
BATH TEMPERATURE(C): 54.2 PRESSURE DROP(CM H2O): 0.0

TWALL1	TWALL2	TWALL3	TWALL4	TWALL5	MEAN
55.3	55.1	53.9	52.7	55.9	54.2

TNASAL1	TNASAL2	MEAN
36.3	38.4	37.4

TTRACHEA1	TTRACHEA2	MEAN
46.0	48.0	46.0

MEAN VELOCITY(CM/SEC): 43.3 REYNOLDS NO: 10792.4

DTWALL(C): 16.8 DT(C): 8.7 NUSSELT NO: 62.7

++

TEST NO 130 ORAL INHALATION
GAS:NITROGEN DEPTH (FSW): 1000.0 FLOW (LPM): 10.4
BATH TEMPERATURE(C): 53.9 PRESSURE DROP(CM H2O): 0.0

TWALL1	TWALL2	TWALL3	TWALL4	TWALL5	MEAN
53.8	54.9	53.7	51.4	55.5	53.5

TNASAL1	TNASAL2	MEAN
30.6	32.7	31.7

TTRACHEA1	TTRACHEA2	MEAN
42.1	44.2	42.1

MEAN VELOCITY(CM/SEC): 136.5 REYNOLDS NO: 34012.4

DTWALL(C): 21.9 DT(C): 10.5 NUSSELT NO: 183.5

++

TEST NO 131 ORAL INHALATION
GAS:NITROGEN DEPTH (FSW): 1000.0 FLOW (LPM): 10.7
BATH TEMPERATURE(C): 53.6 PRESSURE DROP(CM H2O): 0.5

TWALL1	TWALL2	TWALL3	TWALL4	TWALL5	MEAN
54.0	54.8	53.2	49.6	54.8	52.5

TNASAL1	TNASAL2	MEAN
30.3	32.4	31.4

TTRACHEA1	TTRACHEA2	MEAN
37.2	39.5	37.2

MEAN VELOCITY(CM/SEC): 140.4 REYNOLDS NO: 34993.5

DTWALL(C): 21.2 DT(C): 5.9 NUSSELT NO: 109.2

++

TEST NO 132 ORAL INHALATION
GAS:NITROGEN DEPTH (FSW): 1000.0 FLOW (LPM): 12.1
BATH TEMPERATURE(C): 53.1 PRESSURE DROP(CM H2O): 0.6

TWALL1	TWALL2	TWALL3	TWALL4	TWALL5	MEAN
53.4	54.2	52.5	49.6	54.3	52.1

TNASAL1	TNASAL2	MEAN
31.1	33.9	32.0

TTRACHEA1	TTRACHEA2	MEAN
37.4	39.8	37.4

MEAN VELOCITY(CM SEC): 158.8 REYNOLDS NO: 39572.1

DTWALL(C): 20.1 DT(C): 5.4 NUSSELT NO: 119.9

++

TEST NO 133 ORAL INHALATION
GAS:NITROGEN DEPTH (FSW): 1000.0 FLOW (LPM): 6.8
BATH TEMPERATURE(C): 52.7 PRESSURE DROP(CM H2O): 0.1

TWALL1	TWALL2	TWALL3	TWALL4	TWALL5	MEAN
53.0	53.6	52.0	49.9	53.9	51.9

TNASAL1	TNASAL2	MEAN
32.3	34.6	33.5

TTRACHEA1	TTRACHEA2	MEAN
39.8	42.5	39.8

MEAN VELOCITY(CM/SEC): 89.2 REYNOLDS NO: 22238.9

DTWALL(C): 18.5 DT(C): 6.4 NUSSELT NO: 86.3

++

TEST NO 134 ORAL INHALATION
GAS:NITROGEN DEPTH (FSW): 1000.0 FLOW (LPM): 25.2
BATH TEMPERATURE(C): 52.4 PRESSURE DROP(CM H2O): 4.1

TWALL1	TWALL2	TWALL3	TWALL4	TWALL5	MEAN
52.8	53.4	51.9	48.7	53.9	51.5

TNASAL1	TNASAL2	MEAN
30.5	32.5	31.5

TTRACHEA1	TTRACHEA2	MEAN
34.9	37.5	34.9

MEAN VELOCITY(CM/SEC): 330.7 REYNOLDS NO: 82414.6

DTWALL(C): 20.0 DT(C): 3.4 NUSSELT NO: 158.3

++

TEST NO 135 ORAL INHALATION
GAS:HELIUM DEPTH (FSW): 1000.0 FLOW (LPM): 3.6
BATH TEMPERATURE(C): 52.0 PRESSURE DROP(CM H2O): 0.1

TWALL1	TWALL2	TWALL3	TWALL4	TWALL5	MEAN
52.5	52.9	51.4	50.3	53.3	51.7

TNASAL1	TNASAL2	MEAN
36.2	38.2	37.2

TTRACHEA1	TTRACHEA2	MEAN
44.1	48.1	44.1

MEAN VELOCITY(CM SEC): 47.2 REYNOLDS NO: 1505.3

DTWALL(C): 14.5 DT(C): 6.9 NUSSELT NO: 7.8

++

TEST NO 136 ORAL INHALATION
GAS:HELIUM DEPTH (FSW): 1000.0 FLOW (LPM): 15.8
BATH TEMPERATURE(C): 51.8 PRESSURE DROP(CM H20): 0.0

TWALL1	TWALL2	TWALL3	TWALL4	TWALL5	MEAN
51.5	52.8	51.2	48.7	53.2	51.0

TNASAL1	TNASAL2	MEAN
32.0	33.4	32.7

TTRACHEA1	TTRACHEA2	MEAN
38.8	41.7	38.8

MEAN VELOCITY(CM/SEC): 207.3 REYNOLDS NO: 6606.4

DTWALL(C): 18.3 DT(C): 6.1 NUSSELT NO: 24.0

++

TEST NO 137 ORAL INHALATION
GAS:HELIUM DEPTH (FSW): 1000.0 FLOW (LPM): 6.1
BATH TEMPERATURE(C): 51.6 PRESSURE DROP(CM H20): 0.0

TWALL1	TWALL2	TWALL3	TWALL4	TWALL5	MEAN
51.5	52.6	51.2	49.8	53.0	51.4

TNASAL1	TNASAL2	MEAN
33.3	34.9	34.1

TTRACHEA1	TTRACHEA2	MEAN
43.1	44.8	43.1

MEAN VELOCITY(CM/SEC): 80.1 REYNOLDS NO: 2550.6

DTWALL(C): 17.2 DT(C): 9.0 NUSSELT NO: 14.6

++

REFERENCES

1. Keatinge, W. R., Survival in Cold Water, Blackwell Scientific Publications, 1969

2. Hayward, J. S., Eckerson, J. D., and M. L. Collins, "Thermal Balance and Survival Time Prediction of Man in Cold Water," Can. J. Physiol. Pharmacol., Vol. 53, pp. 21-32, 1975.

3. Webb, P., and J. F. Annis, "Respiratory Heat Loss with High Density Gas Mixtures," Final Report Contract NONR 4965(00), Office of Naval Research, Washington, DC, 1966.

4. Goodman, M. W., Colston, J. W., Smith, N. E., and E. L. Rich, "Hyperbaric Respiratory Heat Loss Study," Contract N00014-71-C-0099, Office of Naval Research, Washington, DC, 1971.

5. Guyton, A. C., Textbook of Medical Physiology, Fifth Edition, W. B. Saunders Co., 1976.

6. Hoke, B., Jackson, D. L., Alexander, J., and E. Flynn, "Respiratory Heat Loss from Breathing Cold Gas at High Pressures," Summary of NMRI/NEDU Studies, 1971.

7. Marfatia, S., Donohoe, P. K., and W. H. Hendren, "Effect of Dry and Humidified Gases on the Respiratory Epithelium in Rabbits," J. of Pediatric Surgery, Vol. 10, pp. 583 through 590, 1975.

8. Burton, J. D. R., "Effects of Dry Anesthetic Gases on the Respiratory Mucous Membrane," Lancet 1: 235 through 238, 1962.

9. Webb, P., "Air Temperatures in Respiratory Tracts of Resting Subjects in Cold," J. Appl. Physiol. 4:378 through 382, 1951.

10. Jackson, D. C., and K. Schmidt-Neilsen, "Countercurrent Heat Exchange in the Respiratory Passages," Proceedings Nat. Acad. of Sci., 51:1192 through 1197, 1964.

11. Cole, P., "Some Aspects of Temperature, Moisture, and Heat Relationships in the Upper Respiratory Tract," J. Laryngol. and Otol., 67:449 through 456, 1953.

12. Armstrong, J., A. Burton, and G. Hall, "The Physiological Effects of Breathing Cold Atmospheric Air," J. Aviat. Med. 29:593 through 597, 1958.

13. Spealman, C., N. Pace, and W. A. White, "Heat Exchange by Way of the Respiratory Tract," US Naval Medical Research Institute Research Project X-163, 1944.

14. Moritz, A. R., F. C. Hendriques, and R. McLean, "The Effects of Inhaled Heat on the Air Passages and Lungs - an Experimental Investigation," M. J. of Pathology, 2:311 through 331, 1945.

15. Bouhuys, A., The Physiology of Breathing, Grune and Stratton, Inc., New York, 1977.

16. Collins, J. C., T. C. Pilkington, and K. Schmidt-Nielsen, "A Model of Respiratory Heat Transfer in a Small Mammal", Biophysical Journal 11:886 through 914, 1971.

17. Linderoth, L. S., and E. A. Kuonen, "Heat and Mass Transfer in the Human Respiratory Tract at Hyperbaric Pressures," Final Report Contract ONR N-00014-67-A-0251-00018, 1973.

18. Polgar, G., "Opposing Forces to Breathing in Newborn Infants," Biol. Neonate, 11: 1 through 22, 1967.

19. Moss, M. L., "Veloepiglottic Sphincter and Obligate Nose Breathing in the Neonate," J. Pediatric 67: 330 through 331, 1965.

20. Takagi, Y., Proctor, D. F., Salman, S., and S. A. Evering, "Effects of Cold Air and Carbon Dioxide on Nasal Airflow Resistance," Ann. Otol. 78: 40 through 48, 1969.

21. Patrick, G. A. and G. R. Sharp, "Oronasal Distribution of Inspiratory Flow During Various Activities," J. Physiol. (Lond.) 206: 228 through 238, 1970.

22. Richerson, H. B. and P. M. Seebohm, "Nasal Airway Response to Exercise," J. Allergy, 41: 269 through 284, 1968.

23. Keuning, Jr., "On the Nasal Cycle," Int. Rhinol., 6: 99 through 136, 1968.

24. Braithwaite, W. R., "The Calculation of Minimum Inspired Gas Temperature Limits for Deep Diving," Navy Experimental Diving Unit Report 12-72, 1972.

25. Nuckols, M. L., "Heat Transfer in the Lower Tract of the Human Lung at Hyperbaric Conditions," M. S. Thesis, School of Engineering, Duke University, December 1973.

26. Johnson, C. E., "Deep Diving Respiratory Heat and Mass Transfer," Ph. D. Dissertation, School of Engineering, Duke University, 1976.

27. Dekker, E., "Transition between Laminar and Turbulent Flow in Human Trachea," Journal of Applied Physiology, 16(6): 1060 through 1064, 1961.

28. Harrison, M. R., E. S. Hysing, G. Bo, "Control of Body Temperature: Use of the Respiratory Tract as a Heat Exchanger," J. Pediatric Surgery, 12:6, pp. 821 through 828, 1977.

29. Lloyd, E., N. A. Conliffe, H. Orgel, and P. N. Walker, "Accidental Hypothermia: An Apparatus for Control Rewarming as a First Aid Measure," Scottish Medical Journal, 17: 83 through 91, 1972.

30. Hayward, J. S. and A. M. Steinman, "Accidental Hypothermia: An Experimental Study of Inhalation Rewarming," Aviation Space Environ. Med. 46: 1236, 1975.

31. Weibel, E. R., "Morphometrics of the Lung," Handbook of Physiology, Section 3, Vol. 1, Chap. 7, American Physiol. Soc., Washington, DC, 1964.

32. Horsfield, K. and G. Cumming, "Angles of Branching and Diameters of Branches in the Human Bronchial Tree," Bul. Math. Biophys. 29: 245 through 259, 1967.

33. Electronic Ice Point Manual, Model MCJ, Omega Engineering, Inc., Stamford, Connecticut 06907.

34. DeBoer, B., Stetzner, L., and F. O'Brien, "Thermistor Reliability and Accuracy at High Pressures," American Laboratory, 1975.

35. Temperature Measurement Handbook, Omega Engineering, Inc., 1979.

36. Douglass, R. W., "Flow In A Human Lung Model at High Reynolds Numbers," M. S. Thesis, School of Engineering, Duke University, 1973.

37. Holman, J. P. Experimental Methods for Engineers, McGraw-Hill Co., New York, 1966.

38. Swift, D. L. and D. F. Proctor, Respiratory Defense Mechanisms, Part 1, Chapter 3, Marcel Dekker, Inc., New York, 1977.

39. Personal Communication with D. L. Swift, School of Hygiene and Public Health, Johns Hopkins University.

40. Modern Plastics Encyclopedia, Vol. 54, No. 10A, McGraw-Hill, New York, 1977.

41. Naval Coastal Systems Center Memorandum dated 18 November 1980 from Phil Sexton to G. W. Noble.

42. Bridger, G. P, and D. F. Proctor, "Maximum Nasal Inspiratory Flow and Nasal Resistance," Symposium on the Nose and Adjoining Cavities, Armed Forces Institute of Pathology, Washington, DC, 1 through 3 December 1969.

43. Ferris, B. G., Jr., J. Mead, and L. H. Opie, "Partitioning of Respiratory Flow Resistance in Man," J. Appl. Physiol. 19(4): 653 through 658, 1964.

44. Personal Correspondence with Mr. Rodney Florek, School of Hygiene and Public Health, the Johns Hopkins University.

45. Naval Coastal Systems Center Hydrospace Lab Report Number 1-81, Panama City, Florida, 1981.

46. US Navy Diving-Gas Manual, NAVSHIPS 0994-003-7010, Second Edition, June 1971.

47. McAdams, W. H., Heat Transmission, Third Edition, McGraw-Hill, New York 1954.

48. Siegel, R. and J. R. Howell, Thermal Radiation Heat Transfer, McGraw-Hill, New York, 1972.

49. Kreith, F., Principles of Heat Transfer, Third Printing, International Textbook Co., Scranton, PA, 1960.

50. Sears, F. W., M. W. Zemansky, University Physics, Third Edition, Part 1, Addison-Wesley Publishing Co., Inc., Reading, Massachusetts, 1963.

51. Johnson, C. E., and L. S. Linderoth, Jr., Deep Diving Respiratory Heat and Mass Transfer, School of Engineering, Duke University, 1976.

52. Douglas, R. W., and B. R. Munson, "Viscous Energy Dissipation in a Model of the Human Bronchial Tree," Journal of Biomechanics, Vol. 7 1974, pp 551 through 557.

53. Schroter, R. C. and M. F. Sudlow, "Flow Patterns in Models of the Human Bronchial Airways," Respiration Physiology, No. 7, 1969, pp 341 through 355.

54. Pedley, T. J., Schroter, R. C., Sudlow, M.F., "Energy Losses and Pressure Drop in Models of Human Airways," Respiration Physiology, No. 9, 1970, p 371.

55. Pedley, T. J., Schroter, R. C., Sudlow, M. F., "The Prediction of Pressure Drop in Models of Human Airways," Respiration Physiology, No. 9, 1970, p 387.

56. Pedley, T. J., Schroter, R. C., Sudlow, M. F., "Flow and Pressure Drop in Systems of Repeatedly Branching Tubes," Fluid Mechanics, Vol. 46, Part 2, 1971, pp 365 through 383.

57. Womersley, J. R., "Oscillating Motion of a Viscous Liquid in a Thin Walled Elastic Tube," Phil Mag., Serv. 7, 46, 1955, pp 199 through 221.

58. Schlicting, H., Boundary Layer Theory, McGraw-Hill, New York, 1960.

59. Sudlow, M. F., Olson, D. E., and R. C. Schroter, "Fluid Mechanics of Bronchial Air-Flow," Third International Symposium on Inhaled Particles, 1970.

60. ASHRAE Handbook of Fundamentals, Second Printing, American Society of Heating, Refrigerating, and Air-Conditioning Engineers, Inc., New York, 1974.

61. Bird, R. B., W. E. Stewart, and E. N. Lightfoot, Transport Phenomena, John Wiley and Sons, New York, 1960.

62. Chilton, T. H., and A. P. Colburn, "Mass Transfer (Absorption) Coefficients Prediction from Data on Heat Transfer and Fluid Friction," Industrail and Engineering Chemistry, November 1934, p 1183.

63. Lewis, W. K., "The Evaporation of a Liquid into a Gas," Mechanical Engineering, Vol 55, 1933, p 567.

64. Kays, W. M., Convective Heat and Mass Transfer, McGraw-Hill Co., New York, 1966.

65. Parker, J. D., Boggs, J. H., and E. F. Blick, Introduction to Fluid Mechanics and Heat Transfer, Addison-Wesley Publ. Co., Inc., Reading, Massachusetts, 1970.

66. Jones, J. B. and G. A. Hawkins, Engineering Thermodynamics, John Wiley and Sons, New York, 1960.

67. Smith, L., F. Keyes, and H. Gerry, "Proceedings of American Academy Arts and Science 69: 137, 1934.

68. Thermodynamic Properties of Steam, Joseph Keenan and F. G. Keyes, John Wiley and Sons, Inc., 1936.

69. Shames, I. H., Mechanics of Fluids, McGraw-Hill Co., New York, 1962.

70. Meyers, G. E., Analytical Methods in Conduction Heat Transfer, McGraw-Hill, New York, 1971.

71. Crandall, S. H., Engineering Analysis, McGraw-Hill Co., New York, 1956.

72. Walker, J. E. C., Wells, R. E., Jr., and Merrill, E. W., "Heat and Water Exchange in the Respiratory Tract", Am. J. Med., Vol 30, 1961, pp 259-267.

73. Cole, P., "Further Observations on the Conditioning of Respiratory Air", J. Laryng., Vol 67, 1953, pp 669-681.

74. Breathing; What You Need to Know, National Tuberculosis and Respiratory Disease Association, 1968.

75. Slattery, J. C., and Bird, R. B., "Calculation of the Diffusion Coefficient of Dilute Gases and of the Self-Diffusion Coefficient of Dense Gases", A.I Ch. E Journal, 4, 137 through 142, 1958.

76. Kestin, Joseph, A Course in Thermodynamics, Vol. II, McGraw-Hill Co., New York, 1979.

77. Sherwood, T. K., and Pigford, R. L., Absorption and Extraction, McGraw-Hill Co., New York, 1953.

78. Rohsenow, W. M. and Choi, H. Y., Heat, Mass, and Momentum Transfer, Prentice-Hall, Inc., New Jersey, 1961.

79. Saidel, G. M., Kruse, K. L., and Primiano, F. P., Jr., "Heat and Water Transport in the Trachea," Presented at the 73rd Annual Meeting of the American Institute of Chemical Engineering, Chicago, November 1980.

80. Strauss, R. H., McFadden, E. R., Jr., Ingram, R. H., Jr., Deal, E. C., Jr., and Jaeger, J. J., "Influence of Heat and Humidity on the Airway Obstruction Induced by Exercise in Asthma," J. of Clinical Investigation, Vol. 61, 1978, pp. 433 through 440.

81. Deal, E. C., Jr., McFadden, E. R., Jr., Ingram, R. H., Jr., and Jaeger, J. J., "Hyperpnea and Heat Flux: Initial Reaction Sequence in Exercise-Induced Asthma," J. Appl. Physiol: Respirat. Environ. Exercise Physiol. 46(3): 476 through 483, 1979.

82. Deal, E. C., Jr., McFadden, E. R., Jr., Ingram, R. H., Jr., and Jaeger, J. J., "Esophageal Temperature During Exercise in Asthmatic and Nonasthmatic Subjects," J. Appl. Physiol: Respirat. Environ. Exercise Physiol. 46(3): 484 through 490, 1979.

83. NIH Publ. #81-2019, "Epidemeology of Respiratory Disease," Div. of Lung Dis., Claude Lenfant, Chairman, October 1980.

84. Proctor, D. F., and Adams, G. K., III, "Physiology and Pharmacology of Nasal Function," Pharmac. Ther. B., Vol. 2, 1976, pp. 493 through 509.

85. Scherer, P. W. and Hanna, L. M., "Heat and Water Transport in the Human Respiratory System," Unpublished articles, Department of Bioengineering, University of Pennsysvania.

86. Cole, P., "Recordings of Respiratory Air Temperature", J. Laryng., Vol. 68, 1954, pp 295-307.

87. Cole, P., "Respiratory Mucosal Vascular Responses, Air Conditioning and Thermo Regulation", J. Laryng., Vol. 68, 1954, pp 613-622.

DISTRIBUTION LIST

		Copy No.
427	Commander, Naval Sea Systems Command (SEA 0353) (Attn: Mr. J. Freund)	1
---	Supervisor of Diving (OOC-D), Department of the Navy, Washington, DC	2
---	Commander, Navy Experimental Diving Unit (NEDU 05, CDR J. L. Zumrick)	3
204	Commanding Officer, Naval Medical Research Institute	4
---	Commanding Officer, Naval Medical Research and Development Command, National Navy Medical Center, Bethesda, MD 20014 (CAPT C. Green)	5
054	Chief of Naval Research (Dr. Leonard M. Libber)	6
---	Webb Associates, Inc., Yellow Springs, Ohio 45387	7
001	Chief of Naval Material (MAT 08T24)	8
154	US Naval Academy, Naval Systems Engineering Department, Annapolis, MD (Attn: LCDR A. Sarich)	9
---	University of Texas at Austin, Department of Chemical Engineering, Austin, TX 78712 (Attn: Dr. E. Wissler)	10
---	University of Pennsylvania, Department of Bioengineering, Philadelphia, PA 19104 (Attn: Dr. P. W. Scherer)	11
---	The Johns Hopkins University, School of Hygience and Public Health, 615 N. Wolfe St., Baltimore, MD 21205 (Attn: Dr. D. L. Swift)	12
---	Duke University, Department of Mechanical Engineering, Durham, NC 27706 (Attn: Dr. C. E. Johnson)	13
---	DCIEM, 1133 Sheppard Ave. West, P. O. Box 2000, Downsview, Ont M3M 3B9 (Canada) (Attn: Dr. L. Kuehn)	14
---	Admiralty Marine Technology Establishment Physiological Lab, Fort Road, Alverstoke, Gosort, Hants (England) PO12 2DU (Attn: Dr. Philip Hayes)	15
---	F. G. Hall Laboratory, Duke Medical Center, Duke University, Durham, NC 27706	16
---	Norwegian Underwater Institute, Gravadalsveien 255, 5034 Ytre Lakseva, Norway (Attn: Dr. Geir Evensen)	17
---	Undersea Medical Society, 9650 Rockville Pike, Bethesda, MD 20014 (Attn: Dr. C. W. Shilling)	18
075	Director, Defense Technical Information Center	19-28


DAT
ILM